KEELE UNIVERSITY

The combination of polyhydroxyalkanoates, collagen and stem cells for application in tendon tissue engineering

Thesis submitted to Keele University for the Degree of Doctor of Philosophy

Alexander James Lomas

October 2013

School of Postgraduate Medicine

Institute of Science and Technology in Medicine

Keele University

Declaration Part 1. To be bound in the thesis

SUBMISSION OF THESIS FOR A RESEARCH DEGREE

Part I. DECLARATION by the candidate for a research degree. To be bound in the thesis

Degree for which thesis being submitted Doctor of Philosophy

Title of thesis The combination of polyhydroxyalkanoates, collagen and stem cells for application in tendon tissue engineering

This thesis contains confidential information and is subject to the protocol set down for the submission and examination of such a thesis: NO

Date of submission 30.08.2013 Original registration date 08.10.2009

(Date of submission must comply with Regulation 2D)

Name of candidate Alexander James Lomas

Research Institute ISTM Name of Lead Supervisor Nicholas Forsyth

I certify that:

(a) The thesis being submitted for examination is my own account of my own research
(b) My research has been conducted ethically. Where relevant a letter from the approving body confirming that ethical approval has been given has been bound in the thesis as an Annex
(c) The data and results presented are the genuine data and results actually obtained by me during the conduct of the research
(d) Where I have drawn on the work, ideas and results of others this has been appropriately acknowledged in the thesis
(e) Where any collaboration has taken place with one or more other researchers, I have included within an 'Acknowledgments' section in the thesis a clear statement of their contributions, in line with the relevant statement in the Code of Practice (see Note overleaf).
(f) The greater portion of the work described in the thesis has been undertaken subsequent to my registration for the higher degree for which I am submitting for examination
(g) Where part of the work described in the thesis has previously been incorporated in another thesis submitted by me for a higher degree (if any), this has been identified and acknowledged in the thesis
(h) The thesis submitted is within the required word limit as specified in the Regulations

Total words in submitted thesis (including text and footnotes, but excluding references and appendices) …40000……

Signature of candidate A Lomas …… Date …26.08.2013…

Declaration Part 1. To be bound in the thesis

Note

Extract from Code of Practice: If the research degree is set within a broader programme of work involving a group of investigators – particularly if this programme of work predates the candidate's registration – the candidate should provide an explicit statement (in an 'Acknowledgments' section) of the respective roles of the candidate and these other individuals in relevant aspects of the work reported in the thesis. For example, it should make clear, where relevant, the candidate's role in designing the study, developing data collection instruments, collecting primary data, analysing such data, and formulating conclusions from the analysis. Others involved in these aspects of the research should be named, and their contributions relative to that of the candidate should be specified (*this does not apply to the ordinary supervision, only if the supervisor or supervisory team has had greater than usual involvement*).

Abstract

Polyhydroxyalkanoates (PHA) are biopolymer molecules that have shown increasing evidence of suitability for use as biomaterials. Many different cell types from a range of species have been shown to adhere and develop on PHA scaffolds, with some preliminary *in vivo* studies having been performed and showing promising results.

Several cell types have shown potential for use in tendon tissue engineering. Primary tendon cells (tenocytes) isolated from a rat Achilles tendon (RaT), human Mesenchymal Stem Cells (hMSCs) and human Embryonic Stem Cells (hESCs) have all been utilised throughout this investigation in many different experimental models. To date, research has focused on scaffold design and manufacture, suitability of the polymer for cell culture, *in vitro* testing in both static and dynamic environments and a pilot *in vivo* study. The aims of this study were to find if the PHA molecule Poly (hydroxybutyrate-co-hydroxyhexanoate) (PHBHHx) is able to support tendon cell culture, to design a scaffold using the polymer that could replicate tendon *in vitro* and *in vivo*, to mechanically stimulate cells seeded in scaffolds to encourage extracellular matrix remodelling into tendon like structures and to monitor the construct when placed *in situ* in a pilot *in vivo* model.

Results have shown that PHBHHx can support RaT, hMSC and hESC development. Mechanical testing revealed a design with similar properties to those of a rat Achilles tendon. Bioreactor studies have demonstrated how hMSCs, hESCs and rat tenocytes can remodel collagen gels incorporated into the scaffold towards morphologies resembling tendon. Preliminary *in vivo* studies have found that a PHBHHx and PHBHHx/collagen hybrid scaffold show little immune response when placed *in situ*.

In conclusion, this study has demonstrated the effectiveness of PHBHHx and PHBHHx/collagen hybrid scaffolds for use in tendon tissue engineering, providing scope for future breakthrough products and innovations in both scientific and clinical arenas.

Contents.

List of Figures

List of Tables

Publications and Presentations.

Original research Publications

Alex J. Lomas, George G. Q. Chen, Alicia J. El. Haj, Nicholas R. Forsyth. Poly (3-hydroxybutyrate-co-3-hydroxyhexanoate) supports adhesion and migration of mesenchymal stem cells and tenocytes. World Journal of Stem Cells 2012;26:4(9): 94-100.

Alex J Lomas, William R Webb, JianFeng Han, Xun Sun, Zhirong Zhang, George GQ Chen, Alicia J El Haj, Nicholas R Forsyth. Poly (3-hydroxybutyrate-co-3-hydroxyhexanoate)/collagen hybrid scaffolds for Tissue Engineering Applications. Tissue Eng Part C Methods. 2013;19(8):577-85

William R. Webb, Tina P. Dale, **Alex J. Lomas**, Guodong Zeng, Nicholas R. Forsyth, Alicia J. El Haj, Guo-Qiang Chen. Poly(3-hydroxybutyrate- co-3-hydroxyhexanoate) (PHBHHx) Scaffolds for Tendon Repair in the Rat Model. (Biomaterials 2013;34:6683-6694)

Platform Presentations.

Lomas, AJ. Dynamic Mechanical Force Application for Tendon Tissue Engineering. BOSE user group meeting. Glasgow, UK. 1 May 2012.

Lomas, AJ. Mechanostimulation of human mesenchymal stem cells in phbhhx/collagen hybrid scaffolds for tendon tissue engineering applications. TERMIS World Congress. Vienna, Austria, 4-9 September 2012.

International Conferences and Symposia Published in full in proceedings (Posters)

AJ Lomas, J Han, GQ Chen, AJ El Haj, NR Forsyth. Utilising stem cells and poly (3-hydroxybutyrate-co-3-hydroxyhexanoate)/collagen hybrid scaffolds for tendon tissue engineering. European Cells and Materials 2011 Vol. 22 Suppl. 3 (page 29)

WR Webb, **AJ Lomas**, G Zeng, GQ Chen, AJ El Haj, NR Forsyth. Poly(3-hydroxybutyrate-co-3-hydroxyhexanoate) (PHBHHx) Scaffolds for Tendon Repair in the Rat Model. European Cells and Materials 2011 Vol. 22 Suppl. 3 (page 34)

Lomas AJ, Webb WR, Zeng G, Forsyth NR, El Haj AJ, Chen GQ. Poly(3-hydroxybutyrate- co-3-hydroxyhexanoate) (PHBHHX) scaffolds for tendon repair in the rat model. Histology and Histopathology 2011 Vol. 26 Suppl. 1 (page 160).

Papers in Preparation.

Alex J Lomas, Emily R Britchford, William R Webb, George GQ Chen, Alicia J El Haj, Nicholas R Forsyth. The Effect of Cyclical Mechanical Stress and Growth Factor Addition on Human Stem Cell Seeded PHBHHX/Collagen Hybrid Scaffolds. (European Cells and Materials, submission planned 2013)

Acknowledgments.

My family's support over the past four years has been invaluable. Thank you for your patience and understanding, especially when I was a miserable bugger after a very long day!

First, I would like to thank my supervisory team of Dr Nicholas Forsyth and Prof Alicia El Haj and my PhD advisor Dr Paul Roach for their continued guidance and input throughout the last three years. Without their support and knowledge this research would not have been possible. I am especially appreciative of the opportunities to travel and present my work that they have provided me with, giving me a greater understanding of the work being performed around the world and allowing me to create my own network of contacts which will serve me well in my career. It has been a pleasure to work with all of you over the past three years and I look forward to working with you in the future.

I would also like to thank Prof George Chen and the entire laboratory at Dept. Biological Sciences and Biotechnology, Tsinghua University for inviting me into their laboratory and their help and patience during my academic exchange. It was an honour to work in such a prestigious lab group and I valued my time there immensely.

Throughout my PhD many people have made contributions to the work done. Particular thanks go to Emily Britchford, Saurabh Lal, Jan Feng Han, Petronella Vamanu and Hussna Hussain at Keele University and Dr Rainey Wang, Guo Dong, Xian Li and Gao Rai at Tsinghua University for their help through research project collaboration and performing the tasks I couldn't do alone.

As part of the first intake of the DTC regenerative medicine I have been part of a cohort of fantastic people, all of which I owe a great amount to for their friendship, input on

problems and sharing of experiences. I am greatly thankful to Prof Chris Hewitt, Prof David Williams, Dr Rob Thomas and Dr Karen Coopman for first selecting me to be part of this scheme then guiding me through the first year and beyond. I look forward to working with everyone involved with the DTC on future collaborations.

A big thank you goes to Richard Webb for his help and friendship throughout the three years, especially the times in China when we were a little isolated from the rest of the rest of our friends and family. The Red House and Laowais bar also played their part during this time!

Hareklea Markides is the life and soul of any party. Thank you for changing me for the better and making life so enjoyable.

Finally, a big thank you to everyone at the Guy Hilton research Centre for continually going out of their way to help me in all aspects of PhD life. Special thanks go to Deepak Kumar, Tina Dale, Dr Khondoker Akram, Sammy Wilson, Rupert Wright, Michael Rotherham, James Everett, Abigail Rutter Anne Harrison and Maria Kyriacou who have continuously provided support, knowledge and friendship throughout…especially after a few beers!

This research has been generously funded by the EPSRC Regenerative Medicine Doctoral Training Centre (EP/F/500491/1) and the EU seventh framework scheme (PIRSES-GA-2008-230791).

General Abbreviations

PHA	polyhydroxyalkanoate
PHBHHx	poly (hydroxybutyrate-co-hydroxyhexanoate)
hMSC	human mesenchymal stem cells
hESC	human embryonic stem cells
SDhESC	spontaneously differentiated human embryonic stem cells
RaT	rat Achilles tendon
MEF	mouse embryonic fibroblast
TDSC	tendon derived stem cell
FBS	foetal bovine serum
PBS	phosphate buffered saline
NEAA	non-essential amino acid
L-Glut	L- Glutamine
DMEM	Dulbecco’s modified Eagle’s media
KO DMEM	knock-out Dulbecco’s modified Eagle’s media
SR	serum replacement
PSA	penicillin streptomycin, amphotericin B
BMP	bone morphogenic protein

FGF	fibroblast growth factor
PFA	paraformaldehyde
RM	regenerative medicine
TE	tissue engineering
UTS	ultimate tensile stress
GAG	glycosaminoglycan
IMS	industrial methylated spirits
BSC	biological safety cabinet
UV	ultra violet

Chapter 1.

Introduction

1.1. Introduction.

1.1.1. Regenerative Medicine.

The field of research referred to as regenerative medicine (RM) aims to replace or regenerate human cells, tissues or organs to restore or establish natural function (1). Many different research approaches can be classified within the RM bracket; biomaterials, small pharmaceutical molecules and complex biological molecules, such as proteins, cell based therapies and tissue engineering (2). The development and successful implantation in human of both a functioning tissue engineered trachea (3) and bladder (4) demonstrate the advances made in the field over recent years. Further investigations into the tissue engineering of complete liver (5), kidney (6) organs are also showing promise, although further research is required before human testing can be carried out (7). Skin tissue engineering is currently at a more advanced stage of development and is in wide clinical use (8).

Tendon injury and repair presents a major burden to healthcare systems around the world due to increased life expectancies and a more active lifestyle being adopted by older people (9). Tendons are characterised as slow healing following injury for many reasons including poor vasculature, low cell numbers and long term immobilisation leading to further degeneration (10). New treatment methods and materials are therefore required to improve on current gold standards, such as autografts (11), with polymer based tissue engineered constructs showing great promise in this area (12).

This project aims to apply the principles of tissue engineering in the development of an artificial tendon for use as either a model for treatment assessment or as a treatment itself. During this project novel biopolymers, natural polymers and a range of cells that have

shown promise in other areas of musculoskeletal research will be examined, along with mechanical stimulation bioreactors and hypoxic culture conditions to determine the optimal environment for artificial tendon construct development.

1.2. Tendon.

Tendons form the bridge between muscle and bone. Each muscle has at least two tendons, one at the distal end, the other at the proximal end. Without tendons, the force exerted by the muscle would not be transferred to the skeletal system, meaning movement would not be possible. A secondary function of tendon is in supporting the skeleton during movement. The high loads applied to tendons on a regular basis mean that a highly specialised tissue is required to allow for correct function.

1.2.1. Tendon Structure.

Healthy tendon is brilliant white in colour and can vary in thickness according to its location, from thin cylindrical tendons (like those that control finger movement) to thick ribbon like structures (e.g. connecting the humorous and the bicep). The structure of these tendons does not vary greatly between these different types.

The tendon is surrounded by a network of structures that aid in the lubrication and efficiency of glide along the path of force transmission. These include the retinacula (fibrous sheaths), reflection pulleys, synovial sheaths, paratenon and tendon bursae (13). These structures tend only to be found in areas where very large forces are exerted, (e.g. the Achilles tendon) and most are not present for the majority of tendons throughout the

body. Paratenon is a loose sheath of tissue consisting mainly of collagens I and III, with an inner layer of synovial cells surrounding most tendons acting as a guide for tendon glide. The epitenon is the outer layer of the tendon. Composed primarily of densely aligned cross linked collagen I and III fibrils, these act as a binding tissue for the tendon's internal fibre bundles. Collagen I fibrils are the basic unit of the tendon that create its load bearing capacity by aligning with the direction in which the force acts. These collagen fibrils are organised into structures referred to as tertiary, secondary and primary bundles. Primary fibre bundles (or sub fascicles) consist of a collection of collagen I fibrils (14). Secondary fibre bundles (fascicle) group together the sub fascicles into larger units, which are then grouped into tertiary fibre bundles (15). Endotenon divides the bundles of collagen fibrils into areas that can be supplied with blood and other nutrients. As well as acting as a binding mechanism, endotenon, made up of a "crisscross" pattern of types I and III collagen and high concentrations of glycosaminoglycan molecules, which trap water in the overall structure lubricating the system, allowing the tendon fascicles to glide over each other, and creating a greater range of possible movement and a higher overall tolerance of stress (13).

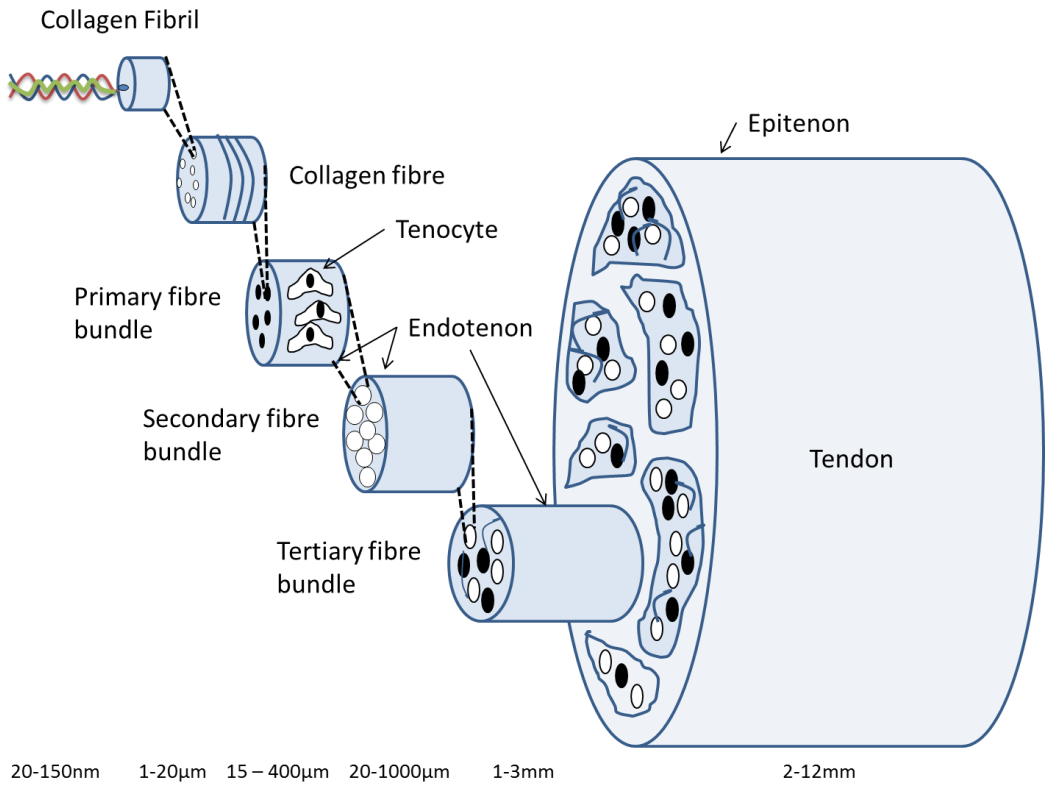

Fig. 1.1 The structure of tendon with approximate diameters of each section. Tendon structure is hierarchical, with many small units coming together to form larger and larger structural units, with connective tissue sheaths (endotenon) aiding in fibril glide. Numerical diameter values from Richardson et al 2007 (16)**.**

1.2.2. Tendon Composition.

Tendons are made up of collagens, proteoglycans, glycoproteins, water and cells(15). Collagen accounts for the majority of a tendon's mass, with type I collagen being by far the most abundant, making up around 70% of total dry mass(17) and around 95% of the total mass of collagen(18). The remaining 5% is made up of types III and V collagen. In healthy tendons, type III collagen is found mainly in the endotenon and epitenon but is found throughout the tendon structure in aged or damaged tissue. Type V collagen is found at the centre of the collagen fibrils acting to establish and mediate fibril diameter growth,

ensuring that a collection of many small collagen I fibrils is formed rather than one large structure (19). For collagen to gain the mechanical properties required to function as a tendon a complex pattern of cross linking is required. This increases both the Young's Modulus (the ratio of the stress along an axis over the strain along that axis in the range of stress in which elastic deformation is maintained) and reduces the strain (the amount a material deforms as a percentage of its original length in one axis) at failure, making the tendon better suited to transmit forces. Cross linking can be achieved either enzymatically with lysyl oxidase, where adjacent amino acids are linked (15) or when reducing sugars bind permanently to the matrix proteins (glycation) (20). Collagen fibrils are linked in many different ways, not just longitudinally, but also horizontally and transversely. Five different cross link patterns are described by Jozsa et al (21). The specific cross links found vary greatly between not only different tendons, but different areas of the same tendon. The variation is thought to be due to differences in the force loading, with the fibrils adapting to transmit load in the most efficient way.

Proteoglycans form a major part of many extracellular matrices (ECM), being responsible for holding water molecules and providing binding sites for cells to adhere to ECM structures. The proteoglycan content of a tendon is dependent on its location and role in the body, with compression bearing regions of bovine tendons being shown to have a significantly higher proteoglycan content than those in tension (3.5% vs. 0.2% of total tendon dry weight) (22). Proteoglycans are mainly found in the extracellular matrix surrounding the tendon cells. The major proteoglycans present in tendon are decorin and aggrecan. Both molecules have been found to play a role in allowing the fibrils to slip over each other during mechanical deformation and allowing tendons to bear compressive forces by trapping water throughout the tendon structure (23) (24). Glycoproteins are also

present in the extracellular matrix. Fibronectin is found on the surface of the collagen fibrils and its synthesis is increased when injury to the tendon occurs. It then aids in healing and remodelling of the tendon structure (13).

Elastin is present in tendon, in the form of elastic fibres and make up around 1-2% of the total dry mass. It is thought that the role elastin plays in tendons is to allow the fibrils to contract and recover after deformation caused by muscle contraction and are responsible for structural flexibility (17).

The predominant cell type found in the tendon is the tenocyte (25). Tencocytes are a specialised form of a fibroblast cell. Fibroblasts are responsible for maintaining extracellular matrix throughout the body. To do this in tendon, large quantities of tropocollagen (the base molecule of collagen) need to be expressed along with the other structural molecules; elastin, decorin and aggrecan (26). Located between the fibrils, tenocytes are found in small numbers and are not very metabolically active, although tendon reconstruction and remodelling does occur in response to injury (10). In total, tenocytes account for around 95% of all cells present in the tendon. Other cells present in tendons are chondrocytes, which are found at the insertion sites, synovial cells in the tendon sheath and vascular cells (13), and in addition there are a very small number of tendon stem cells up to late adolescence (27).

1.2.3. Tendon Blood Supply.

Tendon is a relatively avascular tissue with blood entering from 3 major sources: the musculotendon junction, the osteotendon junction and the surrounding connective tissue

(28). The paratenon is a relatively highly vascularised tissue, supplying around 35% of total blood to the tendon, with the remaining 65% supplied through the junctions with the bone and muscle (29). Blood supply has been implicated in the rupture of tendon, with supply being found to decrease with increased age and physical inactivity, however it is likely that other factors, such as increased activity in older age, have a greater influence (30). It has also been suggested that the low blood supply present in the mid-section of tendon is at least partly responsible for the high incidence of injuries occurring at this position, as external cells cannot easily migrate into the tissue to repair minor damage, although other factors have to be considered such as twisting and thinning (31).

1.2.4. Tendon Mechanical Properties.

The mechanical properties of tendon are typically evaluated using methods that stretch the tissue to failure while continually measuring forces applied. This continual evaluation results in the generation of a stress-strain curve which displays the force required to stretch the tendon to a given elongation. Tendons typically demonstrate four distinct regions while in tension under force (32), which can be seen in Fig. 1.2. Region I is referred to as the toe region. Here, the crimp angles present between the fibres are reduced, resulting in the tendon becoming longer and thinner, however no fibre stretching takes place. Region II is the linear region, where fibres start to be stretched, resulting in some starting to break. In region III the fibres start to break unpredictably throughout the structure, making it a lot weaker as a result. Finally region IV is where the tendon completely fails.

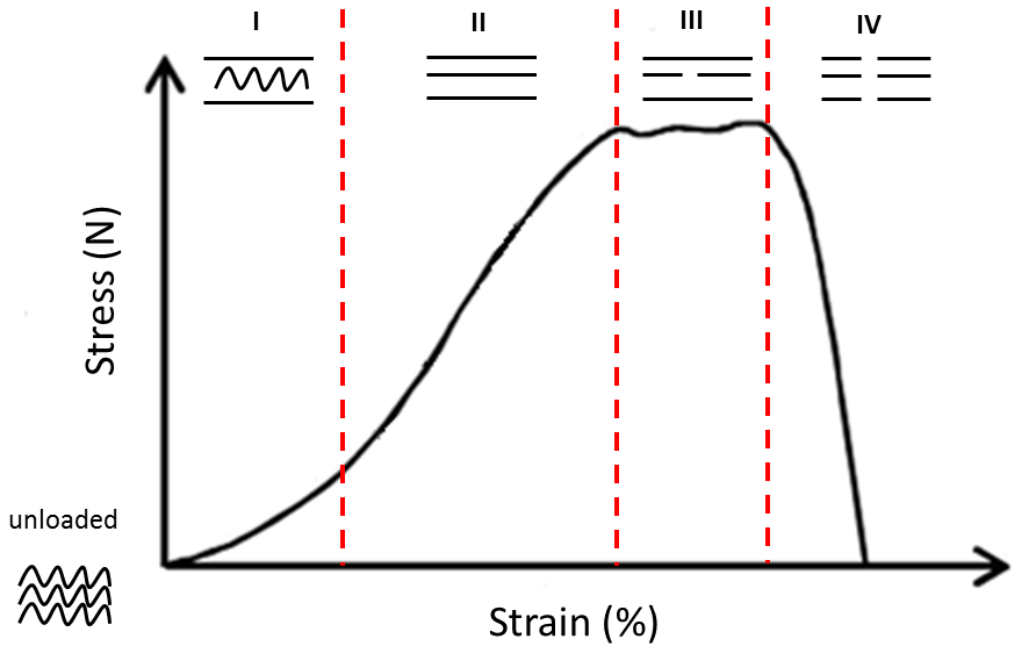

Fig. 1.2 Typical stress strain curve of a tendon. During loading tendon fibrils lose the initial 'crimp' pattern seen in unloaded samples, becoming straightened (region I, toe region). Fibrils begin to elastically stretch in region II (linear region) before fibrils begin to break uncontrollably in region III, before complete tissue rupture in region IV.

The specific mechanical properties change with species and location of the tendon being tested. Normalised tendon analysis demonstrates that typical adult human tendons have a Young's Modulus of 1-2 GPa, an ultimate stress of around 100 MPa and an ultimate strain of 4-10% (33). These figures have proven very difficult to replicate using synthetic materials. In this instance normalisation was performed against the thickness of the tendon sample, with tendons from several areas of the body used to gain a more accurate assessment.

Tendon is a viscoelastic material that it is affected by stress relaxation, creep and hysteresis (34). This means that it does not stretch elastically, and will behave differently at different stages of growth or force application. Stress relaxation occurs when the force needed to

elongate a material to a constant strain decreases over time in a predictable way. Creep is the tendency of a solid material to move deform permanently under the influence of constant high stresses near to, but not at the failure stress (35). This allows for tendons to stretch to beyond normal physiological limits without rupture if forces are applied over a prolonged period of time. Mechanical hysteresis occurs when a material resorts back to its original length after elastic deformation at a slower rate to that which it was loaded, creating an open loop in the stress/strain plot representing energy being dissipated via heat. This has been found to have a value of between 5 and 10% in human tendons (36).

1.2.5. Natural tendon repair.

There are 3 stages in the natural repair cycle of a damaged tendon: exudative, fibroblastic and remodelling (37). The exudative stage occurs between days 0 and 5 after injury in humans. During this time, inflammation occurs and extrinsic cells flood the wound site. The damaged ends of the ruptured tendon also start to soften, allowing for molecules to move into the injury site more easily. By analysing tendon repair in a mouse Achilles defect model it was found that 'tendon gel' (constituting the major compositional molecules of tendon, such as collagens I and III, GAGs, but in an unordered state) was secreted from the damaged tendon end 3 days post injury as identified by transmission electron microscopy. After a further 2 days the 'gel' started to form into an area of denser tissue, which was then subsequently aligned into fibrils after a 21 day period of muscular contraction or *in vitro* mechanical loading (38).

The fibroblastic stage occurs between weeks 1 and 3 post injury. Fibroblasts from the epitenon migrate into and populate the wound site. After an ill-defined critical number of

cells are present, production of extracellular matrix begins, leading to a steady rise in tensile strength with more ECM being produced. The final stage of repair is remodelling where collagen fibrils start to reorganise themselves in accordance with the loads being applied to them, eventually leading to a fully functioning tendon (38). From this, methods of creating artificial tendon can be created. By placing appropriate cells, like autologous tenocytes or MSCs into an area rich with the components of tendon, they may start to remodel the collagen into fibrils, especially if a physiological loading pattern (e.g. simulating general movement) were placed across the new structure (39).

1.2.6. Surgical repair of tendon injury.

Tendon injury is an increasing problem worldwide. In the USA, over 75,000 Achilles tendon ruptures, 55,000 rotator cuff injuries and over 5 million new cases of tennis elbow are diagnosed and treated annually (40). There are three grades of tendon injury: I, II and III. Grade I injuries are small overstretches that do not result in chronic pain. Grade II are the result of small tears in the tendon fibres that can result in some joint instability. Grade III is a complete tear of the tissue and leads to significant joint instability (31). Treatment usually starts by using conservative methods (e.g. physiotherapy). However, surgical intervention is frequently needed if no improvement is observed. Traditional treatment of small lacerations involve suturing the damaged ends together, followed by a programme of physiotherapy designed to manage the weight bearing of the repairing tissue over time. When the defect is too large, constructs are required to bridge the gap. Graft tissues are frequently used with varying effectiveness. Autografts (taking an undamaged section of tendon from another part of the patient – usually hamstring) provide minimal chance of immunorejection, but problems with donor site morbidity and pain are commonly

associated with this procedure (40). Allografts from donor or cadaveric tissue are frequently used, however lack of supply, greater failure rates and immunorejection problems persist (11). Decellularised xenograft tissues from animal sources are starting to be used more widely, however major concerns remain regarding long term viability and cross species disease transmission (12). Commercially available artificial tendon graft products are also in wide clinical use, but a prolonged immune response and post-operative infection have been widely reported (41). Due to the problems associated with tendon repair surgery, new techniques and materials need to be developed in order to meet the increasing clinical need.

1.2.7. Collagen fibril formation.

Fibril formation from a dissolved collagen solution is a diffusion gradient guided process where solvent molecules disperse forcing collagen molecules (oligomers) to gather together, resulting in circular form morphologies. Randomly ordered small diameter fibrils (20-70nm) form in collagen gels when acid soluble collagen molecules are neutralised and the temperature increased to between 20^{o}C and 34^{o}C for 1-2 hours (42). This process occurs in three phases: lag, growth and plateau. When approximately 20% of the available molecules have formed into fibrils, further *de novo* assembly is restricted, resulting in fibrils joining together into a hierarchical structure. Fibril alignment in embryonic tendon formation is controlled intracellularly by specific sites between the Golgi apparatus and cell membrane, which act as ‘fibropositors’. Procollagen (a precursor to collagen that is water soluble as opposed to collagen being acid soluble) molecules are arranged into small diameter collagen fibrils which are then excreted in hexagonally shaped bundles by the cell

from these fibropositors, parallel to the axial direction of the tendon(43). Further fibrilogenesis then occurs via alignment and joining to form larger units.

1.2.8. Growth factors in tendon repair.

Growth factors are molecules which bind with cells to enable a specific cellular function to occur, with the focus in tendon stem cell research being on inducing or maintaining differentiation (44). Several growth factors have been linked with tendon repair and development.

Increased Early Growth Response protein 1 (EGR-1) and Early Growth Response protein 2 (EGR-2) expression in tendon cells is correlated with an increase in collagen expression during tendon cell differentiation in embryonic chick limbs, suggesting a strong link between EGR and *de novo* tendon formation (45). Transforming Growth Factor β (TGFβ) is essential for the maintenance and recruitment of tendon progenitor cells in the embryonic mouse. Through a series of knockout studies it was determined that if TGFβ 2 or 3 were removed between E12.5 and E14.5, tendon and ligament tissue would not develop in limbs (46). Controlled release of basic Fibroblast Growth Factor (bFGF) from scaffold materials has been found to increase the expression of collagen I and increase the stiffness and maximum load capacity of poly(lactic-co-glycolic acid) PLGA electrospun scaffolds seeded with bone marrow stem cells (47).

Bone Morphogenic Protein 12 and 13 (BMP-12/13, also known as Growth Differentiation Factor (GDF-6/7)) are members of the Transforming Growth Factor – Beta (TGF-β)

superfamily that have been found to play important roles in matrix synthesis, differentiation, chemotaxis and proliferation (48) (49) (50). BMP12 can induce tenogenesis in rat bone marrow-derived MSCs. Upregulation of tenomodulin, tenascin C and scleraxis (generally considered as being tendon markers(31)) were all observed in colonies formed in BMP-12 containing media when compared to cells cultured in media containing no growth factors. It was also noted that increased matrix production and remodelling occurred when BMP-12 treated cells were implanted into an injury site in a rat tendon (48,51). BMP-12/13 can promote ectopic tendon formation and repair (48)(52). BMP-12 induced both *in-vitro* and *in-vivo* tenogenesis of MSCs (48)(53)(51). BMP-12 and BMP-13 can both induce increased production of thrombospondin 4 (a specific tendon marker) along with a characteristic wave like pattern found in tendon histological samples after 14 days implantation into a rat defect model (54). A combination of BMP-12, BMP-13 and vitamin C have also been found to induce tenogenisis in human Embryonic Stem Cells (hESCs) in static physiological O_2 (2% O_2) monolayer culture conditions (in house data).

Fibroblast Growth Factors (FGFs) are a group of 23 family members ranging in molecular weight from 17KDa to 34KDa that have been shown to play a vital role in limb development and organogenesis during embryonic development (55)(56). Three members of the FGF family have a prominent role in the maintenance of mesenchyme during limb development; FGF-4, FGF-6 and FGF-8. FGF-4 has been shown to play a role in early stage embryonic patterning and the maintenance of mesenchyme within the developing embryo (56) (57)(58) (59). Further research using FGF-4 knockout studies found that limb buds fail to develop in mice where FGF-4 is not present (57,58)(59). FGF-6 expression has been shown to be present in developing skeletal muscle. Studies conducted using murine models have shown FGF-6 to be exclusively present in the myotomal compartment (early stage of skeletal muscle development) of the somite at E9.5 (60) (61) (62). Due to the close

interaction of tendon, muscle and bone it is feasible that FGF-6 could play an integral role in the development of tendon and muscular-tendon junctions. FGF-8 has also been shown to play a pivotal role in murine limb development by inducing ectopic limb development and replacing the Apical Ectodermal Ridge (the group of cells at the developing front of the embryonic limb) (63) (64). FGF-4, FGF-6 & FGF-8 have been shown to be present in the AER providing signalling to maintain mesenchymal cells in the proliferative state at the limb bud end during development. A brief summary of further growth factors that have been implicated in tendon development and repair can be found in table 1.1.

Table 1.1. Growth factors associated with tendon development and repair. Several factors have been shown to have some effect on the tendon development cycle, acting during different stages to create a final tissue. Tendon development is however poorly defined and as yet, not fully understood.

Growth Factor	Role/Function
TGF-β	Promotes angiogenesis and collagen production(31)
EGF	Induces mitosis in fibroblasts and promotes collagenase activity to remodel the extracellular matrix(31)
PDGF-β	Induces mitosis fibroblasts, chemo attractant to macrophages, and assists angiogenesis(31)
Basic FGF (FGF 2)	Promotes angiogenesis and granulation(31)
VEGF	Vasculogenesis and angiogenesis(31)
Hepatocyte growth factor (HGF)	Expressed in wound fibroblasts to regulate growth, motility, and morphogenesis(31)
Early growth response factor-1 (EGR-1)	Transcription factor that upregulates collagen and accelerates wound closure(31)
FGF 4, 6, 8	Present in early limb bud development and induces stem cell tenogenisis.(64)
BMP-12, 13, 14	Promotes tendon-derived stem cell differentiation into tenocytes(65)

1.3. Cells in Tendon Tissue Engineering.

Many different cell types can be used to produce tendon tissue. These include cells from a donor tendon (primary cells), cells from a different body tissue that can be made into tendon cells (adult stem cells) and cells produced from embryos in the laboratory (embryonic stem cells).

1.3.1. Tenocytes.

Tenocytes are the major cell type present in tendons, making up around 95% of the cellular mass. They are a highly specialised form of fibroblast that is responsible for maintaining the unique tissue capable of sustaining the high loads to which tendons are subjected (25). Their major role is the maintenance of the complex extracellular matrix composed of collagen I (the major component of tendon), collagens III and V, glycosaminoglycans (GAGs), elastin and fibronectin (26), and the reconstruction of tendon tissue either after injury or as part of normal physiological activity.

Under normal physiological conditions, tenocytes are found in small numbers spread between the collagen fibrils. Because of the low cell number and the poor vascularisation (66) of healthy tendon, tenocytes have been shown to have a very low proliferative rate (67), perhaps explaining why tendons take so long to recover after injury. This low proliferative rate becomes problematic when considering cells for use in tissue engineering, as large volumes of tissue will have to be produced from a relatively small sample.

Identifying tenocytes can sometimes be difficult. Visually, tenocytes appear fibroblastic, but with long cytoplasmic processes (25) that form between the cells which aid in cellular communication. Cell surface markers can be used to determine if a cell is 'tenocyte like'. Markers such as CD44 and CD90 have been found to be expressed by tenocytes from both rat and human origin, however Scutt et al (68) found the expression of CD90 to be much higher in rat tenocytes than those from a human. Other markers such as decorin, collagen α1 (26), COL1a2 and scleraxis (69) have also been found to be more specific markers of tenocytes, especially under conditions of tension or stress such as those found in the leg tendons of race horses.

Fibroblast cell culture is well defined, with many different groups using similar methods and gaining good results. As tenocytes are a form of fibroblast, a starting point has already been established. Typically, Dulbeccos Modified Eagles Media (DMEM) is used as a base, with 10% Foetal Bovine Serum (FBS) added to enhance cellular growth. Additional supplements such as L-Glutamine (L-Glut) and Non-Essential Amino Acids (NEAA) can also be added along with anti-bacterial substances such as penicillin/streptomycin to reduce the chance of infection. These antibacterials are more important when using primary tissues. A breakdown of the culture conditions used by different groups culturing tenocytes can be found in table 1.2. In addition to media conditions, the gaseous environment can also be investigated. Cell culture is typically performed in physiologically hyperoxic conditions at 20% O_2 (70), but *in vivo* these conditions rarely exist. Normoxic concentrations *in vivo* are around 3% O_2, (71) however as tendon is so poorly supplied with blood the levels of O_2 a tenocyte would be exposed to would be slightly lower. Multiple types of fibroblasts can be cultured for longer in hypoxic (1.5%- 2% O_2) conditions before the onset of senescence (72). Different seeding densities were

investigated where Schulze-Tanzil et al reported that tenocytes can be successfully cultured in high densities in pellet culture. qRT-PCR revealed gene markers for collagen I and scleraxis were being expressed in significant amounts throughout the culture period, indicating that favourable conditions for tenocyte differentiation were being achieved (25). This study shows how tenocytes can be cultured in different environments and still produce extracellular matrix that is required for generating tendon tissue.

Tenocyte Isolation and Culture Methods.

Many methods have been used to successfully isolate and culture tenocytes from primary tendon tissue. Many of the differences in method come about because of slight changes in the tendons that the specific groups were working with. Even with these differences, many of the steps taken are similar (table 1.2).

Enzymatic Digestion.

Human tenocytes have been isolated in many different ways. Scutt et al (68) isolated both rat and human cells by digestion in 1mg/mL collagenase in DMEM at 37^{o}C for 18 hours on a rotary blood mixer. After this, the samples were sieved through a 70 μm sieve and viability determined before being cultured in media consisting of DMEM with FCS, ascorbate-2-phosphate, ultra glutamine and dexamethasone for at least 2 passages. Anitua et al (73) used a similar method to isolate cells from human skin, synovium and tendon. The samples were removed and placed in sterile PBS with pen/strep and 0.3% collagenase at 37^{o}C and stirred for 90 minutes. The suspension was then centrifuged, re-suspended and cultured in a mixture of DMEM and F12 media (1:1) with 15% human serum, glutamine

and penicillin/streptomycin. A study comparing the effects of isolation method has recently been published, finding that enzymatic digestion by 0.2 % collagenase for 18 hours resulted in 14x more cells being collected from the same volume of human tendon as after 50 days continuous isolation via adhesion culture, without any substantial loss of cellular properties (74). This demonstrates that for any potential clinical use, enzymatic digestion of tissues should be the preferred method of cell isolation.

Animal tenocytes have also been isolated and cultured using enzymatic methods. Collagenase is the most common enzyme used for removing tenocytes from canine (75), bovine (76), murine (77) and rabbit (78) tendons, with alternative enzymes such as trypsin (26) and pronase (76) being used in conjunction with the collagenase for some or part of the digestion process. A breakdown of the isolation methods used for these groups can be found in table 1.2. Enzymatic digestion methods can result in tissues being placed in enzyme solutions for prolonged periods of time, potentially leading to damage to the cells if the enzyme concentration is slightly too high (79). Other methods are therefore also being used to isolate tenocytes from tendon samples.

De Moss et al (80) used an explant method to isolate human tenocytes from tendon with the paratenon layer removed from the samples. The remaining tissue was then cut into $3mm^3$ pieces and placed into a 6 well plate with DMEM, 10% foetal calf serum (FCS), 50 μg/ml gentamicin and 1.5 μg/ml fungizone. After 10 days the fibroblasts in the tendons had migrated onto the tissue culture plastic. Shultz-tanzil et al (25) found a similar effect using human finger tendons. The tendon was placed in media (Ham's F-12/Dulbecco's modified Eagle's medium (50/50) containing 10% foetal calf serum, 25 mg/ml ascorbic acid, 50 IU/ml streptomycin, 50 IU/ml penicillin, 2.5 mg/ml amphotericin B, 1% glutamine and 1% essential amino acids) for 1-2 weeks, during which time cells migrated from

tendon to the culture plastic. Weirich et al 2007 (81) explanted tenocytes from the long biceps tendon from bovine shoulder joints. The surrounding fasciae were removed with the remaining cells detached by digestion with trypsin-EDTA. The remaining tendon tissue was then diced with scissors and rinsed in 70% ethanol, before being placed into Petri dishes containing DMEM/Hams F12 media. Explant methods provide a way of isolating cells from tissues without the need for sometimes damaging enzymatic digestion, however due to the longer times needed for explant methods to gain a large number of cells digestion methods remain popular.

Table 1.2. Methods used to isolate and culture tendon cells. Tendon cells are isolated using two major methods; enzymatic digestion or tissue explant. Variations of enzymes used, times, size of initial sample and media used to culture cells were found according to research group and species of tendon cells being isolated.

	Pronase	**Collagenase**	**Trypsin**	**Minced**	**Media**
Bernard-Beaubois et al 1996.	n/a	1.1mg/mL, 30 mins 37^{o}C, 30 mins room temp + stirring - 25mg/ml (18 hrs)	0.25% trypsin (60 min + collagenase)	Small pieces	Hams F12
Ehlers et al 1998.	60% pronase (1hr)	40mL 0.15% collagenase II in media for 12 hours, 37^{o}C	n/a	4g	McCoys 5A
Archambault et al 2001.	n/a	0.5% (5 min)	0.25% (15 min)	n/a	DMEM, 20mM HEPES (pH 7.2), 100U/mL penicillin, 100µg/mL streptomycin sulphate, 10% FBS.
Ritty et al 2003	n/a	type 1a (4000U/ml) (180 minutes) + mechanical disruption	n/a	3 – 5 mm	DMEM, 2mM PMSF, 1mg/mL BSA
Salingcarnboriboon 2003	n/a	α-MEM containing collagenase at 37°C for 20 min	n/a	n/a	α-MEM, 0.5% FBS.
Shultz-tanzil. 2004	n/a	n/a	n/a	n/a	DMEM/F12 10% FCS, 25mg/mL ascorbic acid, pen/strep, 2.5 mg/ml amphotericin B, 1% glut, 1% essential aa.
De Moss et al. 2007	n/a	n/a	n/a	3mm^2	DMEM, 10% foetal calf serum (FCS), 50 µg/ml gentamicin and 1.5 µg/ml fungizone. 10 days
Weirich et al 2007	n/a	n/a	trypsin-EDTA	n/a	DMEM/Hams F12 pen/strep
Scutt et al 2008	n/a	1mg/ml (18hrs) on blood mixer	n/a	n/a	DMEM, 10% FCS, pen/strep, L-Glut
Anitua et al 2008.	n/a	0.3%% (90 min)	n/a	n/a	DMEM/F12
Mallick et al 2009	n/a	1mg/ml (18hrs)	n/a	n/a	DMEM, 10%FCS, pen/strep

1.3.2. Tendon Derived Stem Cells.

Tendon derived stem cells (TDSCs) are a population of cells resident in tendon that have the capacity to differentiate into bone, cartilage and adipocytes (27) (82). In addition to this differential potential, tendon stem cells (TSCs) have also been found to express the stem cells markers Oct 4 and SSEA-4 (83). These characteristics are not observed with mature tenocytes. TDSCs are isolated from tendon tissue by mincing and enzymatically digesting samples, then resuspending cells in single cell solutions and culturing in 96 well plates, one cell/well. Once colonies have been formed, the further addition of trypsin leads to TDSC detaching before mature tenocytes, allowing for collection and further culture. The concentration of TDSCs has been found to vary with age and position and species, with tendons from younger specimens being generally found to contain higher concentrations (84).

TDSC have different morphologies to mature tenocytes. TDSCs have a “cobblestone” like appearance when cultured to confluency, with an enlarged nucleus. Tenocytes have an elongated “spindle” like morphology when confluent, with little contact seen between cells (Fig. 1.3). TDSCs have also been found to have significantly longer population doubling times when compared to tenocytes isolated from the same tendon source (83).

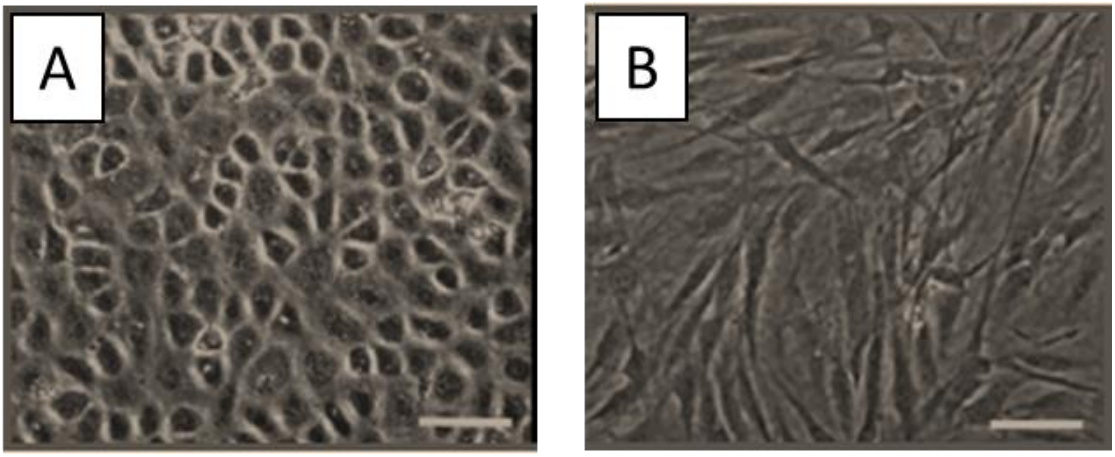

Figure 1.3. Visual comparison of tendon stem cells. Tendon derived stem cells (A) after over 60 days culture appear square and dense in culture. Tenocytes appear elongated when confluent (B). Figure adapted from Zhang et al 2010, figure 5 (83)**.**

Hypoxic (2%) oxygen conditions have been found to have a positive effects on the proliferative capability of several human stem cell types (70) (85). TDSCs have also been found to proliferate faster in 2% O_2 compared to 20% O_2, however differentiation capacity was seen to be reduced (86). This study suggests that hypoxic conditions are suitable for expanding TDSCs for specific use in tendon tissue engineered products/treatments.

1.3.3. Mesenchymal Stem Cells for Tendon Tissue Engineering.

Mesenchymal Stem cells (MSCs) are a multipotent pool of cells that are present in many tissues, with major concentrations found in bone marrow (87) (88) (89) and adipose tissue (90). A well-established approach to isolate MSCs from a bone marrow sample is to place them in complete media on tissue culture plastic (Fig. 1.4.) (87). After a few days MSCs adhere to the plastic surface, leaving the haematopoietic stem cells in suspension. The adhered cells then start to form fibroblast like colonies which undergo expansion (91). By

splitting the cultures before confluence, a more homogeneous cell population that in some instances can proliferate for up to 40 cell divisions, is created (92).

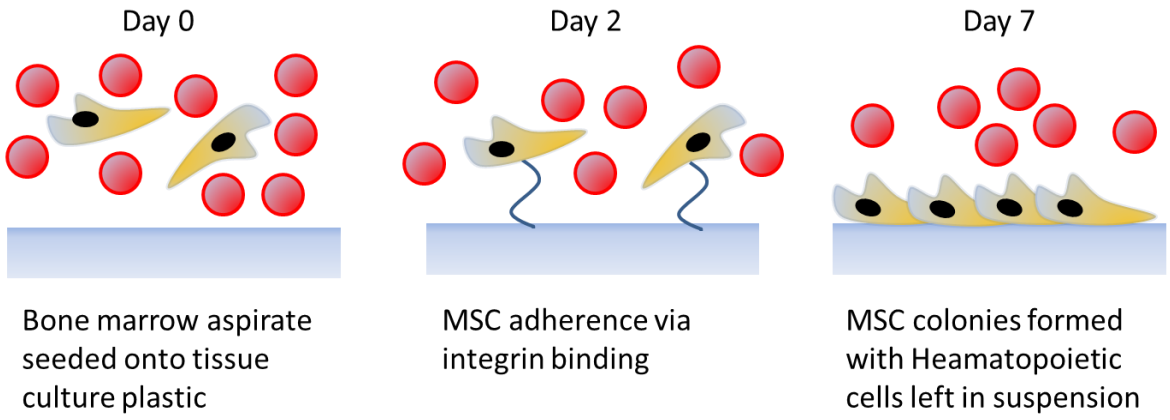

Figure 1.4. Colony forming unit assay: MSC adherence to tissue culture plastic over time. Complete bone marrow aspirate is allowed to settle in tissue culture plastic vessels for a period of time. Mesenchymal stem cells adhere to the surface via integrin binding after around 2 days, forming distinct colonies by 7 days. Media/remaining suspended cells can then be removed, leaving adhered MSCs for further proliferation.

Mesenchymal Stem Cells can be difficult to accurately characterise. Many different surface antigen markers can however be used to characterise a cell as "mesenchymal like", although as yet no single definitive hMSC specific marker exists. Cluster of differentiation / cluster of designation (CD) markers are cell specific surface markers that can be used to form panels to identify specific cell lineages, with both positive and negative markers being used. Several papers have investigated the different markers of human MSCs. Dominici et al identified the key makers of MSCs to be CD105, CD73 and CD90 positive, and lack expression of lineage specific markers such as CD45, CD34, CD14 or CD11b, CD79alpha (CD19) and HLA-DR. hMSCs must also be able to adhere to tissue culture plastic (93). This paper was written as a result of a 2006 meeting of the Mesenchymal and Tissue Stem Cell Committee of the International Society for Cellular Therapy group, and is

still considered as the reference point for defining hMSCs for human theraputical use (94). A further generic stem cell marker has also been used to identify MSCs. CD90 is expressed by human MSCs, haematopoietic stem cells and neural stem cells and has been found to play a role in fibroblastic cell differentiation (95). Further studies have identified similar marker profiles , with Kolf et al summarising that cells derived from bone marrow which show positive test results for Stro-1, CD44 (H-CAM) and CD73 along with negative results for CD31, CD34 and CD45 can be considered to be human MSCs (96). A secondary conclusion from this review is that different species can show different surface antigen markers. Murine MSCs were not consistently negative for CD34, with different groups reporting different outcomes, and mice cells do not express an equivalent to Stro-1, so this cannot be used.

Table 1.3. Common cellular expression markers used to characterise human MSC populations. Cells positive for CD29, CD44, CD73 and CD105 and negative for CD31, CD34 and CD45 are generally considered to be MSC or 'MSC like' in phenotype.

Marker	+ve/-ve	Associated Lineage/role	Reference
CD29	+	Involved in MSC migration in vivo	Kolf et al 2007 (96) (97)
CD44 (H-CAM)	+	stem cell (cancer) homing receptor	Krampera et al 2006 (92)
CD73	+	MSC migration in vivo	Chamberlain et el 2007 (98)(97)
CD105	+	Mediator of cell-cell and cell-matrix interaction	Molchanova et al 2008 (44)
Stro-l	+	Necessary for colony forming ability	Roufosse et al 2004 (89)
CD90	+	Generic human stem cell marker	Kisselbach et al 2009 (95)
CD31	-	Endothelial	Modder et al 2012 (99)
CD34	-	Haematopoietic	Kolf et al 2007 (96)
CD45	-	Haematopoietic	Chamberlain et al 2007 (98)

The potential for MSCs to produce many different types of differentiated tissue is well documented (87). MSCs have been used *in vitro* with varying success to produce muscle (100), fat (101), cartilage (102), bone (103) and cardiac muscle (104). However, this review will focus on what is known in regards to MSC differentiation into tendon/ligament cells.

Mesenchymal stem cells provide a source of cells that can potentially differentiate into tenocytes under the correct culture conditions (100). Several groups report that by adding

BMP-12 to media, MSCs start to exhibit tenocyte like qualities. Horse MSCs were found to differentiate when exposed to 50ng/mL BMP-12 in the media, with tenomodulin and decorin (common tenocyte surface antigen markers) both being expressed by the cells post exposure (65). Similarly, rhesus monkey MSCs transfected with BMP-12 resulted in upregulation of collagen I and scleraxis (two other widely used surface antigen markers for tenocytes) when compared to a non-transfected control group. This study also showed significant increases in CD44 expression (commonly used tenocyte marker), adding to the claims made that tenocytes had been produced (53). BMP-2 is also reported as playing a role in MSC – tenocyte differentiation. Hoffmann et al (105) reported that murine MSC transfection with Smad8 resulted in the emergence of cells with a tenocyte phenotype which showed increased levels of collagen I and scleraxis expression after 7 days post transfection. When co-culturing MSCs with tenocytes in a non-contact culture vessel, MSCs were exposed to the growth factors excreted by the mature cells. After 14 days MSCs started to differentiate, with significant increased expression of scleraxis and collagen I being found when compared to a control group of singularly cultured MSCs (106). BMP12 and 13 are reported to induce increased production of thromobospondin 4 (a tendon marker) along with a characteristic wave like pattern (created by the crimp angles found between collagen fibrils) found in tendon histological samples after 14 days implantation into a rat hamstring muscle defect model (54).

FGF4 was reported to activate the expression of EGR-1 and EGR-2 in cells isolated from chick embryos. Embryos were isolated at different gestation points, and cultured in the presence of FGF4 for 24 or 48 hours. Embryos were then harvested, dissected, and immunologically examined for collagen I, III and V expression. Increased expression was noted in comparison to controls. EGR-1 and EGR-2 expression was also significantly

increased along with expression of collagens I and III at 14.5 days post fertilisation compared to 12.5 days(45).

Transforming growth factor β3 (TGFβ3) has also demonstrated an important role in ESC/MSC – tenocyte differentiation. When human MSCs were suspended in a 3D fibrin constructs and anchored to two fixed points, cells harvested after 5 days culture with TGFβ3 (0.02μg/mL) were incapable of differentiation into osteo, adipo or chondro lineages, even after a further 21 days static culture and showed marked increases in tendon like characteristics (fibril formation, collagen I expression) indicating that cells had permanently differentiated towards the tendon lineage (107).

Many studies have focused on using MSCs to promote new growth or regeneration in damaged tendon tissue *in vivo*. MSCs isolated from a horse's bone marrow and cultured *in vitro* were injected into tendons that had been subjected to injury. After 8 weeks the tendons were examined against a control group which received no MSCs. While no significant differences were apparent, qualitative trends appeared to show that the tendons which had received MSCs were in better condition than the control group, with higher histological scores and improved mechanical properties (108). In a study mentioned earlier, Hoffmann et al (105) implanted either MSCs transfected with Smad8 or non-transfected MScs into surgically damaged rat Achilles tendons. Substantial remodelling of the wound site occurred with the transfected cells, while control group tendons were comprised of non-specific connective tissue. This study demonstrates that MSCs engineered to overexpress Smad8 could provide a more suitable cell source for tendon repair.

A potential problem when developing a tissue engineered tendon is how best to anchor the new tendon to bone. Ju et al (109) found that by adding MSCs to a rat model of a damaged bone tunnel (the junction between bone and tendon) signs of accelerated remodelling of the wound site were noted after 2 weeks when compared to a cell-free control. However, after 4 weeks complete remodelling of the site had occurred in both groups. This demonstrates that external MSCs do have some effect on the healing time, but not necessarily on healing effectiveness.

A further advantage of using MSCs to promote new tissue growth is that they are immunosuppressive. When immune cells were co-cultured with human MSCs, changes in the secreted molecules of the immune cells occurred, allowing the MSCs to remain in culture and not be attacked (110). *In vivo* studies using MSC seeded rat myocardial infarction models found similar conclusions, with immunohistochemistry showing that MSC seeded constructs could modulate immune response, although the mechanism by which this process occurs is still being investigated (111). This could potentially allow MSCs to be used in allogeneic implants, thereby creating a desirable product to industry as a bank of cells could be used for all implants, thus dramatically reducing the costs involved in manufacture.

MSCs have also been shown to be able to produce tissues that would not normally be considered to be mesenchyme in nature. These include neurons (112) (ectodermic) and hepatocytes (113) (endodermic). The wide range of these studies demonstrates the plasticity of the cells and how slightly different culture conditions can alter the tissue capable of being produced.

MSC therapies in equine tendon therapy.

Extensive experience has been gained in the treatment of horse tendon injuries with mesenchymal stem cells. Early studies in this area used full bone marrow extracted from the sternum of the animal and injecting directly into the damaged tendon area (114). This work demonstrated limited success thought to be due to the low concentration of stem cells actually being delivered, but led to the development of therapies where MSCs were isolated from the bone marrow before use, increasing the concentration of 'active' cells being introduced to the wound area, with results showing improvements over traditional treatment methods (115). This therapy has since been commercialised by several companies (Vet Cell, Vet-Stem) and as of 2010, over 1500 horses had been successfully treated with MSC injections into damaged tendons (116), however translation into human therapies has yet to occur.

1.3.4. Embryonic Stem Cells.

Embryonic Stem cells (ESCs) are pluripotent cells isolated from the inner cell mass of a blastocyst (Fig. 1.5) (117) (118). Human ESCs were first isolated by Thomson et al in 1998 (119) using donated excess embryos from an *in vitro* fertilization (IVF) clinic. ESCs are unique in that they are characterised by the ability to differentiate into all three germ layers, endodermal, ectodermal and mesodermal (however ESCs are not considered as totipotent as they cannot differentiate into placental tissue) without showing signs of senescence over a prolonged period due to the high expression of telomerase (120).

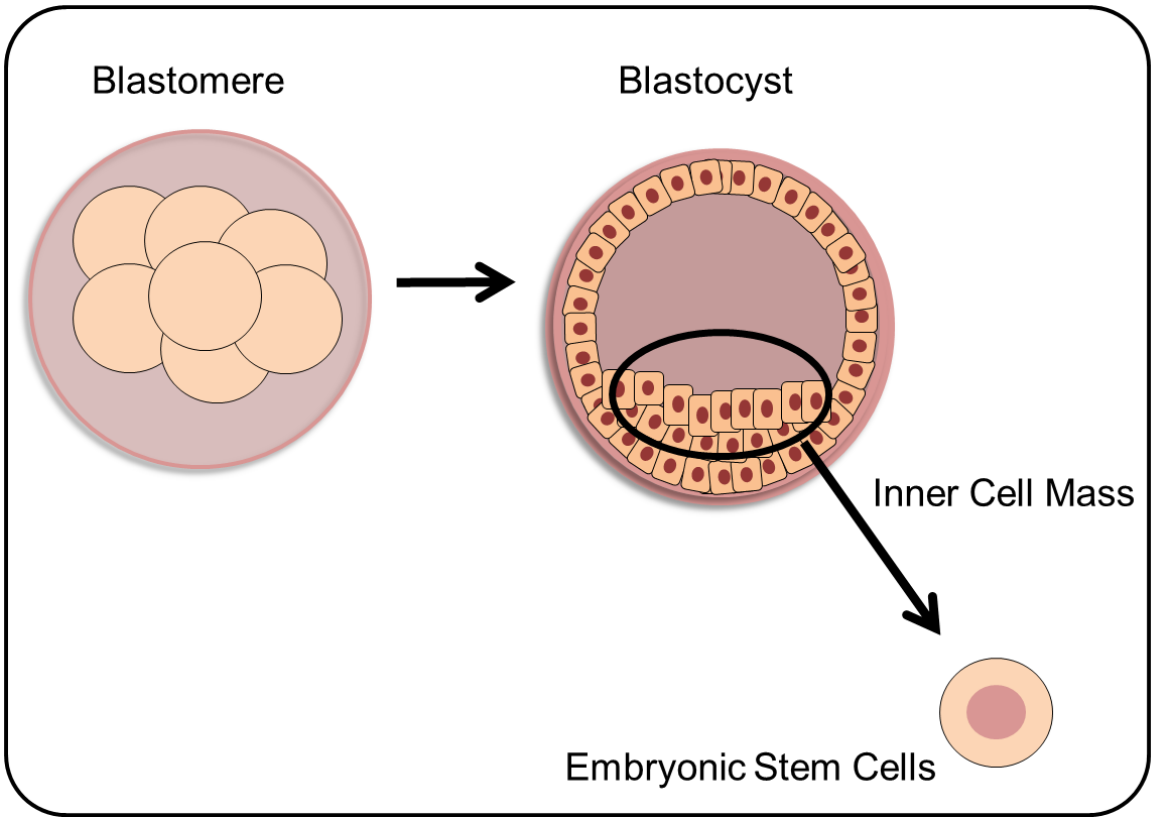

Figure 1.5. Embryonic stem cell isolation. When donor embryos reach the blastocyst stage of development the inner cell mass is isolated using a micro-needle, removed and seeded onto a feeder layer of embryonic fibroblasts. Cell lines can then be established using local protocols.

Human ESC culture.

Human ESC culture has been developed from the procedures originally used for murine ESC culture. Broadly speaking there are two main methods, co culture and feeder free. Co-culture methods use a feeder layer of mouse embryonic fibroblasts (MEFs). ESCs were found to form distinct colonies on the feeder layers, which when isolated, formed teratomas when implanted subcutaneously into an immune-deficient mouse, suggesting pluripotency (119). In feeder free culture, cells are cultured in media pre conditioned by MEFs, with serum replacement substitute and basic fibroblast growth factor (bFGF) (121).

Briefly, MEFs are isolated from mouse 11.5-12.5 day old embryos and cultured to confluency, before sub-passaging. Once around 60% confluent, media is changed to "knock out" media containing serum replacement and BFGF and allowed to culture for 24 hours. This media is then collected and replaced, until MEFs are overly confluent (122).

Embryonic Stem Cells for Tendon Tissue Engineering.

Investigations into the applications of ESC for use in tendon tissue engineering are few in number. Many concentrate on differentiating cells before seeding into scaffold material as a way to induce an ESC population to start to act as tenocytes. Chen et al (123) found that by differentiating human ESCs into MSCs by exposure to foetal bovine serum and FGF 2 they were able to create a tendon like structure when seeded into scaffolds consisting of silk and collagen. Follow-on studies by the same group also found that by mechanically stimulating this structure the effect on the cells was to further take on the characteristics of natural tendon. This study also utilised another two small animal models. The scaffolds described above were ectopically implanted in a nude mouse, sutured between vertebrae allowing for natural cyclical tension to be applied when the animal moved. A second model used Green Fluorescent Protein transfected ESC-MSC to seed the scaffold before implantation into a 6mm defect in the Achilles tendon of a rat, to ensure that the implanted cells were remaining *in situ* for the duration of the experiment. Increases in collagen alignment, expression of common tendon associated cellular markers (Collagen I & III, Epha4 and Scleraxis) and mechanical properties (failure force and stiffness) were observed in cell seeded scaffolds when compared to scaffold only controls, demonstrating that the cells were having a beneficial effect on tendon regeneration (124).

The healing capacity of embryonic sheep tendon when implanted subcutaneously into an adult mouse determined that the adult environment did not affect the healing properties of embryonic tissue. Sections of foetal sheep tendon and adult tendon were isolated and artificially wounded before being implanted into the back of a mouse. Foetal tendon sections demonstrated increased alignment of cells, increased mechanical properties and little inflammation response when compared to adult tendon controls (125). This study demonstrates that embryonic tissues could have a possible advantage over adult derived tissues for tendon regeneration.

Equine embryonic stem cell containing materials have also been investigated as a potential source of cells for tendon repair. By using a commercially available pluripotent cell source and co-culturing with equine embryonic fibroblasts, cells were created that resembled ESCs. These cells were then injected into an induced defect in a race horse tendon and allowed to act for 8 weeks, before animals were sacrificed and further analysis taken. Ultra sound analysis was taken every 2 weeks during the experiment. It was found that cells amplified structural changes in the damaged area, making a more tendon like structure than the scar tissue formed in the acellular group. However, molecular analysis found little difference in the cell types present in the injury site (126). It has also been found that ESCs have a higher survival rate in damaged horse tendons and an increased capacity for migration compared with MSCs, with both cell types initiating no immune response (127).

1.4. Tendon Tissue Engineering Scaffolds.

The scaffold of a tissue engineered product plays a vital role in cellular attachment, proliferation, and signalling as well as providing a mechanical environment that can perform the basic function of the tissue it is replacing before the cellular products begin to produce matrix and remodel independently. Many different materials have been used with varying success for artificial tendon, with both natural and artificial materials being used individually or as part of a hybrid scaffold.

One of the most common materials used in tendon tissue engineering is collagen. Collagen is the major extracellular matrix component produced by tenocytes. Once secreted, collagen is formed into aligned fibrils by the action of a longitudinal force. Groups have tried to artificially induce this realignment in vitro. Building on previous knowledge that fibroblasts cause collagen gels to randomly contract (128), Feng et al (129) seeded tenocytes into type I collagen gels and applied both static and dynamic forces with the aim of trying to align the fibres more precisely, and thus create a more biomimetic tendon structure. Surprisingly, the static gels displayed better mechanical properties after nine days culture time, although no significant differences in the alignment of the collagen fibrils produced by either loading pattern were apparent.

As tendon is composed of around 70% type I collagen (17) many groups see it as a logical ideal starting point, usually combining it with additional materials to add tensional strength. By combining woven silk fibres into a collagen gel Chen et al (130) found that a hybrid material applied to ligament and tendon tissue engineering gave better results than those from silk on its own. This study found that: cells were better aligned, that the

interface between natural tissue and implant was better, that the mechanical loads that can be carried by the implant were much more like natural ligament/tendon and that the internal space in the implant in which the cells grow is preserved when collagen and silk are used, aiding in cellular development. All of these factors indicate that this scaffold could be used to help in tendon regeneration. Chen et al (131) found that by using a hybrid scaffold made of a PLGA polymer mesh containing collagen cells from a canine cruciate ligament, the cells were able to adhere and proliferate, eventually remodelling the collagen and allowing the polymer to be absorbed by the body of the mouse into which the implant had been placed. However in this instance very little mechanical loading of the structure would have been applied to the implant *in vivo*, leading to an uncertainty of if the implant would be suitable for use as a replacement tendon.

Silks have also been used without any other additional materials to culture tenocytes and ultimately replicate tendon tissue. Fang et al (132) found that tenocytes (isolated by enzymatic digestion of rat tail tendon) could be cultured *in vitro* on a braided *A. pernyi* silk scaffold for at least one week. Following this initial test, cell/scaffold constructs were implanted into a surgically damaged rabbit Achilles tendon. It was found that the early signs of tendon regeneration started to occur after 6 weeks, with the damaged tendon being visually almost indistinguishable from the negative control after 16 weeks. It was also found that by 16 weeks, type I collagen was the predominant collagen present, and that around 55% of the tendons tensile strength had been restored. This demonstrates not only that tenocytes can adhere and proliferate on silks *in vitro*, but that that this form of silk could potentially be used to aid in tendon regeneration *in vivo.* Fan et al (133) found that by seeding mesenchymal stem cells into a woven densely rolled scaffold that the cells had differentiated into a fibroblastic like lineage, with the common tendon cellular markers

(collagen I and III) starting to be released after 24 weeks post implantation into the anterior cruciate ligament position of a pig. The mechanical properties of the implant were also tested at this time, with comparable results being found to natural tissue under normal physiological loading conditions. Although the author was looking to create a ligament, the conclusions made in this study could also be applied to tendon, owing to the two tissues being very similar and some of the experimental positive indicators (e.g. maximum tensional stress), being the same as they would be in a tendon investigation.

Polymers are attractive materials to tissue engineers due to the ease with which their chemical and mechanical properties can be altered. Tendon is a particularly complex material to design a biomaterial for due to the high levels of mechanical stress put on it on a regular basis. Despite this, some polymers have been found to be usable for tendon tissue engineering. As stated previously, Chen et al (131) used a PLGA mesh as a strengthening agent in a collagen/polymer hybrid scaffold. The PLGA was found to be still present 8 weeks post implant, but had been totally resorbed after 12 weeks, leaving the restructured collagen to take the mechanical loads.

Commercial synthetic polymer based implants have been used to varying success for tendon and ligament repair. The Leeds-Kieo® implant is a non-absorbable synthetic prosthesis (used to completely replace a damaged ligament or tendon) that has been surgically used for over 20 years. Studies investigating the success of implanting the Leeds-Kieo® device have found that the overall performance of the implants is acceptable, but not to the same standard as the natural tissue or a donor tissue (134). Other problems that have been reported are engraftment tunnel enlarging, laxity in the joint after several years' implantation, immune rejection and complete rupture (135). The Lars® Ligament

replacement device is also a non-absorbable synthetic ligament and tendon prosthesis that is approved for use in many countries. Follow up studies performed on Lars® implantations found failure rate and general satisfaction at 24 months post implantation to be similar to that of autograft controls, however some problems such as stiffness were reported (136). A major advantage over the Leeds-Keio® implant is that as yet, little to no immune rejection has been reported(40).

Commercial biological scaffolds original designed for use in other surgeries are also starting to be used in tendon repair. The Zimmer Patch® is an acellular, cross-linked porcine derived collagen material that has been used for several applications, including rotator cuff repair. Conflicting clinical outcomes have been reported with using this material, with positive patient scores and increased range of movement being found in one study (137), but substantial tearing and inflammation being reported in another (138). This perhaps demonstrates that patch materials such as Zimmer patch® are suitable in some situations, but cannot be considered as being ideal tendon repair scaffolds. Graftjacket® is also used for many different surgical interventions, including Achilles tendon rupture repair. Produced from decellurised human cadaver skin, this product maintains the collagen architecture of the donor tissue while minimising the risk of immune response. Graftjacket® has been used in addition to traditional suturing for Achilles tendon repair, with patients being found to be able to perform a heal raise 6 months post-surgery (139), demonstrating that the scaffold can be used to support traditional therapies even if they are not suitable for use as direct tendon replacements.

A major problem with these currently used tendon/ligament scaffolds is their comparably low mechanical properties to natural tendon. Table 1.4 shows the failure strength of the scaffolds discussed previously along with the tendons they are commonly used to treat. It is apparent that even the scaffold with the highest failure strength is still an order of

magnitude weaker than the lowest strength natural tendon (40). This demonstrates the need for the development of new implant materials and designs and is the focus of many current studies investigating tendon tissue engineering.

Table 1.4. Mechanical properties of tendon and tendon scaffold materials currently available for clinical treatment of tendon and ligament injury. Numbers from Chen et al 2009 (40)**.**

Material	Failure strength (N)
Human Achilles tendon	5089 ± 1199
Human Supraspinatus (rotator cuff)	1978 ± 301
Human Patellar tendon	3855 ± 550
Leeds-Kieo® (ligament)	780 ± 200
Lars® (ligament)	998 ± 148
Graftjacket®	229
Zimmer Patch®	128

1.5. Polyhydroxyalkanoates.

Polyhydroxyalkanoates (PHA) are a family of biopolymers (polymer molecules synthesised by organisms – usually bacteria) consisting of polyesters of many different hydroxycarboxylic acid molecules. They are produced by micro-organisms as an energy storage molecule when they are exposed to unbalanced growth conditions, typically the addition of lauric acid and a limited nitrogen and phosphorous supply during culture (140). Originally seen as a replacement for traditional petrochemical polymers, PHAs have become redundant as everyday materials due to the cost of producing large quantities of polymer being prohibitive (141), despite recent rises in oil cost. However, increasing interest in these new polymers is starting to arise from the medical device sector, where the potential benefits of using PHA mean the cost of materials can be absorbed by the high value added to products during manufacturing. These benefits include not inducing an immune reaction, non-toxicity and complete biodegrability (broken down entirely by the body) (142). It is the recent developments in the potential of PHA materials as scaffolds for implant products that this section will focus on.

Many different implant types have been singled out as potential areas in which PHA could be utilised, ranging from shunts and meshes to bone substitutes and, importantly for this investigation, tendon repair devices (142). By altering the chain molecules used to create these polymers they can be optimised to suit the conditions needed to support the different cells that could be put on it. Properties such as Young's modulus, maximum tensile strain and stress, melting and glass transition temperatures and degradation rates can be optimised easily according to what is required.

1.5.1. PHBHHx.

PHBHHx is the designation of molecules consisting of random co polymers of 3-Hydroxybutyrate and 3-Hydroxyhexanoate (Fig. 1.6) (143). It is one of the few PHA molecules that can currently be produced on a large enough scale to use for both scientific research and medical device construction (140). PHBHHx has a melting temperature of 111.7^{o}C, a glass transition temperature of -0.67^{o}C, a tensile strength of 4.1MPa, an elongation at break of 103.8% and a Young's modulus of 130.4 MPa (144), making it a potential material for many biomaterial applications.

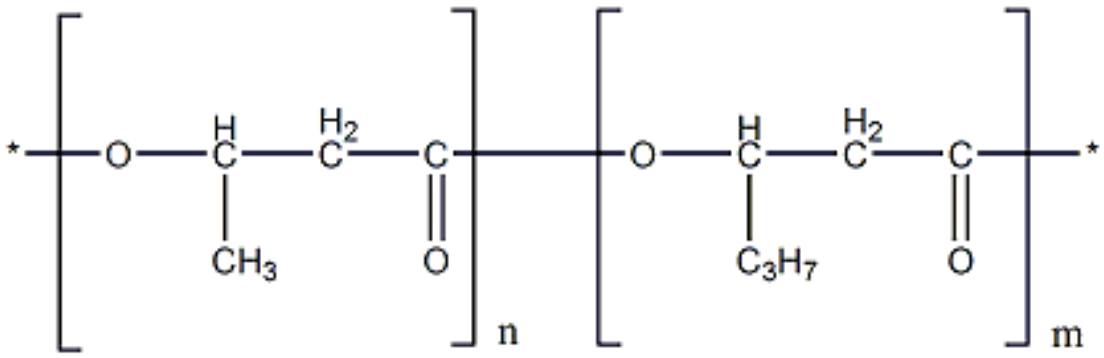

Figure 1.6. Chemical structure of PHBHHx. Monomers of polyhydroxybutyrate p(HB) $C_4H_6O_2$ and polyhydroxyhexanoate p(HHx) $C_6H_{10}O_2$ covalently join to form the complete molecule. Exact compositions of polymer can be altered according to need, with higher %HHx leading to changes in mechanical properties.

Many different cell types have been successfully cultured *in vitro* using PHBHHx scaffolds, including both mature and stem cells. A lot of work has been focussed on using PHBHHx as a scaffold for bone tissue engineering. Wang et al (143) compared rabbit bone marrow cells seeded onto PHBHHx with PLA and PHB, two other widely used materials used for bone scaffolds. They found increases in both cell number and alkaline phosphatase activity, an early indicator of osteoblastic differentiation, demonstrating that

PHBHHx is a suitable material for osteoblast attachment, differentiation and proliferation. Bone marrow stem cells have also been found to proliferate at greater rates on PHBHHx and other similar PHA polymers compared to tissue culture plastic. The conclusions by Hu et al (144) in this study found that other PHA polymers (namely PHBVHHx) are best suited to BMSC culture, but that PHBHHx can still provide the correct environment for this cell type to survive and proliferate. Ji et al (145) made similar conclusions using human keratinocyte cells from the cell line HaCaT. Wang et al (146) found that by altering the surface properties of a PHBHHx scaffold using a lipase treatment they could alter the growth rates of mouse fibroblast cells, concluding the correct hydrophilicity and hydrophobicity are needed for cells to proliferate optimally.

PHBHHx has also been used in successful *in vivo* studies. Ye et al (147) seeded PHBHHx hybrid scaffolds with adipose derived stem cells, differentiating them into chondrocytes. They found that typical indicators of cartilaginous tissue were formed by the cells after 14 days culture, indicating that both adipose derived stem cells and chondrocytes can both be cultured on PHBHHx. The seeded scaffolds were then implanted into a mouse and left *in vivo* for 12 or 24 weeks, with the differentiated 24 week group showing no traces of the polymer and partially formed cartilaginous tissue remaining in its place. Bian et al (148) used porous PHBHHx tubes as conduits to join the damaged ends of nerves in rats. After one month of implantation compound muscle action potentials could be observed within the conduit, indicating that the nerve ends had re-joined and that functional recovery had been achieved. After 3 months *in vivo*, the conduits had been found to have lost between 20 and 24% of their weight, indicating that resorption had started, adding to the claim that PHBHHx can be used as a nerve conduit, or indeed for any biomaterial application that requires resorption of the original material. Wu et al (149) coated decellularised porcine

aortic valves with PHBHHx and implanted the new structure into the pulmonary valve position of a sheep for 16 weeks. Cellular repopulation was found to be higher in valves which had been coated when compared to the uncoated control group, as well as a reduction in the amount of calcification that had occurred. It was also found that by coating the valves, a higher tensile strength could be achieved, creating a stronger implant. PHBHHx has also been investigated for use as a non-adherent film for use during surgery. By dissolving the polymer in non-harmful organic solvents such as dimethyl sulfoxide (DMSO), Dai et al (150) found it could be injected into a wound site to create a non-permeable film upon contact with body fluids. Cells did not adhere to the film surface due to the unfavourable hydrophilic conditions produced using solvents other than chloroform to dissolve the polymer, demonstrating the need to select the correct solvent for the role the polymer scaffold created will be required to perform.

1.5.2. PHBHHx scaffold production.

Films.

Hu et al (144) dissolved 1g of polymer powder in 50 mL organic solvent, in this case chloroform. This was then spread out over a glass container and allowed to dry at room temperature for 24 hours, after which the chloroform had fully evaporated. To ensure no chloroform remained in the structure, vacuum drying was then applied. Sun et al (151) used a similar method, but to ensure purity of the polymer the material was dissolved in dichloromethane and refluxed at 38^{o}C until fully dissolved. This solution was then filtered, then hexane was added to precipitate out the PHBHHx. To form the films, 0.35g polymer

was dissolved in 7mL dichloromethane then poured into a 60mm glass Petri dish to evaporate for 24 hours.

Electro-spun scaffolds.

Cheng et al (152) created an electro-spun PHBHHx scaffold by dissolving polymer at varying concentrations in chloroform/dimethylformamide. This solution was then placed into a syringe pump and a voltage applied between the needle and the target. This was then left until a scaffold was formed that was at the desired thickness (6 hours produced a 70μm thick sheet of material). They found that a polymer concentration of around 5 wt% (5g polymer in 100mL solvent) was needed to produce smooth fibres, and that dimethylformamide was needed as a solvent to prevent the needle from becoming blocked. They also found that by adding more dimethylformamide smaller diameter fibres could be produced.

Porous scaffolds.

Sun et al (151) used a leeching method to produce a porous PHBHHx scaffold. By adding sodium chloride at a ratio of 9:1 with the polymer, then dissolving all of this in dichloromethane a thick paste was formed. This was then poured into a 60mm glass Petri dish and allowed to dry for 24 hours at room temperature, producing a film. The film was then immersed in deionised water, allowing the salt particles to move out of the scaffold, leaving a porous final structure. This process was also replicated by Ye et al (147), with the scaffolds being stored at -70^{o}C and being sterilized with γ-radiation after production.

Tubes.

Bian et al (148) created PHBHHx tubes for use as nerve conduits. To do this they first purified the polymer by dissolving 1g in 10mL 1, 4 dioxane and refluxing at 60^{o}C for 1 hour. Sodium chloride (NaCl) crystals (30-50μm) were then added to the solution homogeneously (achieved by continual stirring). Stainless steel wires (1.5mm diameter) were then dipped into the solution 3 times, rotating to ensure a uniform coating. After this the structures were air dried for 24 hours, allowing the solvent to evaporate. The dry tubes were then dipped in deionised water to remove the NaCl crystals, producing a porous membrane. By altering the size of the NaCl crystals different pore sizes were achieved. Wang et al (153) used a dipping method to create a slightly thicker tube using a different biopolymer to PHBHHx. By dipping and rotating a Teflon coated mandrill in polymer solution for 30 seconds then dipping in water for 5 minutes (repeating the process as necessary) a nerve guide conduit was formed, with a material thickness of over 100μm and a lumen (inner core) diameter of 1mm. This method could be adapted to create a much larger diameter tube than produced here, potentially making one big enough to be used in tendon tissue engineering.

1.6. Mechanical Stimulation Bioreactors in Musculoskeletal Tissue Engineering.

Mechanical stimulation has been shown to be essential in the development of many different tissue types. This is especially true of orthopaedic tissue, where differentiation of progenitor cells, tissue organisation and cellular remodelling have all been linked heavily to mechanical loading.

1.6.1. Bone

Shear stress and compression have been shown to increase greatly the activity of osteoblasts on scaffolds (154). Several different designs and systems have been used successfully, with perfusion flow reactors are most abundant (155). By mechanically pumping media through a chamber containing the cell/scaffold construct conditions similar to those found *in vivo* can be produced, with media flow mimicking the movement of water through the internal bone structure, creating areas of shear where the water comes into contact with the bone architecture, thus encouraging cells to differentiate and behave as though present in a damaged bone.

1.6.2. Cartilage

Bioreactors used for cartilage tissue engineering are very similar to those used for bone. However the principle stress mechanism needed for MSCs to undergo increased chondrogenesis has been shown to be cyclical compression. Oxygen concentrations are also an important variable, with hypoxic (below 2% O_2) conditions shown to further stimulate chondrocyte activity (156). Several studies have demonstrated the superiority of a bioreactor system when compared to a static culture when creating an MSC (or derivative of MSC) cartilage implant (102)

1.6.3. Tendon

Several designs of bioreactor have been utilised for tendon tissue engineering(157). Early designs focussed on using variations of perfusion bioreactors originally designed for bone or cartilage (155), however it has been shown that perfusion alone is not sufficient to recreate the complex environmental stimuli required to create working tendon tissue (158). Direct strain bioreactors work by exposing tissue to a constant, static force in one direction while maintaining the flow of nutrients to the tissue via a sealed chamber (159). Cyclic strain bioreactors (now the most widely used for tendon tissue engineering) create a reciprocal mechanical force over the tissue which can be varied according to the desired loading regime of the investigator (160). Several types of loading patterns have been investigated, from sinusoidal to block waveforms (a period of loading followed by a period of rest (Fig 1.7.)), with positive results being found for most loading regimes when compared to static controls (161). Sinusoidal patterns mimic *in vivo* loading by constantly changing the force being applied to the construct, a situation that has been observed in rabbit Achilles tendons where a force was always found to be applied over the tissue, even in situations where the animal is inactive (162). Block waveforms potentially allow for cells to respond to the mechanical loading more effectively. Cells have been found to react to stimuli over a time period of around 1 second. By applying a force for a period of time longer than this, a greater cellular response can potentially be stimulated (163).

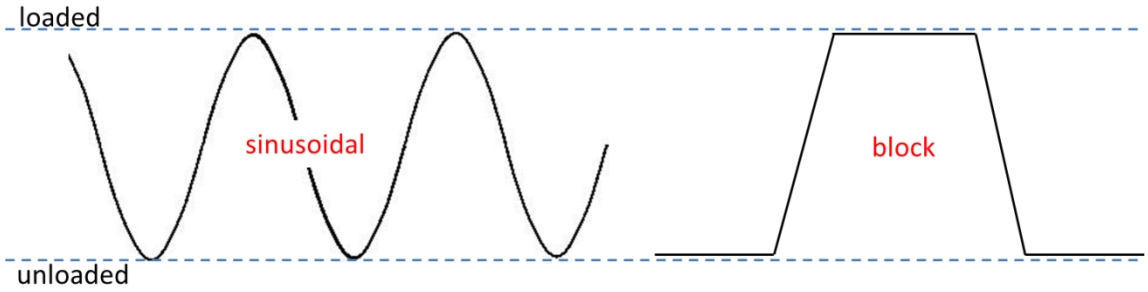

Figure 1.7. Loading wave patterns used in tendon tissue engineering. Sinusoidal wave patterns follow a sine wave, moving in a smooth, unbroken motion from peak to peak. Block patterns have distinct 'on' and 'off' periods, with 'on' representing a sample being loaded and 'off' being a rest period. Typically: y-axis represents displacement, x-axis represents time.

Mechanical loading has been used to influence cell/matrix behaviour in many different ways. It is now thought that in order for stem cells to take on connective tissue morphologies some form of mechanical loading is required (164). Static mechanical force has been used to create neotendonous structures using collagen gels. By applying a strain of 50% using a home-made rack system, greater alignment of collagen fibres has been observed over lower strain conditions (23). This study also found that mechanical properties were significantly improved by applying a strain of over 20%, a peculiar finding considering that this would normally be far beyond the natural maximum strain of a tendon. Comparing static with dynamic mechanical strain has shown collagen content in matrix, mechanical properties and scleraxis (a commonly used expression marker associated with embryonic tendon development) expression all being up regulated in dynamic samples (164).

Further investigation into the effect of cyclic strain on tendon scaffolds has determined that frequencies between 0.017 Hz and 1 Hz with strains between 2% and 10% elongation in a variety of systems (165) (161) (166) result in increased cellular alignment, up regulation of tendon specific cellular markers and improved mechanical properties being observed. It has even been found that very low frequency (0.0034 Hz) low strain (2.4%) mechanical stimulation over a long time period (8 hours/day, 12 days) can result in increased stiffness in MSC seeded collagen scaffolds compared to static controls (167). These studies demonstrate the need for mechanical stimulation when designing materials for tendon tissue engineering and that an ideal loading regime and bioreactor system type is yet to be found.

Human embryonic stem cells have been induced to form tenocytes through a combination of growth factor addition and mechanical force. The addition of BMP-2 and TGF-β, coupled with a cyclic (1Hz) mechanical 10% strain over 14 days resulted in upregulation of collagen 1a, collagen 3a, scleraxis, as well as an increase in fibril density and mechanical properties (123) (124).

1.7. Project aim.

Due to the demand for new advanced materials for tendon repair novel avenues of investigation have to be pursued. Previous work has highlighted PHBHHx as a possible new material to use as a scaffold to encourage tenocytes to remodel collagen, leading eventually to the production of an all-natural 'artificial' tendon, however much optimisation work remains to be completed. This thesis will aim to determine how best to use PHBHHx scaffolds for tendon tissue engineering, with cell type, mechanical loading, media supplements, scaffold design, *in vivo* scaffold breakdown and immune response investigated.

Chapter 2:

Materials and Methods.

2.1. General Abbreviations/Consumables.

The following materials were used in all experimental processes, unless otherwise stated.

DMEM	Dulbeccos Modified Eagles Medium (4.5g/L glucose) (12-604F, Lonza, UK)
FBS	Foetal Bovine Serum (14-501F, Lonza, UK)
NEAA	Non-Essential Amino Acids (13-114E, Lonza, UK),
L-Glut	L-glutamine (17-605E, Lonza, UK)
PSA	Penicillin, Steptomycin and Amphotericin B (15240112, Invitrogen, UK)
Trypsin	Trypsin/EDTA solution (CC-5012, Lonza, UK)
KO DMEM	Knockout DMEM (03382, Gibco, UK)
SR	Serum Replacement (10828-028, Gibco, UK)
DMSO	Dimethyl Sulphoxide (R00550, Invitrogen, UK)
PBS	Phosphate Buffered Saline (17-516F, Lonza, UK)
T-25	Corning 25cm^2 tissue culture flask 430639 (430421, SLS, UK)
T-75	Corning 75cm^2 tissue culture flask 4306 (413290 SLS, UK)
T-175	Corning 175cm^2 tissue culture flask 430825 (354639 SLS, UK)
Well Plates	6: Costar 3516, 12: Costar 3512, 24: Costar 3524, 48: Costar 3548, 96: Costar 96. (all SLS, UK)

Centrifuge tube	15ml SLS8002, 50ml SLS8110 (both SLS, UK)
IMS	Industrial Methylated Spirit (64-17-5 Genta Medical, UK)
PFA	Paraformaldehyde (P6148 Sigma Aldrich, UK)
BSC	Biological Safety Cabinet class II (W05318 Envair, UK)

2.2. Cell Culture.

2. 2. 1. General techniques.

a. Media Change.

Media changes were performed as necessary according to cell type and experimental need. Generally, MSCs and tenocytes had a media change twice weekly, ESCs daily, unless specifically stated. Media was removed from cells by aspiration in a class II Biological Safety Cabinet, tilting the flask/vessel to ensure maximum amount of spent media was removed. New media was pre warmed in a water bath (2828 Thermo Scientific, UK) set to 37^{o}C before being pipetted onto the cells in appropriate measures. Cells were then placed back into the incubator at 37^{o}C.

b. Cell Passage.

Cells were passaged by first aspirating off any media and washing with 5 mL PBS. The PBS was again aspirated off, and replaced with 37^{o}C 1% trypsin/ PBS solution (1mL for T-25, 4mL for T-75) and incubated at room temperature for 5 minutes. If cells remained attached after this time, agitation was used until detachment had taken place. The trypsin activity was then inactivated by adding an equal amount of complete media (DMEM, 10% FBS, 1% NEAA, 1% L-Glut) and mixed with a pipette, with the FBS acting to oversaturate the trypsin molecules. The cell solution was then centrifuged (IECCL30Thermo Scientific, UK) at 200g for 3 minutes, after which the supernatant was aspirated off. The pellet was then resuspended in a known amount of media, allowing for a fractional split to be made (e.g. Resuspend in 1mL media; add 500µL to each new flask if splitting 1:2). The cells were then plated into the appropriate flask with correct amounts of media.

c. Cryopreservation of cells.

Cells were cryopreserved by detaching with 37^{o}C 1% trypsin/PBS solution for 5 minutes, centrifuging (3 minutes, 200g), then re suspended in 1mL solution of 90% FBS: 10% DMSO at room temperature. This was then transferred to a 1.5mL cryovial, placed into a Nalgene 'Mr Frosty' (C1562 Sigma Aldrich, UK) container at room temperature, and put into a -80^{o}C freezer (MDF-U54V Sanyo) for 24 hours. After 24 hours, the cryovials were transferred to liquid nitrogen for long term storage.

d. Thawing of cells.

Cryovials of cells were removed from liquid nitrogen storage and quickly transferred to the cell culture lab. They were then placed in a water bath set at 37^{o}C and gently agitated until defrosted (around one minute). Once defrosted cells were transferred to a flask containing the appropriate media and allowed to adhere to the surface for 24 hours. One adhered; a media change was performed removing any non-viable (unadhered) cells.

e. Cell Counting.

Cells were suspended in a known amount of media. 10µL cell solution was then pipetted into each side of a haemocytometer. Cells were counted at 100x magnification (10x objective, 10x eye piece), using the lines of the haemocytometer to focus and define the area in which cells were counted. For each cell suspension the corner 4x4 square fields (Fig. 2.1 highlighted by red boxes) were counted and the values summed and averaged. Counting was done in a left to right, up to down pattern. If a large number of cells were present, a counter was used. If too many or too few cells (above 100, below 20) cells were

present, the solution was adjusted by either dilution or centrifugation and re suspension in a smaller volume. Once a value was obtained, the figure was multiplied by 1 $x10^4$ to gain a cell concentration in cells/mL of the cell solution.

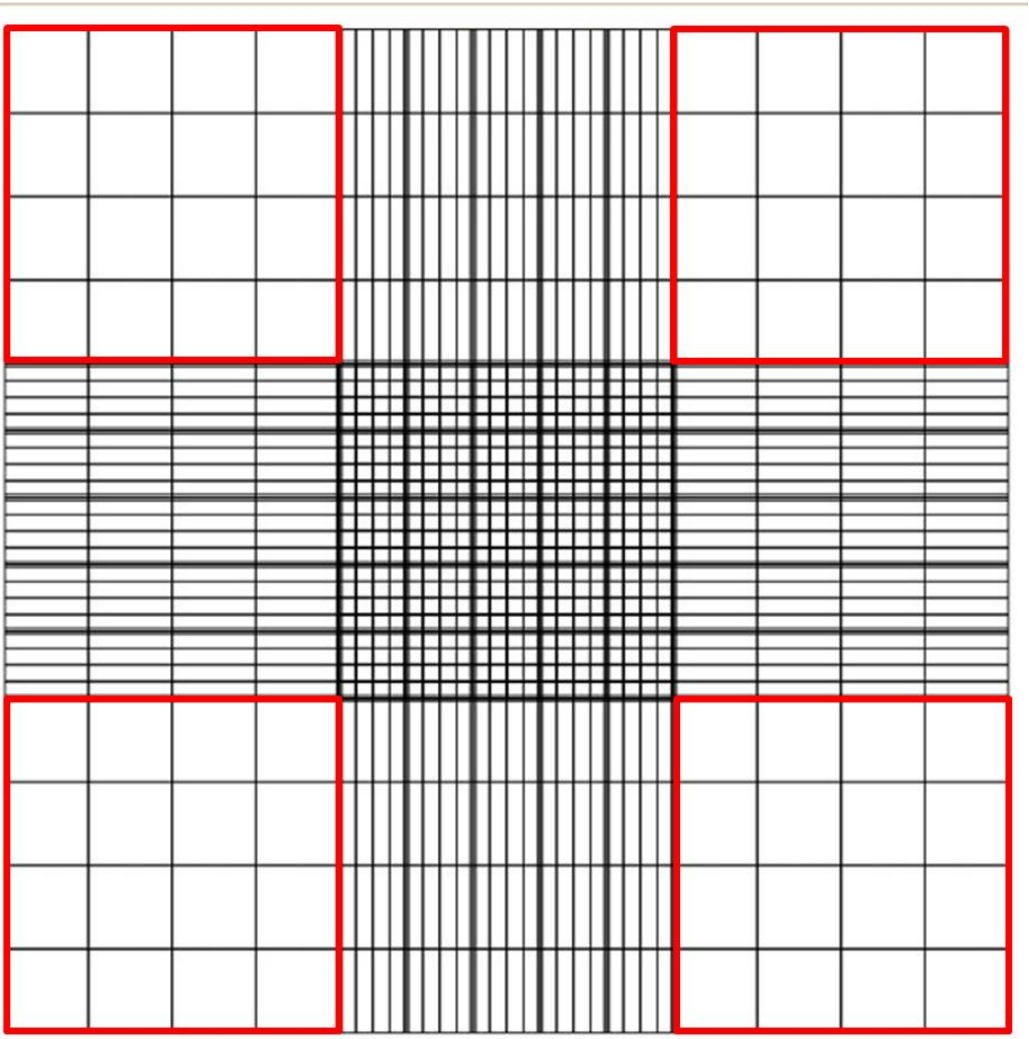

Figure 2.1

Haemocytometer diagram. For all cell counts, cells present in the red boxed areas were counted, summed, then the total number of cells present in all boxes averaged. This number was then multiplied by $1x10^4$ to gain a concentration of cells /mL of solution.

f. Cell Viability.

Cell viability was determined using a trypan blue dye exclusion assay. A cell solution was obtained by trypsin dissociation. The solution was mixed using a pipette to create a more homogenous dispersion of cells, before a 10µL sample was removed and mixed with 10µL of trypan blue solution on a glass slide. 10µL of the mixed solution was then pipetted onto a pre-prepared haemocytometer with a glass cover slip used to seal the chamber. Cells were counted using the method as section 2.2.1.e. with both viable and non-viable cells counted separately and an overall average and percentage viable gained. Live cells appear clear in the centre with a blue outer membrane. Dead cells appear totally blue (Figure 2.2) If cells were suspended in collagen gel, the sample was immersed in 1mL 0.4 % type VI collagenase (Invitrogen)/PBS solution for 2 hours at 37^{o}C, centrifuged at 200g for 3 minutes and the pellet resuspended in media to count cells.

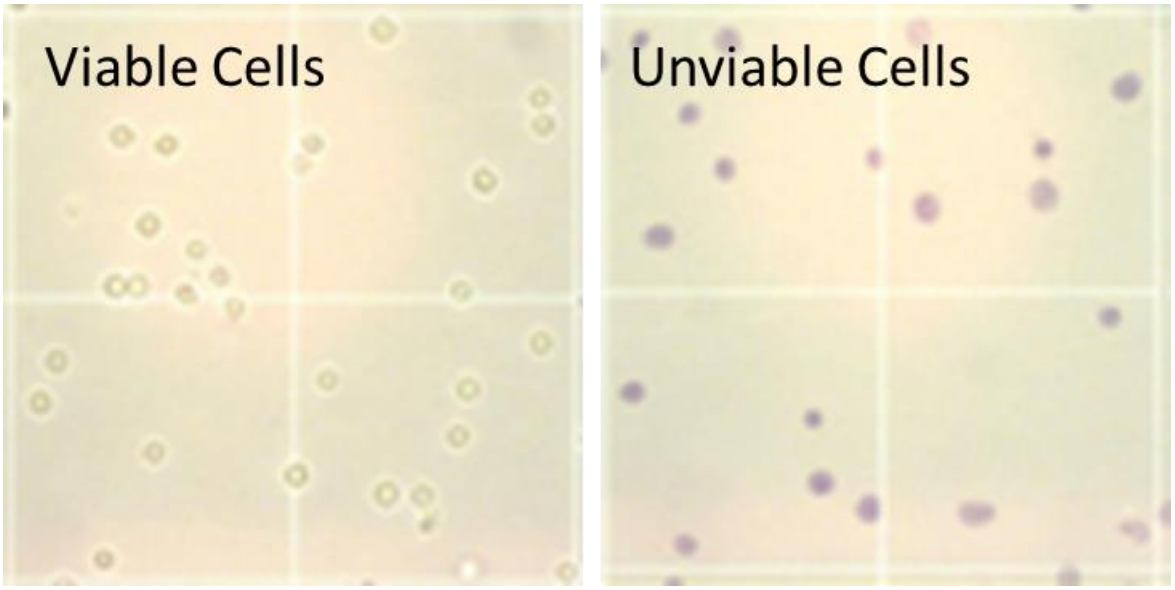

Figure 2.2

Example image of viable and unviable cells stained with trypan blue as they appear on a haemocytometer. Viable (live) cells to not allow the stain to permeate their membrane and appear colourless. Unviable (dead) cells have a permeable membrane to trypan blue and thus appear blue. Image adapted from www.cellbiolabs.com.

g. LIVE/DEAD fluorescence assay.

Fluorescent live dead staining was performed using the LIVE⁄DEAD® Viability⁄Cytotoxicity Kit (L3224Invitrogen, UK). Media was removed from cells using an aspirator, followed by a double PBS wash. A dye solution of 5µL Ethidium-1, 1.2 µL Calcein AM, 2.5 mL PBS (leaving final concentrations of 2µM calcein AM and 4µM Ethidium-1) was made up, with sufficient solution to cover the cell surface used in each well. In cases where 3D structures were being investigated, enough solution to completely immerse the entire scaffold was used. This was then incubated at 37^{o}C for 20 minutes, before reagents were removed by aspiration. Samples were then washed with PBS before a

final immersion of the sample in PBS and storage at 4^{o}C if necessary. Either fluorescent or confocal microscopy was then performed as described in sections **2.8.5** and **2.8.6**.

i. Seeding.

Seeding of cells was achieved by suspending cells at a known concentration using a haemocytometer as described previously.

Scaffolds:

Cells were seeded onto scaffolds by first creating a high density cell suspension. Cells were suspended at 1 x 10^{6} cells/mL by trypsin dissociation, counting and centrifugation. 100µL of this high density solution was the pipetted into the centre of a dry scaffold pre prepared according to experiment. Once seeded, scaffolds were transferred to an incubator at 37^{o}C for 6 hours to allow for cells to adhere to the surface. After 6 hours, scaffolds were immersed in 37^{o}C complete media according to experiment and cell type.

Flasks/Petri dishes:

Cells were suspended at known concentrations as described previously before pipetting directly into flasks containing sufficient complete media pre warmed to 37^{o}C to completely cover the cell growth surface. Flasks were placed into an incubator at 37^{o}C after seeding. Adhesion was checked after 12 hours using light microscopy.

2. 2. 2. Tenocytes.

a. Tenocyte extraction and culture.

Tendons were extracted from 8 week old male rats obtained from Keele University animal house by first sacrificing the animal, then surgically removing the Achilles tendon from

both hind legs. The tendons were then placed in a universal bijou flask containing a solution of phosphate buffered saline supplemented with 1000 U/m PS for transport to the lab. Samples were kept in this solution for a maximum of 1 hour. The tendon was removed from the solution in a Biological Safety Cabinet and placed into a sterile petri dish. One tendon from each rat was minced into approximately $2mm^2$ pieces using a scalpel. Each tendon piece was then placed into the centre of a dry petri dish. The dishes were placed into an incubator at 37^oC for 1 hour, allowing the tendon to loosely adhere to the petri dish surface. Media (DMEM (4.5g/L glucose), 10% FBS, 1% NEAA, 1% L-glutamine) was then carefully dropped into the dishes, immersing the tendon, with care being taken to not detach the tendon piece from the culture plastic surface, and dishes placed back into the incubator for further culture. After around 5 days, cells started to migrate out of the tendon onto the petri dish surface. Once these cells reached confluence in the dish, the tendon piece was carefully removed using sterile tweezers and re-adhered to another petri dish using the same protocol as previously described. The remaining cells from the first dish were then detached from the surface using warm 1% trypsin/PBS solution for 5 minutes, pelleted by centrifuge (3 minutes, 200g), then divided into two T-25 flasks. One flask was then placed in a 2% O_2 incubator (Galaxy R+, RS Biotech), the other into the standard 21% O_2 incubator (MCO-17AI, Sanyo), after which the cells were expanded, passaging the cells when they reached 90-100% confluence. This process was repeated for the second dish the tendon piece was adhered into, with cell labelled as being from the second batch of cells gained from the tissue sample. This process was repeated with each tendon piece until cells were not seen to be migrating onto the culture plastic, up to a maximum of 3 times.

b. Tenocyte characterisation.

Tendon cells were characterised using Tenomodulin immunofluorescence. Cell samples were cultured to around 60% confluence in complete tenocyte media (section 2.2.2.a.) in a 12 well plate before being fixed in 95% methanol for 5 minutes and washed twice with PBS in the well of the plate. Samples were then immersed in 0.01% Triton X (T8787 Sigma Aldrich, UK) solution for 5 minutes, before washing with PBS. Cells were then immersed in 3% bovine serum albumin (A8806 Sigma Aldrich UK) for 1 hour at room temperature, before a further PBS wash. Enough primary antibody (rabbit polyclonal IgG, SC98875 Santa Cruz, USA. 1:200 in PBS) to completely immerse the cells was then applied and left at 4^{o}C overnight. The antibody was then removed by aspiration and samples washed with PBS. The secondary antibody (donkey anti rabbit IgG-FITC conjugated, SC 2090 Santa Cruz, USA. 1:200 in PBS) was applied and left at room temperature for 1 hour, before washing with PBS. A counterstain was then used to highlight the nucleus of the cells by adding 4',6-diamidino-2-phenylindole (DAPI) (Sigma Aldrich D9542) at a 1:500 concentration in PBS for 5 minutes at room temperature. A final PBS wash was then administered before immersing the sample in PBS for imaging. Samples were stored under PBS at 4^{o}C after imaging.

2. 2. 3. Mesenchymal Stem Cells.

a. Fibronectin Coating.

Tissue culture flasks were coated with fibronectin (F0895 Sigma Aldrich, UK) before use. A solution of 10ng/mL fibronectin/PBS was used to coat each flask, with 4mL used for a

T-75 (or enough to completely cover the surface). Flasks were left for at least 2 hours at room temperature before the solution was aspirated off and cells added.

b. Isolation and Culture of Mesenchymal Stem Cells.

Complete human bone marrow aspirate was supplied by Lonza, UK (1M-125). A total mononuclear cell count was performed on the incoming aspirate, before being seeded into fibronectin coated T-75 flasks at 1 x 10^5 mononuclear cells/cm^2 in 15mL media (DMEM (4.5g/L glucose), 5% FBS, 1% NEAA, 1% L-glutamine, 1% PSA). These were then incubated at 37^{o}C for 7 days, before half of the media was changed and cells replaced back into the incubator. A full media change was performed on day 14 of culture. MSCs were initially identified by being the adherent cells that remain in the dish after the second full media change. After isolation, cells were either cryopreserved or expanded.

For cellular expansion, cells were cultured in media (DMEM (4.5g/L glucose), 5% FBS, 1% NEAA, 1% L-glutamine) until 90-100% confluent, when they were split 1:2.

c. MSC characterisation.

Further characterisation of cells was carried out using a Human Mesenchymal Stem Cell Characterisation Kit (Millipore SCR067) according to manufacturer's protocol. Briefly, cells were cultured to around 60% confluence in a 6 well plate before being fixed in 4% PFA for 5 minutes. Cells were then immersed in 0.01% Triton X (T8787 Sigma Aldrich, UK) solution for 5 minutes. Cells were then washed in PBS before 3% bovine serum albumin (BSA) (3%BSA in FBS) blocking solution was applied for 2 hours. Supplied antibodies (mouse anti-THY-1 (CD90), mouse anti-STRO-1, mouse anti-H-CAM (CD44))

were diluted according to specification in PBS (this kit specified 1:500 as optimum). Cells were coated in antibody solution at 4^{o}C overnight, with one antibody solution used per well. Cells were then washed with PBS and blocking solution before secondary antibody (donkey anti mouse IgG) solution was applied for 2 hours at room temperature in darkness. A final PBS wash followed, with cells stored immersed in PBS at 4^{o}C. Imaging was then performed using fluorescence microscopy using FITC and TRITC filters according to the fluorescent tag associated with the antibody.

2. 2. 4. Embryonic Stem Cells.

a. Mouse Embryonic Fibroblast isolation.

Mouse embryonic Fibroblasts (MEFs) were isolated from pregnant female mice at approximately 12 days after being plugged. The mouse was sacrificed by cervical dislocation, before being sprayed with generous amounts of 70% IMS. An incision was then made parallel to the hind legs across the abdomen of the mouse, before two further incisions were made, creating a V shape towards the animals head. The uterine horn was then removed using scissors and forceps into a sterile 90mm petri dish. Each embryo was then separated from the uterine horn, and the membrane surrounding it pierced, draining the amniotic fluid. The embryo was then removed from the membrane and the head removed using a scalpel. The body was then stored in 10%PS/PBS until ready for further processing, with a maximum of 10 embryos per 50mL.

Three dishes of warm PBS were prepared in a Biological Safety Cabinet (BSC) . The embryos were transferred to the first bath, where the bulk of any organs or viscera (red matter) was removed using sharp sterile forceps. The remaining tissue was then washed in the second PBS bath, and then again into the final bath. The tissue was then transferred to pre warmed PBS/1% Trypsin/EDTA solution (2mL/embryo) and incubated for 5 minutes,

vortexed, and then incubated for a further 5 minutes. The trypsin was then neutralised using complete DMEM/10% FBS media and the sample vortexed. The liquid was then allowed to settle for 5 minutes before the top 3mL was removed and added to a T-75 flask containing 15mL complete media (DMEM, 10% FBS, NEAA, L-Glut, 1% PSA). This was then incubated for 48 hours, before a complete media change was performed with media containing no PSA.

b. MEF culture.

MEFs were seeded into a T-75 flask with complete media (DMEM, 10% FBS, NEAA, L-glut) and allowed to reach full confluence. When split, cells were plated at 1:8 and allowed to reach approximately 70% confluence before 25mL conditioning media (KO-DMEM, 20% Serum Replacement, 1%NEAA, 1% L-Glut, 4ng/mL β-FGF (F0291, Sigma Aldrich, UK), 909µL β-mecaptoethanol (M7522, Sigma Aldrich, UK)) was added, replacing the complete media. Conditioning media was removed daily, collected and stored at -20^{o}C until use. Before use, conditioning media was defrosted and filtered (22µm Milipore stericup). At the time of filtering a further 4ng/mL β-FGF was added.

c. Matrigel coating of flasks.

Matrigel (354277 SLS, UK) was defrosted overnight at 4^{o}C and diluted 1:100 in serum free KO DMEM at 4^{o}C. This was then vortexed to ensure complete mixing, before being pipetted into tissue culture vessels, with enough Matrigel solution to completely coat the flask surface being added. Flasks were allowed to sit for at least 1 hour before matrigel solution was aspirated off and the flask used for cell culture. If flasks were stored, they were done so at 4^{o}C for a maximum of 7 days.

d. ESC culture.

SHEF 1 embryonic stem cells (UK Stem Cell Bank) were cultured on matrigel coated T-25 flasks in a 21% O_2, 5% CO_2 incubator at 37^{o}C. Pre conditioned media (from MEFs) was used throughout. Cells were split 1:2 when confluent, with media changed daily. This method was adapted from that originally described by Xu et al (122).

e. Spontaneous Differentiation.

Spontaneous differentiation of ESCs was achieved using the method described by Bandi et al (168). Briefly, 1 x10^{6} SHEF 1 were seeded into a Matrigel coated T-75 flask for 24 hours in standard ES cell media (KO DMEM, 20% Serum Replacement, 4ng/mL b-FGF (100-18B Peprotech UK), 1% L-Glut, 1% NEAA, β-mercaptoethanol (31350-010 Invitrogen, UK)), and allowed to adhere for 24 hours. Spontaneous differentiation was induced by changing the media to standard fibroblast media (DMEM, 10% FBS, 1% NEAA, 1% L-Glut) for 5 days, changing the media after 3 days.

2. 3. Scaffold Production.

2.3.1. Purification of PHBHHx.

Poly-(3-hydroxybutyrate-3-hydroxyhexanoate) (PHBHHx) (Lukang Group, Shandong, China) (Mw 500KDa, 87.9% HB, 12.1% HHx) was purified by immersing in 100% ethanol (CHE1932, SLS UK) for 12 hours, before filtering using a 22µm Milipore stericup. Any remaining ethanol was allowed to evaporate fully at room temperature before use.

2.3.2. PHBHHx films.

Films were made by dissolving PHBHHx powder in Chloroform (472476, Sigma-Aldrich, UK) at varying concentrations between 0.8 and 2.4 weight (%) (0.08-0.24g PHBHHx/10mL Chloroform). This was left for 1 hour with regular shaking to allow the polymer to fully dissolve. 3mL polymer solution was then pipetted into a 60mm diameter glass petri dish on a flat surface in a fume cupboard and the solvent evaporated overnight. After complete evaporation had occurred, the films were removed from the dishes, cut into a circular shape using scissors and a template with a diameter of 35mm and immersed in 70% Ethanol for 2-3 hours in a BSC to sterilise. After washing with sterile PBS 3 times, the films were used.

2.3.3. PHBHHx tubes.

2g PHBHHx powder was dissolved in 20 mL chloroform in a 50 mL conical flask. Tube construction was performed using a 2.5 mm diameter stainless steel mandrill which was dipped into the homogenised PHBHHx/NaCl solution for 1 second, removed, inverted, stood upright with the polymer coated end at the top of the mandrill, and slowly rotated by hand allowing the solvent to evaporate in a flow hood for 2 minutes. This process was repeated 5 times, after which the mandrill was fixed vertically for 60 minutes to allow the solvent to fully evaporate and the polymer to become rigid. The polymer tube was carefully removed by hand and immersed in deionised H_2O overnight to further remove any remaining solvent.

2.3.4. Porous scaffolds.

Porous scaffolds were made by following the same protocol as used for making tubes. Briefly, 1g PHBHHx was dissolved in 10mL chloroform and allowed to stand for 1 hour to

allow the polymer to dissolve fully. 0.04g/10mL of Sodium Chloride particles (433209 Sigma Aldrich, UK) (pre-sieved selecting for particles under 100µm in size) were then added to the solution and homogenised by vortexing. A tube was then formed as described in section 2.3.3. After forming, the construct was allowed to air dry for 24 hours, before removing from the mould by hand. The scaffolds were then placed in de-ionised water for 30 minutes, allowing the NaCl particles to dissolve out of the polymer. Sterilisation by immersion on 70% ethanol for 2 hours, followed by washing with PBS 3 times, preceded use.

2.3.5. Collagen Gels.

Type I collagen gels were produced by combining 10x DMEM (D2554 Sigma Aldrich) with cells at 10x the final desired concentration (e.g. final gel concentration needed 1 x 10^5 cells/mL, 1 x 10^6 cells/mL were suspended in the 10x DMEM before gels were produced), with 1mol NaOH, dH_20 and high concentration type I collagen gel (BD354249 BD Biosciences). 2mL of gel was produced by mixing 980µL collagen (initial conc. 9.41mg/mL), 200µL 10x DMEM/cells, 22µL 1M NaOH and 800 µL H_20 for a 5mg/mL final collagen concentration. Gels were fabricated in the order 10x DMEM, NaOH, water, collagen stock to prevent premature gelation. Gels were mixed by pipette creating a uniform colour solution. All gels were mixed and stored on ice until use.

2.3.6. Collagen Cylinders.

To make a collagen tube, the procedure for making the gel solution is as previously described. To create a tube shape a mould was fashioned using two 1mL plastic syringes. On one syringe the tip was removed using sterile scissors. The plunger from the second

syringe was then used to seal the open end, creating a cylindrical mould. Collagen gel was pipetted into the open end of the syringe, with the plunger as near to the top as possible, withdrawing as the collagen solution filled the space. This stopped any air bubbles forming at the end of the cylinder. When the desired amount of gel solution was in the syringe, the second plunger was carefully placed on the open end sealing the chamber. The whole mould was then incubated at 37^{o}C for 2 hours before carefully removing the cylindrical collagen gel into the desired culture vessel (Fig. 2.3).

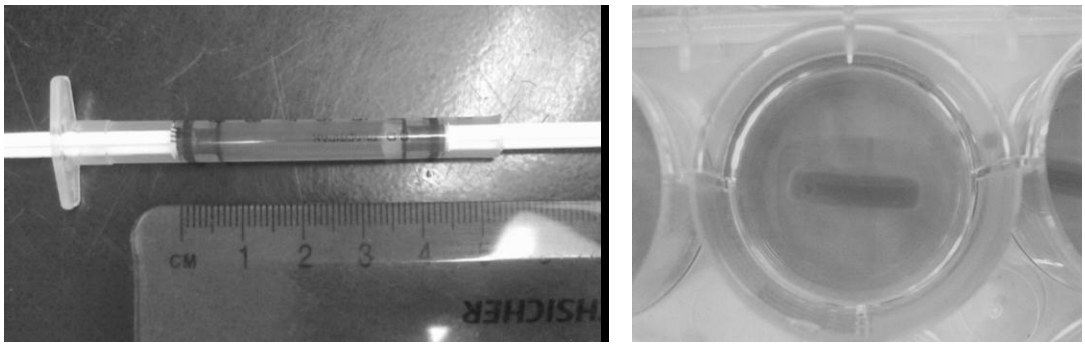

Figure 2.3. Forming a collagen cylinder. Gels were pipetted into an adapted 1mL syringe while still liquid, with a secondary plunger used to seal the gel in place. After 1-2 hours at 37^{o}C, gels can be removed by pushing on one of the plungers, creating a cylinder of collagen gel. Media is then added to maintain gel and prevent dehydration.

2.3.7. Scaffold Preparation for *in vivo* studies.

PHBHHx porous tubes were prepared using the method described in **2.3.c**. PHBHHx fibre was made by melt-spinning using a laboratory-size extruder (Ruojiang Chemical Fibre Machinery Co. Ltd., Beijing, China) with a single nozzle which had an inner diameter of 300 μm. Briefly, PHBHHx powder (87.9% HB, 12.1%HHx) was melted, extruded, isothermally crystallized, drawn and annealed under tension as described in Chinese patent

application No. 200810052461. All fibre was provided by Tsinghua University, Beijing, China.

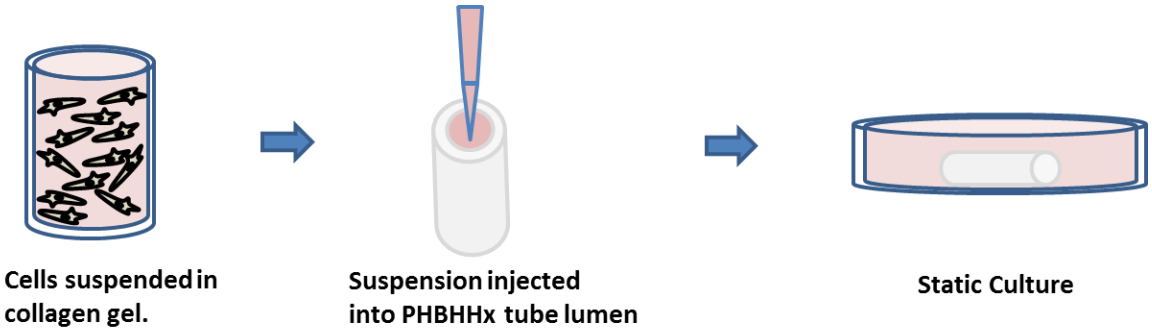

Figure 2.4. PHBHHx/collagen hybrid scaffold. Collagen gel (containing or not containing cells) is pipetted into the centre of a porous PHBHHx tube at 4°C, before elevating the temperature to 37°C for 1-2 hours to allow for the gel to set. Scaffolds were then either placed in static culture, or used for in vivo experimentation.

2.4. *In vitro* testing.

2.4.1. Cellular fluorescent tagging.

Cells were first detached using trypsin and a cell count performed. Cells were suspended at 1 x 10^6 cells/mL concentration, along with 5µL DiO stain solution (V22889 Invitrogen) added for each mL cell suspension. This was then incubated for 10 minutes at 37°C. Solutions were the centrifuged and the pellet washed 3 times with PBS before using cells as required. Cells could then be viewed using fluorescent microscopy.

2.4.2. Mechanical testing.

a. Stiffness was measured using a BOSE Electroforce 3200 system by clamping samples within appropriately sized grips and deforming by 0.5mm at 0.1mm/second in a uniaxial direction with the force required measured. Samples were placed into the grips with the approximate centre of the sample in the gap between the grips (Fig. 2.5). Stiffness was calculated using the equation: $k = F/\delta$, where k = stiffness, F = force and δ = displacement in single direction of freedom (i.e. direction the force acts in).

b. Failure stress was measured by clamping samples within appropriate grips and stretching to failure using a BOSE Electroforce 3200 system. Samples were loaded securely in the grips, with a minimum of 5mm of sample being between the grip tongs. The mid-point of the sample was always between the upper and lower grips. Samples were loaded to failure, or until a drop off in load bearing capability was observed. If samples failed in a position that was not more than 2mm from either the upper or lower grip, the test was considered invalid, minimising the effect of the grip altering the mechanical properties of the sample. A diagram of the set up can be seen in figure 2.5.

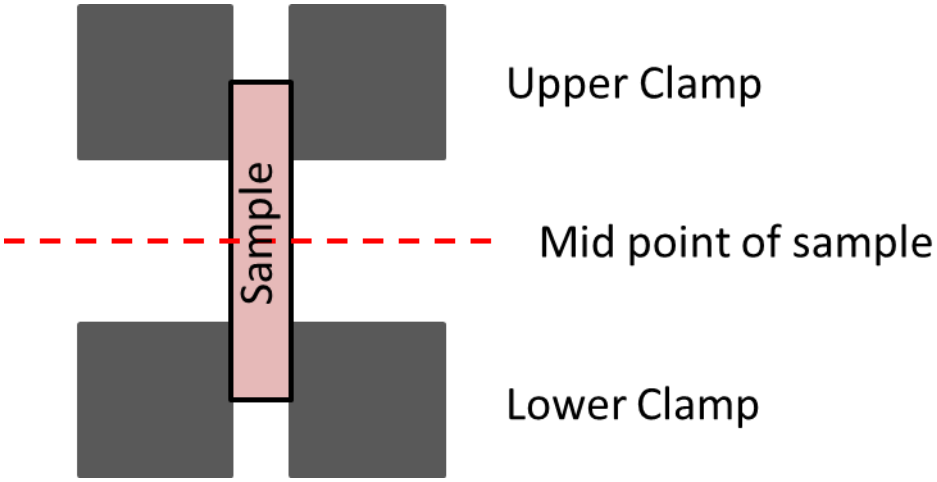

Figure 2.5. Diagram of sample clamping for mechanical testing. Samples were loaded with a minimum of 5mm inside both the upper and lower grips, with the mid-point of the sample being between the upper and lower clamp.

2.4.2. Collagen contraction.

Contraction was monitored over a period of 20 days using callipers. Media was aspirated off gels, with gels then being straightened using sterile forceps to ensure correct values were gained, taking care not to elongate the sample from its original length. Callipers were autoclaved or exposed to ultra violet light prior to use to reduce chance of contamination. Callipers were adjusted to approximate the length of gels prior to moving them into contact with gels, and further adjusted until contact was made. Contraction in diameter was measured using the same method, with readings being taken at 3 random points throughout the length of the gel, and an average taken.

2.4.3. Reverse Transcription –Polymerase Chain Reaction (RT-PCR).

a. Cell lysis.

Cells were pelleted using trypsin and centrifugation. If cells were suspended in collagen gel, samples were pre immersed in 0.4% type IV collagenase at 37^{o}C for 1 hour or until gel was not visible. 350µl lysis buffer was added to the pellet and mixed with the pipette. The lysed cells were then transferred to a QIAShredder tube and centrifuged for 3 minutes at full speed (16000g), disposing of the spin column after use. Samples were stored at -80^{o}C before final extraction.

b. RNA extraction.

1 volume (350µL) of 70% ethanol was added to cell lysate before being transferred to an RNEasy spin column (total 700µL per column). Once transferred, the RNEasy column was centrifuged for 15-30 seconds at 9000g. The flow-through was discarded and the column retained. It was ensured that the column remained untouched through this process to avoid contamination. 700µl buffer RW1 was added to the column and the tube spun for 30 seconds at 9000g. The flow-through was discarded and the column containing RNA retained. 500µl RPE wash buffer was then added to the column and spun for 30 seconds at 9000G before discarding flow-through. RPE wash was repeated followed with centrifugation for 2 minutes at 9000g. The RNEasy spin column containing the extracted RNA was transferred to a new tube and spun again at 16000g for 1 minute. 15µL of RNase free water was added directly onto the polymer of spin column and allowed to stand for 3 minutes. Following this time the column was spun for 1 minute at 9000g. The supernatant

was removed with a pipette and returned to the column and allowed to stand again for 3 minutes prior to a final spin at 16000g. The spin column was then discarded and the microcentrifuge tube containing 15µL of concentrated extracted RNA placed on ice prior to measurement and PCR analysis.

c. RNA Quantification.

Quantification was performed using a Nanodrop 2000 spectrophotometer. Pedestals were cleaned and blanked with dH_2O before use. 1µL RNA sample was loaded onto the pedestal and read using the RNA quantification tool in the associated ND-2000 software. RNA total concentration, 260/280 and 260/230 measurements were recorded. Nanodrop pedestals were cleaned with dH_2O between sample readings.

d. RT-PCR.

A PCR master mix of 12.5µL per sample was created using 2X Reaction mix (6.25µL), forward and reverse primers (0.25µL at concentration 10 µM) SuperScript III RT/Platinum Taq High Fidelity Enzyme mix (0.25µL) and DNAse-free water (4.5µL).

1µL RNA sample was loaded into a 0.2mL PCR tube, with a control of the same RNAse free H_2O used to make up the master mix. 12.5µL master mix was then added to each sample tube and the lid applied before being briefly centrifuged to ensure all product was mixed and at the base of the tubes. Tube strips were then transferred to a pre-programmed PCR thermocycler.

e. PCR cycling.

Samples were run according to the following procedure as previously used by Forsyth et al (85).cDNA synthesis and pre-denaturation: 1 cycle of 50°C for thirty minutes, 94°C for two minutes. PCR Amplification: 40 cycles of 94°C for fifteen seconds (denaturation), annealing temperature for thirty seconds (annealing – see table below) and 68°C for thirty seconds (one minute per kb) (extension).

Final extension: 1 cycle of 68°C for 5 minutes (fully extending any remaining single stranded DNA), then cool to 15°C until retrieved for processing.

f. Annealing Temperatures and Primer Sequences.

Table 2.1. RT-PCR primer sequences, sequence lengths and annealing temperatures. Expression markers investigated were B-Actin (housekeeping gene), SOX-9 (cartilage), RUNX2 (bone), PPARγ (adipose), TNMD (Tenomodulin, tendon), TENC (Tenascin C, tendon), COL1a2 (collagen 1a2), COL3a1 (collagen 3a1), TBSD4 (thrombospondin 4, tendon).

Name	Forward (5'-3')	Reverse (5'-3')	Sequence length	Annealing temperature ^{o}C
B-Actin	GCCACGGCTGCTTCCAGC	AGGGTGTAACGCAACTAAGTC	504	55
SOX-9	TCATGAAGATGACCGACG	CTGGTACTTGTAATCCGG	506	54
RUNX2	CCCCACGACAACCGCACCAT	CACTCCGGCCCACAAATCTC	289	48
PPARγ	CTTTTGCTGAGCTTCTTTCA	TGAAAGAAGCTCAGAAAGC	203	55
TNMD	GCACTGATGAAACATTGG	ATCCAATACATGGTCAGG	274	49
TENC	AAGAGCATTCCTGTCAGC	CAGTTTGCCGGTAAGAGG	217	50
COL1a2	GACTTTGTTGCTGCTTGC	CAAGTCCAACTCCTTTTCC	242	50
COL3a1	AAGGACACAGAGGCTTCG	CTGGTTGACCATCAATGC	210	51
TBSD4	CCCCAGGTCTTTGACCTTCTCCC	ACCTTCCCATCGTTCTTCAGGT	245	59

g. Gel Electrophoresis.

2% agarose gels were made by fully dissolving 2g agarose in 100mL 1x Tris Acetate-EDTA (TAE) buffer (T9650 Sigma Aldrich, UK) with heating for 3 minutes at full power in a microwave. 10mg/mL ethidium bromide was added and mixed thoroughly before pouring into the casting tray and inserting a well comb. It was then allowed to set at room temperature for at least one hour before being immersed in an electrophoresis chamber filled with 1xTAE buffer.

2µL loading dye was added to each sample after being removed from the PCR thermocycler. Samples were then briefly centrifuged and flicked to ensure thorough mixing. 5µL DNA ladder solution (Sigma) was added to control wells in the immersed gel. 5 µL of sample was then loaded in consecutive wells.

Electrophoresis was performed for 60 minutes at 100 V using a BioRad Power PAC 3000 and imaged using a Syngene Gel UV illuminator and GeneSnap imaging software.

2.5. Mechanical Stimulation.

Mechanical stimulation was performed using the BOSE ElectroForce 3200 machine coupled to WinTest software. Scaffold/cell constructs were assembled and cultured in static conditions in complete media for 24 hours before loading took place. Samples were placed within the grips of the Biodynamic chamber adaption, with all vents and outlets sealed, inside a Biological Safety Cabinet (fig. 2.6). Samples were manipulated into place using sterile forceps. Once sealed the unit was transferred to the ElectroForce machine and connected in accordance to manufacturer's protocol. Samples were stressed using an axial strain of 10% (ie. 5mm sample – 0.5mm elongation) in a sine wave pattern, with the high

being 10% strain and the low being the original length of the scaffold. All samples were loaded at a frequency of 1 cycle/minute (0.017 Hz) for 1 hour per day, 5 days on, 2 days' rest.

The Biodynamic chamber was assembled prior to use and autoclaved after 5 days of mechanical loading. After each batch of sample was loaded samples were removed using sterile forceps and placed back into static culture and the chamber comprehensively washed with 70% IMS to remove any remaining residue from samples. IMS was allowed to completely evaporate before new samples were mounted in.

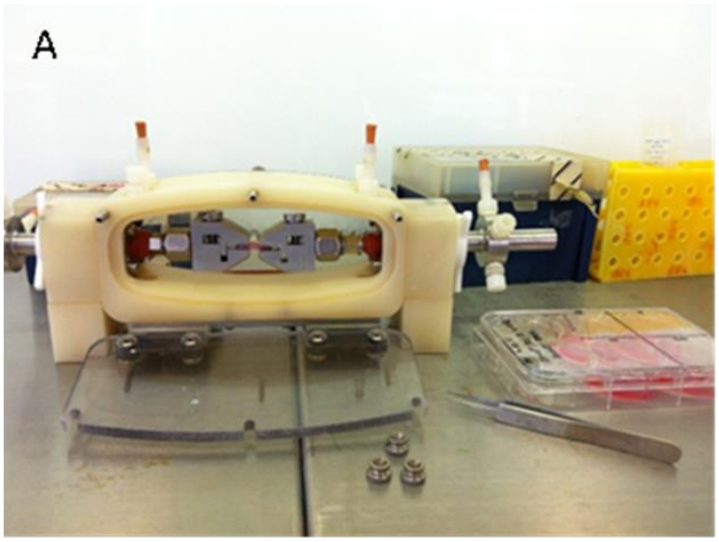

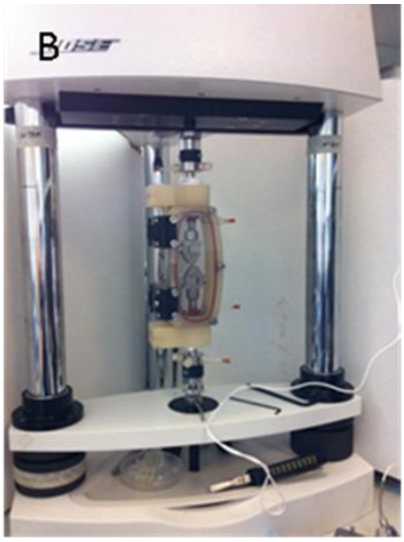

Strain	Loading modality	Frequency	Loading duration	Rest duration
10%	Sinusoidal	0.017 Hz	1 hour/ day – 5/7 days	23 hours/ day

Figure 2.6. BOSE chamber setup and mechanical loading. samples were mounted between the grips of the biodynamic chamber in a BSC before chamber was sealed (A). Samples were then mechanically loaded 'dry' for 1 hour per day for a maximum of 20 days (B) according to the conditions outlined in the figure, before being returned to static culture.

2. 6. Scaffold Characterisation.

2.6.1. Scanning Electron Microscopy.

SEM (FEI Quanta 200, Tsinghua Medical School, Beijing) was carried out using samples of both fibre and tube to determine the topographical structure. Cellular adhesion was also investigated by first allowing rat MSCs and tenocytes to adhere to the polymer for 24 hours before fixing with 70% methanol. Each sample was gold coated (15 nm) prior to analysis.

2.6.2. Pore size.

Pore size was quantified by taking $1mm^2$ areas of electron microscope images and analysing with Image J software. Random areas were taken, with each pore measured along its longest length using the line draw tool, giving a value of pixels for each pore. This was then adjusted using the appropriate scaling factor to convert to millimetres.

2.6.3. Pore density.

Pore density was measured by taking $1mm^2$ areas of electron microscope images and analysing using the grid and counter tools in Image J software. The grid was overlaid over the original image, and all visible pores counted. Pores were defined as being areas of the surface that were not uniform with the surrounding area, i.e., any indent that could be seen.

2.6.4. Fibre diameter.

The diameter of fibres was obtained by viewing at 100x magnification along random area of the fibre length. Point to point lines were then overlaid onto the fibres using the microscope software (FEI Quanta 200), which calculated the length of the line. An average

was then obtained along with a standard deviation to determine how uniform the fibres were.

2.7. *In Vivo* testing.

2.7.1. Animals.

Animal license and experimental design was approved by the Animal Ethical Committee of Tsinghua University, Beijing, 31.8.2010.

15 180-200 g male Sprague-Dawley (SD) rats were purchased from the Centre for Biomedical Analysis, Tsinghua University, China. Animals were returned to the centre post operation and fostered by the staff there for the duration of the experiment. The animals were euthanized at 40 days post operation by cervical dislocation, with the Achilles tendons from both hind legs being removed for analysis.

Experimental Groups: Animals were randomly assigned during surgery into 3experimental groups. Group 1 was a control group, where a 2mm defect was induced in the mid-section of the Achilles tendon of the right hind leg. This injury was then left to heal naturally, with only the outer skin sutured back into place to seal the wound site. Group 2 received the 2mm defect in the same way as group 1, however after injury a PHBHHx tube/fibre scaffold was secured into place, using the fibres to fix the tube into the correct position. The surgical site was then closed using sutures. Group 3 also received a 2mm defect to the right hind Achilles tendon, with a PHBHHX tube/fibre scaffold being placed to bridge the injury site as with group 2, however before suturing the surgical site closed the tube was injected until full with 3mg/mL collagen gel. A full description of surgical method is found in section 2.7.2.

Surgical Preparation: Before surgery all scaffolds (5mm length tube with 3 fibres running through the lumen (Fig. 2.7)) were sterilized using 70% IMS/ deionised H_2O solution overnight in a biological safety cabinet with the ultra violet sterilization system turned on. Scaffolds were then stored and transported in Sterile PBS/10% PSA solution in a sealed 15 mL centrifuge tube. This was only opened prior to surgery and the scaffolds handled using aseptic surgical technique.

2.7.2. Surgical Procedure.

Surgical procedures were carried out by experienced (consultant grade) orthopaedic surgeons at the Surgical Training Centre, Peking University Hospital Number 1, Beijing, China. Animals were anesthetised using 50 mg/Kg sodium pentobarbital according to local practice. Once anesthetised, a lateral incision was made parallel to the Achilles tendon on the distal side of the right hind leg (Fig. 2.8.B) and the tendon exposed (Fig. 2.8.C). In the control group, a 2mm section was removed from the centre of the tendon (Fig. 1D), then the incision closed using 3 cross stitches using dissolvable sutures (Fig. 2.8.I). Experimental groups had a 2mm section removed, after which the gap was bridged using the scaffold. This was done by first knotting together the 3 fibres and passing each individually through one end of the damaged tendon (Fig. 2.8.E). The tube was then passed along the open end of the fibres, and manoeuvred into position (Fig. 2.8.F). The remaining open ends of fibre were then passed through the other damaged end of tendon, and the ends bought together to leave a 2 mm gap between the tendon ends. The fibres were then knotted together as previously, fixing the scaffold in place and the leg at the correct anatomical position (Fig. 2.8.G). In one experimental group, collagen gel was injected into the scaffold after it had been fixed in place using a syringe (Fig. 2.8.H). The surgery was

again then closed with 3 cross stitches using dissolvable sutures. Animals were separated until all had recovered from anaesthesia, then divided according to which experimental group they belonged to.

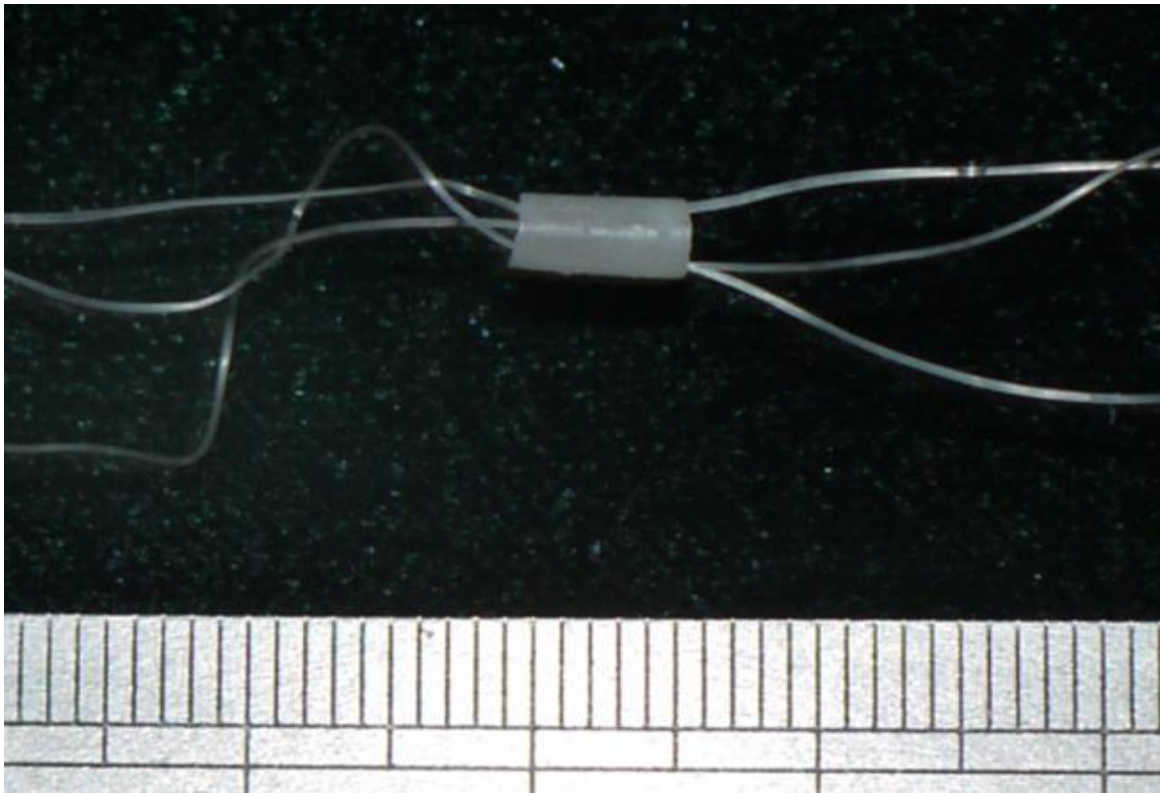

Figure 2.7. Construct as used for in vivo implantation. Final construct consisted of a porous PHBHHx tube with 3 PHBHHx fibres running through the centre. Total construct length was approximately 5 mm to allow for overlap of the injury site.

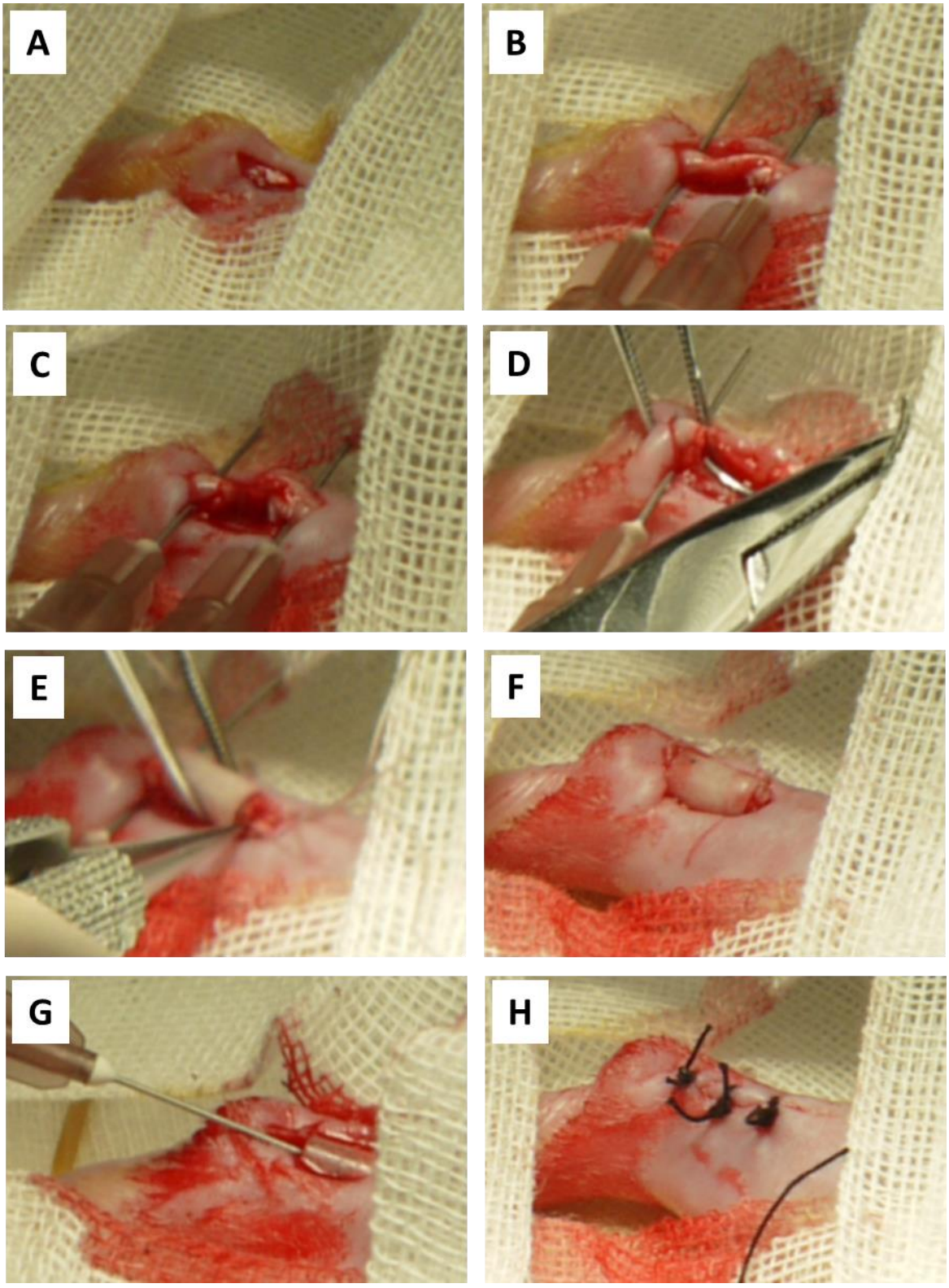

Figure 2.8. Scaffold implant procedure. A: Lateral incision in the right hind leg. B: Isolation and pinning of tendon. C: 2 mm injury induced. D: PHBHHx fibres passed through one end of tendon. E: Tube manoeuvred into place. F: fibres passed through other end of tendon and construct fixed in place. G: Collagen injected into tube. H: Surgery closed using dissolvable sutures.

2.7.3. Blood samples.

Blood was taken from each rat at allotted times throughout the experiment. Rats were first isolated using a restraint tube then blood collected by making a small incision at the tip of the tail. If insufficient blood flow was present after the initial incision, warm water was used to warm the tail. Blood was then collected by drip into an eppendorf micro centrifuge tube. Rats were separated after sampling to ensure no repetition occurred. Rats were monitored for 1 hour after blood collection to ensure no adverse effects were caused during the procedure.

2.7.4. Immune response analysis.

Immune response was monitored by measuring C Reactive Protein (CRP) levels in the rats throughout the experiment. Blood samples were taken from the tail of the rats on days -5, -2, 2, 5, 10, 20 and 40, with day zero referring to the day of surgery. Day 0 blood samples were not possible to collect due to blood loss during surgery. Once collected, samples were immediately centrifuged at 300g for 15 minutes and the serum (clear liquid level at the top) collected and stored at -80^{o}C. Once enough samples had been collected, CRP was measured using a Rabbit anti Rat CRP ELISA kit (557825BD Bioscience) according to the manufacture's protocol and read using a Molecular Devices' VersaMax' Micro plate Reader.

2.7.5. Detection of breakdown molecules.

The breakdown of the scaffold was quantified by measuring the concentration of a breakdown molecule of PHBHHx in the blood serum over time. This was done using a β-hydroxybutyrate detection assay (Pointe Scientific USA, H7587-58, H7587-CTL) using a

scaled down (10x) version of the manufacturer's protocol and read using a Molecular Devices 'VersaMax' Micro plate Reader.

2.7.6. Restoration of mechanical properties.

To test for the restoration of mechanical strength, a stretch to break test was carried out using 3 of the samples from each group. The non-operated tendons were taken as a positive control, demonstrating the strength of a tendon if undamaged and subjected to the same environmental factors. The samples were removed ensuring that the complete tendon was collected. The samples were loaded into the machine (Tension Compression Load Cell Tester, NTS Canada) so that only the ends of the tendon were held by the clamps, and stretched at a rate of 10 mm/min until complete failure was observed.

2. 8. Histological Assessment.

2.8.1. Paraffin wax embedding.

Samples were fixed using 4% paraformaldyhyde (P6148 Sigma Aldrich UK)/PBS solution overnight at 4^{o}C. They were then dehydrated using an ethanol sequence of 70% for 2 hours, 80% for 2 hours, 90% for 2 hours than 100% for 2 hours. After dehydration samples were immersed in xylene for 20 minutes, then at 60^{o}C in melted paraffin wax (Shandon Histoplast, Thermo Scientific) for 1 hour before being loaded onto a cassette in a Shandon Histocentre 2 (Thermo Scientific). They were then aligned in the direction of future sectioning (i.e. longitudinally), before wax was set on a cold plate. Samples were then stored at 4^{o}C.

2.8.2. Microtome Sectioning.

10µm sections of samples were created using a microtome (Shandon AS325, Thermo Scientific). Samples were placed onto pre warmed (around 20^{o}C) glass slides to aid in sample adhesion and a cover slip applied using mounting solution (9369 Sigma Aldrich)

2.8.3. Haematoxylin and eosin stain.

Samples rehydrated by reverse ethanol sequence (immersion in 100% ethanol for 1 hour, 90% ethanol for one hour, 80% ethanol for one hour, 70% ethanol for one hour, 50% ethanol for 2 hours, Xylene for 1 hour) and washed with water. Haematoxylin was applied for 10 minutes before washing with acidified water twice. Eosin was then applied for 5 minutes before washing with water. Cover slips were then placed over the sample and fixed in place using mounting solution before imaging.

2.8.4. Sirius red stain.

Samples were rehydrated with ethanol sequence before haematoxylin was applied for 10 minutes. Samples were washed with water twice before immersing in Sirius red solution for 1 hour at room temperature. Samples were washed of any excess stain with water before coverslips were added and samples imaged.

2.8.5. Fluorescent imaging.

Imaging was performed using a Nikon Ti S microscope coupled with a Nikon DSF11 camera and Nikon C-HGFI fluorescent light source. NIS-Elements software was then used to process the images.

2.8.6. Confocal microscopy.

Confocal microscopy (Olympus Fluoview, Olympus IX71) was performed to determine if cells had migrated into polymer films. A 'z-stack' representation of the polymer cross section was created by taking images at 5µm intervals. When then viewed in the z axis a fluorescent signal was observed where cells were located, allowing for a plane of reference to be made from the images. If all signals are detected in a single straight line, the cells were located on a single plane of reference.

2.8.7. Polarised Light Microscopy.

Samples were prepared according to experimental design. Images were taken using polarised light, with filters at 0^o and 90^o settings (ie. cross polarised) with samples orientated in the same direction. Images were taken with a Nikon N5 camera.

2.8.8. Optical coherence tomography.

Polymer thickness was measured using a home built Optical Coherence Tomogrophy (OCT) system according to a previously published method (169). Briefly, OCT generated images (laser wavelength interference patterns) were taken at random areas of 3 different scaffolds, with 3 images taken of each scaffold. Image J analysis software was then used to determine thickness, using the equation: line length x 0.0055 = length in mm.

2. 9. Statistical analysis

Results were checked for normality before further analysis using the Column Statistics analysis tool in GraphPad Prism® version 5.01.The significance of difference between two groups was determined by paired, two-tailed Student t-test. Differences between three or more groups were analysed by one-way ANOVA with Post-hoc Tukey's Multiple Comparison analysis. A 'p' value less than 0.05 was considered to indicate statistical significance. Data are presented as mean ± standard deviation (SD). Data was analysed using Microsoft Excel 2010® software with an additional stats plug in, or analysis was performed using GraphPad Prism® version 5.01 software for Windows (GraphPad Software, San Diego California USA).

Chapter 3

Cell Isolation, Culture and PHBHHx Compatibility.

3. 1. INTRODUCTION

Polyhydroxyalkanoates (PHA) are a family of biopolymers consisting of polyesters of many different hydroxycarboxylic acid molecules. Originally viewed as replacements for traditional petrochemical-derived polymers, PHAs are now largely redundant as everyday materials due to the prohibitive cost of large quantity production (141). There is now increased interest in these polymers from the medical device sector where the earlier prohibitive costs are reduced due to the reduced scale of operations. In addition PHAs display relatively high immunotolerance, low toxicity, and biodegradability which are all crucial for the medical device sector (142).

PHBHHx is the designation of molecules consisting of random co polymers of 3-Hydroxybutyrate and 3-Hydroxyhexanoate (143). It is one of the few PHA molecules that can currently be produced on a large enough scale for use in both scientific research and medical device construction (140). PHBHHx has a melting temperature of 111.7^{o}C, a glass transition temperature of -0.67^{o}C, a tensile strength of 4.1MPa, an elongation at break of 103.8%, and a Young's modulus of 130.4 MPa making it potentially useful for widespread biomaterial applications and different cell types (144) (148).

As previously mentioned in section **1.2**, tendons form the bridge between muscle and bone. They are typically slow to repair after injury or disease, have a poor blood supply and are relatively acellular when compared to other tissues (39). Tendon is composed mainly of collagen type I fibrils arranged in a hierarchical structure surrounded by a layer of endotenon (13). These fascicles come together to form larger and larger subunits, eventually forming the complete tendon. The arrangement of collagen I fibrils give tendon its strength in tension. Tenocytes are the major cell group present in tendons, making up

around 95% of the cellular mass (25). They are a highly specialized form of fibroblast and are responsible for the maintenance of tendon extracellular matrix (collagen I (the major component of tendon), collagen III, collagen V, glycosaminoglycans, elastin, and fibronectin) and for the repair of tendon tissue either after injury or as part of normal physiological process (16) (53). Under normal physiological conditions, tenocytes are found in small numbers spread between the collagen fibrils (16).

hMSCs are viewed as a candidate cell source for tendon tissue engineering as, unlike tenocytes, they can be readily sourced, isolated and expanded *in vitro*. The exposure of hMSCs to external tensile forces and/or supplementation with additional growth factors can induce differentiation into cells that resemble tenocytes in physiological activity and marker expression profile (53) (92).

Hypoxic cell culture is a term used to describe growing cells in atmospheres with reduced oxygen concentrations to those normally used. Typical values for O_2 would be 1-3 %, compared to 21% in regular atmospheric conditions. Low oxygen tensions have been shown to have beneficial effects on human MSC cell proliferation and on tissue formation potential (170) (171). Tendon derived stem cells have also been recently shown to proliferate faster in hypoxic conditions (86), leading to the conclusion that tenocyte function and cellular activity should be increased by hypoxic atmospheres.

The objective of this investigation was to monitor and quantify the interaction (attachment) and migration of tenocytes and hMSCs with PHBHHx polymer films of a variety of weight: volume ratios to characterize the optimal ratios for use in tissue engineering application.

3. 2. MATERIALS AND METHODS

All materials and reagents were used as described in section **2.1** unless stated otherwise.

Cells

Tenocytes were isolated from rat Achilles tendon (RaT) and cultured according to section **2.2.2** in both 21% O_2 and 2% O_2. Cells were imaged at P0, P4 and P8 at 100x magnification. Image J software was then used to measure cells along the longest axis and at 90^o to the longest axis, giving a value for cell length and width, before a ratio of width to length was found, giving a value of "squareness" or aspect ratio, with 1 being a perfect square and higher numbers denoting a more elongated shape (172). hMSC were isolated from commercially acquired human bone marrow cultured according to section **2.2.3**. Tenocytes were characterised by immunofluorescence with FITC conjugated Tenomodulin (TNMD) using protocol **2.2.2.b**. MSCs were characterised using protocol **2.2.3.c.**

Polymer Characterization

PHBHHx films were made as section **2.3.b**. Polymer thickness was measured using a home built Optical Coherence Tomogrophy (OCT) system according to a previously published method (169). Briefly, OCT generated images (laser wavelength interference patterns) were taken at random sites of 3 different films, with 3 images taken of each film. Image J analysis software was then used to determine thickness using the line draw tool and adjusted using a pre-determined pixel: actual length factor.

Stiffness was measured using a BOSE ElectroForce 3200 system as in section **2.4.2**. Prior to testing, samples were cut to 22 x 5 mm ribbons and placed into the grips, with 10 mm of the polymer in each grip, leaving a 2mm initial sample length.

Cell Attachment

Following preparation PHBHHx films were immersed in 3mL media containing 3 x 10^4 cells/ml in non-adherent, 6 well plates (Costar, UK). After 24 hrs incubation in either 21% O_2 or 2% O_2, films were removed from the dishes, gently washed in PBS, placed in a 15ml centrifuge tube and immersed in pre-warmed Trypsin/EDTA (Lonza, UK) for 5 minutes, before quenching with excess media and removing the film. The surface of the non-adherent dish was also washed once with PBS, exposed to 1 ml Trypsin/EDTA for 5 minutes, before quenching with excess media. After centrifugation cell pellets were re-suspended and cell counts established from both film and non-adherent well by haemocytometer counts of trypan blue (Sigma Aldrich, UK) positive and negative cells gained. A control group where cells were seeded into wells containing no polymer film was also performed. The combined film and well cell counts were treated as 100% and used to establish percentage attachment. Sample cell counts were corroborated by a second, blinded observer experienced in cell culture methods.

Cell Migration

Cell migration was measured by labeling cells with DiO (Vybrant Multicolor Cell Labeling Kit, Invitrogen, UK) and inoculating them as described earlier onto 2% PHBHHx films. These were then incubated in a 21% O_2 or 2% O_2 incubator for 24 or 72 hours, after which time the media was removed, the well washed with PBS, fixed with 4% paraformaldehyde (Sigma Alrich, UK) for 5 minutes, and then re-immersed in PBS. Confocal microscopy (Olympus Fluoview, Olympus IX71) was performed to determine if cells had migrated into polymer films, by creating a ‘z-stack’ representation of the polymer cross section, giving a fluorescent signal where cells are located and allowing for a plane of reference to be made from the images.

Statistical analysis

Results were deemed to be significant if $P \leq 0.05$, or as indicated in figure legends using a 2-tailed, paired, Students t-test using Microsoft Excel 2010 software.

3. 3. RESULTS

Cell Isolation.

Tendon Explant

Tendon samples were isolated from the Achilles region of 6 male wistar rats. After mincing, tendon tissue pieces were allowed to stick to a tissue culture plastic surface for 1 hour before media was added. After 3 days, light microscopy found that a ring of extracellular matrix had formed around the tendon sample (Fig. 3.1). After 6 days, cells had migrated from the tissue sample out onto the culture plastic, with dense areas of cells immediately surrounding the sample, and migration evident in areas further away. Passage 0 (P0) cells were small and spindle like in morphology, with contact inhibition preventing complete confluence. Cells had retained the spindle like morphology through to P4, but cells were found to be larger than P0 examples (Fig. 3.1).

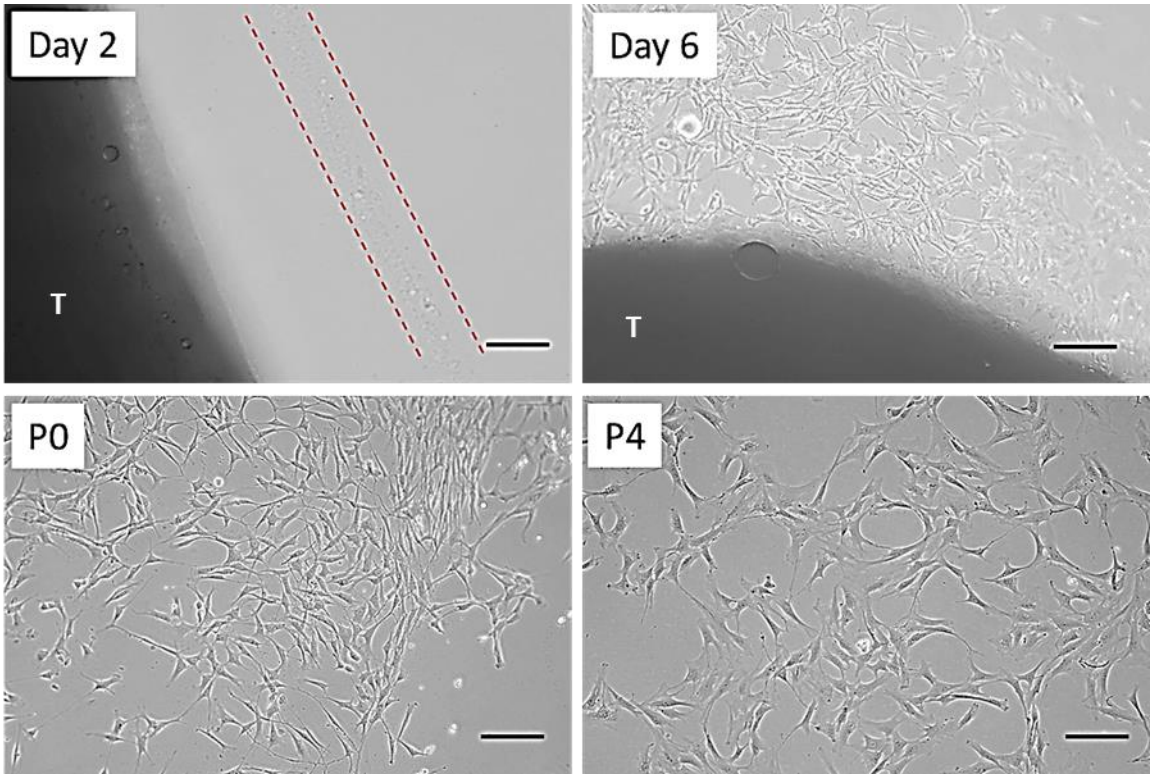

Figure 3.1. Cells migrate from rat tendon samples in 21% O_2. Day 2: ECM seen forming a surrounding layer on tissue culture plastic (area highlighted between dotted lines). Day 6: cells start to migrate from tissue to flask. Passage (P) 0: cells appear spindle like in shape. P4: cells retain spindle like qualities, but appear to gain in size (not quantified). Images at 100x, scale bar = 100µm. T identifies the original tendon piece.

Rat tenocyte isolation was attempted in both 21 and 2% O_2 atmosphere incubators. No evidence of cellular migration from tissue samples was observed in 2% O_2 atmosphere after 12 days culture (Fig. 3.2). When left for longer periods, cells were still not seen migrating from tendon samples (data not shown).

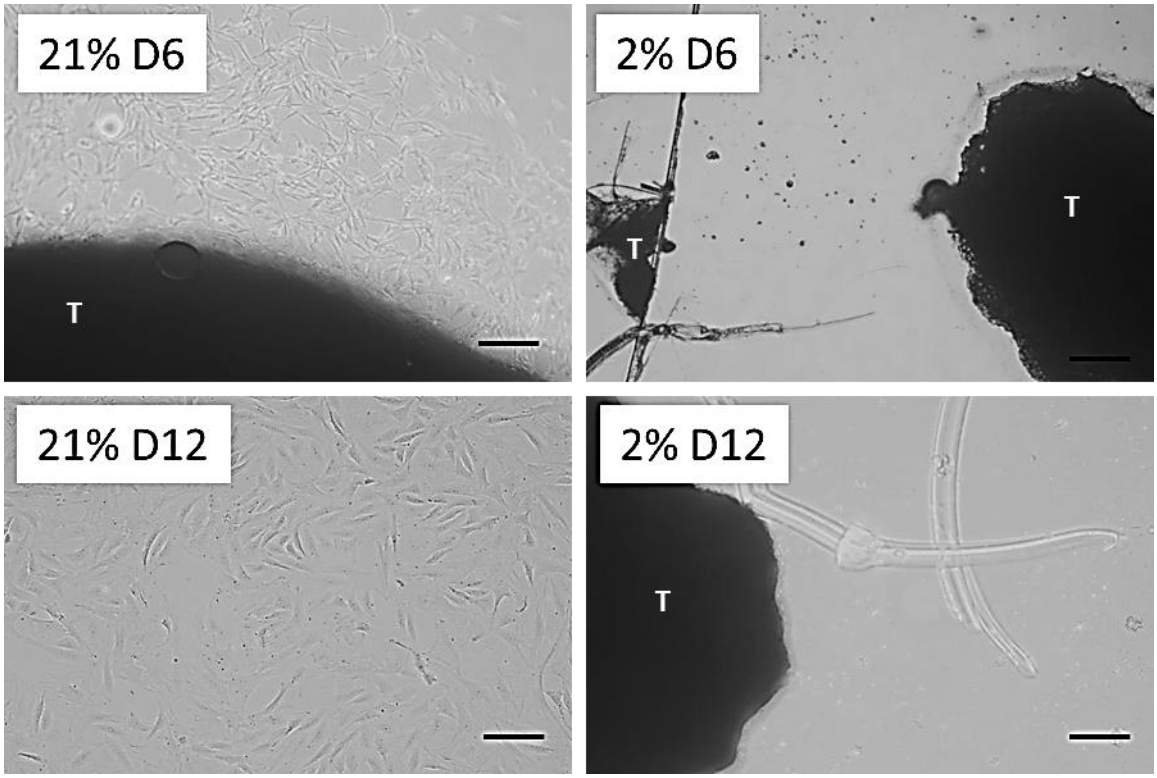

Figure 3.2. Cells do not migrate from rat tendon in 2% O_2 atmosphere. Phase contrast images of cells at 100x magnification. Cells are clearly seen migrating from tendon samples in 21% O_2 after 6 days, with cells being confluent after 12 days. No cells are seen migrating from tendon at any time point in 2% O_2. Images at 100x, scale bar = 100µm. T identifies the original tendon piece.

Tenocyte Characterization

Immunofluorescence was used to determine if the cells isolated from the tendon tissue pieces expressed Tenomodulin (a tendon specific gene(160)) . Cells were found to express tenomodulin at P1, indicating cells were tenocytes.

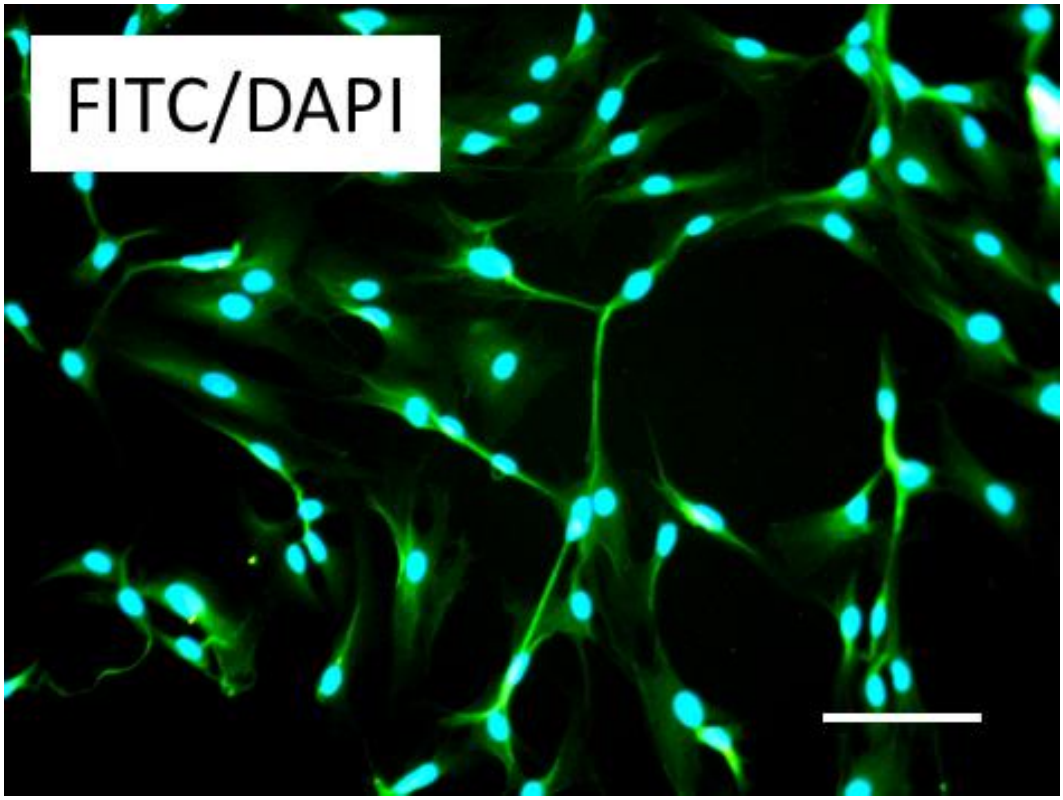

Figure 3.3. Cells isolated from rat tendon express tenomodulin. Nucleus stained blue with DAPI, TNMD stained green with FITC conjugated antibodies. Cells were imaged using fluorescence microscopy, at 200x magnification. Scale bar = 100µm.

Tenocyte phenotype over passage

Cells were visualized over prolonged culture via light microscopy. P0 cells were spindle-like in shape and small, with confluence being reached when cellular contact was achieved. Morphological changes were apparent with continued culture such that P4 cells were 51% larger than those at P0, but retained their elongated, spindle like morphology, as demonstrated by similar length: width ratios. P8 cells had adopted a cobblestone, square appearance, with a length: width ratio of 1.7, losing the spindle like processes which characterized those earlier passage cells (Fig 3.4).

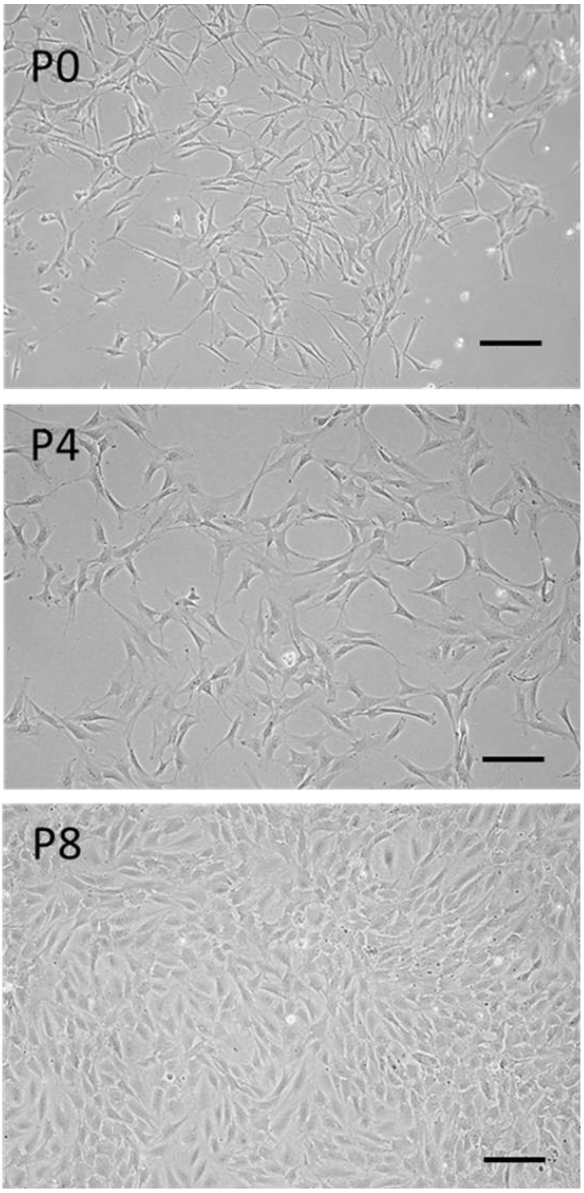

Passage	P0	P4	P8
Length (µm)	60±8	93±7	28±5
Width (µm)	11±3	16±2	16±3
Length:Width	5.4	5.8	1.7

Figure 3.4. Rat tenocytes change morphology with increased passage in 21% O_2. P0 cells appear spindle like and small. P4 cells retain spindle morphology, but become larger. P8 cells appear cobblestone like. Images at 100x in the centre of culture vessels. Scale bar = 100µm. Cell length and width were quantified using ImageJ software using the line draw tool. Cells were measured along the longest axis and perpendicular to the longest axis. Table shows mean ± 1SD, from 3 images, 12 cells measured per image.

Normoxic vs. hypoxic tenocyte culture

Tenocytes are found in an area of the body with low physiological oxygen tension (86). Cells were cultured in both hypoxic (2% O_2) and normoxic (21% O_2) conditions over 10 days, with cell counts performed throughout after cells were isolated in 21% O_2. After 5 days cells were found to have proliferated significantly more ($p = 0.01$) in 2% O_2 compared to 21% O_2, however a difference was not seen at 10 days ($p = 0.45$). The 21% O_2 group was found to increase linearly where the 2% group saw a faster rate of growth in the first 5 days, then a slower rate over the subsequent 5 days (Fig. 3.6).

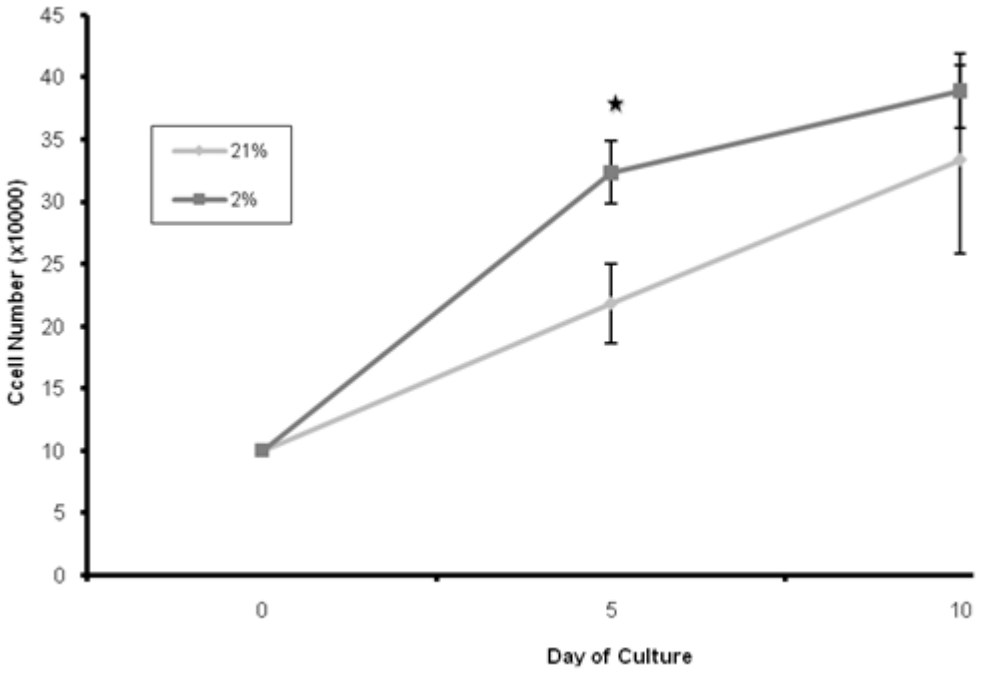

Figure 3.5. Rat tenocytes expand faster in 2% O_2 over 5 days culture, with no difference seen after 10 days. Cells were enzymatically removed from scaffolds and counted using a heamocytometer. Average ± 1SD shown on graph, n = 3. * indicates significant difference ($p \leq 0.05$).

MSC characterization

MSCs were isolated from human bone marrow aspirate using adhesion culture methods. P1 MSCs were characterized using immunofluorescence. Positive stains for HCAM, STRO-1, and THY-1 demonstrated cells were mesenchymal stem cell like (Fig. 3.6)

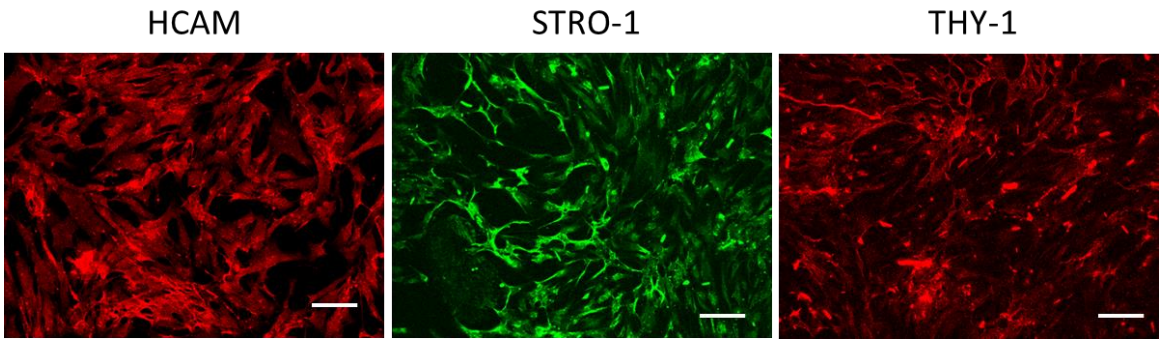

Figure 3.6. hMSC characterization. Positive expression of HCAM, STRO-1 and THY-1 demonstrate cells are mesenchymal stem cells. Images taken using fluorescent microscopy with TRITC and FITC filters, 100x magnification. Scale bar = 100µm.

Polymer film characterization

Films were first characterized by determination of both thickness and stiffness. Thickness was determined by producing wavelength interference patterns of films using an in-house built OCT system, with further analysis performed using the line draw tool in Image J analysis software (Fig. 3.7). The thickness of polymer films correlated directly with the initial polymer input (R^2 = 0.947) where 0.8% wt/vol films had an average thickness 0.10 ± 0.009 mm while the 2.4% wt/vol films had a measured thickness of 0.19 ± 0.018 mm (Fig. 3.8.A). We next sought to determine the stiffness of the polymer films examined above. Stiffness was determined with mechanical testing with the Bose ElectroForce 3200 system as described in Materials and Methods **2.4.2**. The calculated stiffness (resistance to elongation) values ranged from 153 ± 42 N/m (0.8%wt/vol PHBHHx) to 1706 ± 371 N/m (2.4% wt/vol PHBHHx). A biphasic increase in stiffness was observed between ≤1.6% wt/vol (N/m = 135.24*wt/vol, R^2 = 0.9605) and >1.6% wt/vol (N/m = 570*wt/vol, R^2 =

0.9657) A significant increase in stiffness was observed between films ≥ 2% wt/vol when compared to ≤ 1.6% wt/vol ($p \leq 0.024$) (Fig. 3.8.B).

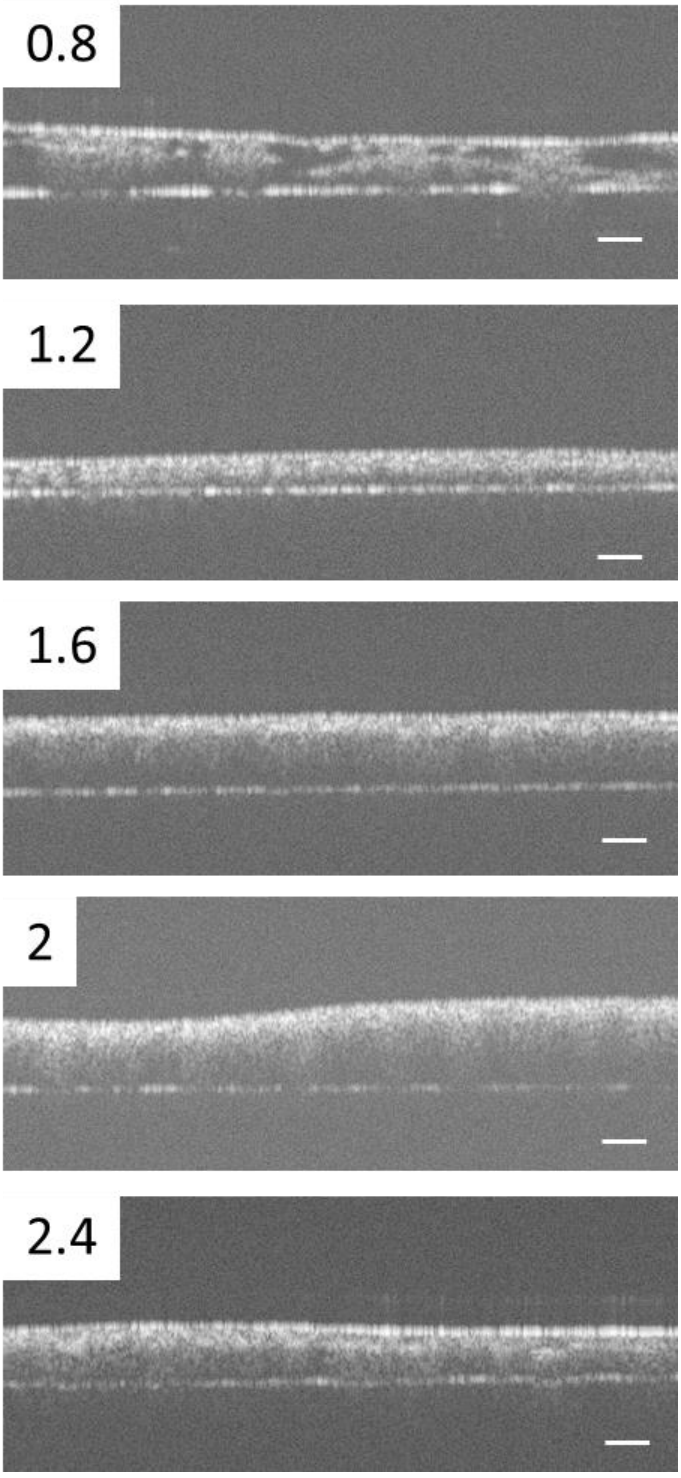

Figure 3.7. Thickness of films varies with increased wt% of PHBHHx. OCT interference patterns of PHBHHx films of 0.8, 1.2, 1.6, 2.0 and 2.4 wt%. Images were generated by measuring reflections of light from below the surface of the polymer sample. Images were then analyzed using image J software, taking an average thickness from 9 randomly chosen sites. Scale bar added using image J, = 0.1mm.

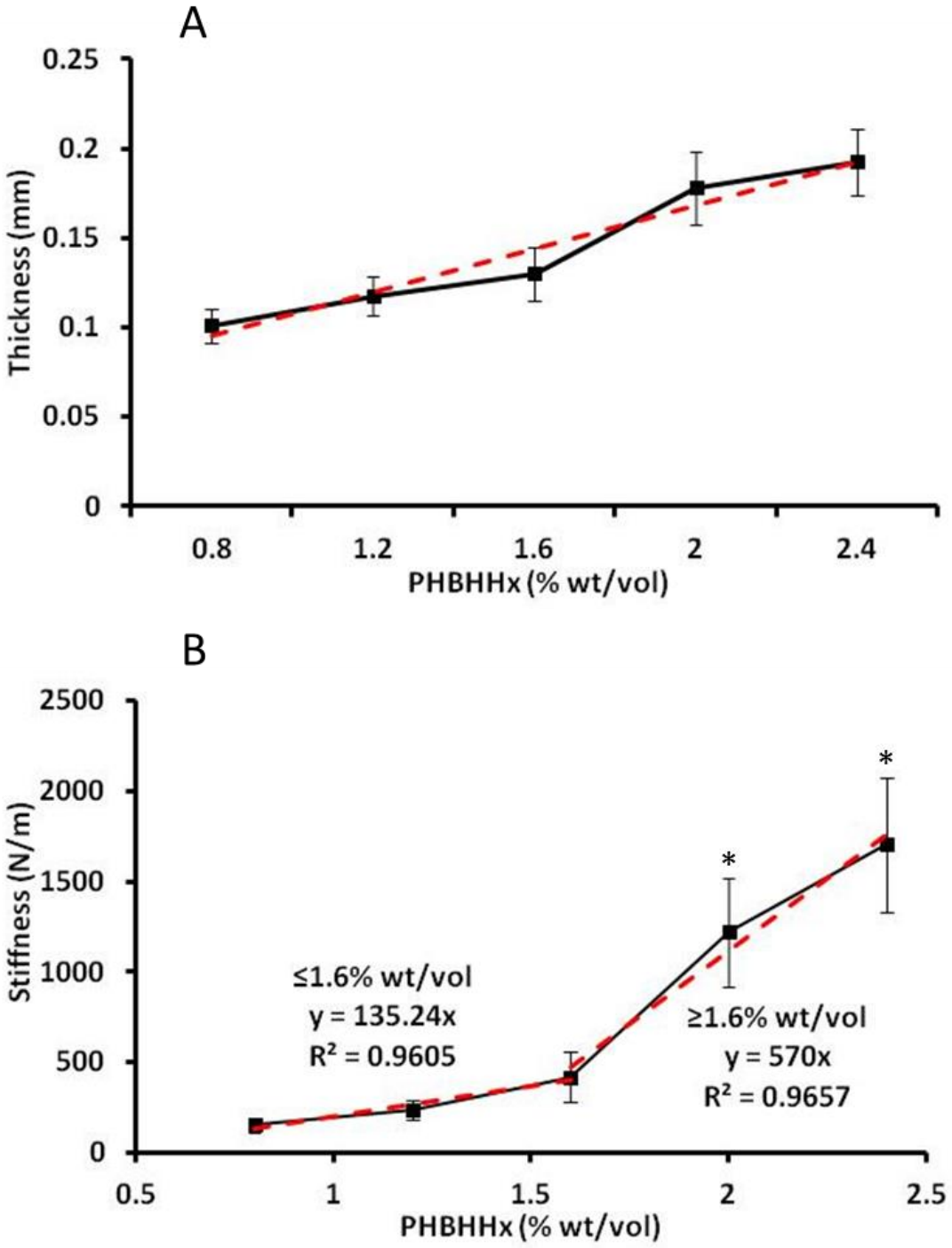

Figure 3.8. Characterisation of PHBHHx films. A: Optical Coherance Tomography and Image J software analysis were used to determine PHBHHx film thickness. Average ± 1SD shown on graph, n = 9. B: PHBHHX film stiffness was measured with the BOSE ElectoForce 3200 system. Average ± 1 SD shown on graph, n = 3. * indicates significant increase compared to ≤ 1.6% wt/vol PHBHHx. Trend lines (line of best fit) are indicated by hatched red lines.

Cellular attachment

Rat tenocytes seeded onto PHBHHx films in 21% O_2 displayed a significant increase in film-adherence between 0.8% wt/vol ($3.87 \times 10^4 \pm 2.73 \times 10^4$ cells/film) and ≤2.0% wt/vol (≤9.47 ± 4.46 cells/film, $p \leq 0.02$) (Fig.3.9.A). Similarly the percentage of cells attached to the film in relation to the overall number of cells in each demonstrated a significant increase between 0.8% wt/vol ($19.36 \pm 4.98\%$) and ≤ 1.6% wt/vol (≤$68.38 \pm 7.31\%$, $p \leq 0.02$) (Fig. 3.9.B). The use of physiological oxygen (2% O_2) in RaT PHBBHx film adherence and percentage attachment studies yielded similar results to above. Significant increases in adherence were noted between films of 0.8% wt/vol and 1.6% wt/vol ($0.87 \pm 0.42 \times 10^4$ vs.$8.67 \pm 3.84 - 13.73 \pm 5.36 \times 10^4$, $p \leq 0.05$) (Fig. 3.9.A), demonstrating that RaT cells displayed greater adherence to substrates with a stiffness ≥ 420 N/m. Significant increases in percentage cell attachment were also noted between films of 0.8% wt/vol ($34.37 \pm 8.27\%$) and ≤1.6% wt/vol (≤$84.36 \pm 3.98\%$, $p \leq 0.01$) (Figure 3.9.B). Direct comparison of attachment profiles in 21% O_2 and 2% O_2 revealed a significant increase in cell attachment to 1.6% wt/vol films in 2% O_2 vs. 21% O_2 ($p = 0.05$) (Fig. 3.9.B).

hMSC adherence to PHBHHx films with varying weight/volume ratios was relatively consistent in 21% O_2 across all films tested though a significant increase was noted between films of 1.2% wt/vol ($5.33 \pm 1.15 \times 10^4$ cells/film) and 2% wt/vol ($8.66 \pm 2.33 \times 10^4$ cells/film) ($p = 0.04$) (Fig. 3.9.C). When expressed as a percentage of total cells present in the dish (film and well) considerable variability was noted. Non-significant increases in cell attachment were noted between 1.2% wt/vol ($19.7 \pm 8.4\%$) and 2% wt/vol ($61.1 \pm 22.9\%$) ($p = 0.059$) (Fig. 3.9.D), suggesting that hMSCs require a stiffer substrate than RaT cells for optimal attachment. Reducing atmospheric oxygen to 2% O_2 created a non-significant rise in cellular attachment between 0.8% wt/vol ($0.73 \pm 0.41 \times 10^4$) and

1.2% wt/vol ($1.0 \pm 0.53 \times 10^4$) ($p = 0.63$) (Fig. 3.9.C). Little variation was seen between films where wt/vol ≥ 1.2%. When expressing values as a percentage of total cells present, non-significant increases were seen between 0.8 % wt/vol (28.7 ± 11.8%) and 1.2% wt/vol (53.8 ± 9.7%). However a significant increase is observed when 0.8% wt/vol (28.7 ± 11.8%) and 2.4% wt/vol (77.1 ± 20.6%) ($p = 0.03$) (Fig. 3.9.D) are compared. Taken together this indicated that hMSC cultured in physiological oxygen display an adherence preference for PHBHHx films with stiffness of 240 N/m (vs. 1220 N/m in 21% O_2).

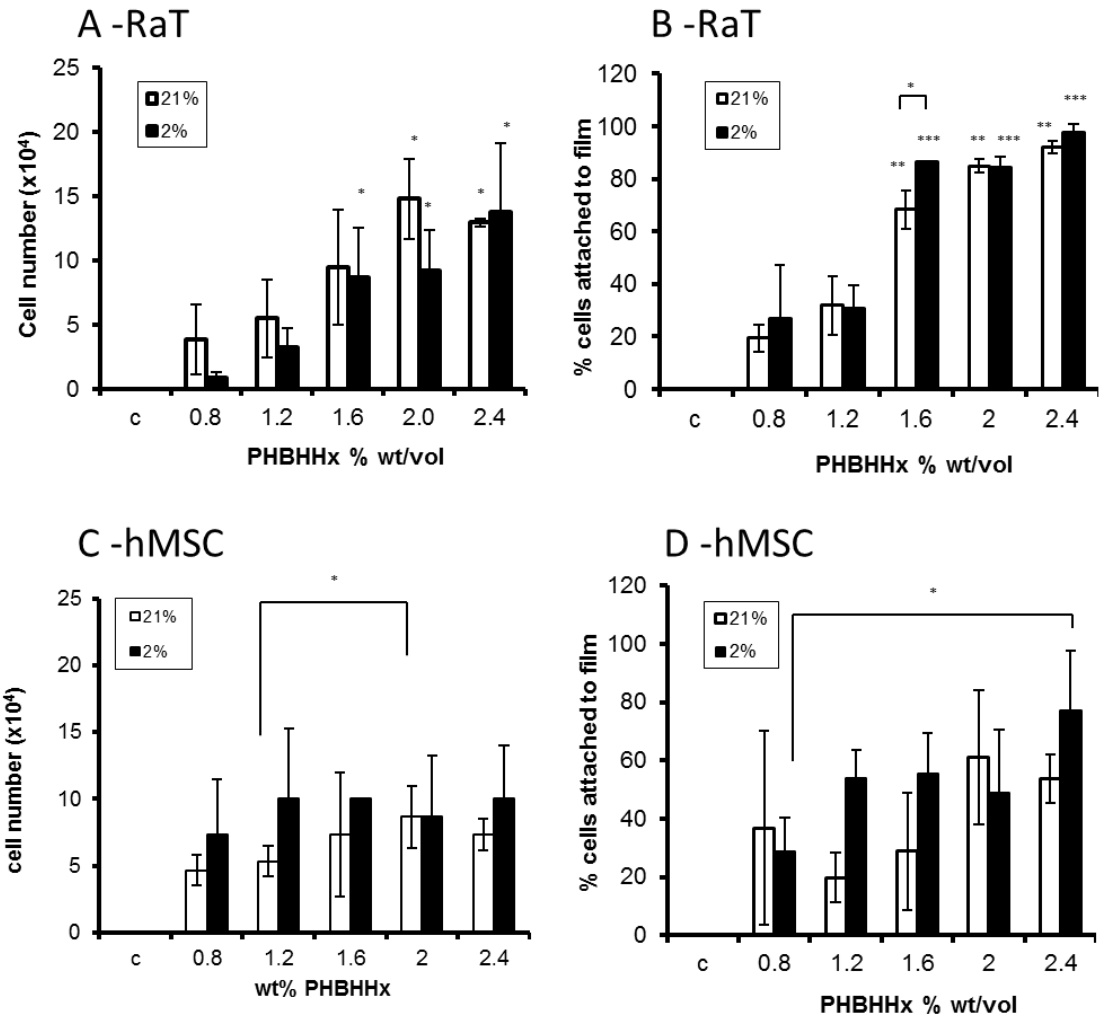

Figure 3.9. Cell attachment to PHBHHx film after 24 hours. A: Number of tenocytes attached to PHBHHx films of varying % wt/vol polymer concentration. B: Tenocyte attachment to films of varying % wt/vol polymer concentration as a percentage of total cell number in the well. C: Number of hMSCs attached to varying % wt/vol concentration of polymer. D: hMSCs attachment to films of varying % wt/vol polymer concentration as a percentage of total cell number in the well. Axes are as labeled, error bars indicate one standard deviation, * indicates p≤0.05, ** p≤0.02, *** p≤0.01 vs. ≤0.8% wt/vol PHBHHx or as indicated.

Cellular Migration

Results so far demonstrate that both MSCs and RaTs adhere to PHBHHx films, with higher stiffness films demonstrating significantly higher MSC and RaT adherence when compared to less stiff films. Our final investigation was intended to determine if cells rapidly migrated into PHBHHx films. As previous observations suggested high MSC and RaT adherence to a 2% PHBHHx film, this concentration was used throughout. No tenocyte or MSC migration was observed into the polymer film after 24 or 72 hours in either O_2 concentration in x-z or y-z directions, as shown by the centre of the green fluorescent signals on the side images being aligned, indicating that cells remained on the film surface (Fig. 3.10). Substantial spreading across the surface of the PHBHHx was apparent after 72 hrs indicating biocompatibility with tenocytes and hMSCs (Figure 3.10 F).

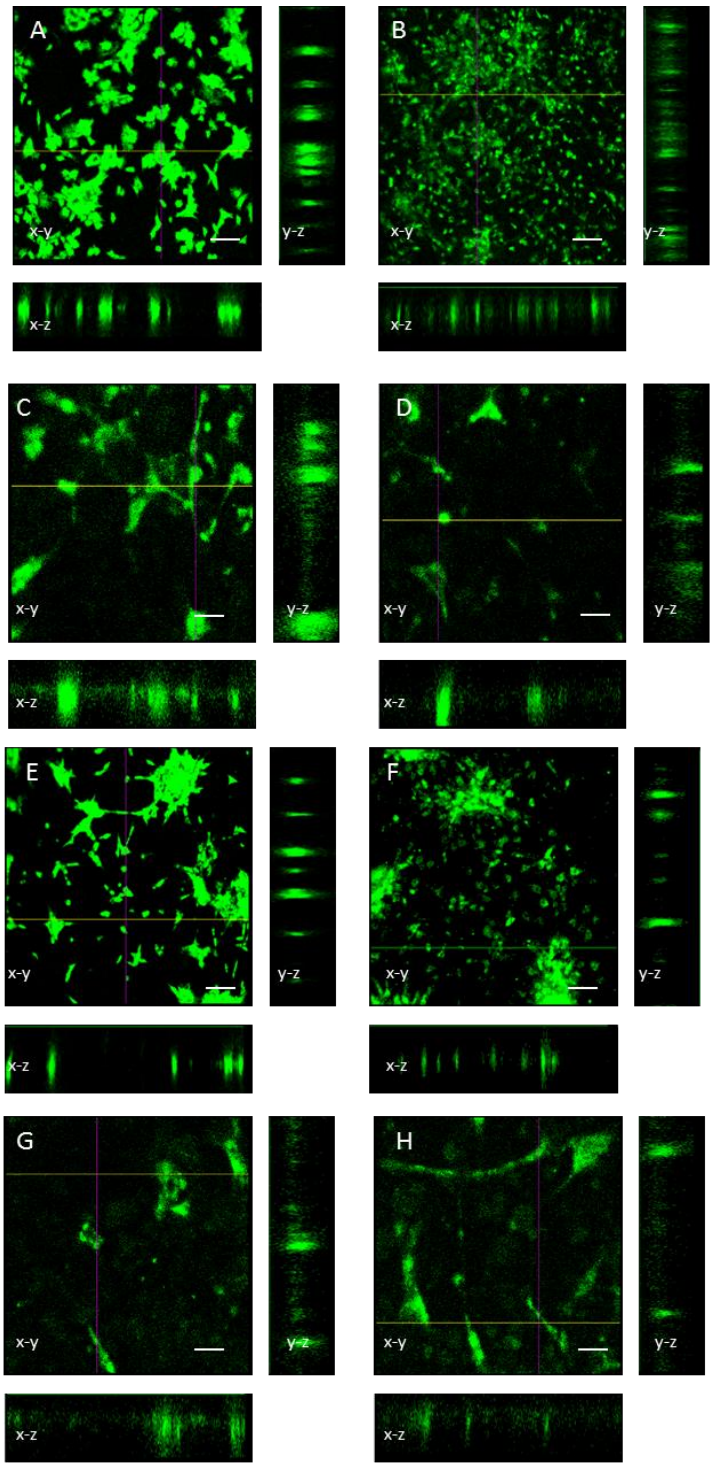

Figure 3.10. Representative images showing surface and cross section views through PHBHHx films gained using confocal microscopy. Cells pre stained with DiO tracking die, appear as a fluorescent signal. A: RaT 21% O_2, 24 hours. B: RaT 21% O_2, 72 hours. C: hMSCs 21% O_2 24 hours. D: hMSCs 21% O_2 72 hours. E: RaT 2% O_2, 24 hours. F: RaT 2% O_2, 72 hours. G: hMSCs 2% O_2 24 hours. H: hMSCs 2% O_2 72 hours. x-y indicates surface view, x-z and y-z indicate reconstructed cross section views through the polymer. Images at 100x magnification, scale bar = 100µm.

3. 4. DISCUSSION

This study demonstrates for the first time that tenocytes will adhere to and spread across PHBHHx polymer films with a preferred rigidity of >420N/m. This supports the assertion of PHBHHx as a candidate material for tendon tissue engineering and adds to the body of literature supporting the biocompatibility of PHBHHx.

PHBHHx has been previously used to culture mesenchymal stem cells, with hMSCs(144)and Adipose derived MSCs (147) being found to adhere to polymer scaffolds in previous studies. Investigation into RaT attachment to PHBHHx films as a total of all cells present in the well demonstrates that when wt/vol ratios of ≥ 1.6% were used a high number of cells adhered to the film in preference to the untreated plastic surface. This can in some part be explained by the increase in stiffness of the polymer film between 1.6% and 2.0% wt/vol. In other words increased polymer rigidity promoted increased tenocyte adhesion. This reinforces a number of previous studies which have demonstrated that material stiffness effects cellular behavior in many ways, including adhesion (173,174). hMSC have previously been shown to adhere to PHBHHx and many other different surfaces with differing mechanical properties (124),(143),(175), explaining why little difference was found between polymer concentrations. As cell fate was not investigated in this study it is not known what, if any, effect on differentiation potency this had. Ongoing 3-D tissue engineering experimentation will address these questions.

Tendon has a poor vascularization and a low mean oxygen concentration (176). We therefore performed our investigation in both room oxygen (21% O_2) and tendon tissue normoxia (2% O_2). Studies looking the effects of different oxygen concentrations on cells have also demonstrated many functional changes in numerous cell types including hMSCs

(70),(71),(85),(177),(178). When comparing 2% O_2 with 21% O_2 only small differences were found between cell number or percentage attachment at the same PHBHHx concentration for either cell type. A non-significant increase was observed in tenocytes (≥ 1.6% wt/vol) in 21% O_2 over 2% O_2, however this was not significant. For reasons we do not fully understand we observed large standard deviations in a number of 2% O_2 sample groups, which could be contributing to this. It should be noted that little difference in the percentage of cells attached to the polymer were observed between the differing oxygen conditions, demonstrating that oxygen tension was not affecting cellular attachment to the films *per se* but that rather reducing the population of cells available for attachment. hMSCs were generally noted to adhere better in hypoxic conditions to all polymer film compositions, however no significant rises were found, possibly due to large inter-group deviations. To our knowledge, this is the first study looking into the *in vitro* effects of oxygen tension on the interaction of primary mammalian cells with polyhydroxyalkanoate scaffolds.

Migration into the polymer surface indicated that cells remained on the surface of the polymer as opposed to migrating into it, suggesting localized polymer degradation had not occurred. This observation is reinforced by reports stating that PHBHHx is broken down *in vivo* (179) and *in vitro* (180) at very slow rates via hydrolysis.

During the early stages of the healing process of damaged tendon *in vivo*, extra cellular matrix secretions have been seen originating from the two damaged ends of the tissue. This ECM was found to contain high concentrations of collagens I and III, and was thus designated “tendon gel” by the author (38). The discovery of ‘tendon gel’ agrees with the

findings of our study, with an ECM prelayer being seen emerging from the tendon samples during explant culture onto which the cells started to migrate after a further few days.

Hypoxic atmosphere (1 – 3% O_2) conditions have been found to be beneficial to cells, delaying senescence and increasing proliferative capacity (72). Mesenchymal stem cells have been shown to have higher proliferation (30 fold increase) in 2% O_2 compared to 21% O_2 (170). Human embryonic stem cell colonies have been found to be less heterogenic and have a more stable self-renewal capacity when cultured in 2% O_2 (85). Tendon derived stem cells have also been found to proliferate faster at 2% O_2 compared to atmospheric conditions (86). This study has demonstrated that tenocytes proliferate faster during the first stages of culture in 2%, but that this difference was not maintained over a longer culture period. It was also noted that cells did not migrate from tendon tissue samples in 2% O_2, leading to the conclusion that tenocyte isolation via explant requires higher than physiological oxygen levels to occur.

3. 5. CONCLUSION.

This investigation demonstrates that tenocytes and hMSCs can adhere to and spread across PHBHHx films over 24 and 72 hour time periods. Film scaffolds fabricated with ≥1.6% wt/vol polymer/solvent, with a stiffness ≥ 420 N/m are the most effective in supporting this activity with RaT cells, however hMSCs displayed a capacity for adhesion to all polymer films of stiffness ≥ 240 N/m. However, other uninvestigated properties of the films could also be contributing to the greater cellular adhesion, such as wettability, porosity or localized surface chemistry. Physiological normoxia (2%O_2) increased hMSC adhesion to most PHBHHx films, however no significant differences were seen due to large intergroup variation and little effect was observed on RaT cell adhesion. PHBHHx can now be considered to be a potential material for use in future tendon tissue engineering application.

Chapter 4.

Design of a PHBHHx/collagen hybrid scaffold for tissue engineering applications.

4.1. INTRODUCTION.

Many different materials have been investigated as possible tissue engineering scaffolds. These include natural materials, such as collagen (130) and silks (132) (133) or manufactured materials such as polymers (142). A current focus for clinical application is on blending these materials to form a hybrid design to both encourage cellular in-growth and provide mechanical support during the remodelling stage of tissue recovery (12) (181).

PHBHHx has great potential as a material for *in vitro* tissue engineering owing to its adaptable mechanical properties, biodegradability and apparent compatibility with many different mesenchymal cell types including rabbit bone marrow derived MSC (143), human adipose derived stem cells, human keratinocytes (145) mouse fibroblasts (146) and rat peripheral nerve cells (148), rat tenocytes and human MSCs (182).

Collagen is a major structural component of many different extracellular matrices. Tissue collagen composition varies according to function. The dry weight of articular cartilage matrix can contain 75 and 80% type II collagen depending on its position in the joint, allowing it to resist the high compression forces found in areas such as joints and intervertebral disks (183). Tendon and ligament dry weight matrices can contain approximately 90% type I collagen arranged in hierarchical fibrils to accommodate high tensional forces (176). Several collagen types (I, III, IV) vary with increased skeletal muscle activity, for example prolonged intense exercise can increasing the abundance of type IV collagen (184), whereas bone contains high amounts of collagens I and III allowing for bones to be slightly flexible during movement (185). Due to its abundance and prevalence collagen is viewed as an appropriate scaffold material, especially in orthopedic tissue engineering due to the wide-scope of potential applications and complementary clinical trial data (186).

Adult tissues contain multiple cell types; however dominant cell types are found within individual tissues. Tenocytes account for over 90% of the cellular mass of a tendon and are responsible for maintaining the collagen based extracellular matrix that forms the tendon structure (25). Cartilage has a similar percentage of chondrocytes that are again responsible for extracellular matrix maintenance (187). Bone has two main cell types responsible for maintaining extracellular matrix, osteoclasts which secrete molecules to break down calcified tissue and osteoblasts which are responsible for rebuilding it (188). Skeletal muscle cells differ from previous examples in that they play a larger role in tissue contractile function rather than extracellular matrix production (92). However, fully differentiated cells can be unsuitable for tissue engineering applications due to their limited proliferation capacity when cultured *in vitro*, so exploration of other less differentiated cells has become widespread (189) (190) (191).

MSCs are a useful cell source for tissue engineering as they can be easily sourced, isolated and cultured *in vitro* (192). Exposure of MSCs to tensile forces and/or growth factor supplementation is described as producing cells that resemble connective tissue cells in expression marker profile and physiological activity (53) (65) (39) (53) (65) (92). Pluripotent human embryonic stem cells (hESC), derived from the inner cell mass of pre-implantation blastocysts are also strong candidates for tissue engineering application (119). They are the precursor to almost all adult tissues in the body, including the mesenchyme layer of cells and thus tendon- (193), cartilage- (194)(195) and bone-like cells (190) have all been derived during *in vitro* and *in vivo* differentiation. hESCs are relatively readily available and could potentially be used to produce an allogeneic “off the shelf” cellular product following on from current safety trials underway in the UK and the USA.

Here we sought to determine the suitability of PHBHHx and collagen hybrid constructs for use with hESC, spontaneously-differentiated hESC (SDhESC), and hMSC with a view to creating a tissue engineered product.

4.2. MATERIALS AND METHODS.

4.2.1. PHBHHx scaffold preparation and characterisation:

PHBHHx tubes were made according to section **2.3.3** and made porous by using the method outlined in section **2.3.4.** Before experimental use scaffolds were sterilised with immersion in 70% IMS followed by 24 hours UV light exposure. Immediately prior to use, scaffolds were immersed in cell specific media for 1 hour. Characterisation of scaffolds was carried out using electron microscopy and image analysis as outlined in sections **2.6.2** and **2.6.3**.

Collagen Scaffolds were formed by using method **2.3.5.** Gels were injected into the casting apparatus and set via temperature elevation to 37^{o}C for 2 hours. Gels were formulated to either 1.5 mg/mL or 3 mg/mL final collagen concentrations. Measurements of tube length and diameter after cell seeding were taken at days 0, 5, 10, 15 and 20.

PHBHHx/Collagen hybrid scaffolds were created by injecting 1.5 mg/mL or 3mg/mL collagen gel (as described previously) seeded with hESC, SDhESC or hMSC at a 1x10^{4} cells/mL concentration into the lumen of the PHBHHx tube before incubation at 37^{o}C for 2 hours. After incubation, constructs were transferred to 6-well plates and immersed in 3 mL cell-specific complete media (**2.2**).

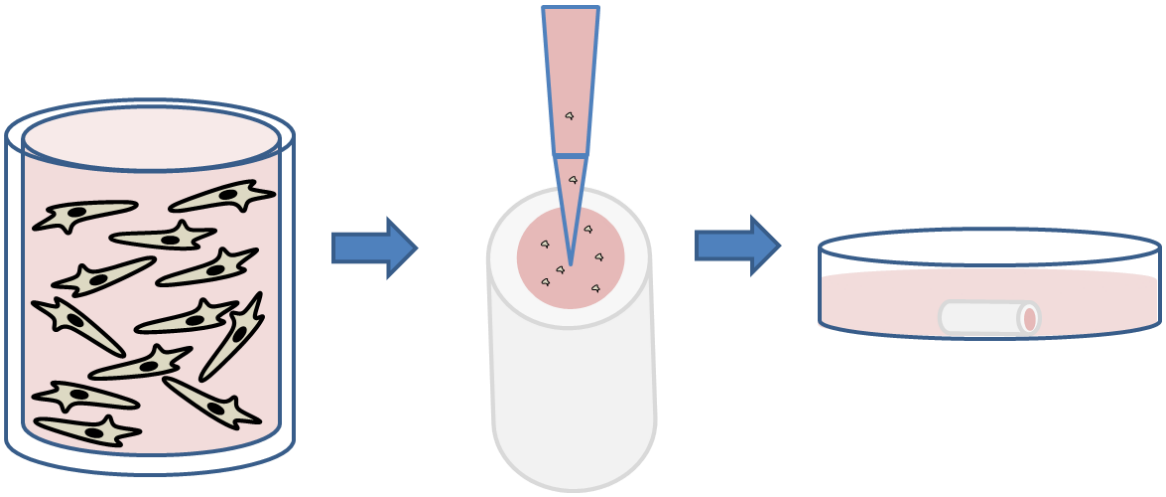

Figure 4.1. Production of PHBHHx/collagen hybrid scaffolds. Cells are suspended in a neutralised collagen gel then quickly injected into a pre prepared PHBHHx tube lumen. Gels were then allowed to set via temperature regulation (37°C for 2 hours) before immersion in complete, cell specific media placed in static culture.

4.2.2. Collagen gel contraction

Collagen gels were made as previously described in section **2.3.5** at final collagen concentrations of 1.5 or 3 mg/mL. hMSCs, SDhESCs and HESCs were seeded into collagen gels at either $1x10^3$, $1x10^4$ or $1x10^5$ cells/mL, as section **2.3.6**. With gels solidifying at 37°C for 1.5 hours, before immersion in complete, cell specific media. Measurements of gel length and diameter were made at 0, 5 10 and 20 days, with the zero time point being before media immersion. Measurements were made using sterile callipers, with measurements being taken at both ends and the centre point of the gel, with an average being taken as section **2.4.2**.

4.2.3. PHBHHx tube pore size and density

Pore size was quantified by taking $1mm^2$ areas of electron microscope images and analysing with Image J software. Random areas were taken, with each pore measured

along its longest length using the line draw tool, giving a value of pixels for each pore. This was then adjusted using the appropriate scaling factor to convert to millimetres. Pore density was measured by taking $1mm^2$ areas of electron microscope images and analysing using the grid and counter tools in Image J software. The grid was overlaid over the original image, and all visible pores counted. Pores were defined as being areas of the surface that were not uniform with the surrounding area, i.e., any indent that could be seen.

4.2.3. Cell Culture.

hMSCs were isolated from human bone marrow using adherence culture as described in section **2.2.3**. Culture media was changed twice weekly and cells passaged at 90% confluency using method **2.2.1.b**. according to 1:2 split ratios.

hESC: SHEF1 were cultured in feeder free conditions according to the methodology outlined in section **2.2.4** using media pre conditioned by mouse embryonic fibroblasts (MEF). During expansion hESC media was changed daily and cells were split 1:2 at 90% confluency with fresh Trypsin/EDTA dissociation for <1 minute. Centrifugation and passage regimes are as described for hMSC.

Spontaneous Differentiation of hESC: hESC (SHEF1) were seeded into Matrigel-coated T-75 flasks at fixed densities (1×10^6 per flask) in conditioned hESC media. Spontaneous differentiation was induced using protocol **2.2.4.e**.

Cell Viability: Cell viability was determined with the trypan blue dye exclusion assay (Sigma Aldrich) according to the method outlined in **2.2.1.f**.

4.2.4. Cellular positioning and viability.

The position and spread of cells was found by fluorescence microscopy. Gels were removed from the tubes, dissected longitudinally down the centre with a scalpel blade and

placed cut side down on a well plate. A fluorescent live dead stain was then performed using protocol **2.2.1.g** and images taken using a Nikon microscope (section **2.8.5**), with representative images taken of the edge and centre of the gel. Image J analysis was then used to count viable (green) and non-viable (red) cells, gaining a percentage of viable cells at the centre and edge of the gel.

4.2.5. Osteogenesis.

Osteogenic differentiation was induced by the use of osteogenic differentiation media (DMEM, 10% FBS, l-glut, NEAA, 0.1μM Dexamethasone, 10mM β- Glycerophosphate) (196). Cells were suspended in constructs and cultured in static culture for a maximum of 20 days, with sampling at days 0, 5, 10 and 20. A control of standard MSC media was run concurrently. At each time point, gels were removed from tubes, immersed in 0.4% type IV collagenase for 1 hour at 37^{o}C, pelleted and resuspended in lysis buffer, after which molecular characterisation was performed.

4.2.6. Molecular characterisation

RNA isolation, Reverse transcriptase polymerase chain reaction and electrophoresis were performed using the methods described in section **2.4.3**. Primers investigated were BACT (housekeeping), SOX9 (cartilage), RUNX2 (bone), TNMD (tendon) and PPARγ (adipose).

4.2.6. Statistical analysis

Differences between groups were analysed by one-way ANOVA with Post-hoc Tukey's Multiple Comparison analysis. A 'p' value less than 0.05 was considered to indicate statistical significance. Data are presented as mean ± standard deviation (SD).

4.3. RESULTS.

4.3.1. Collagen Gel Contraction

We first sought to determine the maximal cell seeding density of hESC, hMSC, and SDhESC into collagen gel tubes at which contraction would not occur and cell viability was maintained. hESCs did not contract collagen gels at any collagen concentration or cell density combination explored over a 20 day time (Fig. 4.2 A, D, G, J). Unlike the parental hESC, SDhESCs with an initial cell seeding density of 1 x 10^5 cells/mL contracted 1.5 mg/mL collagen gel length and diameter after 10 days (1.63 ± 0.15 cm vs. 2.43 ± 0.06 cm, p = 0.02) (Fig. 4.2 B). Contraction continued progressively at days 15 (1.46 ± 0.25cm vs. 2.24 ± 0.06 cm, p = 0.04) and 20 (0.87 ± 0.31 vs. 2.37 ± 0.15 cm, p = 0.02). Gel diameter contracted across these time points ($p \leq 0.03$) (Fig. 4.2 E). SDhESC did not contract 3 mg/mL gel length or diameter irrespective of initial cell seeding density (Fig. 4.2 H, K).

hMSCs contracted both the length (1.26 ± 0.07 cm vs. 2.93 ± 0.05 cm, p=0.002) and diameters (0.23 cm ± 0.03 cm vs. 0.46 cm ± 0.06 cm ± , p = 0.035) of 1.5 mg/mL collagen gels after 10 days with an initial seeding density of 1 x 10^5 cells/mL (Fig. 4.2C, F). Continued contraction was also apparent for both gel length and diameter at days 15 (p = 0.02) and 20 (p = 0.002). Gel diameter also significantly reduced at these time points ($p \leq 0.02$). Where initial cell seeding densities of ≤1 x 10^4 cells/mL were used no significant collagen gel contraction was observed (Fig. 4.2C, F). hMSCs did not contract 3 mg/mL collagen gels (Fig. 4.2 I, L).

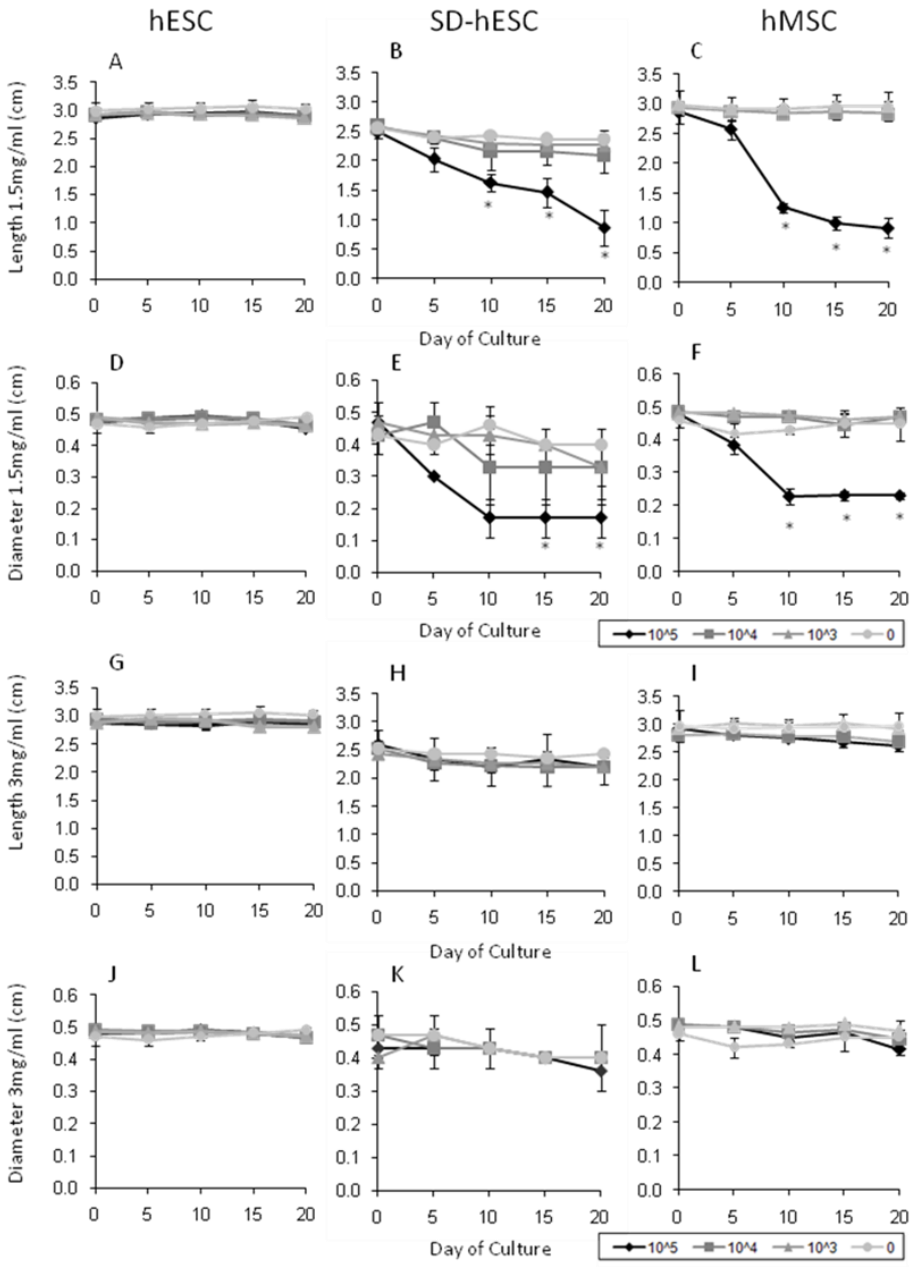

Figure. 4.2. Collagen gel contraction is dependent on both collagen concentration and cell concentration. A, D. 1.5 mg/mL gels do not contract when seeded with hESCs. B, E. significant contraction in both length and diameter seen after 10 days culture in 1.5 mg/mL gels seed with 1 x10^5 SDhESCs/mL. C, F. significant contraction in both length and diameter seen after 10 days culture in 1.5 mg/mL gels seed with 1 x10^5 hMSCs/mL. G, J. 3 mg/mL gels do not contract when seeded with hESCs. H, K. 3 mg/mL gels do not contract when seeded with SDhESCs. I, L. 3 mg/mL gels do not contract when seeded with hMSCs. Graphs show mean ± 1SD, n = 3. Significance determined using one way ANOVA and Tukeys post hoc analysis, $p \leq 0.05$.

4.3.2. PHBHHx Tube Pore Characterisation

PHBHHx tubes were manufactured to contain salt crystals that could be leached out to generate pores distributed across and within the tube structure. Analysis determined that pores had an average diameter of 0.025 ± 0.019 mm (n = 330) at a density of 68.6 ± 10.55 pores/mm^2 (n = 5) (Fig. 4.3). The majority of pores had a diameter of ≤ 0.04 mm [89.1 % (294/330)] while 33.0% had diameters in the range of 0.02 mm ≥ 0.03 mm, and. 1.5% (5/330) of pores had diameters ≥ 0.1 mm.

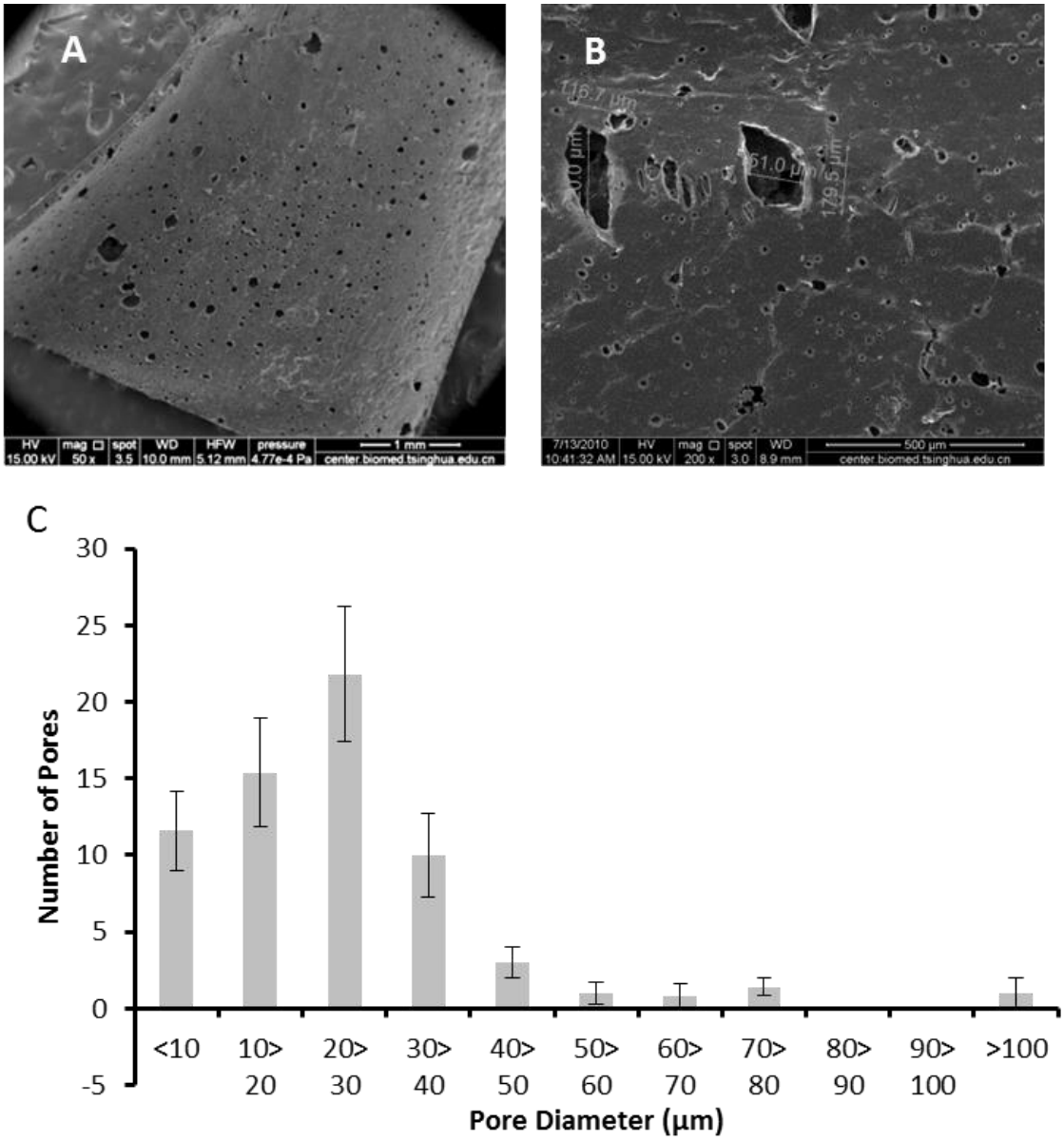

Figure 4.3. PHBHHx tube pore size determination. A: PHBHHx tube structure at 50x magnification. B: Representative tube section at 200x with line measurement indicators showing pore diameter. C: Pore diameter histogram. Measurements were taken from random 1 mm^2 regions of polymer tube (n=5, total number of counted pores = 330). Error bars indicate one standard deviation.

4.3.3. Cell Viability in Collagen Gels

Subsequent analysis of hESC cell viability at day 20 demonstrated that with 1.5 mg/mL gels ≤ 8.4 ± 7.5 % of cells remained viable (Fig. 4.4 A) and in 3 mg/mL gels ≤ 1.4 ± 2.4 % cells were viable (Fig. 4.5 B). SDhESC viability after 20 days was determined as ≥ 48.6 ± 6.8% in 1.5 mg/mL gels (Fig. 4.4 A) and ≥ 52.3 ± 6.6 % in 3 mg/mL gels (Fig. 4.4 B) for all cell densities. hMSC viability after a 20-day incubation period within collagen gels was ≥ 78 ± 6.3 % in 1.5 mg/mL (Fig. 4.4 A) and ≥ 89 ± 8.5% in 3 mg/mL (Fig 4.4 B) gels at all cell densities tested.

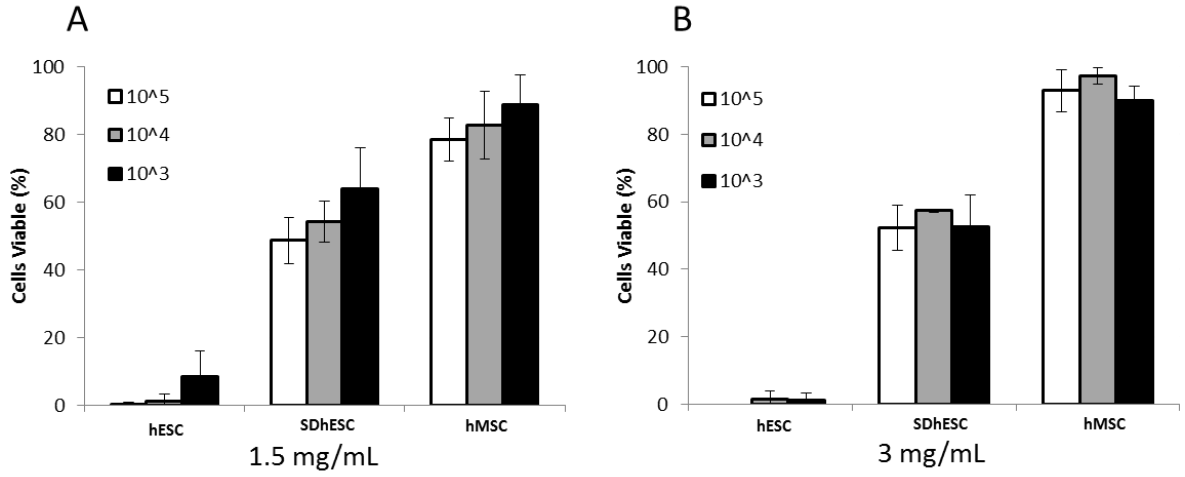

Figure. 4.4. hMSC and SDhESC retain high viability levels after 20 days collagen gel suspension. % of trypan blue negative cells found as a total of all cells. A: cells seeded in 1.5 mg/mL collagen gels. B: cells seeded in 3 mg/mL collagen gels. Graph shows mean ± 1 standard deviation, n = 3.

4.3.4. Viability in PHBHHx/Collagen hybrid scaffolds

PHBHHx/collagen/cell scaffolds were immersed in culture medium and maintained over a 20 day period before cell removal by enzymatic digestion. hMSCs retained high viability, 87.7 ± 4.6% after 20 days in culture (Fig. 4.5). SDhESCs displayed lower viability, with 46.2 ± 16.1% viable after 20 days in culture when compared to hMSC. These values are broadly similar to those obtained following on from incubation in collagen gels alone indicating that the porous PHBHHx scaffold had little impact on cell viability.

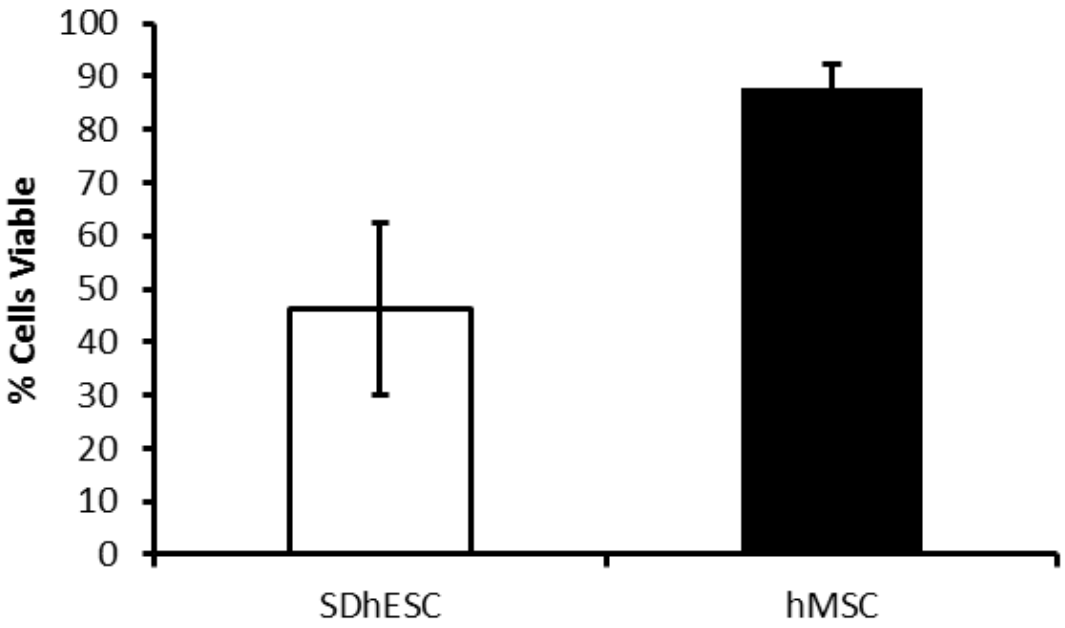

Figure 4.5. hMSC and SDhESC retain viability after 20 days in a PHBHHx/Collagen gel hybrid scaffold. An initial seeding density of 1 x 10^4 cells/mL was evaluated for viability with Trypan Blue staining after 20 days. % of viable (trypan blue negative) cells shown, (n = 5). Error bars indicate one standard deviation.

4.3.5. Cell positioning

Positioning in gels was monitored by removing gels from constructs, transversely slicing and imaging at representative areas of the edge and centre using fluorescence microscopy. Day 0 images were taken immediately after gelation. Cells were evenly spread throughout the gel, with high viability seen. At day 5 cells had become more fibroblastic in shape, becoming more elongated compared to day 0. Day 10 cells were again evenly spread throughout the gel, with more non-viable cells seen than on previous days. Cells at day 20 were found to be evenly spread and viable at both the centre and edge of the gel (Fig.4.6).

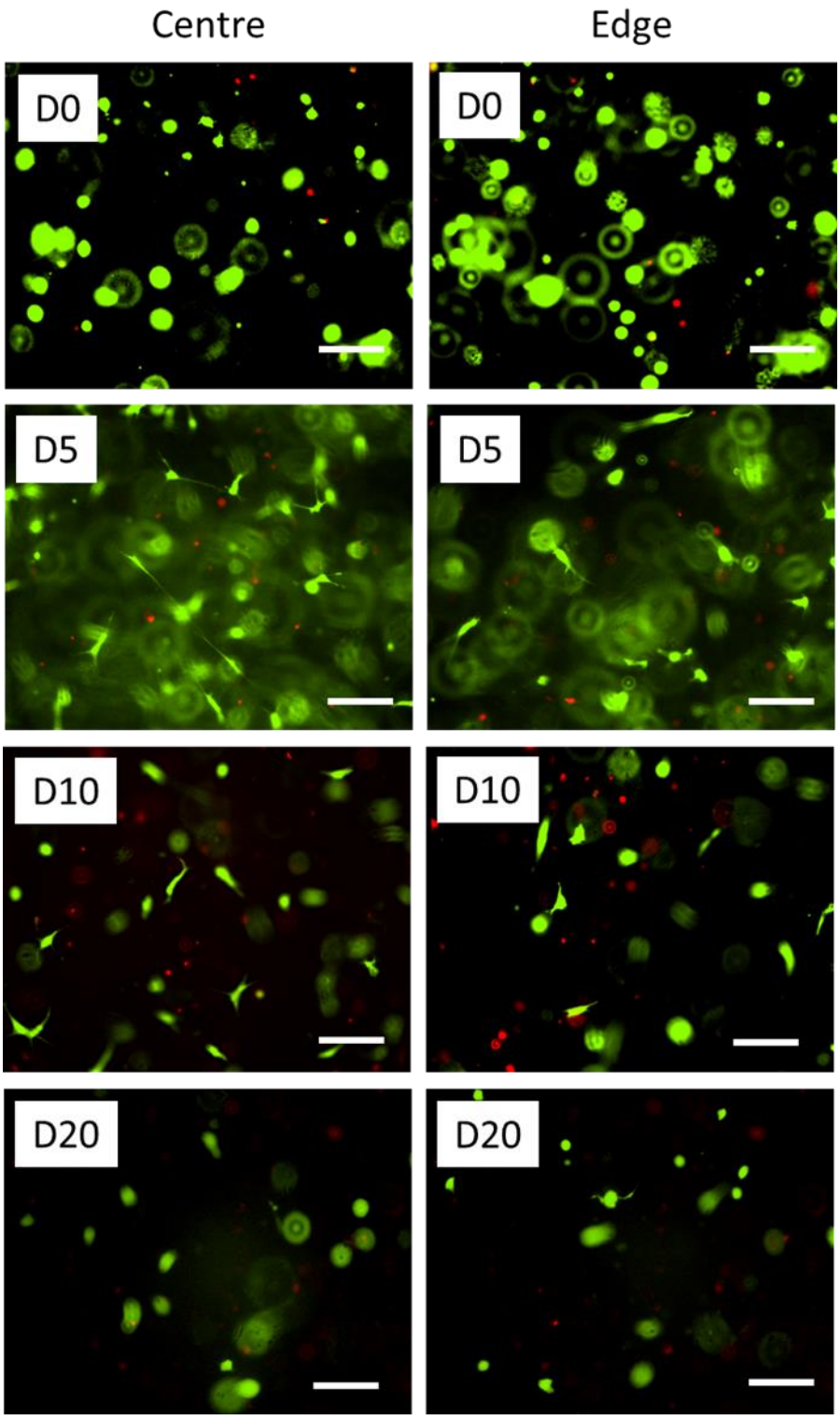

Figure 4.6. hMSCs spread throughout the gel throughout 20 days culture. Gels were removed intact from PHBHHx tubes, sliced transversely in half and images taken using a live dead fluorescence assay in representative areas of the edge and centre of gels, using fluorescence microscopy. Images at 100x, scale bar = 100µm.

Image analysis was performed using image J software, using the counter tool. Viability at day 0 was found to be 91.1 ± 2.5 % in the centre and 88.3 ± 2.3 % at the edge. Day 5 viability was found to have dropped to 79.2 ± 1.9% and 74.9 ± 5.2% at the centre and edge respectively, with a larger drop observed at day 10 at the edge of the gel compared to the centre (58.6 ± 0.7% vs. 76.2 ± 4.1%). Day 20 viability was found to be similar in both locations (71.9 ± 2.7% centre, 74.3 ± 2.0% edge) (Fig. 4.7).

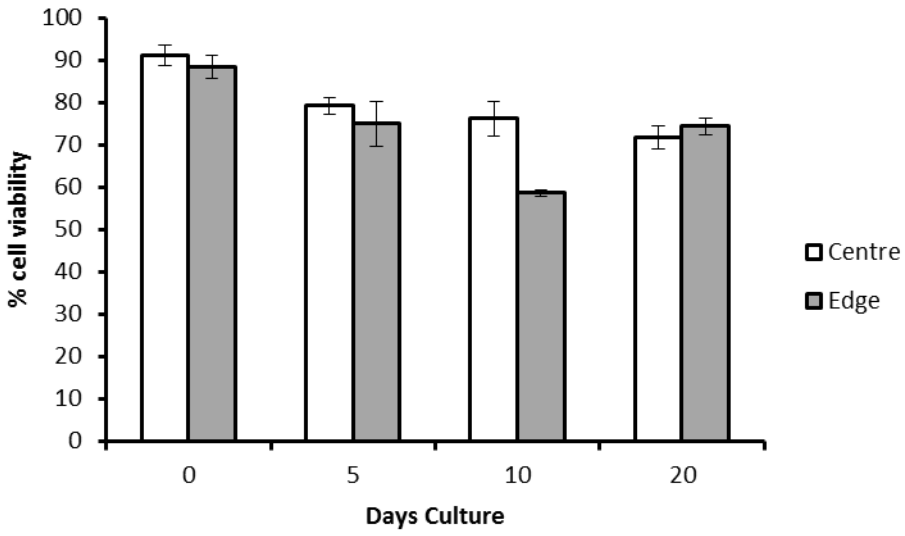

Fig. 4.7. Viability of hMSCs at the centre and edge of gels removed from PHBHHx tubes over time. Gels were removed, transversely sectioned, stained and imaged using fluorescence microscopy, before image analysis using image J software. Graph shows mean ± 1SD, n =3.

4.3.6. Molecular characterisation

We finally sought to determine if the PHBHHx/Collagen hybrid scaffold played a role in directing spontaneous differentiation of hMSC or SDhESC into select musculoskeletal lineages. SOX-9 expression was maintained until Day 10 but lost thereafter whereas RUNX2 expression was rapidly lost in hMSC (Fig. 4.8.A). SOX-9 expression was again maintained until Day 10 but lost thereafter while RUNX2 expression was not detected at any time point in SDhESC (Fig. 4.8.A). BACT was included as a loading control. We were unable to detect expression of either PPARγ or TNMD in experimental samples indicating the absence of differentiation into either adipose or tendon lineages.

4.3.7. Induced differentiation

As a proof of concept and confirmation that differentiation can be achieved in stem cells in the construct, osteogenesis, chondrogenesis and adipogenesis was induced in hMSCs by changing culture media. RT-PCR for the RUNX 2 gene was found to be absent after day 0 in control media. Osteogenic media prolonged RUNX2 expression throughout 20 days culture, although expression was reduced at days 5 and 10 (Fig. 4.8.B.)

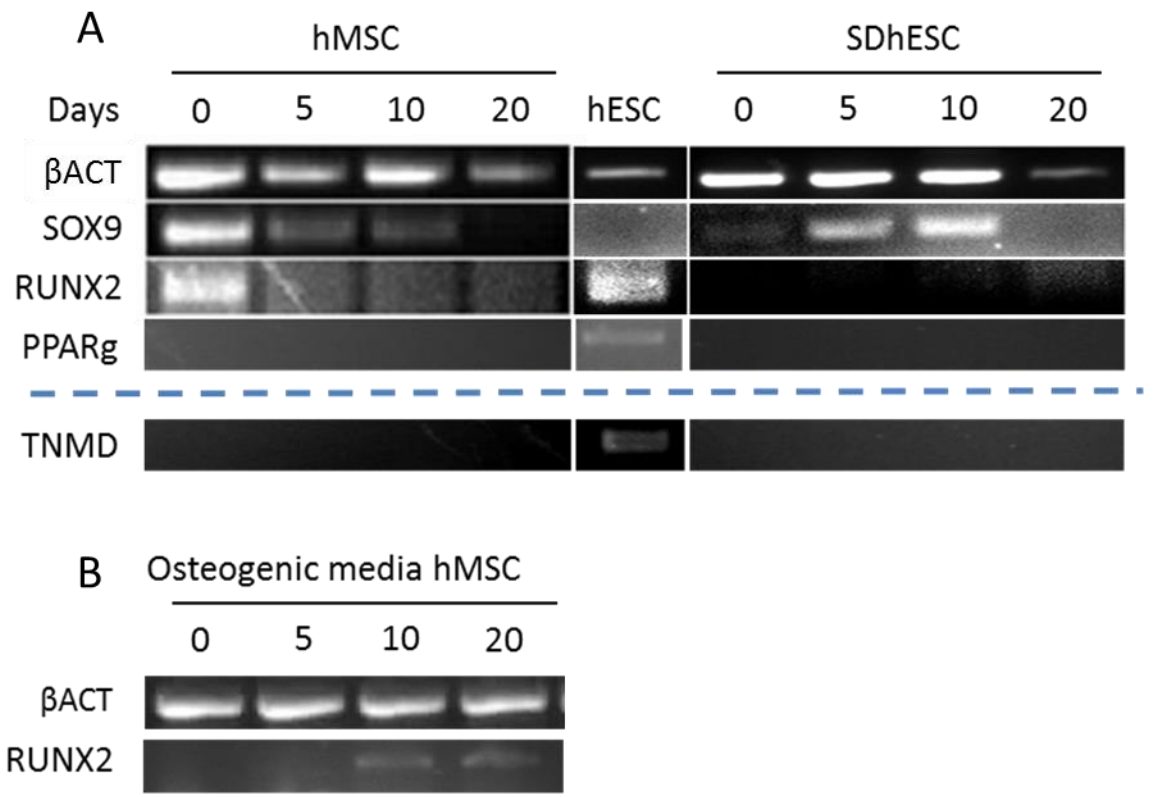

Figure 4.8. A: hMSC and SDhESC did not undergo spontaneous differentiation after 20 days PHBHHx/Collagen gel scaffold encapsulation. RT-PCR-based evaluation of BACT, SOX9, and RUNX2 expression levels after 0, 5, 10 or 20 days in construct. Undifferentiated hESC are included as control for SDhESC. TNMD used a pre-established positive control. B: Osteogenic media supplementation results in RUNX2 being expressed in hMSCs over 20 days in PHBHHx/collagen hybrid scaffolds. Scaffolds were immersed in osteogenic media in static culture conditions, with cell lysates taken at days 0, 5, 10 and 20 and RT-PCR performed as described previously.

4.4. DISCUSSION.

Tissue engineering and regenerative medicine aim to use scaffolds and cells to regenerate and restore function of tissue lost through damage, disease, and disorder. The use of PHBHHx has been explored by many labs investigating multiple potential applications including cellular interactions and its use as a scaffold in tissue engineering)(142),(143),(145),(146),(148),(182). Here we demonstrated the interaction of human embryonic and mesenchymal stem cells with collagen gels and PHBHHx/collagen hybrid scaffolds using a range of static *in vitro* experimentation to assess suitability for further tissue engineering applications. We show that hMSCs and SDhESCs can be cultured for extended periods on PHBHHx/collagen hybrid scaffolds and thereby confirm its suitability as a model system.

The application and suitability of PHBHHx as a scaffold material in orthopaedic models and for human and animal stem cell biocompatibility has been described elsewhere (14), (36),(38),(182),(122),(197),(114),(180),(34),(35), with bone tissue being formed by rat MSCs (197) and cartilage like structures formed by human adipose derived stem cells when seeded onto PHBBHx scaffolds (147). We therefore conclude that PHBHHx is a suitable material for stem cell based tissue engineering and does not prevent differentiation toward the osteogenic lineage when osteogenic supplements are added to media.

Type I collagen gels supported the differentiation of murine ESCs into either osteogenic or chondrogenic lineages when seeded into 2D and 3D 1.2 mg/mL scaffolds. The additional presence of lineage specific supplements was found to further increase differentiation above that found in control collagen gels, with apparent high cell viability after 15 days in culture (198). Human and murine ESC culture in 0.75 mg/mL type I collagen gels has also been achieved by pre differentiating cells into embryoid bodies before seeding onto gels

and covering with DMEM/F12 media, stimulating differentiation into fibroblast like cells over a 21 day period (199). Undifferentiated ESCs were not compatible with our PHBHHx/collagen gel hybrid scaffold system. Our study has demonstrated that hESCs required a prior spontaneous differentiation step induced by exposure to foetal bovine serum prior to collagen gel suspension to shift cell phenotype away from that of a self-renewing ESC into a partially differentiated heterogeneous population. We found that pre-differentiated hESC in PHBHHx/collagen gel hybrid scaffolds demonstrate a 40-60% cell viability after 20 days continuous static culture.

Collagen gel contraction by fibroblastic cells is well established (200). This investigation sought to find the concentrations of collagen and cells that would not result in large collagen contraction over 20 days, potentially allowing for the construct to be implanted into a wounded tendon and the gel remain in contact with the damaged tendon ends for as long as possible, potentially increasing the probability of tissue integration. Decreasing collagen gel concentrations from 2.6 to 1.3 mg/mL was reported as having a greater impact on gel contraction kinetics than increasing the rabbit MSC density by the same fold increase (500K to 1M cells/mL) (167). Similarly human corneal fibroblasts can contract a 4.5mg/mL collagen gel over a 25 day static culture period when seeded at a cell concentration of 5×10^5 cells/mL, but not 1×10^5 cells/mL (169). These reports correlate with our observations where little contraction was observed in the 3 mg/mL groups, and the rate of contraction slowed with 1.5 mg/mL gels seeded with lower cell densities. We have successfully identified a cell: collagen ratio with very little collagen contraction over 20 days static culture, yet retain high cell viability in the absence of additional stimuli, for application in *in vitro* studies utilising either hMSCs or SDhESCs.

SOX-9 is a master regulator of chondrogenic differentiation and is expressed by cells in both pre-cartilaginous and mature cartilage tissue (201). A cyclical, compressive

mechanical loading regime promotes chondrogenic differentiation of rabbit MSCs as demonstrated by increased SOX-9 and collagen II expression (202). We found that in the absence of either mechanical or biochemical stimuli SOX-9 expression was lost rapidly in hMSC or after approximately 10-days in SDhESC.

B-actin is frequently used as a housekeeping gene due to its consistent presence as a cytoskeletal component of mammalian cells, and is commonly used as a marker of cellular viability (203). We noted expression of β-Actin at all-time points which when coupled to the high cell viability provides an additional demonstration of viable cell transcriptional activity. RUNX2 transcription factor is critical for the promotion of osteogenic differentiation (204). A cyclic compressive strain upregulated RUNX2 in MSC seeded collagen-alginate gels demonstrated up regulation after 21 days (205). Mouse ESCs cultured on collagen I coated flasks displayed little RUNX2 expression change over tissue culture plastic after 21 days in static culture, remaining low throughout the experiment(206). Similar to our observations with SOX-9 we did not detect noticeable upregulation of RUNX2 during our experimental time course in the absence of mechanical stimuli.

4.5. CONCLUSION

Herein we have demonstrated that undifferentiated hESCs are not viable after 20 days culture within a PHBHHx/Collagen gel hybrid scaffold whereas hMSCs and SDhESCs demonstrated good viability over the long term. Gel contraction was negligible with collagen concentrations of 3 mg/mL with all cell types at all investigated seeding densities over 20 day's static *in vitro* culture. We were unable to detect any evidence of spontaneous differentiation into fat, bone, cartilage, or tendon lineages in static culture, but osteogenesis was achieved using osteogenic media. In summary we have developed a porous PHBHHx/Collagen gel hybrid scaffold which features good cell compatibility and an absence of spontaneous lineage-forming differentiation cues. This scaffold system is readily translatable into dynamic systems and differentiation models across multiple lineages.

Chapter 5

Mechanical Stress and Growth Factors with Cell Seeded PHBHHx/Collagen Hybrid Scaffolds.

5.1. INTRODUCTION.

Mechanical loading has been used to influence cell/matrix behaviour in many different ways. A current hypothesis suggests that for stem cells to take on connective tissue morphologies some form of mechanical loading is required (164). Static mechanical force, where a load was applied to the construct continuously for a period of time, has been used to create neotendinous structures from collagen gels. By applying a constant strain of 50% for 24 hours to acellular unstructured collagen before adding a decorin cross linker, a structure similar to rat tail tendons could be created (23). More recent studies have focussed on evaluating different mechanical stimulation methods. Comparisons between static and dynamic mechanical strain (1% strain, 1Hz, 30 minutes/day, 7 days) in MSC seeded collagen gels revealed that matrix collagen content, mechanical properties (stiffness, maximum tensional load) and scleraxis gene expression (a commonly used expression marker associated with embryonic tendon development) were all upregulated in dynamic samples (164). Cyclic strain at frequencies between 0.017 Hz and 1 Hz with strains between 2% and 10% elongation applied to collagen based tendon scaffolds resulted in increased cellular alignment, up regulation of tendon specific cellular markers (Scleraxis, Collagen I, Collagen III) and improved mechanical properties being observed (165) (161) (166). It has even been found that very low frequency (0.0034 Hz) low strain (2.4%) mechanical stimulation over a long time period (8 hours/day, 12 days) can result in increased stiffness in MSC seeded collagen scaffolds compared to static controls (167). These studies demonstrate the need for mechanical stimulation when designing materials for tendon tissue engineering, but that an ideal loading regime is yet to be found.

Growth factors are molecules which bind with cells to enable a specific cellular function to occur, with the focus in tendon stem cell research being on inducing or maintaining

terminal differentiation into tendon specific cells (44). Bone Morphogenic Protein 12 and 13 (BMP-12/13, also known as GDF(growth differentiation factor)-6/7) are members of the Transforming Growth Factor – Beta (TGF-β) superfamily and play important roles in matrix synthesis, differentiation, chemotaxis and proliferation (48) (49)(50). BMP-12/13, have also been found to promote ectopic tendon formation and repair (48) (52). Singularly, BMP-12 has been reported to induce both *in-vitro* and *in-vivo* tenogenesis of MSCs (48) (53) (51). BMP-12 and BMP-13 have been found to separately induce increases in production of thromobospondin 4 (a specific tendon marker) along with a characteristic wave like pattern found in tendon histological samples after 14 days implantation into a rat defect model (54). A combination of BMP-12, BMP-13 and vitamin C has also been found to induce tenogenesis in hESCs in static physiological O_2 (2% O_2) culture conditions by our research group (in house data).

Fibroblast growth factors (FGFs) are a group of 23 growth factors which play a vital role in limb and organ development during embryogenesis (55) (56). Three members of the FGF family have a prominent role in the maintenance of mesenchyme during limb development; FGF-4, FGF-6 and FGF-8. FGF-4 has an integral role in early embryonic patterning and the maintenance of mesenchyme within the developing embryo (56) (57) (58) (59). FGF-4 knockouts revealed that limb buds fail to develop (57) (58) (59). FGF-6 expression is found in developing skeletal muscle. Studies conducted using murine models have shown FGF-6 presence at E9.5 and to be exclusively present in the myotomal compartment (early stage of skeletal muscle development) of the somite (60) (61) (62). Due to the close interaction between muscle and tendon as the conductor of forces between muscle and bone it is feasible that FGF-6 could play an integral role in the development of tendon and muscular-tendon junctions. FGF-8 has also been shown to play a pivotal role in murine limb development by inducing ectopic limb development and replacing the Apical

Ectodermal Ridge (AER)(a collection of cells at the front of the developing embryonic limb) (63)(64). FGF-4, FGF-6 and FGF-8 are all present in the AER and provide the signalling required to maintain mesenchymal cells in the proliferative state at the limb bud end during development. In house experimentation has shown that combinations of FGF-4, 6 and 8 may be required for the control of differentiation and proliferation of stem cells towards the tendon lineage in 2D cell culture.

We therefore sought to investigate the effect of dynamic mechanical stress and growth factor addition in conjunction with 3D PHBHHx/ collagen hybrid scaffolds seeded with human stem cells in relation to tendon tissue engineering.

5.2. MATERIALS AND METHODS.

5.2.1. Cells.

hMSCs were isolated from human bone marrow using adherence culture as described in methods section **2.2.3**. SHEF1 hESCs were cultured in feeder free conditions according to methodology **2.2.4**. Spontaneous differentiation of hESC was performed by seeding into Matrigel-coated T-75 flasks at fixed densities (1 $x10^6$ cells per flask) in conditioned hESC media. Spontaneous differentiation was induced by changing base media to MEF media for 5 days, changing the media after 3 days as method **2.2.4.e**. RaT cells were isolated from the Achilles tendon of 6 week old Wistar rats and cultured as method section **2.2.2**.

5.2.2. Growth factor supplementation.

Growth factors were reconstituted before use by defrosting and dissolving product in either water or sodium hydroxide according to the manufacturer's protocol. Basic media was

supplemented with a combination of either: BMP 12 (R&D Systems, UK) at 10ng/mL, BMP13 (Peprotech, USA) at 10ng/mL and Vitamin C 2ng/mL (concentrations as used by Berasi et al (54)) or a combination of FGF 4, FGF6, FGF8 all at 50ng/mL and Vitamin C 2ng/mL (found to be optimal for tenocyte differentiation in hESCs, in house data) for each cell type during static culture throughout the 20 day experimental period. A control group with no growth factor additions was also run. 1% Penicillin, Streptomycin and Amphotericin B (PSA) (15240112, Invitrogen, UK) was also added during the experimental mechanical loading period. Table 5.1 provides an overview of the different media types used throughout this investigation.

Table 5.1. Media compositions as used in experiments. Basic media was used as a control, with bone morphogenic protein (BMP) media and fibroblast growth factor (FGF) media used to determine the effects of growth factors on cells in dynamic culture conditions.

Basic media	BMP media	FGF media
DMEM, 10% FBS, 1% l-Glutamine, 1% NEAA, 1% PSA	DMEM, 10% FBS, 1% l-Glutamine, 1% NEAA, 1% PSA	DMEM, 10% FBS, 1% l-Glutamine, 1% NEAA, 1% PSA
	BMP 12 10ng/mL	FGF 4 50ng/mL
	BMP 13 10ng/mL	FGF 6 50ng/mL
	Vitamin C 2ng/mL	FGF 8 50ng/mL
		Vitamin C 2ng/mL

5.2.3. Scaffold

Porous PHBHHx tube scaffolds were produced as described in section **2.3.4**. At least 4 scaffolds were produced for every experimental condition and time point. Polymer tubes were cleaned and sterilised in 70% IMS for 2 hours before collagen gels were added. Collagen gels were formed by first neutralising type I rat tail collagen as section **2.3.5.** with 5mg/mL final collagen concentrations. Gels were injected into the lumen of tubes using a 1mL Gilson pipette, before cross-linkage through temperature elevation to 37^{o}C for 2 hours.

5.2.4. Mechanical stimulation.

Mechanical stimulation was performed using a BOSE ElectroForce 3200 machine coupled to WinTest software as described in Section **2.5**. Scaffold/cell constructs were assembled and allowed to sit in complete media for 24 hours before loading took place. All samples were maintained in static culture when not in the BOSE chamber throughout the experiment, with groups of scaffolds stimulated for 0 days (no loading), 5 days, 10 days and 20 days. All measurements were carried out at each end point, i.e. day 20.

5.2.5. Histological analysis.

Samples were fixed using 4% paraformaldyhyde (P6148 Sigma Aldrich UK)/PBS solution overnight at 4^{o}C. They were then embedded in paraffin wax (section **2.8.1**) and sectioned using a microtome (section **2.8.2**) Haematoxylin and eosin stain (section **2.8.3**) and Sirius red (section **2.8.4**) stains were applied to sections after rehydration and mounted on glass microscope slides. Polarised light microscopy was performed as section **2.8.9** and images of a single field of view were taken with polarisers set at 0^{o} and 90^{o} differences using a

Nikon N5 camera, with constant light brightness. A corresponding bright field image of the same view field was also taken as a reference.

5.2.6. Mechanical testing.

Stiffness and ultimate tensile stress (maximum load) were measured as method **2.6.1.** using a BOSE Electroforce 3200 system.

5.2.7. Cellular Viability

A 2 x 2 x 2mm section of collagen gel from each sample were removed, digested in 0.4% type IV collagenase (C5138, Sigma Aldrich UK)/PBS solution for 1 hour before a trypan blue exclusion assay was performed to assess cell viability (**2.2.1.f.**).

5.2.8. Control.

An acellular group was used as a control. Tubes and collagen were made as with cellular constructs, with cells left out of the collagen gel. Constructs were mechanically loaded and stained as with the cellular groups.

5.2.9. Molecular Characterisation.

Gels were removed from tubes and immersed in 0.4% type IV collagenase for 1 hour. Molecular characterisation was performed via RT-PCR (method **2.4.3**). Genes investigated were Beta Actin (BACT), Collagen 1a2 (COL1a2), collagen 3a1 (COL3a1), tenascin-C (TEN-C), tenomodulin (TNMD) and thrombospondin-4 (TBSD-4). Primer sequences and annealing temperatures can be found in **table 2.1**.

5.2.10. Statistical analysis

Results were deemed to be significant if $P \leq 0.05$, or as indicated in the text using a 2-tailed paired Students t-test or one way ANOVA with Tukey's post hoc test.

5.3. RESULTS.

5.3.1. Cell viability.

Cell viability in PHBHHx/collagen hybrid scaffolds was measured using a trypan blue exclusion assay. The number of cells in all media conditions was reduced by around 50% (42.4 – 52.9%) after 5 days loading. Cell viability remained high throughout the culture period (95.8 ± 8.3 - 82.5 ± 13.70 %) in all conditions at all-time points (Fig. 5.1).

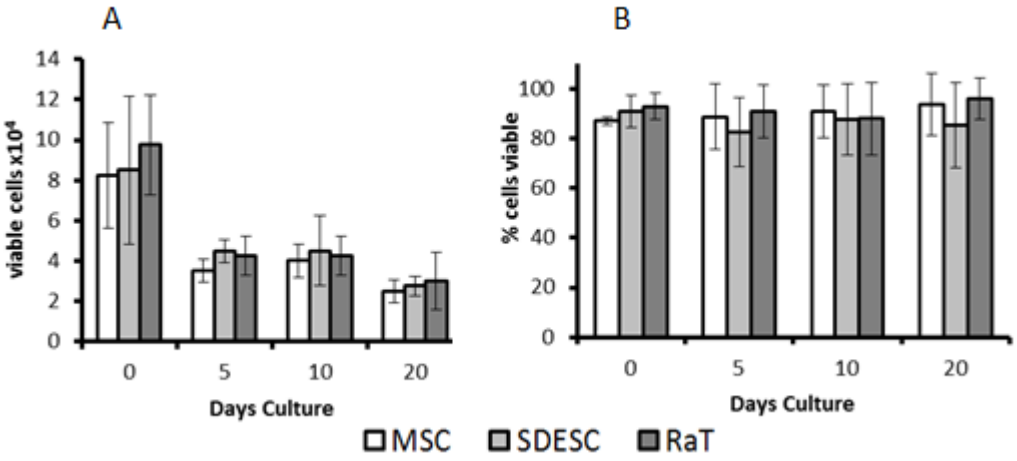

Figure 5.1. Cell number and cell viability in PHBHHx/collagen hybrid scaffolds after 0, 5, 10 and 20 days mechanical loading. A: total number of viable cells present in the collagen gel after loading. B: percentage of viable cells in collagen gel after loading. White bars indicated hMSCs, light grey bars SDhESC and dark grey bars RaT cells. Mean ± 1SD. n = 3.

5.3.2. Mechanical testing.

Mechanical testing (maximum load and stiffness) was performed using a BOSE Electroforce 3200 by applying a tensional elongation of 0.1mm/s until failure. Freshly dissected rat Achilles tendon controls had a maximum load of 3.24 ± 0.30 N and a stiffness of 3826 ± 261 N/m.

hMSC seeded scaffolds ranged in maximum load from 2.13 ± 0.82 N to 3.7 ± 0.06 N, and 4073 ± 120 N/m and 6724 ± 1052 N/m stiffness. Unstimulated constructs had similar load to failure to rat achilles tendon controls. Stimulation led to maximum load increases being seen in standard media after 20 days ($p=0.01$), but decreases after 5 days loading in BMP media ($p = 0.04$). Significant increases were seen in construct stiffness after 5 days stimulation in standard and FGF media ($p =0.01, 0.00$ respectively), but not in BMP media ($p = 0.8$). hMSC seeded constructs were significantly stiffer after 10 days in standard media, with no difference seen in FGF media and a reduction seen in BMP media. Significant increases were seen after 20 days loading in standard media ($p=0.01$), but not BMP ($p=0.2$) or FGF ($p=0.08$) medias (Fig. 5.2). Statistical significance was determined by one way ANOVA followed by Tukey's post hoc test.

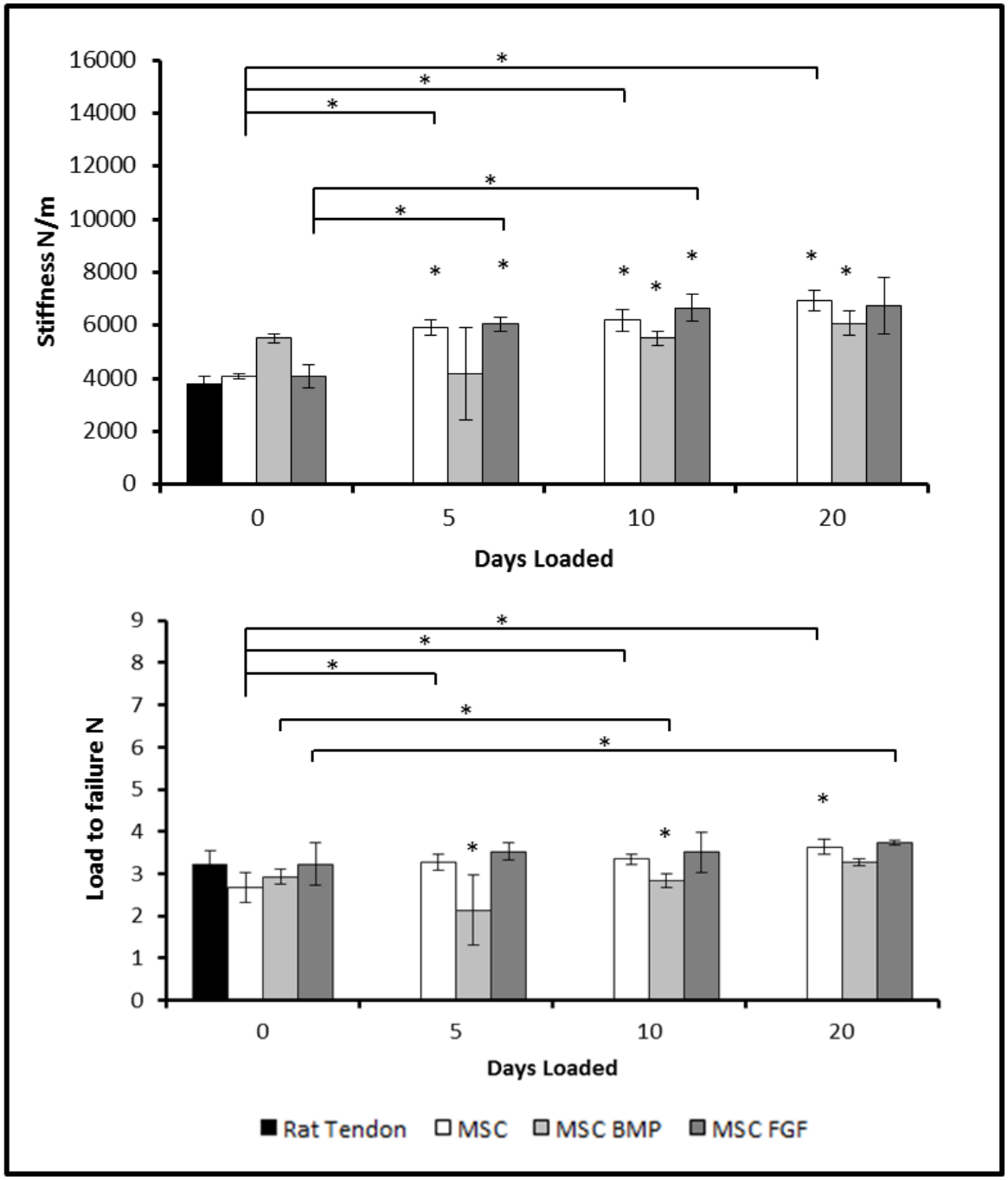

Figure 5.2. Stiffness and maximum load of hMSC seeded constructs increases with length of time of mechanical stimulation. Significant increases in stiffness are seen in most sample types after 5 days stimulation, Mean ± 1SD. n = 3, * significant ($p \leq 0.05$) compared to rat tendon control or as indicated.

Maximum loads between 2.13 ± 0.30 N and 4.07 ± 0.04 N, and stiffness of 7766 ± 147 and 3833 ± 450 N/m were recorded for SDhESC seeded constructs. Unloaded samples had a significantly lower maximum load in all media types compared to rat Achilles tendon controls. Mechanical stimulation increased maximum load in all media after 5 days, showing no difference from rat Achilles tendon. Significant increases in maximum load were seen in all media types after 10 days stimulation when compared to unloaded controls ($p \leq 0.03$). This trend was repeated after 20 days stimulation ($p \leq 0.04$). Stiffness of SDhESC seeded scaffolds was found to be similar in all unloaded samples to rat tendon controls. Stimulation increased seeded scaffold stiffness after 5 days in FGF media ($p=0.05$) and all conditions after 10 days ($p \leq 0.03$) and 20 days ($p \leq 0.03$) (Fig. 5.3). Statistical significance was determined by one way ANOVA followed by Tukey's post hoc test.

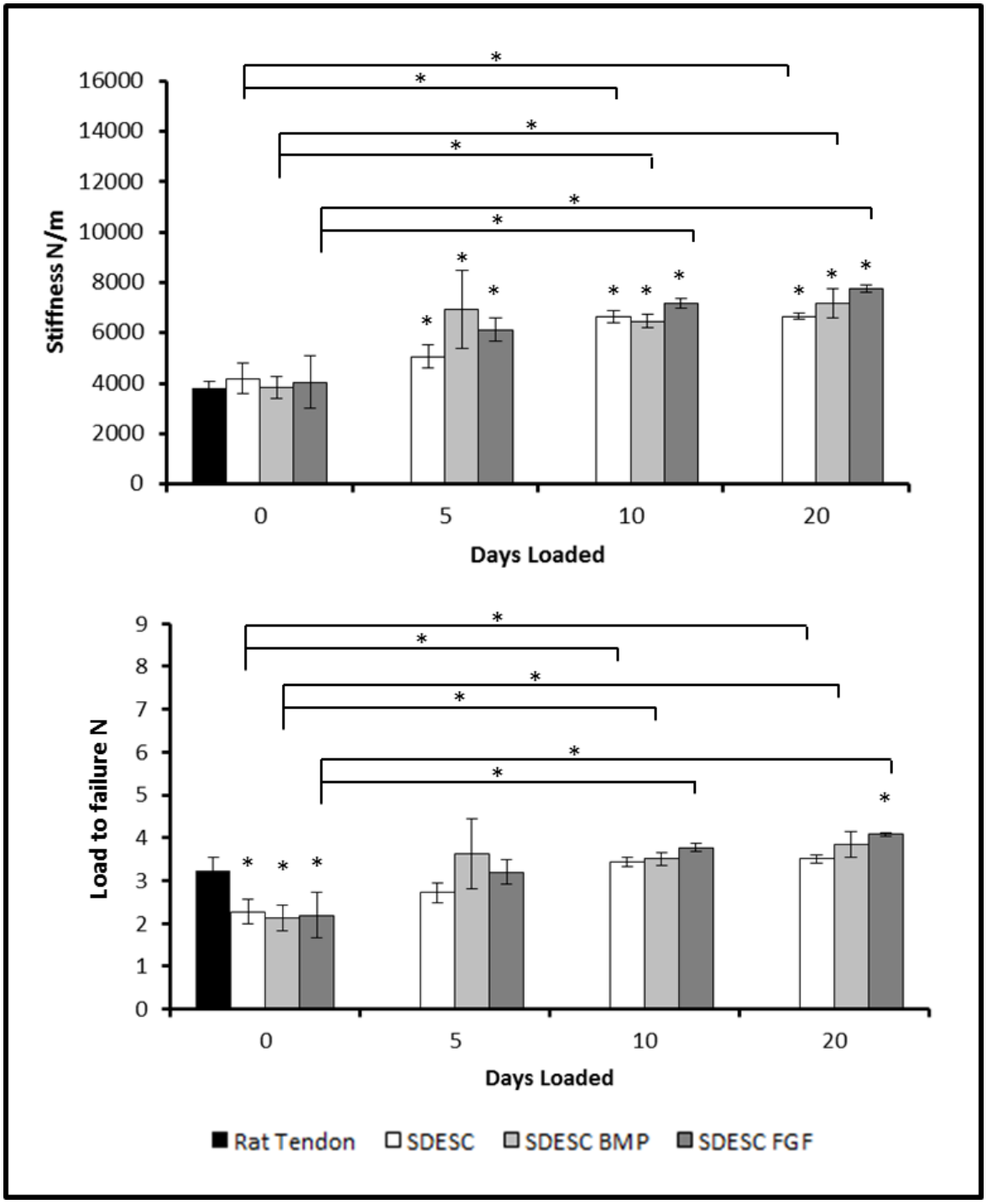

Figure 5.3. Stiffness and maximum load of SDhESC seeded constructs increases with length of time of mechanical stimulation. significant increases in both maximum load and stiffness are found after 10 days stimulation. Mean ± 1SD. n = 3 * significant ($p \leq 0.05$) compared to rat tendon control or as indicated.

RaT seeded constructs had the highest overall load to fail at 2.56 ± 0.22 and 5.12 ± 1.40 N and stiffness at 4680 ± 783, 9840 ± 1334 N/m, seen after 5 days stimulation in basic media and FGF media correspondingly. Differences between conditions were obscured by high standard deviations, leading to constructs being similar in both maximum load and stiffness in all conditions, however significant increases in maximum load were seen after 10 and 20 days in standard media ($p=0.03$, 0.02 respectively) compared to unstimulated controls. Significant increases in stiffness were also observed after 10 and 20 days in standard media ($p= 0.01$, 0.01 respectively), but not in other media types (Fig. 5.4). Statistical significance was determined by one way ANOVA followed by Tukey's post hoc test.

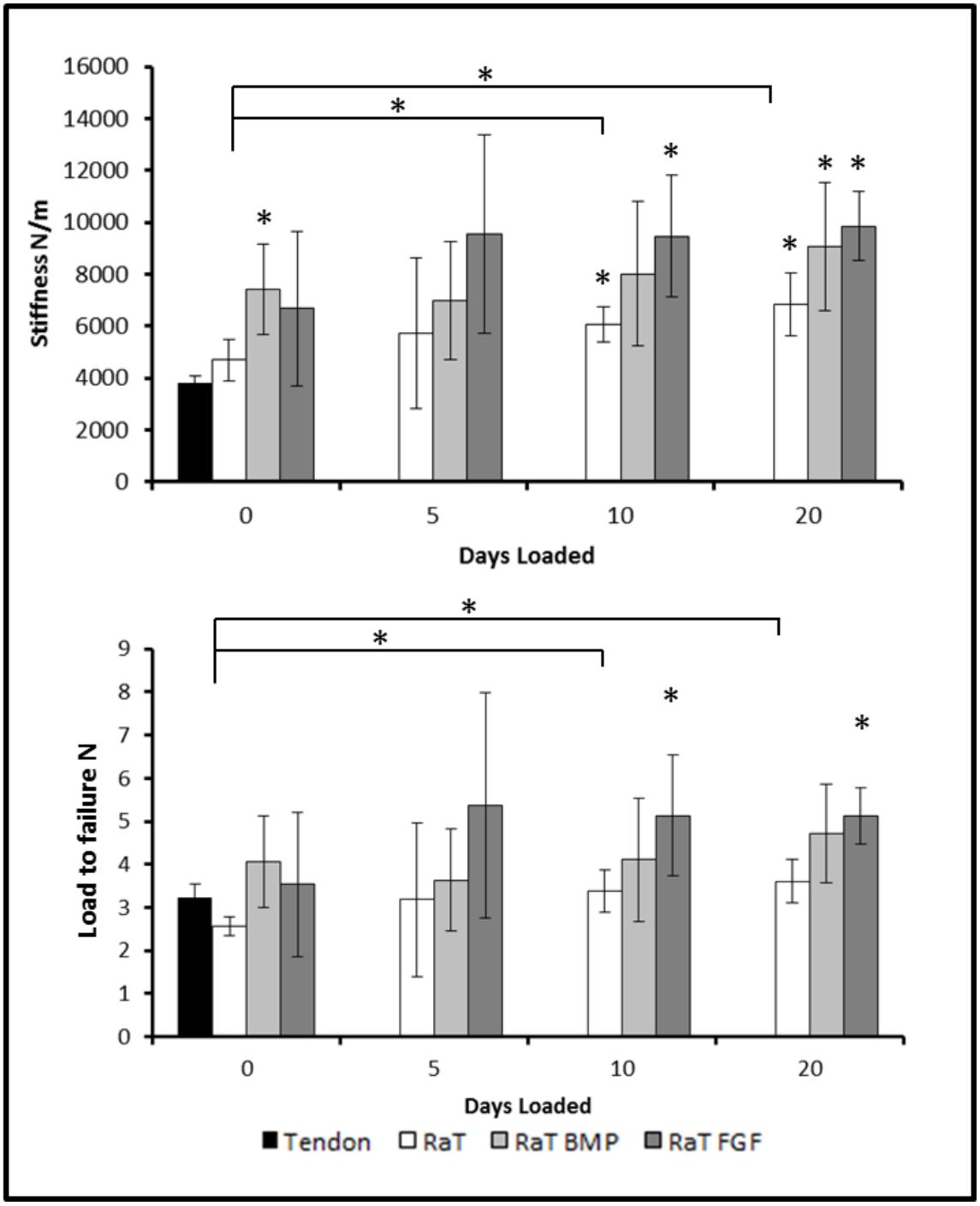

Figure 5.4. Stiffness and load to fail of RaT seeded constructs increases with length of time of mechanical stimulation. large variation prevents statistical significance in many samples. Mean ± 1SD. n = 3 * significant ($p \leq 0.05$) compared to rat tendon control or as indicated.

5.3.2. Normalised mechanical properties.

Normalised values of ultimate tensile stress were gained by subtracting acellular values from cellular construct results, giving a trend of the effect of the cells on the mechanical properties of the final constructs. Although these results cannot be taken as absolute, as only average values were taken into account, it is possible to ascertain where the duration of mechanical stimulation using these conditions has the largest general effect on the mechanical properties on the constructs.

hMSC seeded constructs without mechanical stimulation were less stiff than acellular constructs in all media. Load to fail was unafected, with unloaded constructs found to be within ±0.5N of acellular. Stimulation led to increases in both stiffness and max stress in both no growth factor and FGF media, with maximal values for all media types found after 10 days stimulation. FGF had the largest effect, with load to fail of 1.52N and stiffness of 3314N/m. Further stimulation to 20 days had a negative effect on mechanical properties. hMSCs in BMP media were found to reduce stiffness and load to fail after 5 days stimulation, with normalised values dropping to 0.82N and -1480N/m (Fig. 5.5 a, b).

Unloaded SDhESC seeded constructs had lower stiffness and max stress than acellular controls in all media. Stimulation increased stiffness and load to fail in all conditions, with maximal vaules at day 10 and FGF media having the largest effect with 1.79N and 3826N/m. Further stimulation had a negative effect on mechanical properties (Fig. 5.5 c, d).

RaT cells had the largest effect on mechanical properties. Unloaded samples without growth factors had similar normalised load to fail (-0.12N) but lower stiffness (-1100N/m) values compared to acellular controls. BMP and FGF media increased unloaded sample max stress and stiffness (BMP: 1.38N, 1640N/m. FGF: 0.85N, 800N/m) in unloaded

samples. Mechanical stimulation for 5 days increased properties in no growth factor and FGF media, but not in BMP media. Maximum values were seen after 10 days stimulation with the largest effect being seen in FGF media (3.14N, 6106N/m). Further loading had a negative effect on properties (Fig. 5.5 e, f).

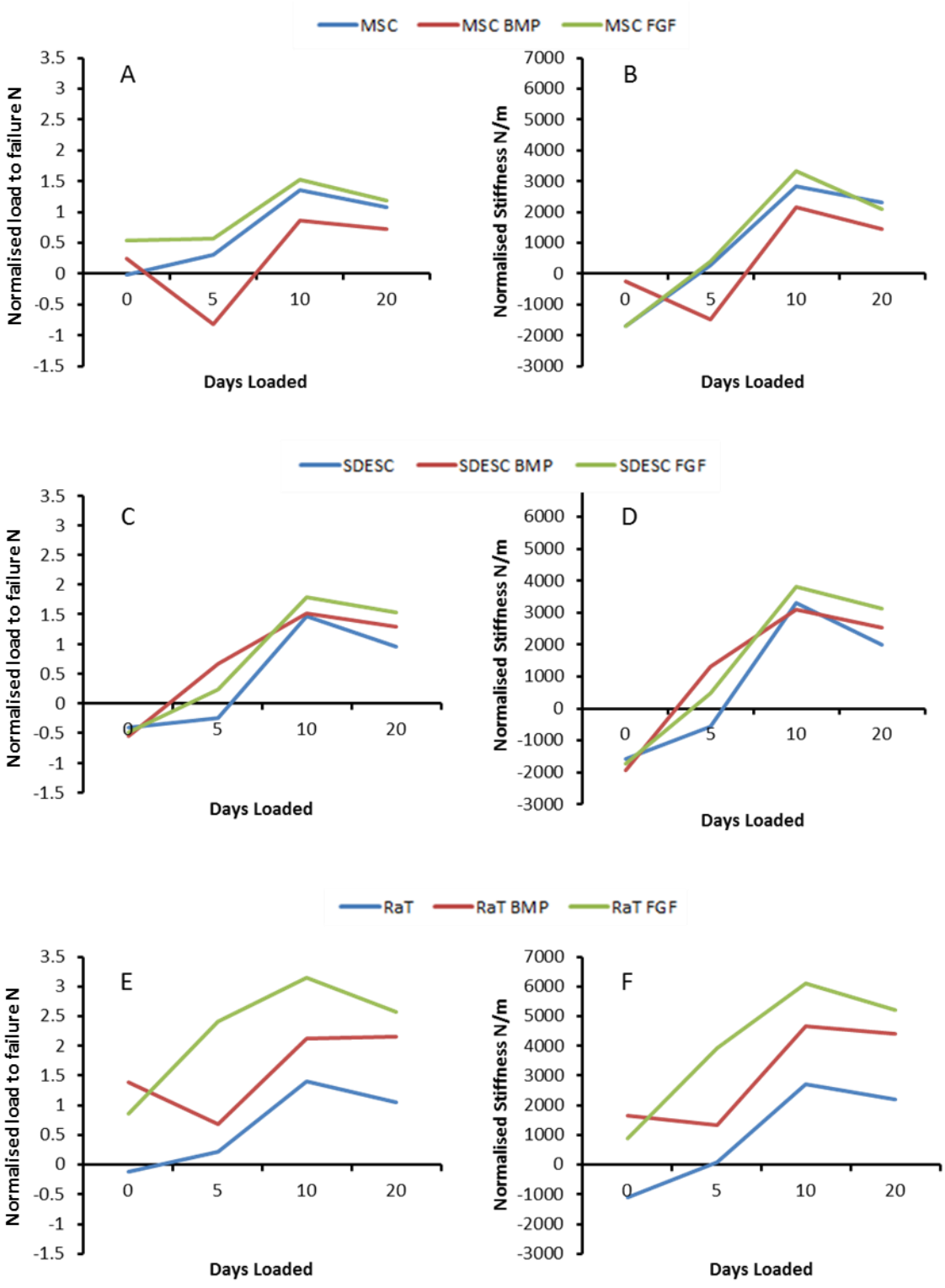

Figure 5.5. Normalised effect of cells. Graphs show average values from mechanical testing normalised to an acellular control. Trends show initial slow increase in properties between days 0 and 5, with large increases being made between days 5 and 10, before plateauing to day 20. RaT cells had the largest impact on construct properties.

5.3.3. Polarised light microscopy.

Polarised light can be used to identify areas of birefringence or areas where structural order exist (207). Problems with sectioning being inconsistent, with folds and air bubbles sometimes present, restrict the conclusions that can be made to overall observations, and prevent quantitative assessment being made.

Little evidence of remodelling was present in MSC seeded samples in the absence of growth factors, with only small areas of birefringence being seen at day 20. BMP12/13 increased the amount of birefringence in comparison to no growth factors, with increased mechanical stimulation also increasing the amount of sample visible when viewed through cross polarisers at day 20, perhaps suggesting increased matrix organisation. FGF 4/6/8 increased the amount of sample visible compared to no growth factor samples, with almost complete birefringence of the sample visible at day 20 (Fig. 5.6).

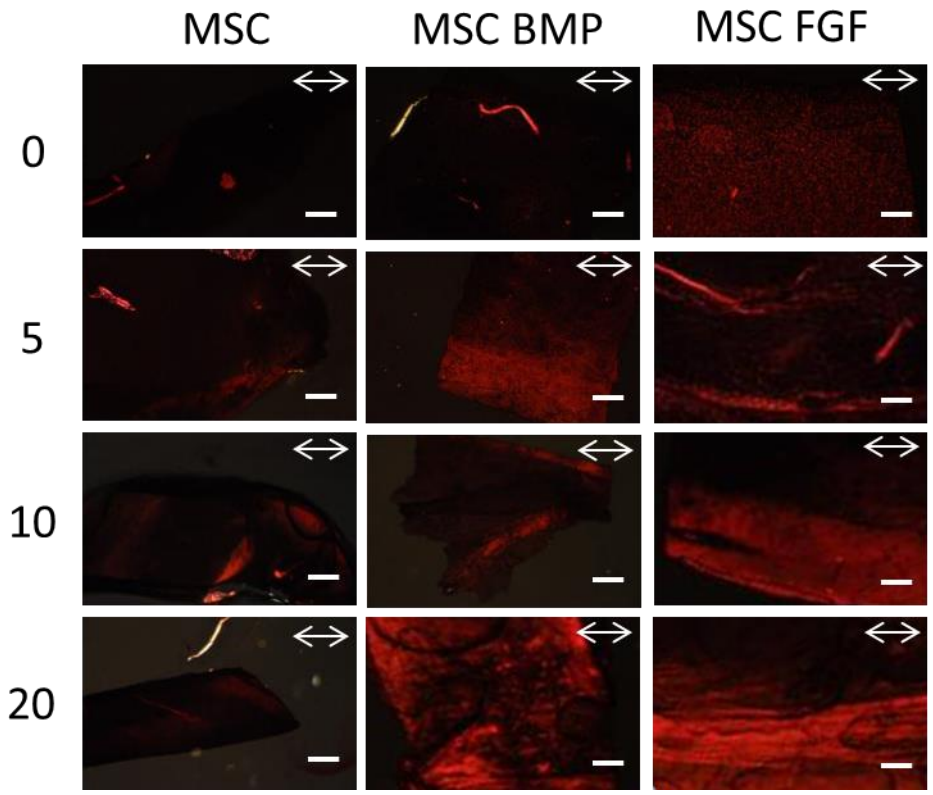

Figure 5.6. Growth factors induce matrix remodelling of hMSC seeded constructs over 5, 10 or 20 days stimulation. Little matrix ordering is apparent in no growth factor media. Extensive matrix ordering was seen after 10 days stimulation when growth factors present. Sections stained with Sirius red. Shown are images taken through crossed polarizers (at 90^{o} to each other). White arrows indicate loading orientation. Images taken at 100x magnification. Scale bar = 100µm.

Embryonic stem cell seeded scaffolds displayed increased sample birefringence with increased mechanical stimulation. Samples had remodelled after 10 days stimulation in all media conditions, with large areas of sample demonstrating birefringence. The addition of FGF 4/6/8 increased the amount of birefringence, but little difference was seen between BMP12/13 media and no growth factor samples (Fig. 5.7).

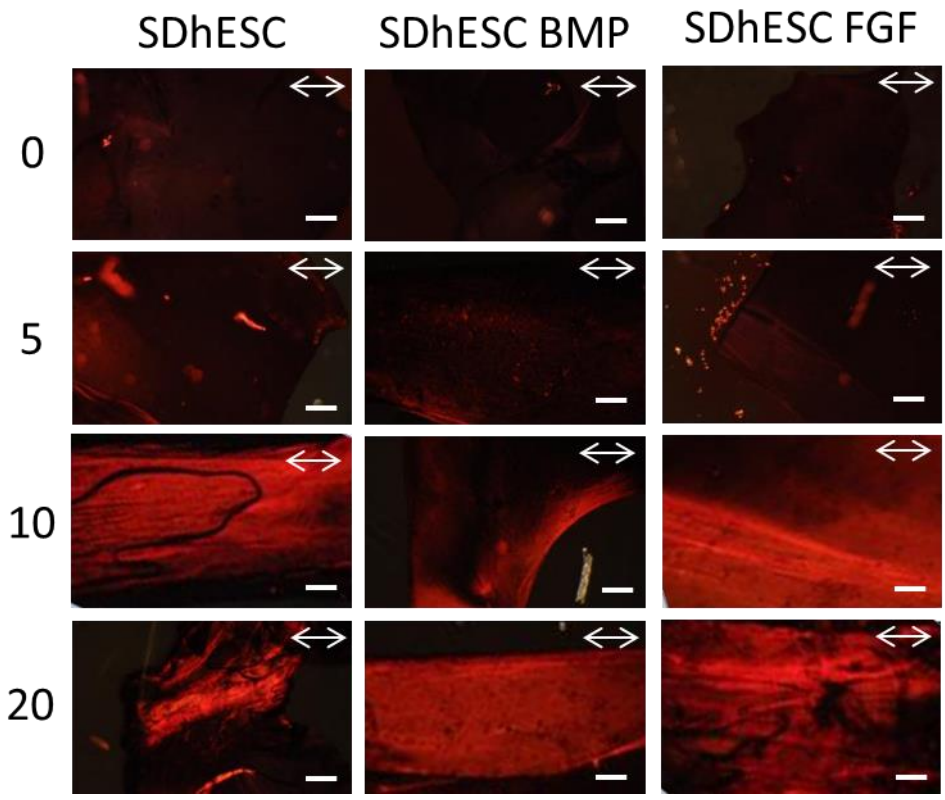

Figure 5.7. SDhESCs remodel matrix with mechanical stimulation over 5, 10 or 20days. Stimulation resulted in matrix ordering in all media types after 10 days. Extensive matrix ordering observed after 10 days stimulation in all media. Sections stained with Sirius red. Shown are images taken through crossed polarizers (at 90^{o} to each other). White arrows indicate loading orientation. Images taken at 100x magnification. Scale bar = 100µm.

Rat tenocyte seeded constructs showed increased birefringence after 20 days stimulation in no growth factor and BMP 12/13 media, but not to any great extent in other conditions. A halo like artefact was present on the FGF media day 20 sample (yellow arrow) (Fig. 5.8). Acellular constructs showed little or no birefringence and therefore no evidence of ordered collagen remodelling occurring at any time point (Fig. 5.9).

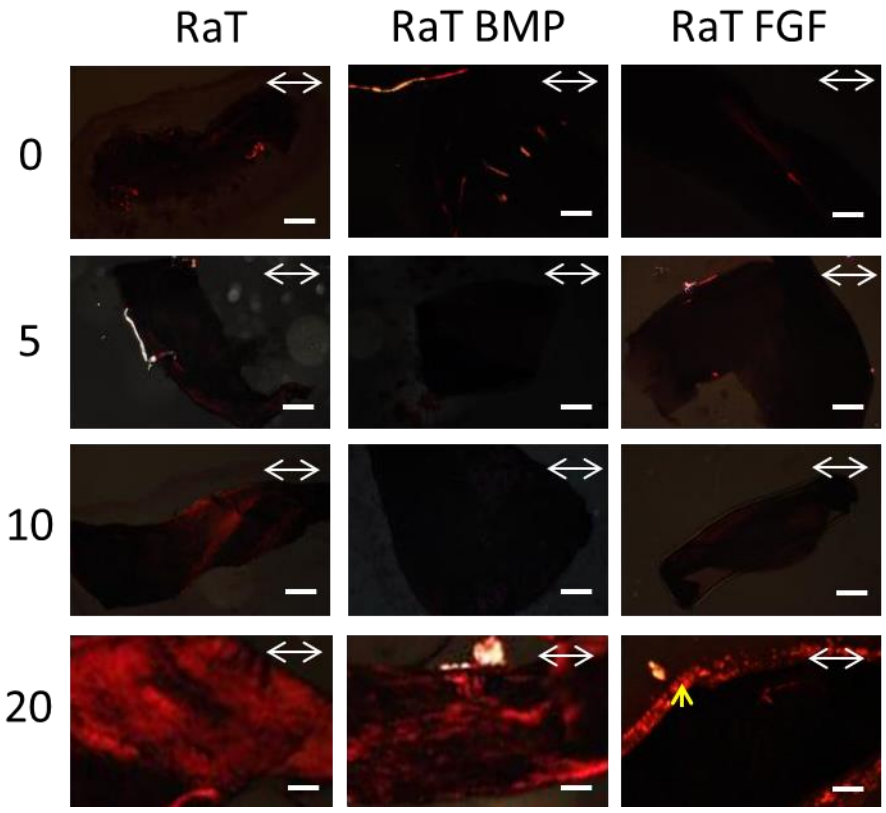

Figure 5.8. Rat tenocytes remodel collagen in response to mechanical stimulation over 5, 10 or 20 days. Evidence of matrix ordering was seen after 20 days stimulation in no growth factor and BMP media. No ordering was seen in FGF media. Sections stained with Sirius red. Shown are images taken through crossed polarizers (at 90^{o} to each other). White arrows indicate loading orientation yellow arrow indicates "halo" artefact surrounding sample. Images taken at 100x magnification. Scale bar = 100µm.

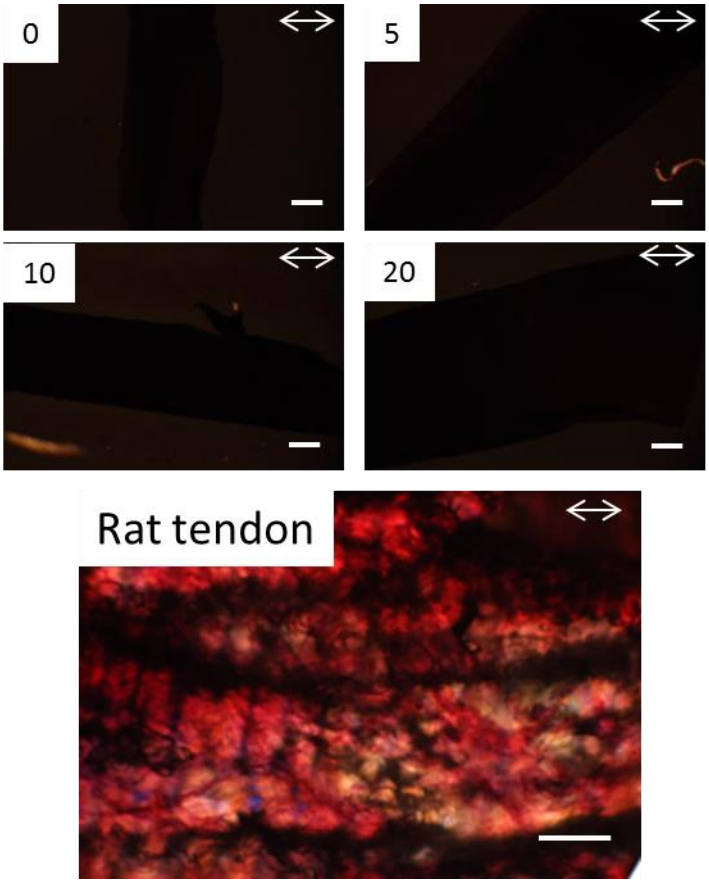

Figure 5.9. No matrix remodelling observed in acellular constructs over 20 days mechanical stimulation. No light is seen to be refracted by the sample, indicating that little to no ordering is present in the structure. Rat tendon shows high levels of birefringence throughout its structure. Sections stained with Sirius red. Shown are images taken through crossed polarizers (at 90^{o} to each other). White arrows of acellular images indicate loading orientation. White arrows on tendon indicate longitudinal tendon direction. Images taken at 100x magnification. Scale bar = 100μm.

5.3.4. Histology.

Collagen gels were removed from the PHBHHx tube and sectioned and stained with Haematoxylin and Eosin. Evidence of collagen fibril formation was seen in no growth factor samples with 20 days mechanical stimulation in small distinct areas (white arrows) (Fig. 5.10). Little evidence was seen at other time points. BMP 12/13 addition increased the amount of fibril formation and alignment seen, especially in day 10 samples (white arrows) (Fig. 5.10). FGF addition increased the amount of matrix alignment with increased stimulation, with large areas of collagen being seen to be ordered (white arrows) (Fig. 5.10).

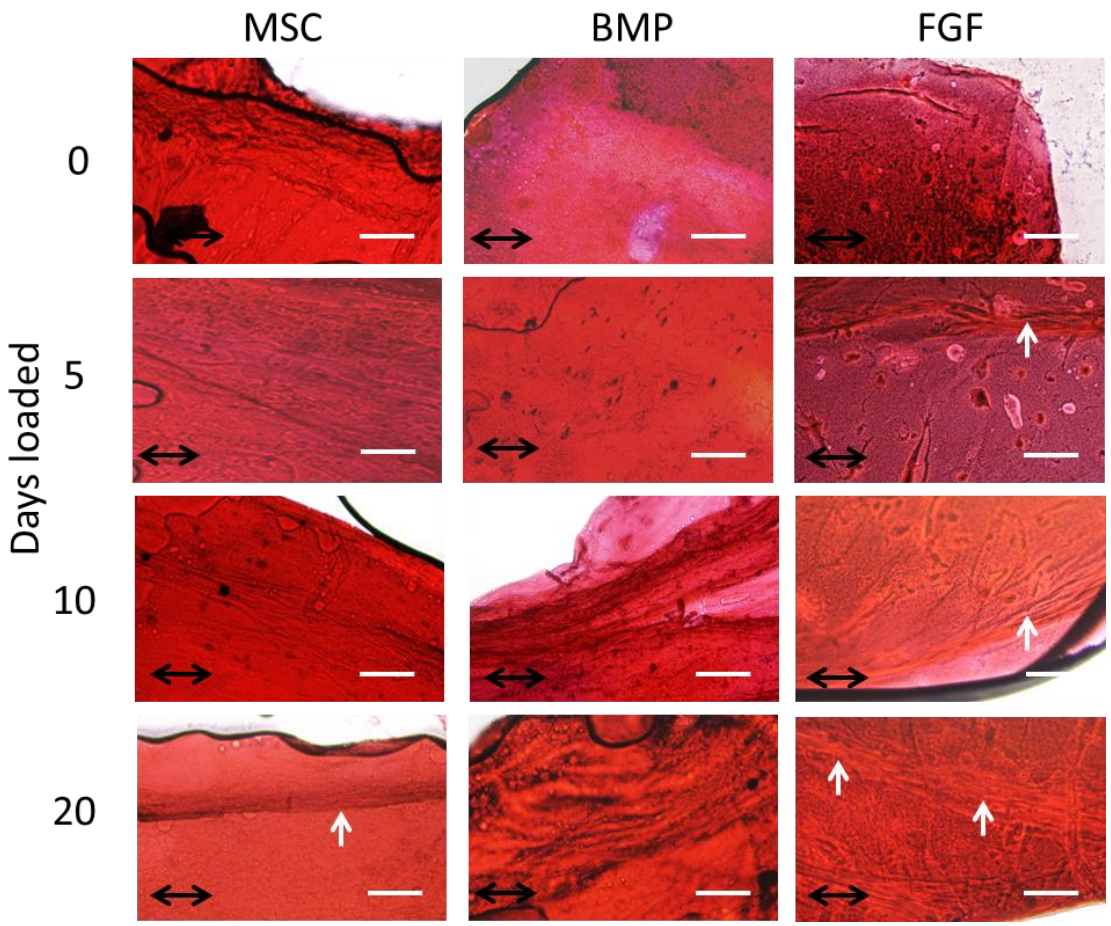

Figure 5.10. Cellular and matrix remodelling of hMSC seeded scaffold collagen core. Regions of matrix ordering became visible after 20 days loading in standard media. No clear evidence of matrix ordering was seen in BMP supplemented media (white arrows). Regions of ordering were apparent after 5 days stimulation with FGF supplementation, becoming larger at day 10 and almost completely covering the gel volume after 20 days (white arrows). Black arrows indicate loading orientation. Images at 200x magnification. Scale bar = 100µm.

Distinct regions of matrix alignment were seen in SDhESC samples in no growth factor media after 5 days stimulation, with regions becoming larger with increased stimulation (white arrows) (Fig. 5.11). BMP 12/13 addition increased the size of matrix aligned regions at day 5, with most of the matrix being ordered at day 20 (white arrows) (Fig. 5.11). FGF 4/6/8 addition resulted in ordered areas of matrix alignment in unloaded samples, with stimulation leading to large cellular and ECM ordering after 5 days and complete ordering after 20 days (white arrows) (Fig. 5.11).

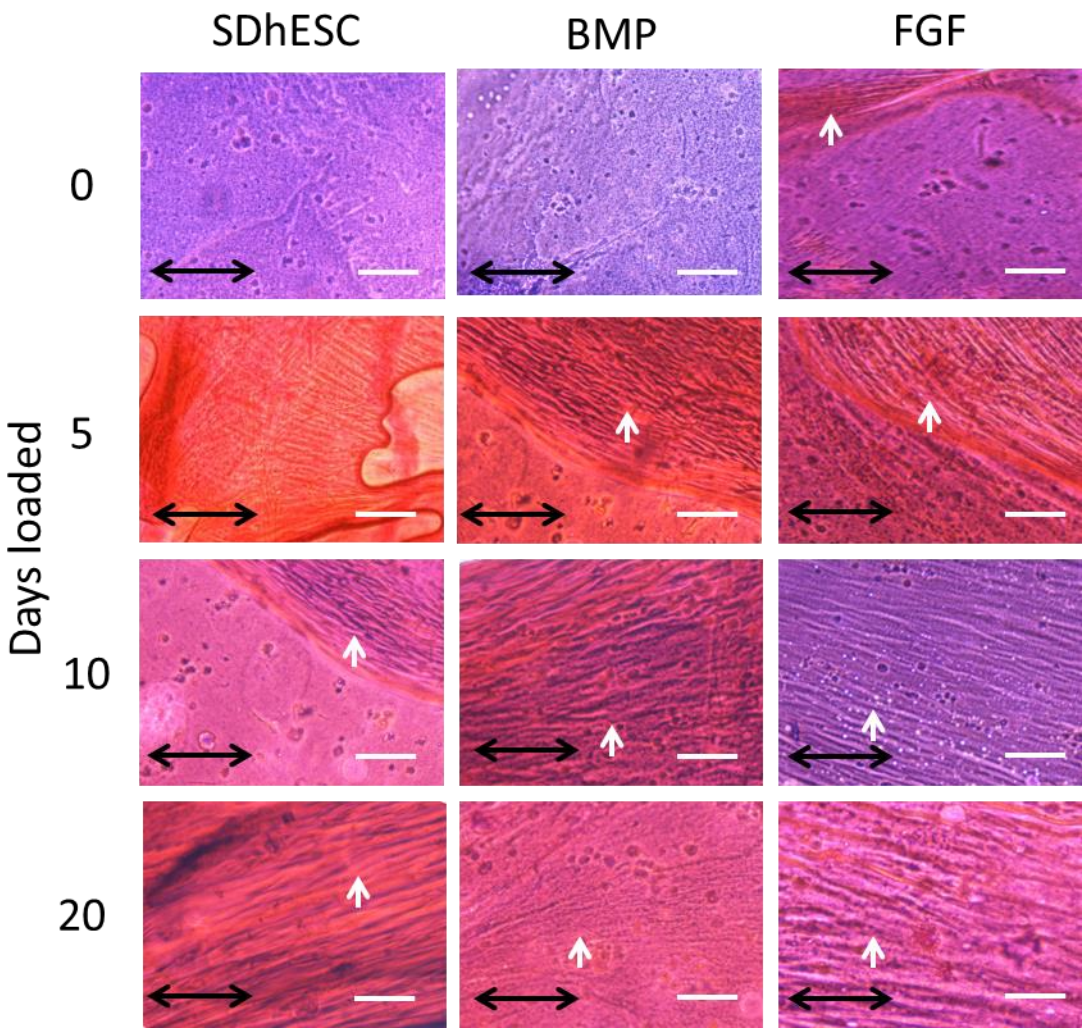

Figure 5.11. Matrix remodelling and cellular alignment of SDhESC seeded scaffold collagen core. Remodelling and cellular alignment became apparent after 5 days stimulation, with regions becoming larger at 10 and 20 days (white arrows). Ordering and cellular alignment of SDhESC seeded scaffolds supplemented with BMP media was apparent at day 5, with complete matrix alignment seen after day 10 (white arrows). Matrix ordering and cellular alignment of SDhESC seeded scaffolds supplemented with FGF media was apparent in samples with no stimulation. Larger areas are ordered at days 5, 10 and 20 (white arrows). Black arrows indicate loading orientation. H&E stain. Images taken at 200x magnification. Scale bar = 100µm.

Evidence of matrix remodelling and cellular organisation in rat tenocyte seeded scaffolds was observed in unloaded samples without growth factor additions, with further limited remodelling being seen after increased stimulation (Fig. 5.12). BMP 12/13 addition led to no matrix ordering being seen in unloaded samples, with distinct areas of ordering being seen after 5 days stimulation, getting larger with further stimulation (Fig. 5.12). No order was seen in FGF 4/6/8 unloaded samples, with areas forming after 5 days stimulation with little improvement seen at later time points (white arrows) (Fig. 5.12). Little to no matrix ordering or alignment was seen at any time point in acellular samples. Rat Achilles tendon shows cellular and matrix alignment in the direction of the tendon's main orientation (Fig. 5.13).

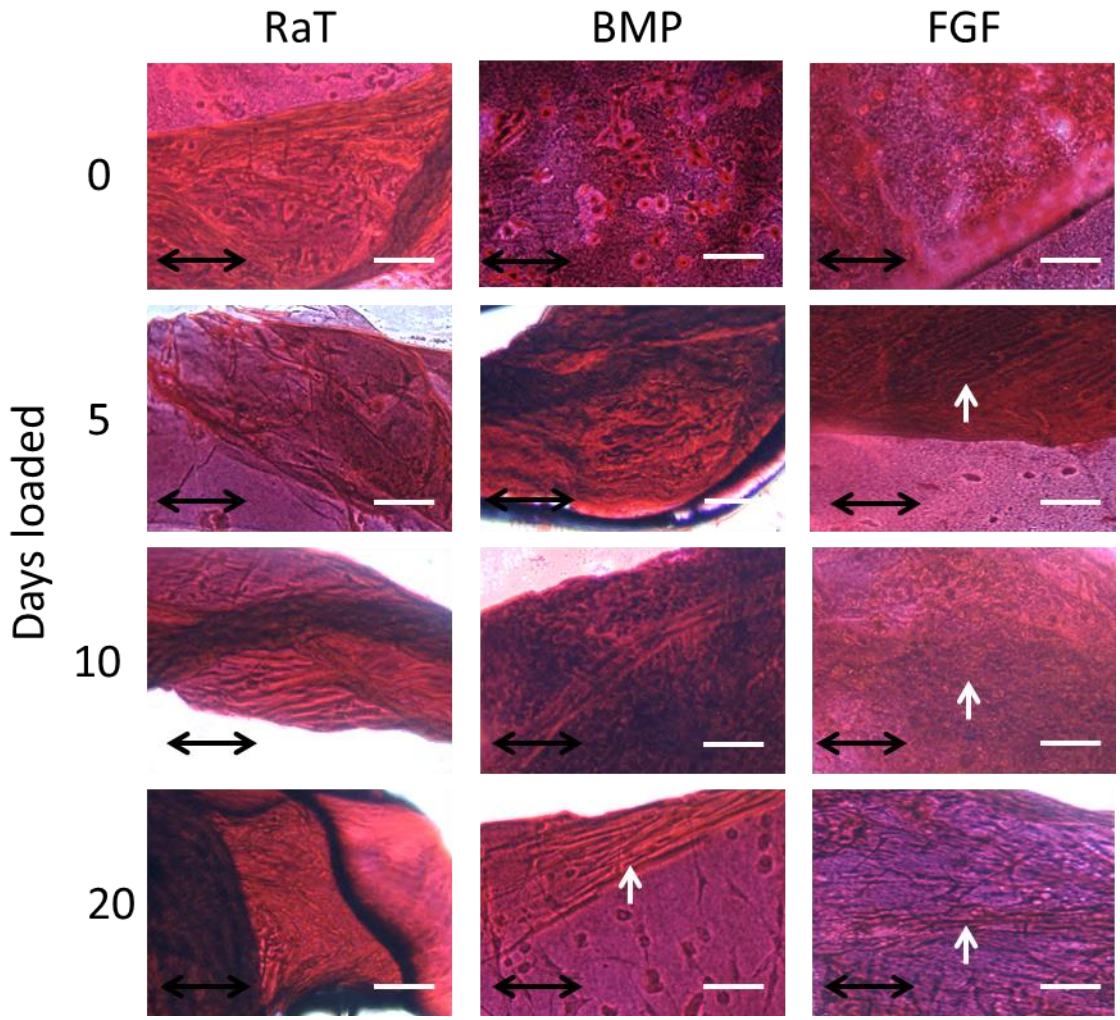

Figure 5.12. Cellular and matrix remodelling of RaT seeded scaffold collagen core. Matrix ordering was apparent in samples with no stimulation. Mechanical stimulation does not appear to have a large effect on ordering, with little difference seen between unloaded and loaded samples. Unloaded samples showed little sign of matrix ordering in BMP supplemented RaT seeded scaffolds. Distinct areas of ordering were seen after 20 days stimulation (white arrow). Regions of matrix alignment were seen after5 days stimulation in FGF supplemented RaT seeded scaffolds, with little further effect being evident (white arrows). Black arrows indicate loading orientation. H&E stain. Images taken at 200x magnification. Scale bar = 100µm.

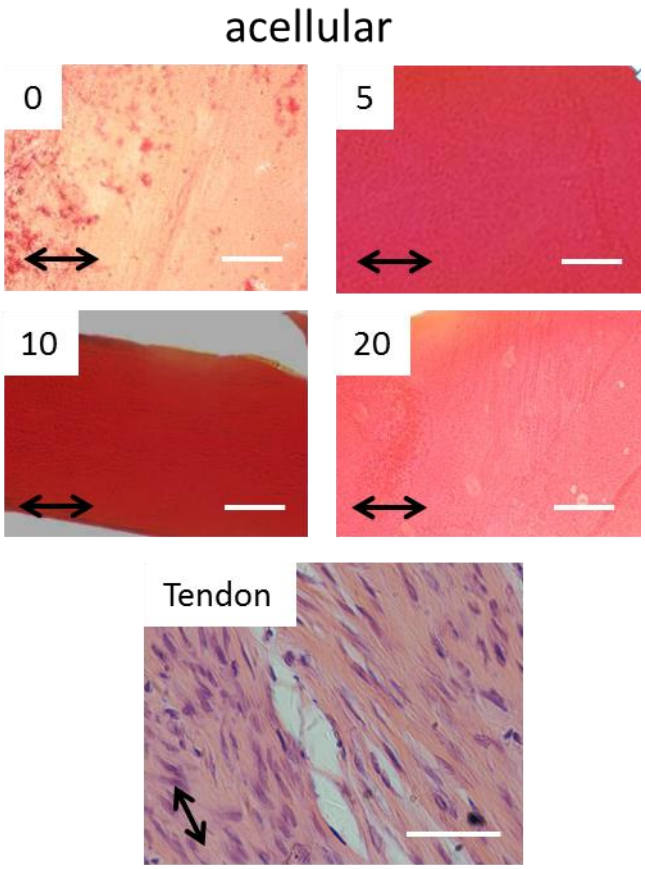

Figure 5.13. Matrix remodelling of acellular collagen core and healthy tendon at 200x magnification. No evidence of matrix alignment is apparent in any sample. (H&E stain). Tendon section taken from a rat Achilles tendon, and stained and imaged at Tsinghua University centre for biological research. Black arrow indicates loading or tendon direction. H&E stain. Images taken at 100x magnification. Scale bar = 100µm.

5.3.5. Molecular Characterisation.

Cell fate was assessed using reverse transcriptase polymerase chain reaction (RT-PCR). Due to small yields of cells, samples were pooled from 3 scaffolds into one before RNA isolation in order to give sufficient amounts of RNA to test for multiple markers. Beta Actin (BACT) was expressed in all cell types at all-time points, demonstrating cellular viability, however expression was limited in hMSCs after 20 days loading and BMP media at 10 days loading. Expression of COL1a2 was maintained in MSCs in standard media and BMP media to day 20, and day 5 in FGF media. COL3a1 was expressed by MSCs at all-time points in all media types. TENC expression was maintained throughout 20 days in BMP and FGF media, and up to day 5 in standard media. TBSD-4 was present in unloaded hMSCs, with some evidence of expression after 20 days stimulation in FGF media only (Fig. 5.14.). RNA extraction of sufficient amounts from SDhESC and RaT cells was not found to be possible for unknown reasons.

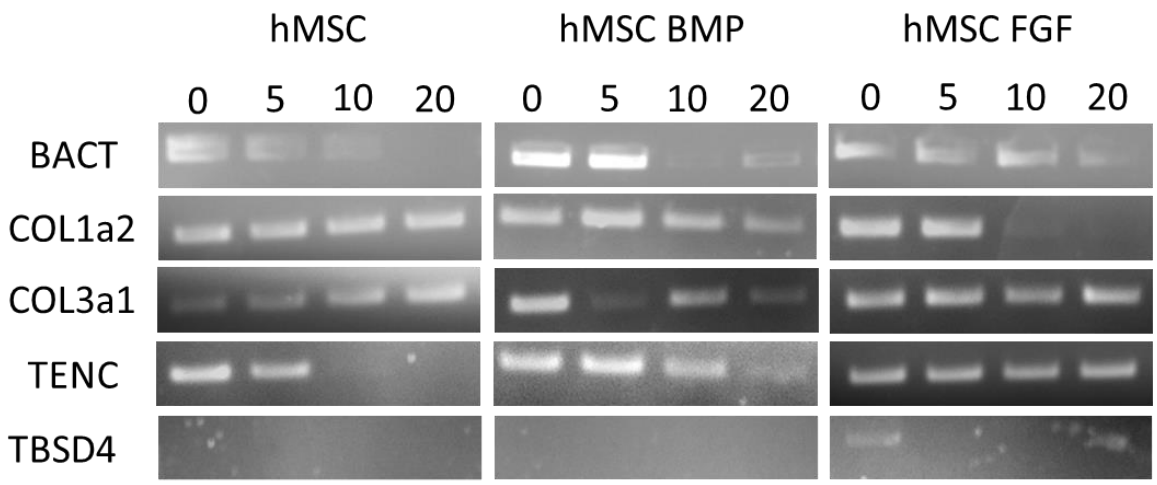

Figure 5.14. Molecular Characterisation of cells isolated from collagen tubes. Tendon specific markers expressed in FGF and BMP media. Markers: BACT beta actin, COL1a2 Collagen 1a2, COL1a3, Collagen 1a3, TENC tenascin C, TBSD4 Thrombospondin-4.

5.4. DISCUSSION.

Tendon injury and disease is notoriously difficult to cure, with the chance of success of treatment being dependent on many factors, including patient age, type of injury and time between injury and medical intervention (10). As a result there remains a need for new treatments to be developed incorporating novel biomaterials and cellular components that provide a clinical advantage over current best treatment methods (39). This investigation has for the first time investigated the effects of growth factors, mechanical stimulation and PHBHHx/collagen hybrid scaffolds on human stem cells, finding that mechanical stimulation has positive effects on hMSC seeded scaffolds, with increased matrix organisation and maintenance of commonly used tendon molecular markers over a 20 day culture period.

Cellular viability in 3D PHBHHx/collagen has been found to be above 82% throughout long term *in vitro* culture. Previous studies investigating other additions to collagen gels have also demonstrated its suitability for long term cell culture. Silk/collagen hybrid scaffolds have been shown to sustain high viability and function of differentiated hESCs (ESC-MSC cells) over 14 days with mechanical stimulation (124). Viability of all cell types was found to be high throughout the experimental time period, building on previous work demonstrating the suitability of PHBHHx/collagen hybrid scaffolds for tendon tissue engineering applications. Cell numbers were reduced after mechanical stimulation. This could be due to collagen gel being lost from the centre of the tube during the BOSE chamber stimulation process, although this loss was not quantified. Our investigation also identified a drop in viability of around 50% in SDhESC cells. This can be explained by the number of cells that had not differentiated or remained embryonic stem cell like, which were found in previous chapters to be unviable in this construct design.

Human movement is controlled by contracting muscles acting through tendons. As a result, tendon tissue is consistently under high levels of mechanical stress, usually applied in a cyclical motion (158). Investigations into the mechanical stimulation of tendon tissue engineered constructs have been shown to influence cell behaviour in many ways. Long term mechanical stimulation resulted in tenocyte seeded PGA constructs becoming dense fibrillar structures with higher levels of tendon specific proteins being expressed by cells in the overall matrix, with higher mechanical properties when compared to non-loaded controls (160). This work corresponds with our findings, with mechanical stimulation significantly increasing both load to fail and stiffness in tenocyte seeded samples where growth factors were added.

The effect of mechanical loading was found to be highest using these loading conditions after a period of 10days. Continued loading over a period of 20days was found to contribute to a drop in overall mechanical integrity. This could have been caused by the high amplitude being used to load the constructs being quite close to the natural ultimate strain a tendon can withstand *in vivo* (33), which could have led to some damage being caused to the developing collagen fibres (158). Alternatively, the repetitive moving of the constructs from static culture to the bioreactor could also have led to small defects being formed in the tube structure, which could have led to reduced overall mechanical properties (208).

Bone marrow derived human mesenchymal stem cells have been shown to create tendon like structures when exposed to dynamic cyclical mechanical stress when seeded in collagen scaffolds. Up regulation of fibrillar collagen marker expression, along with embryonic tendon markers were seen in samples after 7 days, 30 minutes per day loading (164). This study also demonstrated the need for continued dynamic stress to be applied to maintain tendon like cellular characterisation. This study agrees with our findings, with

collagen 1a2, collagen 3a1 and tenascin C expression maintained in hMSC seeded collagen scaffolds exposed to dynamic stress with the addition of BMP 12 and BMP13 or FGF4, FGF6 and FGF8 added to media.

MSC seeded collagen constructs have been found to become stiffer after 14 days of low level, low frequency loading. The authors found that the direct contact with cells that collagen sponges provide created a system that was more efficient at transmitting forces to cells than basic collagen gels. This study also suggests that the original scaffold architecture that cells initially adhere to is an important factor when designing materials for tendon tissue engineering. (209). It has also found that slow stretching of collagen scaffolds increased the amount of fibrillar alignment and overall scaffold mechanical properties, significantly increasing stiffness and ultimate tensile stress after 4 days continuous loading (159). These studies agree with our findings, with mechanical loading significantly increasing both stiffness and ultimate tensile stress (load to fail) of scaffolds seeded with any of rat tenocytes, human adult or embryonic stem cells.

Fibril alignment in embryonic tendon formation has been found to be controlled by intracellular specific sites between the Golgi apparatus and cell membrane. Procollagen molecules are arranged into small diameter collagen fibrils which are then excreted in hexagonally shaped bundles by the cell parallel to the axial direction of the tendon (43). It has been suggested that further fibrillogenesis then occurs when other small collagen fibrils start aligning and joining together to form mature tendon after birth (210). No evidence of these intracellular sites in adult cells has yet been found, perhaps explaining the increases in mechanical properties seen in embryonic stem cell seeded scaffolds when compared to MSC seeded constructs, with both load to fail and stiffness being found to be higher. It has also been found that the absence of mechanical loading leads to the loss of fibropositors in embryonic tendon cells (211), explaining how constructs seeded with ESCs were generally

mechanically stronger and stiffer after mechanical loading and showed increased matrix organisation when compared to other cell types exposed to similar culture conditions.

This investigation has for the first time investigated the combined effect of FGF 4, FGF 6 and FGF 8 on cells seeded into a 3D scaffold environment. FGF 4 has been shown to play a crucial role in mesenchyme patterning during embryonic development (57) (58). FGF 6 is strongly linked with skeletal development in embryos (60),(61), with studies also finding that it is needed during adult skeletal muscle development and repair (212). FGF 8 is associated with embryonic patterning of mesenchyme tissues and in embryonic limb bud development (63),(64),(213). As tendon tissue forms in the developing embryo at similar time points to muscle tissue, shortly after the development of a limb bud, it can be assumed that combinations of FGFs 4, 6 and 8 are closely associated with the formation of the collagen extracellular matrix of both tissue types. We have demonstrated in this study that a combination of FGF 4, FGF 6 and FGF 8 lead to tendon specific cellular expression markers being expressed by hMSCs in 3D PHBHHx/collagen hybrid scaffolds in static culture conditions, with mechanical loading prolonging the expression of TBSD-4 indicating that cells are maintaining a tendon like molecular characterisation.

BMP 12 has been found to induce tenogenesis in rat bone marrow derived MSCs (48). BMP13 has been previously shown to play a role in tendon matrix regeneration after injury (214). Previous work performed in our laboratory has also found strong evidence of BMP12/13 influencing human ESCs towards tenogenic lineages in 2D culture. Our work adds to the body of evidence linking BMP12 and 13 with tendon development and repair, reporting for the first time the influence of these molecules in conjunction with PHBHHx/collagen hybrids scaffolds, finding that growth factors are needed to maintain tenascin C expression in hMSCs for over 5 days culture.

Experimental issues regarding the sectioning of samples greatly limited the conclusions that can be made from the histological analysis. During the sectioning process it was found that the blade was not slicing the sample consistently and as a result, sections were frequently too thick, folded or contained air bubbles, factors which prevented solid conclusions from being made from the polarised light images (207). This could have been prevented by using a cryostat, however due to equipment malfunction and time constraints this option was not available. A potential alternative to polarised light that could have been used is immunohistochemistry, looking for collagen I or other commonly used tendon markers such as scleraxis or collagen I expression (215).

During the RNA extraction process for RT-PCR it became apparent that sufficient amounts of RNA could not be extracted from SDhESCs or RaT seeded samples. This could have been caused by insufficient homogenisation during the enzymatic steps of the isolation procedure, resulting in cells being lost or cells being retained in solid sections of tissue that were filtered out during the cell lysis process(216). A potential way of remedying this problem in future studies would be to use higher concentrations or volumes of collagenase and lysis solution. Repeating the centrifugation step through the QIA Shredder (section **2.4.3**) by placing the flow through back onto the Shredder membrane, leaving for 3 minutes, then re centrifuging, ensuring that all the sample has passed through into the collecting tube could also lead to more RNA being collected from the samples.

5.5. CONCLUSION.

This investigation has demonstrated the need for mechanical pre conditioning of cell seeded constructs before use in tendon tissue engineering. All cell types used showed potential evidence of increased matrix modelling in response to low frequency cyclical mechanical stress, resulting in constructs adopting higher mechanical properties, similar to those found in similarly sized natural tendon tissue. Mesenchymal stem cells were found to maintain or adapt tendon like molecular characteristics, with tendon specific RNA sequences being expressed by cells in response to mechanical stimulus. Mechanical loading was found to have no effect on acellular controls, with no signs of matrix ordering being noted at any time point. PHBHHx/collagen hybrid scaffolds, in conjunction with tendon specific growth factors and cyclical mechanical stimulus have been found to maintain expression of cellular markers associated with tendon by hMSCs over a 20 day culture period.

Chapter 6

Pilot *in vivo* Study of a PHBHHx/collagen construct

6.1. INTRODUCTION.

Tendon injury is an increasing problem in medicine, with over 300,000 tendon procedures performed annually in the United States (217). Tendon is characterised by poor repair following injury or disease, is relatively acellular and has a poor blood supply (176). Treatment can involve many different types of surgical intervention, such as a xenograft or an allograft to treat large tendon defects, however potential problems with this method (such as foreign body reaction) can occur (12). A lack of adequate strategies for repair of tendons had led to development of engineered replacement tendon tissues for use in surgical transplantation. It is because of these reasons that tendon has been identified as an area where tissue engineering could be used to aid in tissue repair (39).

Traditionally, small tendon lacerations are treated by suturing the damaged ends together, followed by a programme of physiotherapy designed to manage the forces exposed to the repairing tissue. For large defects constructs can be required to bridge the gap. Graft tissues are frequently used with varying effectiveness. Autografts (taking a section of donor tissue from another part of the patient – usually the hamstring) provide the current gold standard treatment, with minimal chance of immunorejection, however donor site morbidity and pain are commonly associated (40). Allografts from donor or cadaveric tissue can also be used, however immunorejection, low numbers of donors, and greater failure rate problems are common (11). Xenograft tissues from animal sources are starting to be investigated for use; however major concerns regarding long term viability and cross species disease transmission remain (12). Commercially available artificial tendon graft products are in clinical use; however prolonged immune response and post-operative infection have been widely reported (41). Due to the problems associated with tendon repair surgery, new

techniques and materials need to be developed in order to meet the increasing clinical need.

Several *in vivo* models for tendon injury have been used to determine the effectiveness of novel treatments. Induced defect models are commonly used and generally fall into three categories according to the problem being investigated: taking a small area out of the overall tissue (119), bisecting the tissue and reconnecting the severed ends (222), or completely removing a section of tissue leaving a gap between the severed ends (124). Small animal models used include mouse (123), rat (222) and rabbit (116), (203), with the Achilles tendon usually investigated, owing to its ease of access, relative comparative size to larger animal tendons and direct comparability with the undamaged tendon on the other limb (223). Larger animal models can be used to determine if graft constructs can be scaled up in size to match the dimensions and mechanical properties of human tissue. A common large animal model is the equine digital flexor tendon, where constructs placed into an induced defect model (119) and autologous stem cell (bone marrow MSC) treatment for induced tendonitis (103) have provided data that could lead to future clinical applications in humans.

PHBHHx is one of the few PHA molecules that can currently be produced on a sufficiently large scale to use both in scientific research and medical device construction (140). The aim of this study was to explore the use of PHBHHx and PHBHHX/collagen hybrid scaffolds for the *in vivo* treatment of damaged tendon, monitoring *in vivo* immune response, scaffold breakdown and restoration of mechanical properties and tendon microstructure.

6.2. MATERIALS AND METHODS.

6.2.1. Animals.

15 male Sprague-Dawley (SD) rats 180-200 g were obtained from the Centre for Biomedical Analysis, Tsinghua University, China. Animals were treated as section **2. 7. 1**., being kept in authorised facilities and under local ethical and handling guidelines throughout the experiment.

6.2. Scaffold Preparation.

PHBHHx/ collagen hybrid constructs were prepared using the method as section **2. 3. 7**. Overnight salt leeching resulted in scaffolds having a porous overall structure (Fig. 1 A). PHBHHx fibres were included in the final scaffold design to aid in suturing and positioning of the constructs into the injury site. Construct designs consisting of multiple combinations of fibres and tubes were analysed, with fibres either passed individually through the tube or woven in a French braid (Fig. 6.1).

PHBHHX/collagen gel hybrids were created by injecting pre made collagen gel (section **2. 3. e.**) into the centre of the tube after implantation using a 12 gauge hypodermic syringe. Individual gels were created for each rat used in the experiment, with the gel being injected into the scaffold once fixed in the animal (described below).

Before surgery scaffolds were sterilized using 70% IMS/ deionised H_2O solution overnight in a biological safety cabinet under UV. Scaffolds were then stored and transported in sterile PBS / 10% antibiotic PSA solution in a sealed 15 mL centrifuge tube. Scaffolds were then only handled using aseptic surgical technique.

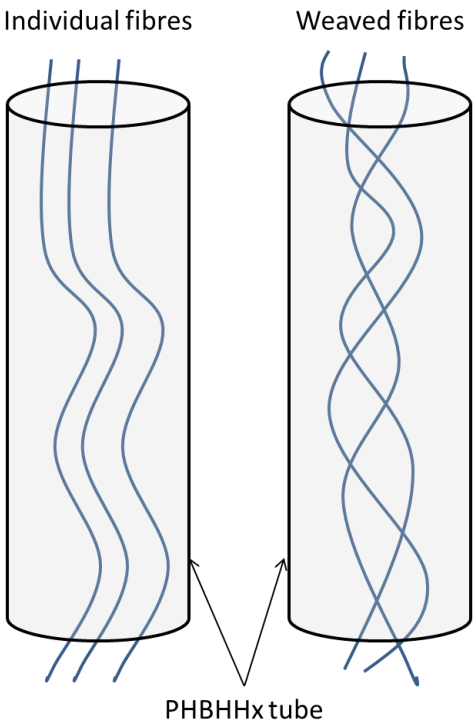

Figure 6.1. PHBHHx scaffold design. Constructs were constructed using a PHBHHx outer tube and up to 3 PHBHHx fibres. Fibres were included to aid in the suturing of scaffolds in the animal model. Several designs were considered for use, with 3 fibres woven in a French braid pattern being the final design chosen.

6.2.3. Scaffold Characterisation.

Scanning electron microscopy was used to determine the microstructure of the tube and the fibre elements of the scaffold as section **2.6.3**. Measurements were taken using the supplied electron microscope software, with 8 measurements of 3 fibres taken at random points along the fibre diameter. Stretch to break testing was carried out on a variety of scaffold combinations to determine which was most closely aligned to natural tendon strength using a material testing machine (Tension Compression load Cell Tester, NTS Canada) at a rate of 10 mm/minute. A control of healthy tendon from rats of comparable age was used as a benchmark. All samples were immersed in warm complete media for 2 hours prior to

testing, with samples tested in a wet state. 3 samples were tested for each scaffold type, with each sample being prepared separately.

Scanning electron microscopy (SEM) (FEI Quanta 200, Tsinghua Medical School, Beijing) was carried out using samples of both fibre and tube to explore the topographical structure.

6.2.4. Surgical Procedure.

Surgical procedures were carried out by experienced (consultant) orthopaedic surgeons at the Surgical Training Centre, Peking University Hospital Number 1, Beijing, China. Surgery was carried out as per the procedure described in section **2. 7. 2**. A brief description and overview of the surgical groups and the differences in surgery can be found in figures 6.2. and 6.3.

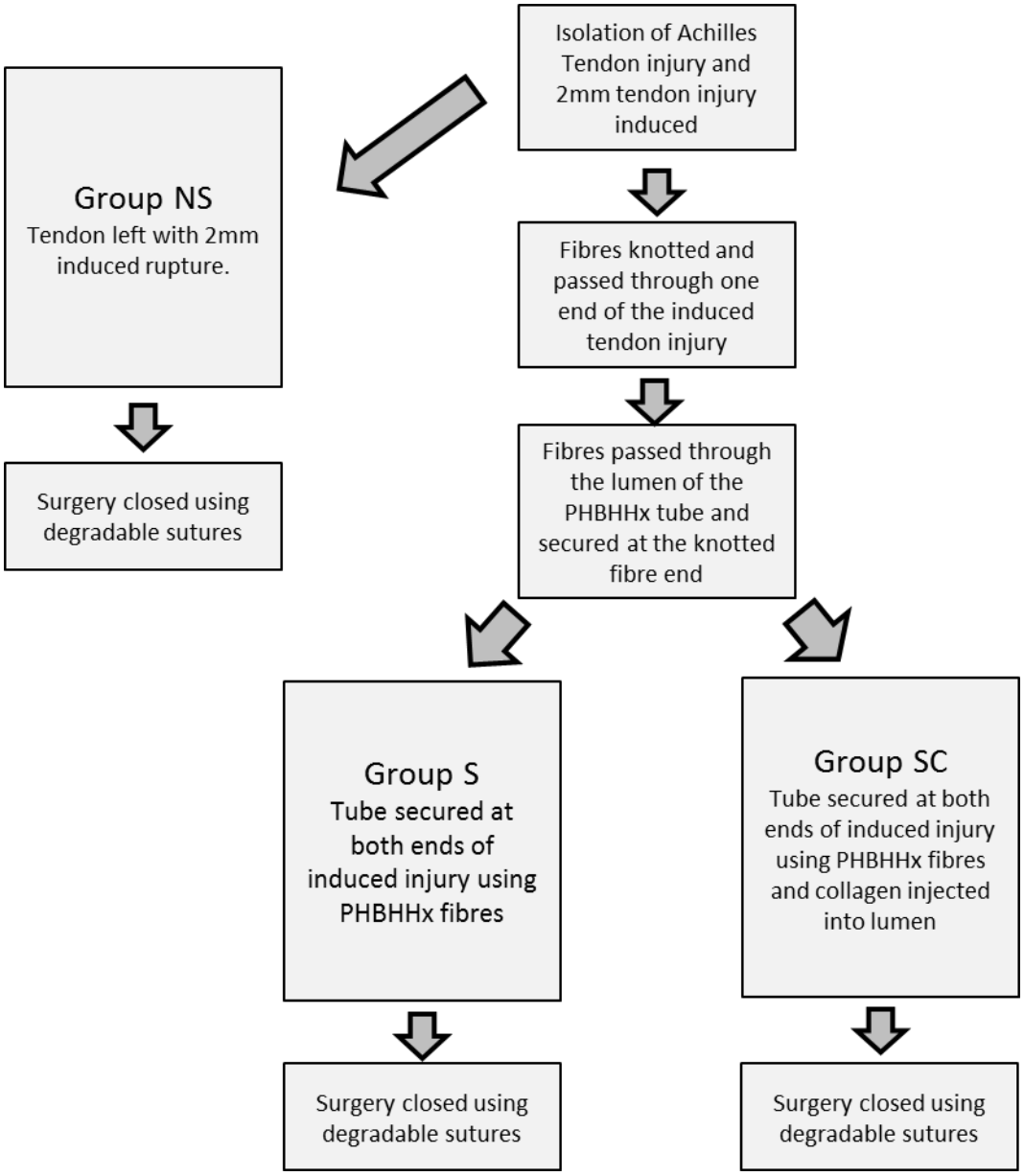

Figure 6.2. Surgical procedure diagram explaining experimental groups. Group NS (no scaffold) were animals with an induced 2mm defect injury that was left open and allowed to heal naturally. Group S (scaffold) were animals with an induced 2mm injury with a PHBHHx tube/fibre construct implanted into the wound site. Group SC (scaffold + collagen) were animals with an induced 2mm defect injury with a PHBHHx tube/fibre scaffold that was filled with collagen gel.

Experimental Groups							
Group	**Description**	**Scaffold Components**	**Cells**	**Number of Animals**	**CRP/AFI animals sampled**	**Mechanical testing**	**Histological Analysis**
NS	Control#	-	-	5	3*	3**	2
S	Scaffold Only	3 x PHBHHx Fibres and 1 x PHBHHx Tube	-	5	3*	3**	2
SC	Scaffold and Collagen	3 x PHBHHx Fibres , 1 x PHBHHx Tube and Collagen gel	-	5	3*	3**	2
# 2mm section of tendon excised with no surgical repair							
* n=3 sampled randomly from each experimental group of 5 animals at each time point, ** n=3 picked at random from each experimental groups of 5 after 40 days with the remaining 2 samples used for histological analysis							

Figure 6.3. Experimental groups and numbers of animals used for each analytical procedure. 5 animals were chosen at random from a 15 strong colony of 180 – 200g male Sprague-Dawley (SD) rats during surgery. Blood samples were taken from 3 randomly chosen rats at each consequent time point after surgery, with 3 rats being chosen post sacrifice for mechanical evaluation, with the remaining 2 rats being used for histological analysis.

6.2.5. Immune response analysis.

Immune response was monitored by measuring C Reactive Protein (CRP) levels in blood. Blood samples were taken from rat tail veins, with serum isolated by centrifugation and analysed using an ELISA kit and plate reader according to method **2. 7. 4**.

6.2.6. Detection of breakdown molecules.

The breakdown of the scaffold was quantified by measuring the concentration of β-hydroxybutyrate in blood serum over time. Serum was isolated by immediate

centrifugation (within 5 minutes of the blood being collected) from blood samples taken from tail veins, before analysis with a colorimetric assay according to method **2. 7. 5**.

6.2.7. Restoration of mechanical properties.

To test for restoration of mechanical strength to pre injury levels, a stretch to break test was carried out using 3 of the samples from each group. The non-operated tendons were taken as positive control. Following removal the tendon was loaded into the Tension Compression Load Cell Tester (NTS Canada) so that the tendon ends were held by the clamps, and stretched at a rate of 10 mm/min until complete failure was observed.

6.2.8. Histological Assessment.

Structural analysis of one sample from each group was performed using H & E according to standard procedures. Prior to staining the sample was first fixed using 70% methanol for 24 hours, then embedded in paraffin wax before sectioning into 8 μm thick sections and placing onto a glass slide. Sections from the injury site and healthy areas of tendon were analysed. Images were taken using an Olympus IX 71 microscope and TH4-200 digital camera.

6.2.9. Statistical Analysis.

Results were deemed to be significant if $P<0.05$ using a 2 tailed Students T-test.

6.3. RESULTS.

6.3.1. Scaffold design and characterisation.

SEM was used to determine the microstructure of both the fibre and the tube elements of the scaffold. The fibre had an average diameter of 247.1 ± 20.3 µm (Fig. 6.4).

Rat Achilles tendon has an average breaking load of 17.35 ± 1.76 N (Fig. 6.5). Several designs of porous PHBHHX scaffold with 1-3 fibres (woven and non-woven) had their mechanical properties evaluated. The nearest in mechanical performance to natural tendon was a tube with 3 fibres running through the centre of it (Fig. 6.5), with comparable breaking loads observed (23.73 ± 1.08 N) compared to rat Achilles tendon (p=0.24). The addition of collagen gel to the centre of the scaffold was found to have minimal effect on the initial mechanical strengths of the constructs, registering break forces of 25.14 ± 1.25 N, which was significantly higher (p=0.03) than rat Achilles tendon.

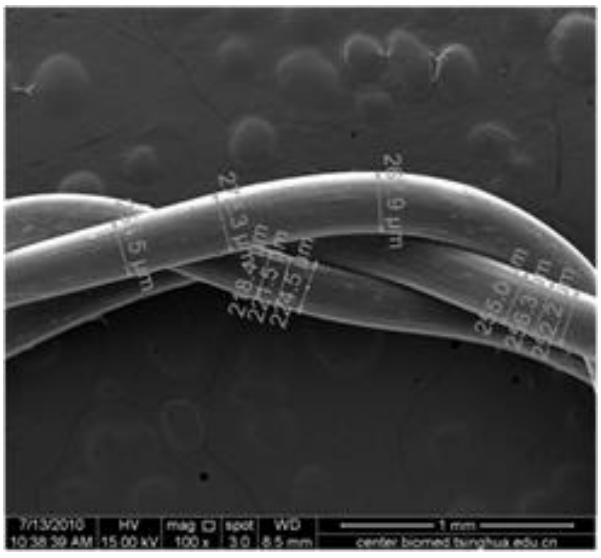

Figure 6.4. SEM images of fibre. 3 fibres at 100x with markers indicating diameter. Image taken at Tsinghua University Medical School.

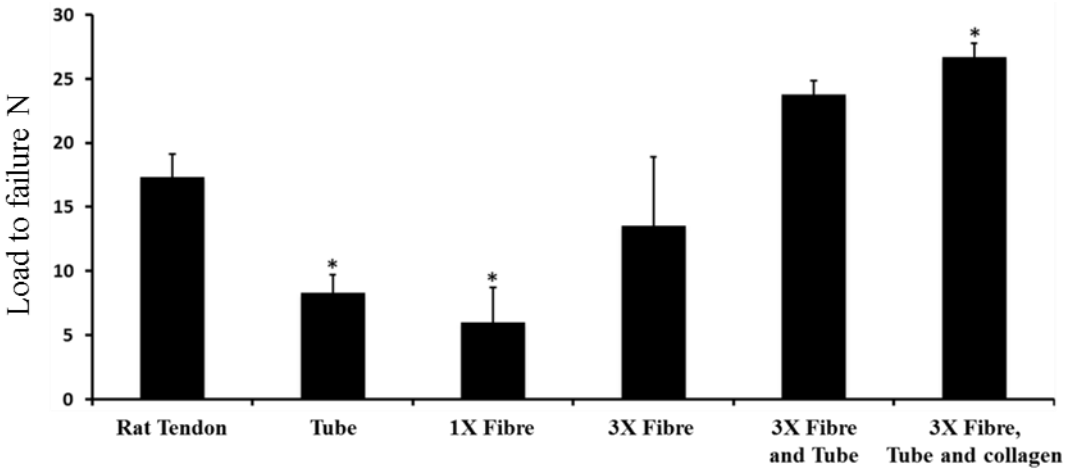

Figure. 6.5. Mechanical loading of scaffold designs. Scaffolds were immersed in PBS for 1 hour before tensional mechanical properties were established. Ultimate tensile stress was established by a stretch to break test. Scaffold designs tested included a single tube, a single fibre, 3 fibres, 3 fibres combined with a tube and 3 fibres combined with a tube filled with collagen. A control of a freshly dissected rat Achilles tendon was also included. Graph shows mean ± 1SD, n = 3. * significant difference (p≤0.05) compared to rat tendon.

6.3.2. Mechanical strength.

Once removed from the animals at day +40 stretch to break tests were performed on the excised repairing tendon/scaffold samples. The scaffold/collagen group had comparable load at failure (18.02 ± 7.45 N) to undamaged tendon (17.35 ± 1.78 N) (Fig. 6.6). The no scaffold and scaffold only groups were found to have lower average breaking loads than healthy tendon, but had similar values to each other, (no scaffold: 10.99 ± 7.62 N, scaffold: 9.55 ±4.49 N) indicating that an implant of both scaffold and collagen is required to achieve tendon-like stretch to break test scores. The scaffold only group was found to have significantly lower load to failure ($p = 0.04$) compared to undamaged tendon.

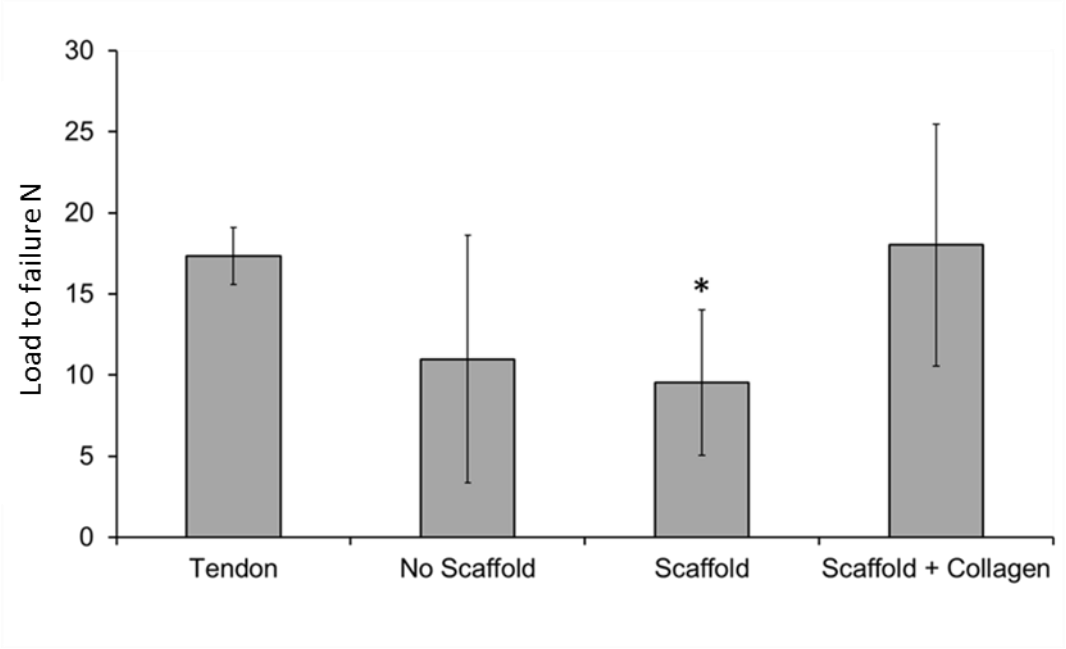

Figure. 6.6. Mechanical testing of remodelling tissue/constructs 40 days post implantation. Tissue was removed from sacrificed animals and stored in PBS until testing. Ultimate tensile stress was obtained using a stretch to break test, with tissue from animals with no scaffold, a PHBHHx tube/fibre scaffold and a PHBHHx tube/fibre + collagen gel scaffold. An undamaged tendon was included as a control. Graph shows mean ± 1 standard deviation (n=3). (* indicates significant to undamaged tendon control).

6.3.3. Histological analysis.

Microscopic evaluation of the damaged tendon sites with Haematoxylin and Eosin demonstrated evidence of cellular infiltration and partial structure regeneration to varying degrees dependent upon the scaffold implanted. Cellular migration into the defect site was apparent throughout where increased migration was observed SC group implant had been introduced to the wound site when compared to either healthy tendon (Fig. 6.7) or a wound site with Group S (Fig. 6.7). A characteristic of tendon tissue is the crimp pattern which is presented by the elongated sinusoidal wave like patterning of the nuclei and cytoplasm of the cells as apparent in the undamaged tendon sample. The emergence of the wave-like

patterning was observed in the SC group (yellow arrows). Cells formed a consistent wave pattern when in contact/close proximity to the fibre or tube component of the implant. This demonstrates that morphological tendon-like cell presence within the tissue was observed being created around the implant, rather than just overlaying fibrous tissue. This was less evident in the group S (Fig. 6.7), indicating that tendon regeneration was more efficient in the SC implant group.

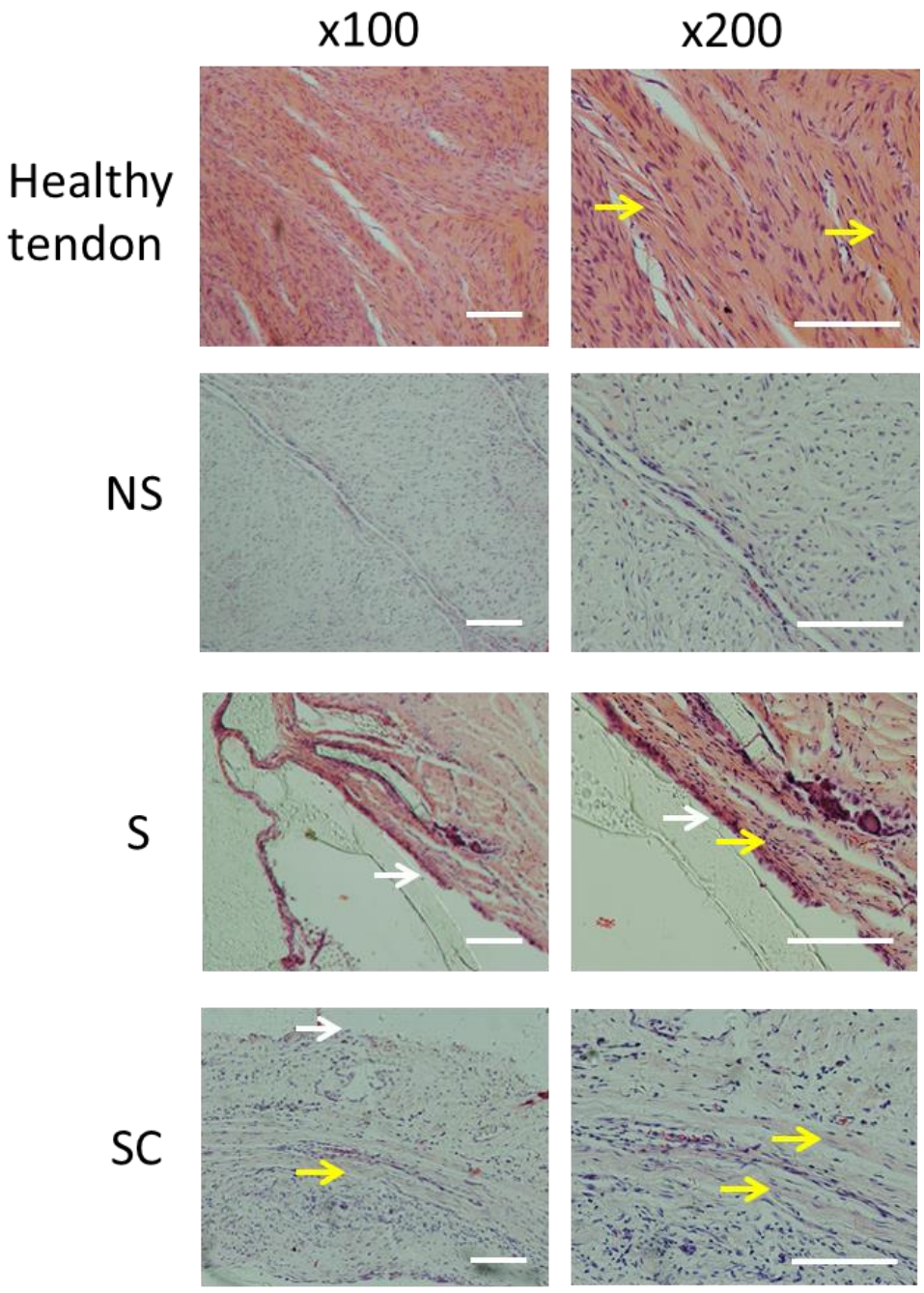

Figure 6.7. H&E stained samples taken from the damaged region of the tendon and from the same region of an uninjured control tendon. Samples were taken from either the inside of the scaffold or the injury site where no scaffold was present. NS: no scaffold implanted into injury site. S: PHBHHx tube and fibre construct implanted into injury site. SC: PHBHHx tube and fibre construct filled with collagen implanted into the wound site. White arrows show areas of scaffold/tissue interaction. Yellow arrows indicate wave like alignment of cells and matrix. Scale bar = 100µm. Sectioning and staining were performed by Tsinghua University centre for biological research.

6.3.4. Polymer breakdown.

β-hydroxybutyrate (HB) is a naturally occurring molecule found in the body. The base level concentration was found by measuring blood serum samples from animals with no scaffold implantation at days 10 and 40, finding an average value of 0.16 mM. When scaffold and scaffold/collagen groups were normalised to this value it was apparent that the scaffold only group was degrading at a greater rate than scaffold/collagen up to days 2 (p= 0.03) and 10 (p= 0.05), after which the trend was reversed at day 20 (p=0.01) (Fig. 6.8).

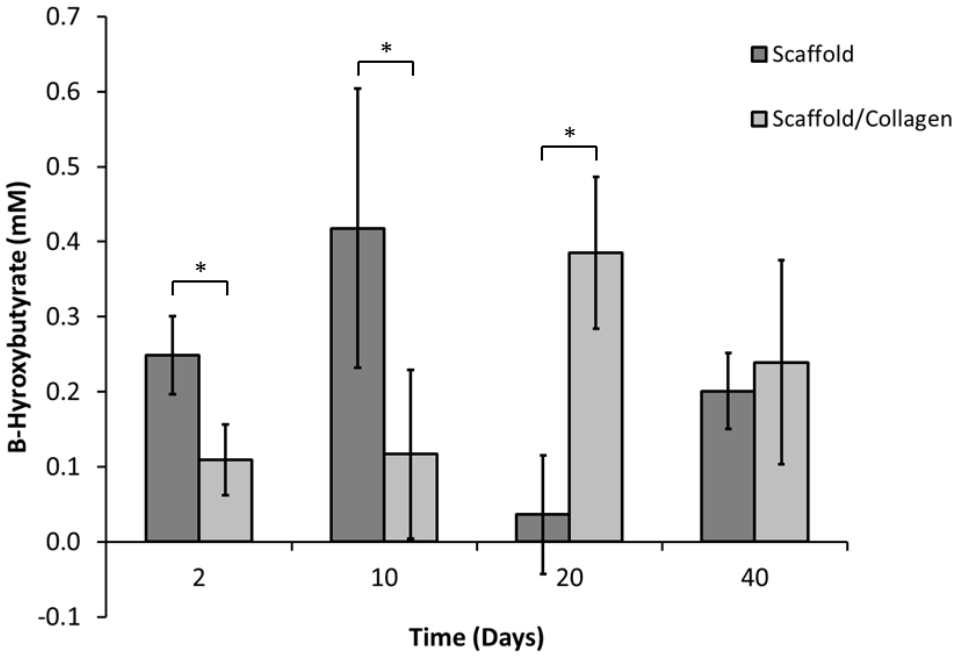

Figure. 6.8. Normalised β-Hydroxybutyrate levels in blood serum over time. Values of PHBHHx and PHBHHx/collagen scaffold groups normalised to no scaffold group values. Graph shows mean values zeroed to average levels found in no implant group ± 1 standard deviation (n=3). (* significant difference between groups (p≤0.05).

6.3.5. Immune response.

Immune response was quantified by measuring the concentration of C-Reactive Protein (CRP) in the blood serum. Samples were taken at time points pre- and post-surgery. Prior to surgery all rats were considered as one group (n=15) with an initial CRP concentration at day -5 found to be 878.06 ± 147.80 µg/L (Fig. 6.9). This was elevated slightly at day -2 to 985.47 ± 128.92 µg/L possibly due to the injury caused by taking a blood sample. Surgery was performed on day 0. Blood samples were not taken at day 0 due to blood loss during surgery. CRP was found to have increased significantly in all groups at day +2 after surgery, with the largest reaction being seen in the scaffold only group (1299.05 ± 121.23 µg/L) and the lowest in the scaffold/collagen group (1131.35 ± 117.40 µg/L). CRP was found to be the highest 48 h post-surgery. No statistical difference between the groups at this time point was observed. By day +5, CRP dropped back to pre-surgery levels, and levels continued to drop slightly at day +10, with the scaffold only group recording the lowest level at 905.78 ± 54.00 µg/L. A small secondary response was observed in both no scaffold and scaffold groups at day+ 20 which was significantly higher ($p=0.004$, 0.0003 respectively) than the level of the scaffold/collagen group. At day +40 all animals were found to have CRP at or below pre surgery levels with the scaffold/collagen group showing the lowest (727.77 ± 42.30) and scaffold only the highest (817.71 ± 21.7) concentrations (Fig. 6.9).

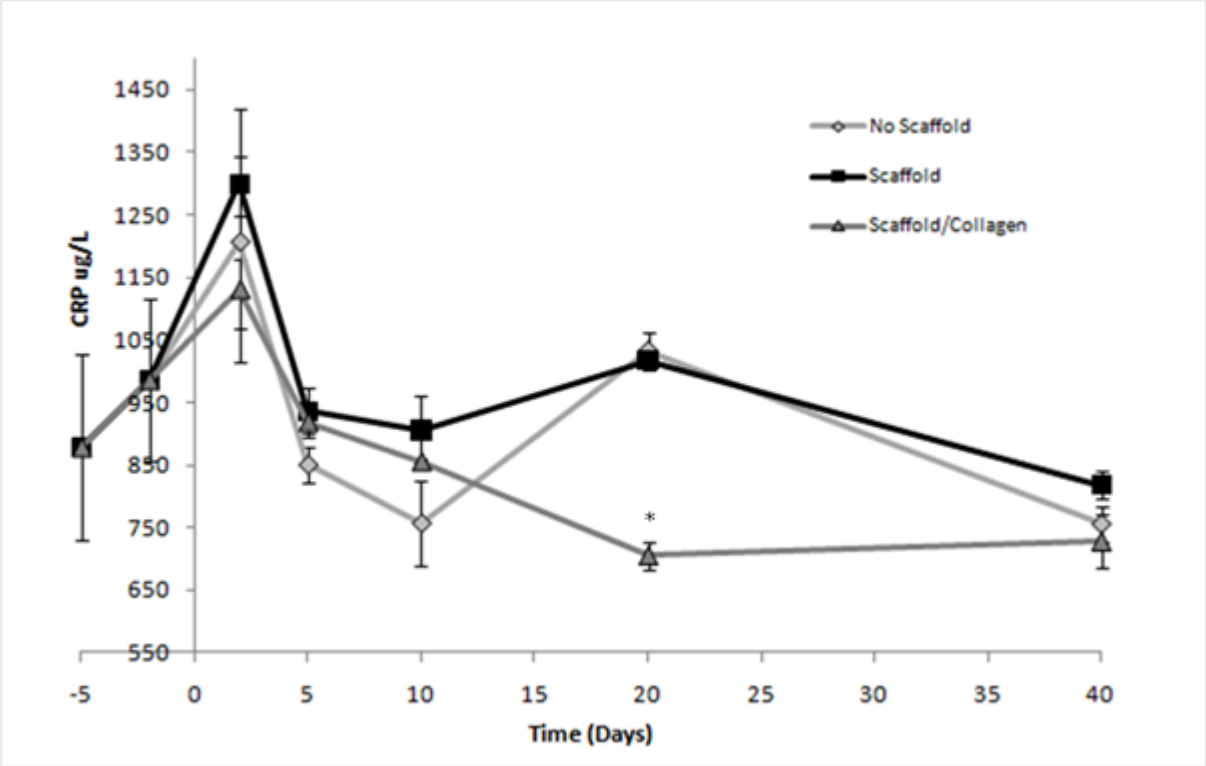

Figure. 6.9. Blood concentration of CRP in recipient rats. No scaffold: rat with induced 2 mm tendon injury. Scaffold: rats with injury bridged with PHBHHx construct. Scaffold/Collagen: rats with injury bridged with PHBHHx/collagen construct. Surgery occurred on day 0. Pre surgery all rats were considered as one group (n=15). Post surgery animals were separated into separate groups (n=5*). Graph shows mean ± 1 standard deviation with group numbers as described. *Group A lost one rat during surgery, and one at day 29. Group B lost one rat on day 30. (* significantly lower than other groups at time point).

6.4. DISCUSSION.

The aim of this investigation was to identify a PHBHHx scaffold design that could be used to improve the rate of damaged tendon tissue healing while not initiating a prolonged immune response. To do this a design that would induce cellular migration and tissue remodelling while at the same time allowing for limited restoration of movement was required and found. The physiological demands placed on tendon tissue are high. A design consisting of a porous tube containing three individual fibres was identified as being mechanically similar to the rat Achilles tendon and to other commercially available human tendon repair materials (208). Further analysis of the scaffold using SEM revealed a consistent porosity across the tube structure and a constant fibre diameter.

Mechanical testing of samples recovered from the rats at day +40 found that the scaffold/collagen group had a comparable mechanical load capability to undamaged tendon, matching the performance of traditional tendon laceration treatments (218), and bettering the performance shown by porcine intestinal sub mucosa (219) and PLGA based (7), (29) (131),(220) treatment methods. However, the success of the implant and the healing rate caused was variable. This could be explained by variability in manufacturing although intra-group mechanical properties were within a narrow range. It has also been shown that small differences in components of the surgical procedure, such as suturing, can affect the failure rate of tendon implants (208). What is apparent that the addition of the scaffold/collagen implant at the wound site increased the mechanical strength significantly when compared to the no scaffold control group, and that the scaffold alone increased the overall mechanical strength. This highlights the importance of collagen in the remodelling of tendon and concurs with previous studies suggesting collagen is a beneficial inclusion in tendon graft material (37), (131).

C-Reactive Protein (CRP) is an early marker for inflammatory response caused by an implanted material (221). As expected, CRP rose dramatically after surgery in all experimental groups to a maximum value after 48 hours, returning to pre surgery levels at day +5 [31]. Day +10 results showed that CRP levels either continued to fall or remained stable, however at day +20 a small increase was observed in no scaffold and scaffold only groups. This could have been caused by several factors, including small re-injury (such as one of the stitches becoming dislodged) (208) or that the rats started causing injury to themselves (fighting). It could also be caused by the tendon's natural development cycle creating a small amount of inflammation around the wound site, which would not be unusual at around 2 weeks post injury (37). Day +40 results show low CRP concentrations in all groups, indicating that no long term immunological response was occurring due to the presence of a PHBHHx scaffold; improving on similar conclusions made by previous studies (222). This also creates a possible advantage over many commercially available synthetic tendon graft materials which have been found to present long term immunological risk (40). The drop in CRP concentration to levels seen below those measured before the surgery could be explained by the longer periods of time between blood sample collections, allowing for any potential inflammation caused by the collection process to subside. It could also be caused by the relative size of the injury in comparison to the size of the animal being smaller as the rats became larger (223).

β-Hydroxybutyrate is a constituent monomer of PHBHHx (143). Measurement of HB concentration in blood over time demonstrated that scaffold breakdown was erratic, with large error bars showing the discrepancies between the individual samples. The trend shows that scaffolds without collagen seemed to breakdown at an earlier stage than those containing collagen, with higher values found at days 2, 5 and 10. At days 20 and 40 this trend was reversed. Further refinement of the production method should improve the

variation. By comparing the β-hydroxybutyrate concentration with the CRP level it becomes apparent that there is no link between the factors. This agrees with a previous study (179) in suggesting that the breakdown products of PHBHHx are immunologically inert, as when large increases in HB concentration are present no rise in CRP is seen.

Cellular infiltration into the scaffold was observed in both the Group S and Group SC designs along with sinusoidal cellular alignment, a key marker in the histological analysis of tendon tissue, signifying the presence of crimp angles between collagen fibrils (224). However, Group SC showed a denser cellular presence with sinusoidal morphology along the surface of the PHBHHx scaffold, implying a more favourable environment for cells is produced when a collagen lumen is present within the scaffold design (15). The sinusoidal-elongated morphology could indicate force transmission from the fibre to the cells resulting in mechano-transduction promoted tendon cell proliferation and alignment. Earlier studies highlighted that the addition of collagen within scaffold design can aid integration within the implanted tissue (131). This further highlights the importance of collagen addition, not only in the tissue integration and remodelling of tendon but as a means of delivering cells to a point of repair, and further adds to previous studies suggesting collagen is a beneficial inclusion in tendon graft material (124), (129).

Cellular therapies for tendon healing have been found to produce promising results in the equine model (116), (127); however the relative high costs and secondary surgical procedures required to harvest cells for inclusion in tendon repair scaffolds could be preventing their current widespread use in the clinic (39). Our study suggests that the inclusion of exogenous or endogenous cells is not necessarily required to produce tendon healing, although further experimentation with the addition of cells to the construct would be required before absolute conclusions can be made.

6.5. CONCLUSION.

This study has demonstrated that PHBHHx can be used as a scaffold material for the treatment of damaged tendon tissue *in vivo* and that its breakdown products are immunologically inert in the rat model. It has also shown that cells migrate into a PHBHHx scaffold *in vivo* and begin remodel damaged tissue, with a PHBHHx plus collagen scaffold resulting in the greatest mechanical properties of the healing tissue after a 40 day time period. When considered together, these results provide a foundation to proceed with a larger, more in depth *in vivo* study, where further indications can be investigated.

Chapter 7.

Discussion.

Tendon injury and disease is increasingly prevalent and notoriously difficult to cure. Treatment success is dependent on many factors, including patient age, type of injury and time between injury and medical intervention, with many injuries being untreatable (10). Because of these issues, a strong clinical need exists for new treatments to be developed, incorporating novel biomaterials and cellular components to provide a clinical advantage over current best treatment methods (39). Tissue engineering or regenerative medicine aims to use scaffolds and cells to regenerate and restore function of tissue lost through damage, disease, and disorder (1). The use of PHBHHx has been explored by many groups investigating multiple potential applications including cellular interactions and its use as a scaffold in tissue engineering (142), (143), (145), (146), (148), (182).

A key consideration when designing a tissue engineered construct is how cells interact with the scaffold material. Many cells require contact adhesion to remain viable (225). It is therefore vital to establish early on in the design of tissue engineering scaffolds that the specific cell type to be used is compatible with the materials chosen. PHBHHx has been previously used to culture many different cell types. A previous report demonstrated that hMSC adherence was greatly improved on PHBHHx films when compared to both tissue culture plastic and other PHA molecules (144). Adipose derived MSCs were also successfully cultured in 3D PHBHHx scaffolds before being stimulated into chondrogenic differentiation (147). This chapter and corresponding journal manuscript (182) demonstrate that rat tenocytes and human mesenchymal stem cells adhere to and spread across PHBHHx polymer films, with a preferred rigidity of >420N/m over at least a 72 hour culture period. This supports the assertion of PHBHHx as a candidate material for tendon tissue engineering and adds to the body of literature supporting the biocompatibility of PHBHHx.

Investigation into rat tenocyte attachment to PHBHHx films as a total of all cells present in the well demonstrates that when wt/vol ratios of ≥ 1.6% were used over 90% of cells adhered to the film in preference to the untreated plastic surface. This could in some part be explained by the increase in stiffness of the polymer film between 1.6% and 2.0% wt/vol, suggesting that increased polymer rigidity promoted increased tenocyte adhesion. This reinforces a number of previous studies which have demonstrated that material stiffness affects cellular adhesion and behaviour (173) (174). hMSC have previously been shown to have less preference when adhering to surfaces with differing mechanical properties, although differentiation and proliferative capacity are altered (124), (143), (175) explaining why little difference was found between polymer concentrations.

Tendon tissue is poorly vascularised with a low mean oxygen concentration (176). Hypoxic atmospheric (1 – 3% O_2) conditions have been found to be beneficial to cells, delaying senescence and increasing proliferative capacity (72). Mesenchymal stem cells have been shown to have higher proliferation (30 fold increase) in 2% O_2 compared to 21% O_2 (170). Human embryonic stem cell colonies have been found to be less heterogenic and have more stable self-renewal capacity when cultured in 2% O_2 (85). Tendon derived stem cells have also been found to proliferate faster at 2% O_2 compared to atmospheric conditions (86). Initial investigations were therefore performed in both room oxygen (21% O_2) and tendon tissue normoxia (2% O_2). Previous studies into the effects of different oxygen concentrations on cells have demonstrated enhanced proliferation, enhanced clonogenicity, reduced karyotypic abnormalities, reduced spontaneous differentiation, altered transcriptional profiles, and altered FTIR profiles across numerous cell types including hMSCs (70), (71), (85), (177), (178). When comparing 2% O_2 with 21% O_2 only small differences were found between cell number or percentage attachment at the same PHBHHx concentration for either cell type. hMSCs were generally noted to adhere better

in hypoxic conditions to all polymer film compositions, however no significant rises were found, possibly due to large inter-group deviations. To our knowledge, this was the first study looking into the *in vitro* effects of oxygen tension on the interaction of primary mammalian cells with polyhydroxyalkanoate scaffolds. In our study, rat tenocytes were found to proliferate faster during the first stages of culture in 2% O_2, but this difference was not maintained over a longer culture period. It was also noted that cells did not migrate from tendon tissue samples in 2% O_2; leading to the conclusion that tenocyte isolation via explant requires atmospheric oxygen to take place. The proportion of HHx in the polymer has been proposed as an important modulator of cell behavior. Proliferative capacity of rat smooth muscle cells was enhanced by 20% HHx though attachment at seeding was optimal with 12% HHx (226). In our study we have also found robust attachment of hMSC and RaT to 12% HHx polymer films when used at the optimal wt/vol ratio, although further work is required to identify the optimum %HHx in the polymer for use any potential future tendon therapeutic products.

Cell spreading was monitored across polymer surfaces in the absence of mechanical stimuli or directional forces over a period of 72 hours by marking cells with fluorescent tracker dye (DiO). This method was essential due to polymer opacity. After 24 hours the cells were clumped together on the surface of the polymer. This behavior is not uncommon in cell culture and can be explained by the cells not being separated sufficiently when re-suspending after centrifugation. After 72 hours the cells were seen to move apart from each other, filling the available space on the polymer. Yang et al (227) found that mouse islet cells showed increased metabolic activity when cells were cultured on PHBHHx in comparison to tissue culture plastic and Poly Lactic Acid. This investigation also looked into cell migration across a PHBHHx film surface, finding that cells were moving from an

even distribution to clump together to start to form functional units. These findings agree with our work that cell locomotion is possible across PHBHHx surfaces.

DiO and other similar dyes used for tracking cells can be expelled by the ABCG2 multi-drug transporter pathway (228). HMSCs retained dye more efficiently than tenocytes although both had undergone reductions in intensity after 72 hours suggesting that some of the dye may have been exocytosed. Migration into the polymer surface was measured with confocal microscope generated z-stacks, allowing for cross sectional views to be created in both the x-z and y-z directions. Cells were always found to be in one plane of view, with no further fluorescent signatures being seen above or below the single plane. This indicated that the cells remained on the surface of the polymer as opposed to migrating into it indicating that localized polymer degradation had not occurred over the time period tested. This observation is reinforced by previous reports which state that PHBHHx is broken down *in vivo* (179) and *in vitro* (180) at very slow rates via hydrolysis.

Tendon stem cells are a sub population of cells present in tendon that are capable of differentiating into bone, cartilage and adipocytes (27). TDSC have different morphologies to mature tenocytes. TDSCs have a “cobblestone” like appearance when cultured to confluence, with an enlarged nucleus, whereas tenocytes have an elongated “spindle” like morphology when confluent, with little contact seen between cells. TDSCs have also been found to have significantly longer population doubling times when compared to tenocytes isolated from the same tendon source (83). After passage 8, it was found that cells isolated from tendons started to change morphology, becoming shorter and squarer in appearance. Due to this apparent shift in cell phenotype, experimentation using cells isolated from tendons was performed using cells at or below passage 4, making it far more likely that a population of tenocytes were used rather than tendon stem cells.

This work has demonstrated the potential of using PHBHHx as a material for tendon tissue engineering, promoting cellular adherence and migration across a 2D scaffold surface and maintaining viability over a 3 day time period in both 21% O_2 and 2% O_2, providing a solid foundation for further work investigating the polymer's use for potential tissue engineering applications.

The next stage in construct development was to identify a scaffold design that was both capable of withstanding the mechanical loading of tendon tissue and allowing for cellular growth and matrix development. By incorporating the major constituent molecule of tendon (collagen I), a hybrid scaffold of a PHBHHx tube and a collagen core was found that was mechanically similar to rat tendon and capable of maintaining cellular viability and phenotype over a 20 day culture period. The interaction of human embryonic stem cells with the construct was also assessed, providing for the first time a study on the effects of PHBHHx/collagen scaffolds on human embryonic stem cells *in vitro*.

The application and suitability of PHBHHx as a scaffold material in 3D models for human and animal stem cell biocompatibility has been described in several previous studies (148), (222), (147), (122), (197), (114), (180). The microstructure of PHBHHx scaffolds has also been shown to influence cellular behaviour. Rat MSCs adhere to and elongate along the length of electrospun PHBHHx scaffolds, demonstrating that fibre orientation played a strong role in promotion of differentiation toward a specific lineage (aligned promoted osteogenesis whereas random promoted adipogenesis) (197). Cartilage like structures have also been formed by human adipose derived stem cells pre-seeded onto salt leached, porous 3D PHBHHx foams, then successfully implanted subcutaneously into a nude mouse model (147).

Type I collagen gels supported the differentiation of murine ESCs into either osteogenic or chondrogenic lineages when seeded into 2D and 3D 1.2 mg/mL scaffolds. The additional presence of lineage specific supplements (beta-glycerol phosphate – bone, chondroitin sulphate – cartilage) was found to further increase differentiation above that found in control collagen gels, with greater expression of SOX-9 measured using qRT-PCR after 15 days culture. Viability within the collagen gels was unclear but surface viability was approximately 60% after 15 days culture(198). Human and murine ESC culture in 0.75 mg/mL type I collagen gels has also been achieved by pre differentiating cells into Embryoid Bodies before suspension (199). Undifferentiated ESCs were not compatible with our PHBHHx/collagen gel hybrid scaffold system. Our study has demonstrated that hESCs required a prior spontaneous differentiation step induced by exposure to foetal bovine serum prior to collagen gel suspension to shift cell phenotype away from that of a self-renewing ESC into a partially differentiated heterogeneous population for long term culture in type I collagen gels. Here we report viability and contractile behaviour of hESC and pre-differentiated hESC in PHBHHx/collagen gel hybrid scaffolds after a pre-differentiation stage, and demonstrate a 40-60% cell viability of SDhESC after 20 days continuous static culture. Viability of hMSCs in constructs was found to be 70-80% after 20 days, indicating no adverse effects of the scaffold in the cells.

Differentiation of MSCs in hydrogel based scaffolds has been well researched. Bone marrow derived MSCs and umbilical cord derived MSCs were compared in a study investigating differentiation on collagen I/III gels, finding that in the absence of lineage specific media, neither osteogenesis nor adipogenesis was stimulated, however osteogenesis was induced in both cell types after 21 days (185). Mechanostimulation has been suggested as an alternative to chemostimuli when inducing MSC differentiation on collagen scaffolds. A cyclic compressive strain study on hMSC seeded collagen-alginate

gels demonstrated up regulation of CBFA-1 (RUNX2) after 7 days when compared to static unloaded controls (205). This suggests cells were becoming more osteoblastic, as the RUNX2 transcription factor has been shown to be critical for the promotion of osteogenic differentiation (204). By inducing chondrogenic differentiation of MSCs in collagen I gels it was found that increased chondrogenesis could be achieved by increasing both collagen concentration in the gel and the initial cell seeding density. However, similar to our study, they found that little evidence of chondrogenesis was induced in 3mg/mL collagen gels seeded with $1x10^5$ MSCs (229). B-actin is frequently used as a housekeeping gene due to its consistent presence as a cytoskeletal component of mammalian cells, and is commonly used as a marker of cellular viability (203). We noted expression of β-actin throughout the 20 day period which, when coupled to the high cell viability provided an additional demonstration of viable cell transcriptional activity. Expression of lineage specific molecular markers for multiple tissue lineages also suggested that cells were maintaining phenotype over 20 day static culture in PHBHHx/collagen hybrid scaffolds.

For this scaffold design, minimal collagen contraction is essential to facilitate the integration of implanted cells into host tissue when placed *in vivo*, increasing the likeliness of cellular infiltration and the overall rate of recovery (230). Collagen gel contraction by fibroblastic cells is well established (200). Cells interact with the surrounding ECM via strong inward tractions located at the tips of long slender extensions, similar to those used by a cell to migrate across a surface (231). Platelet derived growth factor (PDGF) is believed to be one of the stimuli considered to be responsible for causing the extensions to contract (232) (233). Decreasing collagen gel concentrations from 2.6 to 1.3 mg/mL was reported as having a greater impact on gel contraction kinetics than increasing the rabbit MSC density by the same fold increase (500K to 1M cells/mL) (167). This suggests that availability of fibril binding sites in the collagen is the major factor in gel contraction and

not seeding density *per se*. Similarly human corneal fibroblasts can contract a 4.5mg/mL collagen gel over a 25 day static culture period when seeded at a cell concentration of 5 x 10^5 cells/mL, but not 1 x 10^5 cells/mL (169). These reports correlate with our observations where little contraction was observed in the 3 mg/mL groups, and the rate of contraction slowed with 1.5 mg/mL gels seeded with lower cell densities. We have therefore identified a cell:collagen ratio with negligible collagen contraction at cell seeding densities of 1 x 10^6 cells/mL or lower, and provide high cell viability in the absence of additional stimuli for application in studies utilising either hMSC or SDhESC.

The use of mechanical loading has been highlighted in several papers as being necessary for long term expression of cellular markers for many different tissue lineages in 3D culture models. These tissues include tendon (165), muscle (234) and bone (154). Further work investigating the effects of mechanical stimulus to PHBHHx/collagen scaffolds seeded with several cell types was therefore required to establish further if forces could act through the construct and induce cells towards a tendon specific lineage. This investigation demonstrated for the first time the effects of growth factors, mechanical loading and PHBHHx/collagen hybrid scaffolds on human stem cells, finding mechanical loading to have positive tenogenic effects on hMSC seeded scaffolds, with increased mechanical properties and maintenance of tendon specific molecular markers over a 20 day culture period.

Cellular viability in PHBHHx has been found to be high throughout long term *in vitro* culture. Cells previously cultured on PHBHHx include rabbit MSCs (197), murine islet cells (227), smooth muscle cells (226) and osteoblasts (143). 3D collagen gels have also demonstrated the ability to sustain high cell viability throughout long term culture. Silk/collagen hybrid scaffolds were found to sustain high viability and function of differentiated hESCs (ESC-MSC cells) over 14 days with mechanical loading (124). Our

studies demonstrated that viability of hMSCs, hESCs and rat tenocytes was high throughout the experimental time period, building on previous conclusions demonstrating the suitability of PHBHHx/collagen hybrid scaffolds for tissue engineering applications. Our theory is that total cell numbers were reduced after mechanical loading due to collagen gel being lost from the centre of the tube during the BOSE chamber loading process, although loss was not quantified.

Human movement is controlled by contracting muscles acting through tendons. As a result, tendon tissue is consistently under high levels of mechanical stress, usually applied in a cyclical motion (158). Investigations into the mechanical stimulation of tendon tissue engineered constructs have been shown to influence cell behaviour in many ways. Long term mechanical loading has been found to result in tenocyte seeded PGA constructs into dense fibrillar structures with higher levels of tendon specific proteins being expressed by cells and being found in the overall matrix when compared to non-loaded controls (160). This work corresponds with our findings, with mechanical loading significantly increasing both load to fail and stiffness in tenocyte seeded samples where specific combinations of growth factors were added.

Bone marrow derived human mesenchymal stem cells have been shown to create tendon like structures when exposed to dynamic cyclical mechanical stress when seeded in collagen scaffolds (164). Up regulation of collagen I and III expression, along with embryonic tendon markers were seen in samples after 7 days of 30 minutes per day loading. This study also demonstrated the need for continued dynamic stress to be applied to maintain tendon like cellular characterisation. This study agrees with our findings, with collagen 1a2, collagen 3a1 and tenascin C expression maintained in hMSC seeded collagen scaffolds exposed to dynamic stress and fibroblast growth factors 4, 6 and 8 over a 20 day period. MSC seeded collagen constructs have been found to become stiffer after 14 days of

low level, low frequency loading (209). This study suggests that the original scaffold architecture that cells initially adhere to is an important factor when designing materials for tendon tissue engineering, finding that the direct contact with cells that collagen sponges provide were more efficient at transmitting forces to cells than basic collagen gels. It has also found that slow stretching of collagen scaffolds increased the amount of fibrilar alignment and overall scaffold mechanical properties, significantly increasing stiffness and ultimate tensile stress after 4 days loading (159). These studies agree with our findings, with mechanical loading significantly increasing both stiffness and load to failure of scaffolds seeded with both rat tenocytes and human adult and embryonic stem cells, with an insignificant increasing trend observed in hMSC seeded scaffolds.

Fibril alignment in embryonic tendon formation has been found to be controlled intracellularally by specific sites between the Golgi apparatus and cell membrane. Procollagen molecules become arranged into small diameter collagen fibrils which are excreted in hexagonally shaped bundles through the cell membrane parallel to the axial direction of the embryonic tendon (43). Further fibrillogenesis occurs when other small collagen fibrils start aligning and joining together to form mature tendon after birth (210). No evidence of these intracellular sites in adult cells has yet been found, perhaps explaining why embryonic stem cells were found to show greater remodelling of collagen than MSCs and increases in both load to fail and stiffness. It has also been found that the absence of mechanical loading leads to the loss of fibropositors in embryonic tendon cells (211), providing a potential explanation of how constructs seeded with hESCs were generally mechanically stronger and stiffer after mechanical loading and showed increased matrix organisation when compared to other cell types exposed to similar culture conditions.

Vitamin C was added to media in conjunction with growth factors in small concentrations as it has been found by several studies to aid in tendon regeneration (235) and increases the cellular production of the major components of tendon (236). Ascorbic acid also acts as an anti-oxidant (237), helping to maintain the growth factor stability in the media for longer and prolonging the effectiveness of the molecules.

This investigation has for the first time investigated the combined effect of FGF 4, FGF 6 and FGF 8 on cells seeded into a 3D scaffold environment. FGF 4 has been shown to play a crucial role in mesenchyme patterning during embryonic development, with an absence of FGF 4 leading to a failure of proper development (57), (58). FGF 6 is strongly linked with skeletal development in embryos (60,61), with studies also finding that it is needed during adult skeletal muscle development and repair, possibly acting to recruit satellite cells to the wound site (212). FGF 8 is associated with embryonic patterning of mesenchyme tissues and in embryonic limb bud development (63), (64), (213). As tendon tissue forms in the developing embryo at similar time points to muscle tissue, shortly after the development of a limb bud, it was assumed that combination of FGFs 4, 6 and 8 would be closely associated with the formation of the collagen extracellular matrix of both tissue types. We have demonstrated in this study that a combination of FGF 4, FGF 6 and FGF 8 lead to tendon specific cellular expression markers being maintained or stimulated by hMSCs, but not in hESCs in 3D PHBHHx/collagen hybrid scaffolds. BMP 12 has been found to induce tenogenesis in rat bone marrow derived MSCs, with increases in scleraxis, tenomodulin, tenascin C and collagen 1a2 expression noted in treated cells compared to control samples, and tendon like tissues being formed when pre-treated cells were seeded into collagen scaffolds and implanted *in vivo* (48). BMP13 has been previously shown to play a role in tendon matrix regeneration after injury (214), with knockout studies in mice finding similar results (238). Unpublished work performed in our laboratory has also found

strong evidence of BMP12/13 influencing human ESCs towards tenogenic lineages in 2D culture. The data presented here adds to the body of evidence linking BMP12 and 13 with tendon development and repair, reporting for the first time the influence of these molecules in conjunction with PHBHHx/collagen hybrids scaffolds, finding that growth factors are essential for the maintenance of tenascin C expression in hMSCs for over 5 days culture, and that FGFs 4, 6 and 8 are needed for expression of Thrombospondin-4 in hMSCs in 3D PHBHHx/collagen hybrid scaffolds.

PHBHHx has been found to be an effective material as an implant device in several studies (148), (150), (222). Further investigation into the effect of implanting a PHBHHx/collagen hybrid scaffold into a tendon wound site was required to gain an understanding of how the construct reacts *in vivo*, with mechanical properties, breakdown characteristics and immune response needed to be evaluated to gain a greater understanding of how these materials could be used in future therapeutic treatments.

There are three grades of tendon injury; I, II and III, with grade III the most severe and most likely to not respond to treatment (31). When tendon defects are too large to heal naturally, constructs are required to bridge the gap and aid the regeneration process. Graft tissues are frequently used with varying effectiveness, with autografts providing the most reliable source of transplant material (40). Allografts from donor or cadaveric tissue are currently used, however lack of supply, greater failure rates and immunorejection problems prevent further development (11). Decellularised xenograft tissues are starting to be used more widely in the clinic, however major concerns remain regarding long term viability and cross species disease transmission (12). Artificial tendon grafts have been in wide clinical use for many years, however prolonged immune response and post-operative infection have been widely reported (41). Due to these problems associated with tendon

repair surgery, new techniques and materials are needed to meet the increasing clinical need. This investigation used an induced Achilles defect in the rat model to monitor an implanted PHBHHx and PHBHHx/collagen hybrid construct that could be used to improve the rate of damaged tendon tissue healing while not initiating a prolonged immune response.

Mechanical testing of samples recovered from the rats 40 days post implantation found that the scaffold/collagen group had a comparable mechanical load capability to undamaged tendon, matching the performance of traditional tendon laceration treatments (218), and bettering the performance shown by porcine intestinal sub mucosa (219) and PLGA based (131), (220) treatment methods. However, the success of the implant and the healing rate caused was variable. This could be explained by variability in manufacturing although intra-group mechanical properties were within a narrow range. It has also been shown that small differences in components of the surgical procedure, such as suturing, can affect the failure rate of tendon implants (208). It was apparent that the addition of the PHBHHx/collagen hybrid implant at the wound site increased the mechanical strength significantly when compared to the no scaffold control group. This highlights the importance of collagen in the remodelling of tendon, concurring with previous studies suggesting collagen is a beneficial inclusion in tendon graft material (37), (131).

Regular sinusoidal cellular alignment is a key marker in the histological analysis of tendon tissue, signifying the presence of crimp angles between collagen fibrils (224). Evidence of cellular alignment was seen in samples of damaged tissue from all three experimental groups; however it was most apparent in those with the scaffold/collagen implant, potentially suggesting a faster healing rate. It was also most evident when cells were in direct contact with the scaffold. This was observed with scaffold-collagen implants,

indicating that force transmission through the fibre to the cells promoted tendon cell proliferation and alignment.

C-Reactive Protein (CRP) acts as an early marker for inflammatory response caused by an foreign object material or to tissue damage (221). As expected, CRP levels in blood serum rose dramatically after surgery in all experimental groups to a maximum value after 48 hours, returning to pre surgery levels after 5 days (181). Further stability of CRP was seen after day 5, however small peaks were seen after 20days in animals where constructs were placed. Long term (40 days post-surgery) low CRP levels demonstrate that no chronic inflammatory response was occurring, demonstrating immunological compatibility in the rat model. These findings indicate a possible advantage over the available synthetic tendon graft materials which have been found to present long term immunological risk (40), however longer term assessment of constructs would be required before more conclusive statements can be made.

β-Hydroxybutyrate is a constituent monomer of PHBHHx (143). Measurement of HB concentration in blood over time demonstrated that scaffold breakdown was erratic, with large error bars showing the discrepancies between the individual samples. Trends in the data show that constructs without collagen breakdown at an earlier stage than those containing collagen, where this trend was reversed, however wide variations seen in the groups hinder the conclusions that can be made from this. Further refinement of the production method should improve the variation, with more close control of both porosity and polymer volume aiding to make the process more consistent. When β-hydroxybutyrate and CRP concentrations were compared it became apparent that there is no link between the factors, further suggesting the immunological inertness of PHBHHx and its in vivo breakdown products (179).

Chapter 8

Conclusion and Future Perspectives

8.1. Conclusion.

This study has demonstrated the effectiveness of PHBHHx and combinations of PHBHHx and collagen for tendon tissue engineering applications. Early work found cellular viability and migration capacity to be high on PHBHHx films, providing evidence that the polymer was nontoxic to both human and rodent derived cells. It was also found that hMSCs adhere better to stiffer films, providing further evidence to the body of knowledge on cellular adherence being influenced by material properties.

Polymer and collagen constructs were designed that closely resembled the mechanical properties of native rat Achilles tendon. Cell viability and phenotype were maintained throughout 20 days static culture. It was also established that a cell concentration of under 1×10^5 cells/mL in 3mg/mL collagen gels would not lead to collagen contraction, potentially increasing the probability of an *in vivo* construct integrating with native tissue and thus creating an overall more successful implant.

Mechanical stimulation of cells in constructs was found to increase mechanical properties and tendon like matrix morphologies of PHBHHx/collagen scaffolds. It was also found that mechanical stimulation was essential for continued expression of tendon specific cellular markers. Supplementation of tenogenic growth factors was found to increase the mechanical properties of cell seeded scaffolds, although these increases were largely observational rather than statistically significant.

Implantation of PHBHHx/collagen hybrid scaffolds in an induced rat Achilles tendon defect model found that scaffolds did not initiate a prolonged immune response over a 40 day experimental period, despite increased levels of scaffold breakdown products being found in blood serum. Evidence of cellular migration and matrix remodelling was also

apparent, providing strong evidence that scaffolds were being incorporated into the wound site and starting to aid in the healing process.

This thesis has proven through a series of *in vitro* and *in vivo* experiments that PHBHHx and collagen can be seeded with human stem cells or rat tenocytes to form constructs suitable for tendon tissue engineering applications.

8.2. Future Perspectives and Avenues of Research.

This thesis has demonstrated that PHBHHx can be used to culture human stem cells and animal tenocytes, and that combination of PHBHHx and collagen can be formed into scaffolds suitable for tissue engineering of tendon. This research acts as a foundation for further work in the field, with several potential avenues of research remaining to be explored.

The integration of musculotendon and osteotendon tissue boundaries provides the next logical step for further research. Integration of these tissues would provide a working model of a complete tendon system, allowing for future drug and treatment testing to be carried out and effect seen over the differing tissues found in and around tendons. A proposal to integrate graphine into the tube structure to encourage osteoblastic differentiation has been generated, as has a proposed collaboration with groups working in muscle tissue engineering areas.

Different variants of PHBHHx can also be investigated. This research has focussed on using PHHBBx with an HHx mass percentage of 12.1%, due to its availability and compatibility with other musculoskeletal cell types. Mass percentage can vary according to initial culture conditions present when the polymer is produced from 8% to 20%, with varying properties associated with this change.

Growth factors have been added as a media supplement as part of this investigation. Further research into the controlling of cellular exposure to growth factors could result in much stronger effects being seen. One way in which growth factors could be introduced to the system could be via the use of nanoparticles. These particles would breakdown at a controlled rate, allowing release to be temporally and spatially controlled. Another option would be to introduce angiogenic growth factors into the outer PHBHHx tube, adding to

the properties held by the polymer and better replicating the highly vascularised tissues surrounding large tendons.

Further *in vivo* analysis of the construct would also be required before any potential use in humans can be made. This investigation has already determined that PHBHHx/collagen scaffolds do not initiate any prolonged immune response. Further experimentation using more advanced versions of the scaffold should provide greater insight into how this type of construct could be utilised in humans, with higher mechanical strengths and more accurate tissue architecture allowing for greater integration of tissue and thus a lower chance of implant failure.

References

(1) Mason C. A brief definition of regenerative medicine. Regenerative Medicine. 2008;3(1):1-5.

(2) Mason C. Regenerative medicine cell therapies: numbers of units manufactured and patients treated between 1988 and 2010. Regenerative Medicine. 2010;5(3):307-313.

(3) Macchiarini P, Jungebluth P, Go T, Asnaghi MA, Rees LE, Cogan TA, Dodson A, Martorell J, Bellini S, Parnigotto PP, Dickinson SC, Hollander AP, Mantero S, Conconi MT, Birchall MA. Clinical transplantation of a tissue-engineered airway. Lancet. 2008;372(9655):2023-2030.

(4) Atala A, Bauer SB, Soker S, Yoo JJ, Retik AB. Tissue-engineered autologous bladders for patients needing cystoplasty. Lancet. 2006;367(9518):1241-1246.

(5) Barakat O, Abbasi S, Rodriguez G, Rios J, Wood RP, Ozaki C, Holley LS, Gauthier PK. Use of decellularized porcine liver for engineering humanized liver organ. Journal of Surgical Research. 2012;173(1):11-25.

(6) Ross EA, Williams MJ, Hamazaki T, Terada N, Clapp WL, Adin C, Ellison GW, Jorgensen M, Batich CD. Embryonic stem cells proliferate and differentiate when seeded into kidney scaffolds. Journal of the American Society of Nephrology. 2009;20(11):2338-2347.

(7) Badylak SF, Weiss DJ, Caplan A, Macchiarini P. Engineered whole organs and complex tissues. Lancet. 2012;379(9819):943-952.

(8) Guenou H, Nissan X, Larcher F, Feteira J, Lemaitre G, Saidani M, Del Rio M, Barrault CC, Bernard FX, Peschanski M, Baldeschi C, Waksman G. Human embryonic stem-cell derivatives for full reconstruction of the pluristratifi ed epidermis: a preclinical study. Lancet. 2009;374(9703):1745-1753.

(9) Sharma P. Tendinopathy and tendon injury: The future. Disability and Rehabilitation, 2008 2008;30(20-22):1733-1745.

(10) Sharma P. Tendon Injury and Tendinopathy: Healing and Repair. The Journal of Bone and Joint Surgery 2005;87:187-202.

(11) Pallis M, Svoboda SJ, Cameron KL, Owens BD. Survival comparison of allograft and autograft anterior cruciate ligament reconstruction at the united states military academy. American Journal of Sports Medicine. 2012;40(6):1242-1246.

(12) Longo UG, Lamberti A, Maffulli N, Denaro V. Tendon augmentation grafts: a systematic review. British Medical Bulletin 2010;94:165-188.

(13) Kannus P. Structure of the tendon connective tissue. Scandinavian Journal of Medical Science Sports 2000;10:312-320.

(14) Butler DL, Grood ES, Noyes FR, Zernicke RF. Biomechanics of ligaments and tendons. Exercise and Sport Sciences Reviews 1978;6:125-81.

(15) Wang JHC. Mechanobiology of tendon. Journal of Biomechanics 2006;39:1566-1582.

(16) Richardson LE, Dudhia J, Clegg PD, Smith R. Stem cells in veterinary medicine – attempts at regenerating equine tendon after injury. Trends in Biotechnology 2007;25(9):409-416.

(17) Birch HL, Worboys S, Eissa S, Jackson B, Strassburg S, Clegg PD. Matrix metabolism rate differs in functionally distinct tendons. Matrix Biology 2008;27:182-189.

(18) Riley GP, Harrall RL, Constant CR, Chard MD, Cawston TE, Hazleman BL. Glycosaminoglycans of humanrotator cuff tendons: changes with age and in chronic rotator cufftendinitis. Annals of the Rheumatic Diseases 1994;53:367-376.

(19) Birk DE, Fitch JM, Babiarz JP, Doane KJ, Linsenmayer TF. Collagen fibrillogenesis in vitro: interaction of types I and V collagenregulates fibril diameter. Journal of Cell Science 1990;95(4):649-657.

(20) Bailey A.J, Paul RG, Knott L. Mechanisms of maturation and ageing of collagen. Mechanisms of Ageing and Development 1998;106:1-56.

(21) Jozsa L, Kannus P, Balint Jb, Reffy A. 3-dimensional ultrastructure of human tendons. Acta Anatomica 1991;142(4):306-312.

(22) Samiric T, Parkinson J, Ilic MZ, Cook J, Feller JA, Handley CJ. Changes in the composition of the extracellular matrix in patellar tendinopathy. Matrix Biology 2009;28:230-236.

(23) Pins GD, Christiansen DL, Patel R, Silver FH. Self-assembly of collagen fibers. Influence of fibrillar alignment and decorin on mechanical properties. Biophysical Journal 1997;73(4):2164-2172.

(24) Yoon JH. Tendon proteoglycans: biochemistry and function. journal of Muskuloskeletal andd Neuronal Interactions 2005;5(1):22-34.

(25) Schulze-Tanzil G, Mobasheri A, Clegg PD, Sendzik J, Shakibaei JM. Cultivation of human tenocytes in high-density culture. Histochemistry and Cell Biology 2004;122:219-228.

(26) Bernard-Beubois K, Hecquet C, Houcine O, Hayem G, Adolphe M. Culture and characterisation of juvinile rabbit tenocytes. Cell Biology and Toxicology 1997;13:103-113.

(27) Bi Y, Ehirchiou D, Kilts TM, Inkson CA, Embree MC, Sonoyama W, Li L, Leet AI, Seo BM, Zhang L, Shi S, Young MF. Identification of tendon stem/progenitor cells and the role of the extracellular matrix in their niche. Nature Medicine. 2007;13(10):1219-1227.

(28) Maffulli N. Rupture of the achilles tendon. Journal of Bone and Joint Surgery 1999;81(7):1019-1036.

(29) Benjamin TP, Nokes M, Pugh N. Review of the vascularisation of the human Achilles tendon. Injury. 2005;36(11):1267-1272.

(30) Langberg H, Olesen J, Skovgaard D, Kjaer M. Age related blood flow around the Achilles tendon during exercise in humans. European Journal Applied Physiology 2001;84(3):246-248.

(31) Thaker H. Engaging stem cells for customized tendon regeneration. Stem Cells International. 2012:309187.

(32) Maganaris CN, Narici MV, Maffulli N. Biomechanics of the achilles tendon. Disability and Rehabilitation 2008;30(20-22):1542-1547.

(33) Arampatzis A, Karamanidis K, Morey-Klapsing G, De Monte G, StafilidisS. Mechanical properties of the triceps surae tendon and aponeurosis in relation to intensity of sport activity. Journal of Biomechanics 2007;40:1946-1952.

(34) Gajdosik RL, Lentz DJ, McFarley DC, Meyer KM, Riggin TJ. Dynamic elastic and static viscoelastic stress-relaxation properties of the calf muscle-tendon unit of men and women. Isokinetics and Exercise Science 2006;14:33-44.

(35) Ryan ED, Herda TJ, Costa PB, Walter AA, Hoge KM, Stout JR, Cramer JT. Viscoelastic creep in the human skeletal muscle–tendon unit. European Journal of Applied Physiology 2010;108(1):207-211.

(36) Screen HRC. Investigating load relaxation mechanics in tendon. Journal of the Mechanical Behavior of Biomedical Materials 2008;1(1):51-58.

(37) Koob TJ. Biomimetic approaches to tendon repair. Comparative Biochemistry and Physiology Part A 2002;133:1171-1192.

(38) Torigoe K, Tanaka HF, Yonenaga K, Ohkochi H, Miyasaka M, SatoR, Kuzumaki T, Yoshida K, Yoshida T. Mechanisms of collagen fibril alignment in tendon injury: from tendon regeneration to artificial tendon. Journal of Orthopaedic Research 2011;29(12):1944-1950.

(39) Bullough R, Finnigan T, Kay A, Maffulli N, Forsyth NR. Tendon repair through stem cell intervention: Cellular and molecular approaches. Disability and Rehabilitation 2008;30(20-22):1746-1751.

(40) Chen J, Xu J, Wang A, Zheng M. Scaffolds for tendon and ligament repair: review of the efficacy of commercial products. Expert Reviews Medical Devices 2009;6(1):61-73.

(41) Basiglini L, Iorio R, Vadalà A, Conteduca F, Ferretti A. Achilles tendon surgical revision with synthetic augmentation. Knee Surgury Sports Traumatology and Arthroscroscopy. 2010;18(5):644-647.

(42) Kadler KE, Holmes DF, Trotter JA, Chapman JA. Collagen fibril formation. Biochemical Journal. 1996;316:1-11.

(43) Canty EG, Lu Y, Meadows RS, Shaw MK, Holmes DF, Kadler KE. Coalignment of plasma membrane channels and protrusions (fibripositors) specifies the parallelism of tendon. Journal of Cell Biology 2004;165(4):553-563.

(44) Molchanova EA, Payushina OV, Starostin VI. Effects of growth factors on multipotent bone marrow mesenchymal stromal cells. Biology Bulletin 2008;35(6):555-570.

(45) Lejard V, Blais F, Guerquin MJ, Bonnet A, Bonnin MA, Havis E, Malbouyres M, Bidaud CB, Maro G, Gilardi-Hebenstreit P, Rossert J, Ruggiero F, Duprez D. EGR1 and EGR2 involvement in vertebrate tendon differentiation. Journal od Biological Chemistry 2011;286(7):5855-5867.

(46) Pryce BA, Watson SS, Murchison ND, Staverosky JA, Dünker N, Schweitzer R. Recruitment and maintenance of tendon progenitors by TGFβ signaling are essential for tendon formation. Development 2009;136:1351-1361.

(47) Sahoo S, Toh SK. Goh GHC. A bFGF-releasing silk/PLGA-based biohybrid scaffold for ligament/tendon tissue engineering using mesenchymal progenitor cells. Biomaterials 2010;31:2990-2998.

(48) Lee JY, Zhou Z, Taub PJ, Ramcharan M, Li Y, Akinbiyi T, Maharam ER, Leong DJ, Laudier DM, Ruike T, Torina PJ, Zaidi M, Majeska RJ, Schaffler MB, Flatow EL, Sun HB. BMP-12 Treatment of Adult Mesenchymal Stem Cells In Vitro Augments Tendon-Like Tissue Formation and Defect Repair In Vivo. PLoS One 2011;11(6):e17531.

(49) Wang EA, Rosen V, Cordes P, Hewick RM, Kriz MJ, Luxenberg DP, Sibley BS, Wozney JM. Purification and characterization of other distinct bone-inducing factors. Proceedings of the National Acadamy of Sciences U S A. 1988;85(24):9484-9488.

(50) Sieber C, Kopf J, Hiepen C, Knaus P. Recent advances in BMP receptor signaling. Cytokine Growth Factor Reviews 2009;20(5-6):343-355.

(51) Lou J, Tu Y, Burns M, Silva MJ, Manske P. BMP- 12 gene transfer augmentation of lacerated tendon repair. Journal of Orthopeadic Research 2001;19(6):1199-1202.

(52) Wolfman NM, Hattersley G, Cox K, Celeste AJ, Nelson R, Yamaji N, Dube JL, DiBlasio-Smith E, Nove J, Song JJ, Wozney JM, Rosen V. Ectopic Induction of Tendon and Ligament in Rats by Growth and Differentiation Factors 5, 6, and 7, Members of the TGFb Gene Family. Journal of Clinical Investigation 1997;100(2):321-330.

(53) Wang QW, Chen ZL, Piao YJ. Mesenchymal Stem Cells Differentiate into tenocytes by Bone Morphogenic Protien (BMP) 12 Gene transfer. Journal of Bioscience and Bioengineering 2005;100(4):418-422.

(54) Berasi SP. Varadarajan U. Archambault J. Cain M. Souza TA. Abouzeid A. Li J. Brown CT. Dorner AJ. Seeherman HJ. Jelinsky SA. Divergent activities of osteogenic BMP2, and tenogenic BMP12 and BMP13 independent of receptor binding affinities. Growth Factors 2011;29(4):128-139.

(55) Ornitz DM IN. Fibroblast growth factors. Genome Biology Reviews 2001;2(2)1–12.

(56) Kosaka N, Sakamoto H, Terada M, Ochiya T. Pleiotropic function of FGF-4: Its role in development and stem cells. Developmental Dynamics 2009;238:265-276.

(57) Niswander L MG. Fgf-4 expression during gastrulation, myogenesis, limb and tooth development in the mouse. Development 1992;114(3):755-768.

(58) Niswander L, Tickle C, Vogel A, Martin G. Function of FGF-4 in Limb Development. Molecular Reprodive Development 1994;39(1):83-89.

(59) Sun X, Lewandoski M, Meyers EN, Liu YH, Maxson RE Jr, Martin GR. Conditional inactivation of Fgf4 reveals complexity of signalling during limb bud development. Nature Genetics 2000;25(1):83-86.

(60) deLapeyrière O, Ollendorff V, Planche J, Ott MO, Pizette S, Coulier F, Birnbaum D. Expression of the *Fgf6* gene is restricted to developing skeletal muscle in the mouse embryo. Development 1993;118(2):601-611.

(61) Han JK MG. Embryonic expression of FGF-6 is restricted to the skeletal muscle liniage. Developmental Biology 1993;158(2):549-554.

(62) Zhao P HE. Embryonic myogenesis pathways in muscle regeneration. Developmental Dynamics 2004;229:380-392.

(63) Moon AM. Fgf8 is required for outgrowth and patterning of the limbs. Nature Genetics 2000;26(4):455-459.

(64) Boulet AM, Moon AM, Arenkiel BR, Capecchi MR. The roles of Fgf4 and Fgf8 in limb bud initiation and outgrowth. Develpmental Biology 2004;273:361-372.

(65) ViloniniS, RamelliP, Pisani LF, Gorni C, Mariani P. Horse bone marrow mesenchymal stem cells express embryo stem cell markers and show the ability for tenogenic differentiation by in vitro exposure to BMP-12. BMC Cell Biology 2009;10:29-39.

(66) Ahmed IM, Lagopoulos M, McConnell P, Soames RW, Sefton GK. Blood supply of the Achilles tendon. Journal Of Orthopaedic Research 1998;16(5):591-596.

(67) MilleBF, Olesen JL, Hansen M, Døssing S, Crameri RM, Welling RJ, Langberg H, Flyvbjerg A, Kjaer M, Babraj JA, Smith K, Rennie MJ. Coordinated collagen and muscle protein synthesis in human patella tendon and quadriceps muscle after exercise. Journal of Physiology 2005;567(3):1021-1033.

(68) Scutt N, Rolf CG, Scutt A. Tissue specific characteristics of cells isolated from human and rat tendons and ligaments. Journal of Orthopaedic Surgery and Research 2008;3(32).

(69) Taylor SE, Vaughan-Thomas A, Clements DN, Pinchbeck G, Macrory LC, Smith RKW, Clegg PD. Gene expression markers of tendon fibroblasts in normal and diseased tissue compared to monolayer and three dimensional culture systems. BMC Musculoskeletal Disorders 2009;10(27).

(70) Holzwarth C, Vaegler M, Gieseke F, Pfister SM, Handgretinger R, Kerst G, Müller I. Low physiologic oxygen tensions reduce proliferation and differentiation of human multipotent mesenchymal stromal cells. Cell Biology 2010, 11:11 2010;11(11).

(71) Forsyth NR, Musio A, Vezzoni P, Simpson AH, Noble BS, McWhir J. Physiologic oxygen enhances human embryonic stem cell clonal recovery and reduces chromosomal abnormalities. Cloning Stem Cells 2006;8(1):16-23.

(72) Poulios E, Trougakos IP, Chondrogianni N, Gonos ES. Exposure of human diploid fibroblasts to hypoxia extends proliferative life span. Molecular Mechanisms And Models Of Aging 2007;1119:9-19.

(73) Anitua E, Sánchez M, Zalduendo MM, de la Fuente M, Prado R, Orive G, Andía I. Fibroblastic response to treatment with different preparations rich in growth factors. Cell Proliferation 2009;42:162-170.

(74) Wagenhäuser MU, Pietschmann MF, Sievers B, Docheva D, Schieker M, Jansson V, Müller PE. Collagen type I and decorin expression in tenocytes depend on the cell isolation method. BMC Musculoskeletal Disorders 2012;8(13):140.

(75) Ritty TM, Roth R, Heuser JE. Tendon cell array isolation reveals a previously unknown fibrillin-2-containing macromolecular assembly. Structure 2003;11:1179-1188.

(76) Ehlers TW, Vogel KG. Proteoglycan synthesis by fibroblasts from different regions of bovine tendon cultured in alginate beads. Comparative Biochemistry and Physiology Part A 1998;121:355-365.

(77) Mallick E, Scutt N, Scutt A, Rolf C. Passage and concentration-dependent effects of Indomethacin on tendon derived cells. Journal of Orthopaedic Surgery and Research 2009;4(9).

(78) Archambault JM, Elfervig-Wall MK, Tsuzaki M, HerzogaW , Banes AJ. Rabbit tendon cells produce MMP-3 in response to fluid flow without significant calcium transients. Journal of Biomechanics 2002;35:303-309.

(79) Sutradhar BC. Park J, Hong G, Choi SH. Kim G. Effects of Trypsinization on Viability of Equine Chondrocytes in Cell Culture. Pakistan Veterinary Journal. 2010;30(4):232-238.

(80) de Mos M, Koevoet WJLM, Jahr H, Verstegen MA, Heijboer MP, Kops N, van Leeuwen JPTM, Weinans H, Verhaar JAN, van Osch GJVM. Intrinsic differentiation potential of adolescent human tendon tissue: an in-vitro cell differentiation study. BMC Musculoskeletal Disorders. 2007;8(16).

(81) Weirich , Keene DR, Kirsch K, Heil M, Neumann E, Dinser R. Expression of PSACH-associated mutant COMP in tendon fibroblasts leads to increased apoptotic cell death irrespective of the secretory characteristics of mutant COMP. Matrix Biology. 2007;26(4):314-323.

(82) Rui YF, Lui PP, Li G, Fu SC, Lee YW, Chan KM. Isolation and characterization of multipotent rat tendon-derived stem cells. Tissue Engineering Part A. 2010;16(5):1549-1558.

(83) Zhang J, Wang JHC. Characterization of differential properties of rabbit tendon stem cells and tenocytes. BMC Musculoskeletal Disorders. 2010;11(10).

(84) Lui PP. Tendon-Derived Stem Cells (TDSCs): From basic science to potential roles in tendon pathology and tissue engineering applications. Stem Cell Reviews. 2011;7(4):883-897.

(85) Forsyth NR, Kay A, Hampson K, Downing A, Talbot R, McWhir J. Transcriptome alterations due to physiological normoxic (2% O-2) culture of human embryonic stem cells. Regenerative Medicine. 2008;3(6):817-833.

(86) Lee WY, Lui PP, Rui YF. Hypoxia-mediated efficient expansion of human tendon–derived stem cells in vitro. Tissue Engineering Part A. 2012;18(5):484-498.

(87) Pittenger MF, Mackay AM, Beck SC, Jaiswal RK, Douglas R, Mosca JD, Moorman MA, Simonetti DW, Craig S, Marshak DR. Multilineage potential of adult human mesenchymal stem cells. Science. 1999;284(5411):143-147.

(88) Jiang Y, Jahagirdar BN, Reinhardt RL, Schwartz RE, Keene CD, Ortiz-Gonzalez XR, Reyes M, Lenvik T, Lund T, Blackstad M, Du J, Aldrich S, Lisberg A, Low WC, Largaespada DA, Verfaillie CM. Pluripotency of mesenchymal stem cells derived from adult marrow. Nature. 2002;418(6893):41-49.

(89) Roufosse CA, Direkze NC, Otto WR, Wright NA. Circulating mesenchymal stem cells. The International Journal of Biochemistry & Cell Biology. 2004;36:585-597.

(90) Zuk PA, Zhu M, Mizuno H, Huang J, Futrell JW, Katz AJ, Benhaim P, Lorenz HP, Hedrick MH. Multilineage cells from human adipose tissue: implications for cell-based therapies. Tissue Engineering. 2001;7(2):211-228.

(91) Molchanova EA, Payushina OV, Starostin VI. Effects of growth factors on multipotent bone marrow mesenchymal stromal cells. Biology Bulletin 2008;35(6):555-570.

(92) Krampera M, Pizzolo G, Aprili G, Franchini M. Mesenchymal stem cells for bone, cartilage, tendon and skeletal muscle repair. Bone. 2006;39:678-683.

(93) Dominici M, Le Blanc K, Mueller I, Slaper-Cortenbach I, Marini F, Krause D, Deans R, Keating A, Prockop Dj, Horwitz E. Minimal criteria for defining multipotent mesenchymal stromal cells. The International Society for Cellular Therapy position statement. Cytotherapy. 2006;8(4):315-317.

(94) Fernández Vallone VB, Romaniuk MA, Choi H, Labovsky V, Otaegui J, Chasseing NA. Mesenchymal stem cells and their use in therapy: What has been achieved? Differentiation. 2013;85(1):1-10.

(95) Kisselbach L, Merges M, Bossie A, Boyd A. CD90 Expression on human primary cells and elimination of contaminating fibroblasts from cell cultures. Cytotechnology. 2009;59(1):31-44.

(96) Kolf CM, Cho E, Tuan RS. Biology of adult mesenchymal stem cells: regulation of niche, self-renewal and differentiation. Arthritis Research & Therapy. 2007;9(1):204-214.

(97) Ode A, Kopf J, Kurtz A, Schmidt-Bleek K, Schrade P, Kolar P, Buttgereit F, Lehmann K, Hutmacher DW, Duda GN. Kasper G. CD73 and CD29 concurrently mediate the mechanically induced decrease of migratory capacity of mesenchymal stromal cells. European Cells and Materials. 2011;22:26-42.

(98) Chamberlain G, Fox J, Ashton B, Middleton J. Concise Review: Mesenchymal Stem Cells: Their Phenotype, Differentiation Capacity, Immunological Features, and Potential for Homing. Stem Cells. 2007;25:2739-2749.

(99) Mödder UI, Roforth MM, Nicks KM, Peterson JM, McCready LK, Monroe DG, Khosla S. Characterization of mesenchymal progenitor cells isolated from human bone marrow by negative selection. Bone. 2012;50(3):804-810.

(100) Pittenger M, Vanguri P, Simonetti D, Young R. Adult mesenchymal stem cells: Potential for muscle and tendon regeneration and use in gene therapy. J Musculoskel Neuron Interactions. 2002;2(4):309-320.

(101) Justesen J, Stenderup K, Eriksen EF, Kassem M. Maintainance of osteoblastic and adipocytic differentiation potential with age and osteoporosis in human marrow stromal cell cultures. Calcified Tissue International. 2002;71:36-44.

(102) Chao PG, Grayson W, Vunjak-Novakovic G. Engineering cartilage and bone using human mesenchymal stem cells. Journal of Orthopaedic Science. 2007;12:398-404.

(103) Waese EYL, Kandel RR, Stanford WL. Application of stem cells in bone repair. Skeletal Radiology. 2008;37:601-608.

(104) Leor J, Amsalem Y, Cohen S. Cells, scaffolds, and molecules for myocardial tissue engineering. Pharmacology & Therapeutics. 2005;105(2):151-163.

(105) Hoffmann A, Pelled G, Turgeman G, Eberle P, Zilberman Y, Shinar H, Keinan-Adamsky K, Winkel A, Shahab S, Navon G, Gross G, Gazit D. Neotendon formation induced by manipulation of the Smad8 signalling pathway in mesenchymal stem cells. Journal Of Clinical Investigation. 2006;116(4):940-952.

(106) Luo Q, Song G, Song Y, Xu B, Qin J, Shi Y. Indirect co-culture with tenocytes promotes proliferation and mRNA expression of tendon/ligament related genes in rat bone marrow mesenchymal stem cells. Cytotechnology 2009;61:1-10.

(107) Kapacee Z, Yeung CY, Lu Y, Crabtree D, Holmes DF, Kadler KE. Synthesis of embryonic tendon-like tissue by human marrow stromal/mesenchymal stem cells requires a three-dimensional environment and transforming growth factor β3. Matrix Biology. 2010;29(8):668-677.

(108) Schnabel LV, Lynch ME, van der Meulen MCH, Yeager AE, Kornatowski MA, Nixon AJ. Mesenchymal stem cells and insulin-like growth factor-i gene- enhanced mesenchymal stem cells improve structural aspects of healing in equine flexor digitorum superficialis tendons. Journal Of Orthopaedic Research. 2009;27(10):1392-1398.

(109) Ju YJ, Muneta T, Yoshimura H, Koga H, Sekiya I. Synovial mesenchymal stem cells accelerate early remodeling of tendon-bone healing. Cell and Tissue Research. 2008;332(3):469-478.

(110) S. Aggarwal MFP. Human mesenchymal stem cells modulate allogeneic immune cell responses. Blood 2005;105(4):1815-1822.

(111) Du YY, Zhou SH, Zhou T, Su H, Pan HW, Du WH, Liu B, Liu QM. Immuno-inflammatory regulation effect of mesenchymal stem cell transplantation in a rat model of myocardial infarction. Cytotherapy 2008;10(5):469-478.

(112) Brohlin M, Mahay D, Novikov LN, Terenghi G, Wiberg M, Shawcross SG, Novikova LN. Characterisation of human mesenchymal stem cells following differentiation into Schwann cell-like cells. Neuroscience Research 2009;64(1):41-49.

(113) Stock P, Staege MS, Müller LP, Sgodda M, Völker A, Volkmer I, Lützkendorf J, Christ B. Hepatocytes derived from adult stem cells. Transplantation Proceedings 2008;40(2):620-623.

(114) Herthel DJ. Enhanced suspensory ligament healing in 100 horses by stem cell and other bone marrow components. AAEP Proceedings 2001;47:319-321.

(115) Smith RK., Korda M, Blunn GW, Goodship AE. Isolation and implantation of autologous equine mesenchymal stem cells from bone marrow into the superficial digital flexor tendon as a potential novel treatment. Equine Veterinary Journal 2003;35(1):99-102.

(116) Frisbie DD. Clinical update on the use of mesenchymal stem cells in equine orthopaedics. Equine Veterinary Journal 2010;42(1):86-89.

(117) Martin GR. Isolation of a pluripotent cell line from early mouse embryos cultured in medium conditioned by teratocarcinoma stem cells. Proclemations of the National Acadamy of Science U S A. 1981;78(12):7634-7638.

(118) Evans MJ KM. Establishment in culture of pluriopotential cells from mouse embryos. Nature. 1981;292(5819):154-156.

(119) Thomson JA, Itskovitz-Eldor J, Shapiro SS, Waknitz MA, Swiergiel JJ, Marshall VS, Jones JM. Embryonic stem cell lines derived from human blastocysts. Science 1998;282:1145-1147.

(120) Bishop AE, Buttery LD, Polak, JM. Embryonic stem cells. Journal of Pathology 2002;197:424-429.

(121) Amit M IJ. Derivation and spontaneous differentiation of human embryonic stem cells. Journal of Anatatomy. 2002;200(3):225-232.

(122) Xu C, Inokuma MS , Denham J,Golds K , Kundu P, Gold JD, Carpenter MK. Feeder-free growth of undifferentiated human embryonic stem cells. Nature Biotechnology 2001;19:971-974.

(123) Chen X, Song XH, Yin Z, Zou XH, Wang LL, Hu H, Cao T, Zheng M, Ouyang HW. Stepwise differentiation of human embryonic stem cells promotes tendon regeneration by secreting fetal tendon matrix and differentiation factors. Stem Cells 2009;27(6):1276-1287.

(124) Chen JL, Yin Z, Shen WL, Chen X, Heng BC, Zou XH, Ouyang HW. Efficacy of hESC-MSCs in knitted silk-collagen scaffold for tendon tissue engineering and their roles. Biomaterials 2010;36:9438-9451.

(125) Favata M, Beredjiklian PK, Zgonis MH, Beason DP, Crombleholme TM, Jawad AF, Soslowsky LJ. Regenerative properties of fetal sheep tendon are not adversely affected by transplantation into an adult environment. Journal of Orthopeadic Research. 2006;24(11):2124-2132.

(126) Watts AE, Yeager AE, Kopyov OV, Nixon AJ. Fetal derived embryonic-like stem cells improve healing in a large animal flexor tendonitis model. Stem Cell Research and Therapy. 2011;2(1):4.

(127) Guest DJ, Smith MR, Allen WR. Equine embryonic stem-like cells and mesenchymal stromal cells have different survival rates and migration patterns following their injection into damaged superficial digital flexor tendon. Equine Veterinary Journal. 2010;42(7):636-642.

(128) Dallon JC, Ehrlich HP. Wound Repair and Regeneration 2008;16(4):472-479.

(129) Feng Z, Tateishi Y, Nomura Y, Kitajima T, Nakamura T. Construction of fibroblast–collagen gels with orientated fibrils induced by static or dynamic stress: toward the fabrication of small tendon grafts. J Artif Organs 2006;9:220-225.

(130) Chen X, Qi YY, Wang LL, Yin Z, Yin GL, Zou XH, Ouyang HW. Ligament regeneration using a knitted silk scaffold combined with collagen matrix. Biomaterials 2008;29:3683-3692.

(131) Chen G, Sato T, Sakane M, Ohgushi H, Ushida T, Tanaka J, Tateishi T. Application of PLGA-collagen hybrid mesh for three-dimensional culture of canine anterior cruciate ligament cells. Materials Science and Engineering C 2004;24:861-866.

(132) Fang Q, Chen D, Yang Z, Li M. In vitro and in vivo research on using Antheraea pernyi silk fibroin as tissue engineering tendon scaffolds. Materials Science and Engineering C 2009;29:1527-1534.

(133) Fan H, Liu H, Toh SL, Goh JHC. Anterior cruciate ligament regeneration using mesenchymal stem cells and silk scaffold in large animal model. Biomaterials 30 2009;30:4967-4977.

(134) A. W. Murray, M. F. Macnicol. 10–16 year results of Leeds-Keio anterior cruciate ligament reconstruction. The Knee 2004;11(1):9-14.

(135) Zaffagnini S, Maria G, Muccioli M, Chatrath V, Bondi A, De Pasquale V, Martini D, Bacchelli B, Marcacci M. Histological and ultrastructural evaluation of Leeds-Keio ligament 20 years after implant: a case report. Knee Surgery Sports Traumatology Arthroscopy 2008;16(11):1026-1029.

(136) Nau T, Lavoie P, Duval N. A new generation of artificial ligaments in reconstruction of the anterior cruciate ligament. Two-year follow-up of a randomised trial. J Bone Joint Surg Br. 2002;84(3):356-360.

(137) Proper SIW, Aladin A, Lam K, Lunn PG. Evaluation of a porcine dermal xenograft (PDX) in the treatment of chronic, massive rotator cuff defects. J Bone Joint Surg Br 2003;85(B Supp I 69).

(138) Soler JA, Gidwani S, Curtis MJ. Early complications from the use of porcine dermal collagen implants (Permacol) as bridging constructs in the repair of massive rotator cuff tears. A report of 4 cases. Acta Orthop Belg. 2007;73(4):432-436.

(139) Lee DK. A preliminary study on the effects of acellular tissue graft augmentation in acute Achilles tendon ruptures. J Foot Ankle Surg. 2008;47(1):8-12.

(140) Chen GQ, Zhang G, Park SJ, Lee SY. Industrial scale production of poly(3-hydroxybutyrate co-3-hydroxyhexanoate). Applied microbiology and biotechnology 2001;57(1-2):50-55.

(141) Chen GQ. A microbial polyhydroxyalkanoates (PHA) based bio- and materials industry. Chemistry Society Reviews 2009;38:2434-2446.

(142) Chen GQ Wu Q. The application of polyhydroxyalkanoates as tissue engineering materials. Biomaterials 2005;26(33):6565-6578.

(143) Wang YW, Wu Q, Chen GQ. Attachment, proliferation and differentiation of osteoblasts on random biopolyester poly(3-hydroxybutyrate-co-3- hydroxyhexanoate) scaffolds. Biomaterials 2004;25:669-675.

(144) Hu YJ, Wei X, Zhao W, Liu YS, Chen GQ. Biocompatibility of poly(3-hydroxybutyrate-co-3-hydroxyvalerate-co- 3-hydroxyhexanoate) with bone marrow mesenchymal stem cells. Acta Biomaterialia 2009;5:1115-1125.

(145) Ji Y, Li YT, Chen GQ. Interactions between a poly(3-hydroxybutyrate-co-3-hydroxyvalerate-co-3-hydroxyhexanoate) terpolyester and human keratinocytes. Biomaterials 2008;29:3807-3814.

(146) Wang YW, Wu Q, Chen GQ. Reduced mouse fibroblast cell growth by increased hydrophilicity of microbial polyhydroxyalkanoates via hyaluronan coating. Biomaterials 2003;24:4621-4629.

(147) Chuan Ye, Ping Hu, Min-Xian Ma, Yang Xiang, Ri-Guang Liu, Xian-Wen Shang. PHB/PHBHHx scaffolds and human adipose-derived stem cells for cartilage tissue engineering. Biomaterials 2009;30:4401-4406.

(148) Bian YZ, Wang Y, Aibaidoula G, Chen GQ, Wu Q. Evaluation of poly(3-hydroxybutyrate-co-3-hydroxyhexanoate) conduits for peripheral nerve regeneration. Biomaterials 2009;30:217-225.

(149) Wu S, Liu YL, Cui B, Qu XH, Chen GQ. Study on Decellularized Porcine Aortic Valve/Poly (3-hydroxybutyrate-co-3-hydroxyhexanoate) Hybrid Heart Valve in Sheep Model. Artificial Organs ;31(9):689-697.

(150) Dai ZW, Zou XH, Chen GQ. Poly(3-hydroxybutyrate-co-3-hydroxyhexanoate) as an injectable implant system for prevention of post-surgical tissue adhesion. Biomaterials 2009;30:3075-3083.

(151) Sun M, Zhou P, Pan LF, Liu S, Yang HX. Enhanced cell affinity of the silk fibroin-modified PHBHHx material. Journal of Material Science: Materials in Medicine 2009;20:1743-1751.

(152) Cheng ML, Lin CC, Su HL, Chen PY, Sun YM. Processing and characterization of electrospun poly(3-hydroxybutyrate-co-3-hydroxyhexanoate) nanofibrous membranes. Polymer 2008;49:546-553.

(153) Wang S, Wan ACA, Xu X, Gao S, Mao HQ, Leong KW, Yu H. A newnerve guide conduit material composed of a biodegradable poly(phosphoester). Biomaterials 2001;22:1157-1169.

(154) Jaasma MJ, O'Brien FJ. Mechanical Stimulation of Osteoblasts Using Steady and Dynamic Fluid Flow. Tissue Engineering: Part A 2008;14(7):1213-1223.

(155) Huang-Chi Chen YH. Bioreactors for tissue engineering. Biotechnology Letters 2006;28:1415-1423.

(156) Yang KJ, Saris DBF, Geuze RE, Van der Helm YJM, Van Rijen MHP, Verbout AJ, Dhert WJA, Creemers LB. Impact of expansion and redifferentiation conditions on chondrogenic capacity of cultured chondrocytes. Tissue Engineering 2006;12(9):2435-2447.

(157) Wang T, Gardiner BS, Lin Z, Rubenson J, Kirk TB, Wang A, Xu J, Smith DW, Lloyd DG, Zheng MH. Bioreactor Design for Tendon/Ligament Engineering. Tissue Engineering Part B Rev. 2013;19(2):133-146.

(158) Kjær M, Langberg H, Heinemeier K, Bayer ML, Hansen M, Holm L, Doessing S, Kongsgaard M, Krogsgaard MR, Magnusson SP. From mechanical loading to collagen synthesis, structural changes and function in human tendon. Scandanavian Journal of Medicine Science and Sports 2009;19:500-510.

(159) Kalson NS, Holmes DF, Herchenhan A, Lu Y, Starborg T, Kadler KE. Slow stretching that mimics embryonic growth rate stimulates structural and mechanical development of tendon-like tissue in vitro. Developmental Dynamics 2011;240(11):2520-2528.

(160) Jiang Y, Liu H, Li H, Wang F, Cheng K, Zhou G, Zhang W, Ye M, Cao Y, Liu W, Zou H. A proteomic analysis of engineered tendon formation under dynamic mechanical loading in vitro. Biomaterials 2011;32(17):4085-4095.

(161) Saber S, Zhang AY, Ki SH, Lindsey D, Pham HM, Chang J. Optimization of flexor tendon tissue engineering using bioreactor cyclic strain. Journal Of The American College Of Surgeons 2008;207(3):s64-s64.

(162) Malaviya P, Butler DL, Korvick DL, Proch FS. In vivo tendon forces correlate with activity level and remain bounded: evidence in a rabbit flexor tendon model. Journal of Biomechanics 1998;31(11):1043-1049.

(163) Vogel V. Local force and geometry sensing regulate cell functions. Nature Reviews Molecular Cell Biology 2006;7(4):265-275.

(164) Kuo CT, Tuan RS. MechanoactiveTenogenic Differentiation of Human Mesenchymal Stem Cells. Tissue Engineering. Part A. 2008;14(10):1615-1627.

(165) Issa R, Engebretson I, Rustom B, McFetridge L, Sikavitsas VI. The effect of cell seeding density on the cellular and mechanical properties of a mechanostimulated tissue-engineered tendon. Tissue Engineering. Part A. 2011;17(11):1479-1487.

(166) Butler DL, Juncosa-Melvin N, Boivin GP, Galloway MT, Shearn JT, Gooch C, Awad H. Functional tissue engineering for tendon repair: a multidisciplinary strategy using mesenchymal stem cells, bioscaffolds, and mechanical stimulation. Journal Of Orthopaedic Research 2008; 26(1):1-9.

(167) Nirmalanandhan, VS. Levy, MS. Huth, AJ. Butler, DL. Effects of Cell Seeding Density and Collagen Concentration on Contraction Kinetics of Mesenchymal Stem Cell–Seeded Collagen Constructs. Tissue Engineering 2006;12(7):1865-1873.

(168) Bandi S, Cheng K, Joseph B, Gupta S. Spontaneous origin from human embryonic stem cells of liver cells displaying conjoint meso-endodermal phenotype with hepatic functions. J Cell Sci 2012;125(5):1274-1283.

(169) Ahearne M. Wilson SL. Liu KK. Rauz S. El Haj AJ. Yang Y. Influence of cell and collagen concentration on the cell matrix mechanical relationship in a corneal stroma wound healing model. Experimental Eye Research 2010;91:584-591.

(170) Grayson WL, Zhao F, Bunnell B, Ma T. Hypoxia enhances proliferation and tissue formation of human mesenchymal stem cells. Biochemical and Biophysical Research Communications 2007;358:948-953.

(171) van Vlimmeren MA, Driessen-Mol A, van den Broek M, Bouten CV, Baaijens FP. Controlling matrix formation and cross-linking by hypoxia in cardiovascular tissue engineering. Journal of Applied Physiology 2010;109(5):1483-1491.

(172) English A, Azeem A, Gaspar DA, Keane K, Kumar P, Keeney M, Rooney N, Pandit A, Zeugolis DI. Preferential cell response to anisotropic electro-spun fibrous scaffolds

under tension-free conditions. Journal of Materials Science Materials in Medicine. 2012;23(1):137-148.

(173) Chatterjee K, Lin-Gibson S, Wallace WE, Parekh SH, Lee YJ, Cicerone MT, Young MF, Simon CG Jr. The effect of 3D hydrogel scaffold modulus on osteoblast differentiation and mineralization revealed by combinatorial screening. Biomaterials 2010;31(19):5051-5062.

(174) Georges PC. Cell type-specific response to growth on soft materials. Journal of Appllied Physiology 2005;98(4):1547-1553.

(175) Lyons FG, Al-Munajjed AA, Kieran SM, Toner ME, Murphy CM, Duffy GP, O'Brien FJ. The healing of bony defects by cell-free collagen-based scaffolds compared to stem cell-seeded tissue engineered constructs. Biomaterials 2010;31(35):9232-9243.

(176) Doral MN, Alam M, Bozkurt M, Turhan E, Atay OA, Do¨nmez G, Maffulli N. Functional anatomy of the Achilles tendon. Knee Surgery, Sports Traumatology, Arthroscopy 2010;18:638-643.

(177) Pijanka JK, Kumar D, Dale T, Yousef I, Parkes G, Untereiner V, Yang Y, Dumas P, Collins D, Manfait M, Sockalingum GD, Forsyth NR, Sulé-Suso J. Vibrational spectroscopy differentiates between multipotent and pluripotent stem cells. Analyst. 2010;135(12):3126-3132.

(178) Ezashi T, Das P, Roberts RM. Low O2 tensions and the prevention of differentiation of hES cells. Proceedings of the National Acadamy of Science 2005;102(13):4783-4788.

(179) Qu XH, Wu Q, Zhang KY, Chen GQ. In vivo studies of poly(3-hydroxybutyrate-co-3-hydroxyhexanoate) based polymers: biodegradation and tissue reactions. Biomaterials 2006;27(19):3540-3548.

(180) Liu Q. In vitro biocompatibility and degradation of terpolyester 3HB-co-4HB-co-3HHx, consisting of 3-hydroxybutyrate, 4-hydroxybutyrate and 3-hydroxyhexanoate. Journal of Biomaterial Science Polymer Edition 2008;19(11):1521-1533.

(181) Hoeferlin A. Estimation of the inflammatory reaction by CRP-levels following prosthetic hernia repair. Hernia 2000;4:248-249.

(182) Lomas AJ, Chen GQ, El Haj AJ, Forsyth NR. Poly(3-hydroxybutyrate-co-3-hydroxyhexanoate) supports adhesion and migration of mesenchymal stem cells and tenocytes. World Journal of Stem Cells 2012;26(9):94-100.

(183) Chung C, Burdick JA. Engineering cartilage tissue. Advanced Drug Delivery Reviews 2008;60:243-262.

(184) Mackey AL, Donnelly AE, Turpeenniemi-Hujanen T, Roper HP. Skeletal muscle collagen content in humans after high-force eccentric contractions. Journal of Applied Physiology 2004;97:197-203.

(185) Schneider RK, Puellen A, Kramann R, Raupach, K , Bornemann J, Knuechel R, Pe´ rez-Bouza A, Neuss S. The osteogenic differentiation of adult bone marrow and perinatal umbilical mesenchymal stem cells and matrix remodelling in three-dimensional collagen scaffolds. Biomaterials 2010;31:467-480.

(186) Cunniffe GM, O'Brien FJ. Collagen scaffolds for orthopaedic regenerative medicine. Journal of Minerals, Metals and Materials 2011;63(4).

(187) Iwasa J, Ochi M, Uchio Y, Katsube K, Adachi N, Kawasaki K. Effects of cell density on proliferation and matrix synthesis of chondrocytes embedded in atelocollagen gel. Artificial Organs 2003;27:249-255.

(188) Clover J, Dodds RA, Gowen M. Integrin subunit expression by human osteoblasts and osteoclasts in situ and in culture. Journal of Cell Science 1992;103:267-271.

(189) Seong, JM. Kim, BC. Park, JH. Kwon, IL. Mantalaris, A.Hwang, YS. Stem cells in bone tissue engineering. Biomedical Materials. 2010;5:6. 2010;5(6).

(190) Jukes JM, Both SK, Leusink A, Th. Sterk LM, van Blitterswijk CA, de Boer J. Endochondral bone tissue engineering using embryonic stem cells. Proceedings of the National Academy of Sciences USA 2008;105(19):6840-6845.

(191) Jukes JM, Moroni L, van Blitterswijk CA, de Boer J. Critical Steps toward a Tissue-Engineered Cartilage Implant Using Embryonic Stem Cells. Tissue Engineering: Part A 2008;14(1):135-147.

(192) Tuan RS, Boland G, Tuli R. Adult mesenchymal stem cells and cell-based tissue engineering. Arthritis Research and Therapy 2002;5(1):32-45.

(193) Vallier L. Touboul T. Chng Z. Brimpari M. Hannan N. Millan E. Smithers LE. Trotter M. Rugg-Gunn P. Weber A. Roger A. Pedersen RA. Early Cell Fate Decisions of Human Embryonic Stem Cells and Mouse Epiblast Stem Cells Are Controlled by the Same Signalling Pathways. PLoS One 2009;4(6):1-13.

(194) Vats A, Bielby RC, Tolley N, Dickinson SC, Boccaccini AR, Hollander AP, Bishop AE, Polak JM. Chondrogenic differentiation of human embryonic stem cells: the effect of the micro-environment. Tissue Engineering 2006;12:1687-1697.

(195) Forsyth N, McWhir J. Human embryonic stem cell telomere length impacts directly on clonal progenitor isolation frequency. Rejuvenation Research 2008;11(1):5-17.

(196) Kanczler JM. Osteogenesis and angiogenesis: the potential for engineering bone. European Cells and Materials 2008;15:100-114.

(197) Wang Y, Gao R, Wang PP, Jian J, Jiang XL, Yan C, Lin X, Wu L, Chen GQ, Wu Q. The differential effects of aligned electrospun PHBHHx fibers on adipogenic and osteogenic potential of MSCs through the regulation of PPAR gamma signaling. Biomaterials 2012;33:485-493.

(198) Krawetz RJ, Taiani JT, Wu YE, Liu S, Meng G, Matyas JR, Rancourt DE. Collagen I scaffolds cross-linked with beta-glycerol phosphate induce osteogenic differentiation of embryonic stem cells in vitro and regulate their tumorigenic potential in vivo. Tissue Engineering Part A 2012;18(9):1014-1024.

(199) Togo S, Sato T, Sugiura H, Wang X, Basma H, Nelson A, Liu X, Bargar TW, Sharp JG,.Rennard SI. Differentiation of embryonic stem cells into fibroblast-like cells in three-dimensional type I collagen gel cultures. In Vitro Cellular & Developmental Biology. 2011;47(2):114-124.

(200) Dallon JE. A review of fibroblast-populated collagen lattices. Wound Repair and Regeneration 2008;16:474-479.

(201) Lefebvre V, de Crombrugghe B. Toward understanding SOX9 function in chondrocyte differentiation. Matrix Biology 1998;16(9):529-540.

(202) Huang CY, Reuben PM, Cheung HS. Temporal expression patterns and corresponding protein inductions of early responsive genes in rabbit bone marrow-derived mesenchymal stem cells under cyclic compressive loading. Stem cells 2005;23(8):1113-1121.

(203) Spencer VA, Costes S, Inman JL, Xu R, Chen J, Hendzel MJ, Bissell MJ. Depletion of nuclear actin is a key mediator of quiescence in epithelial cells. Journal of Cell Science 124, 123-132. 2011;124:123-132.

(204) Lee KS, Kim HJ, Li QI, Chi XZ, Ueta C, Komori T, Wozney JM, Kim EG, Choi JY, Ryoo HM, Bae SC. Runx2 is a common target of transforming growth factor β1 and bone morphogenetic protein 2, and cooperation between runx2 and smad5 induces osteoblast-specific gene expression in the pluripotent mesenchymal precursor cell line C2C12. Molecular Cell Biology 2000;20(23):8783-8792.

(205) Michalopoulos E, Knight RL, Korossis S, Kearney JN, Fisher J, Ingham E. Development of methods for studying the differentiation of human mesenchymal stem cells under cyclic compressive strain. Tissue Engineering Part C Methods. 2012;18(4):252-262.

(206) Evans ND, Gentleman E, Chen X, Roberts CJ, Polak JM, Stevens MM. Extracellular matrix-mediated osteogenic differentiation of murine embryonic stem cells. Biomaterials 2010;31(12):3244-3252.

(207) Komatsu K, Mosekilde L, Viidik A, Chiba M. Polarized light microscopic analyses of collagen fibers in the rat incisor periodontal ligament in relation to areas, regions, and ages. The Anatomical Record 2002;268(4):381-387.

(208) Barber FA, Herbert MA, Coons DA. Tendon augmentation grafts: Biomechanical failure loads and failure patterns. Arthroscopy 2006;22:534-538.

(209) Nirmalanandhan VS, Rao M, Shearn JT, Juncosa-Melvin N, Gooch C, Butler DL. Effect of scaffold material, construct length and mechanical stimulation

on the in vitro stiffness of the engineered tendon construct. Journal of Biomechanics 41 (2008) 822–828.

(210) Canty EG, Starborg T, Lu Y, Humphries SM, Holmes DF, Meadows RS, Huffman A, O'Toole ET, Kadler KE. Actin filaments are required for fibripositor-mediated collagen fibril alignment in tendon. The Journal of Biological Chemistry 2006;281(50):38592-38598.

(211) Kapacee Z, Richardson SH, Lu Y, Starborg T, Holmes DF, Baar K, Kadler KE. Tension is required for fibripositor formation. Matrix Biology 2008;27(4):371-375.

(212) Floss T, Arnold HH, Braun T. A role for FGF-6 in skeletal muscle regeneration. Genes & Development 1997;11(16):2040-2051.

(213) Lewandoski M, Sun X, Martin GR. FGF-8 signalling from the AER is essential for normal limb development. Nature Genetics 2000;26(4):460-463.

(214) Wong YP, Fu SC, Cheuk YC, Lee KM, Wong MW, Chan KM. Bone morphogenetic protein 13 stimulates cell proliferation and production of collagen in human patellar tendon fibroblasts. Acta Orthopaedica 2005;76(3):421-427.

(215) Jelinsky SA, Archambault J, Li L, Seeherman H. Tendon-selective genes identified from rat and human musculoskeletal tissues. Journal of Orthopaedic Research 2010;28(3):289-297.

(216) Yu C, Young S, Russo V, Amsden BG, Flynn LE. Techniques for the isolation of high-quality rna from cells encapsulated in chitosan hydrogels. Tissue Eng Part C Methods 2013:[Epub ahead of print].

(217) Pennisi E. Tending tender tendons. Science 2002;295:1011-1011.

(218) Palmes D, Spiegel HU, Schneider TO, Langer M, Stratmann U, Budny T, Probst A. Achilles tendon healing: long-term biomechanical effects of postoperative mobilization and immobilization in a new mouse model. Journal of Orthopeadic Research 2002;20(5):939-946.

(219) Zantop T, Gilbert TW, Yoder MC, Badylak SF. Extracellular matrix scaffolds are repopulated by bone marrow-derived cells in a mouse model of achilles tendon reconstruction. Journal of Orthopeadic Research 2006;24(6):1299-1309.

(220) Ouyang HW, Goh JC, Thambyah A, Teoh SH, Lee EH. Knitted poly-lactide-co-glycolide scaffold loaded with bone marrow stromal cells in repair and regeneration of rabbit Achilles tendon. Tissue Engineering 2003;9(3):431-439.

(221) M. Lo¨ bler M, Saß C, Kunze KP, Schmitz UT. Biomaterial implants induce the inflammation marker CRP at the site of implantation. Journal of Biomedical Material Research 2002;61:165-167.

(222) Zhou J, Peng SW, Wang YY, Zheng SB, Wang Y, Chen GQ. The use of poly(3-hydroxybutyrate-co-3-hydroxyhexanoate) scaffolds for tarsal repair in eyelid reconstruction in the rat. Biomaterials 2010;31(29):7512-7518.

(223) Ishida H, Nakada H, Yokoyama M, Hayashi Y, Ohsawa T, Inokuma S, Hoshino T, Hashimoto D. Minilaparotomy approach for colonic cancer: initial experience of 54 cases. Surgical Endoscopy 2005;19(3):316-320.

(224) Yahia LH. Microscopical investigation of canine anterior cruciate ligament and patellar tendon: collagen fascicle morphology and architecture. Journal of Orthopeadic Research 1989;7(2):243-251.

(225) Schwartz MA, DeSimone DW. Cell adhesion receptors in mechanotransduction. Current Opinions in Cell Biology 2008;20:551-556.

(226) Qu XH, Wu Q, Liang J, Zou B, Chen GQ. Effect of 3-hydroxyhexanoate content in poly(3-hydroxybutyrate-co-3-hydroxyhexanoate) on in vitro growth and differentiation of smooth muscle cells. Biomaterials. 2006 May;27(15):2944-50. 2006;27(15):2944-2950.

(227) Yang XD, Li HM, Chen M, Zou XH, Zhu LY, Wei CJ, Chen GQ. Enhanced insulin production from murine islet beta cells incubated on poly(3-hydroxybutyrate-co-3-hydroxyhexanoate). Journal of Biomedical Material Research A. 2010;92(2):548-555.

(228) Sales-Pardo I, Avendaño A, Barquinero J, Domingo JC, Marin P, Petriz J. The Hoechst low-fluorescent profile of the side population: clonogenicity versus dye retention. Blood 2006;108(5):1774-1775.

(229) Hui TY, Cheung KMC, Cheung WL, Chan D, Chan BP. In vitro chondrogenic differentiation of human mesenchymal stem cells in collagen microspheres: Influence of cell seeding density and collagen concentration. Biomaterials 2008;29:3201-3212.

(230) Beason DP, Connizzo BK, Dourte LM, Mauck RL, Soslowsky LJ, Steinberg DR, Bernstein J. Fiber-aligned polymer scaffolds for rotator cuff repair in a rat model. Journal of Shoulder Elbow Surgery. 2012;21(2):245-250.

(231) Legant WR, Miller JS, Blakely BL, Cohen DM, Genin GM, Chen CS. Measurement of mechanical tractions exerted by cells within three-dimensional matrices. Nature Methods 2010;7(12):969-971.

(232) Knapp DM, Tower TT, Tranquillo RT, Barocas VH. Estimation of Cell Traction and Migration in an Isometric Cell Traction Assay. AICHE Journal 1999;45(12):2628-2640.

(233) Grinnell F. Fibroblast–collagenmatrix contraction: growth-factor signalling and mechanical loading. Trends Cell Biology 2000;10(9):362-365.

(234) Nea S. Cyclic strain induces mouse embryonic stem cell differentiation into vascular smooth muscle cells by activating PDGF receptor beta. Journal of Applied Physiology 2008;104:766-772.

(235) Omeroğlu S, Peker T, Türközkan N, Omeroğlu H. High-dose vitamin C supplementation accelerates the Achilles tendon healing in healthy rats. Archives of Orthopeadic Trauma and Surgery 2009;129:281-286.

(236) Tajima S. Ascorbic acid preferentially enhances type I and III collagen gene transcription in human skin fibroblasts. Journal of Dermatological Science 1996;11:250-253.

(237) Niki E. Action of ascorbic acid as a scavenger of active and stable oxygen radicals. American Journal of Clinical Nutrition 1991;54(6):1119S-1124S.

(238) Mikic B, Rossmeier K, Bierwert L. Sexual dimorphism in the effect of GDF-6 deficiency on murine tendon. Journal of Orthopeadic Research 2009;27(12):1603-1611.